Adela Kalivoda

# Solubility enhancement of poorly water-soluble drugs by solid dispersion

## a comparison of two manufacturing methods

Cuvillier Verlag Göttingen
Internationaler wissenschaftlicher Fachverlag

# Solubility enhancement of poorly water-soluble drugs by solid dispersion

# Solubility enhancement of poorly water-soluble drugs by solid dispersion

a comparison of two manufacturing methods

Inaugural-Dissertation

zur
Erlangung des Doktorgrades
der Mathematisch-Naturwissenschaftlichen Fakultät
der Heinrich-Heine-Universität Düsseldorf

vorgelegt von

**Adela Kalivoda**

aus Opava (Troppau), Tschechische Republik

Düsseldorf, April 2012

**Bibliografische Information der Deutschen Nationalbibliothek**
Die Deutsche Nationalbibliothek verzeichnet diese Publikation in der Deutschen Nationalbibliografie; detaillierte bibliografische Daten sind im Internet über http://dnb.d-nb.de abrufbar.
1. Aufl. - Göttingen: Cuvillier, 2012
Zugl.: Düsseldorf, Univ., Diss., 2012

978-3-95404-141-1

aus dem Institut für Pharmazeutische Technologie und Biopharmazie
der Heinrich-Heine Universität Düsseldorf

Gedruckt mit der Genehmigung
der Mathematisch-Naturwissenschaftlichen Fakultät
der Heinrich-Heine-Universität Düsseldorf

Referent: Prof. Dr. P. Kleinebudde
Koreferent: Prof. Dr. J. Breitkreutz
Tag der mündlichen Prüfung: 05.06.2012


Nonnenstieg 8, 37075 Göttingen
Telefon: 0551-54724-0
Telefax: 0551-54724-21
www.cuvillier.de


1. Auflage, 2012
Gedruckt auf säurefreiem Papier

978-3-95404-141-1

# Contents

# List of abbreviations

| | |
|---|---|
| API | active pharmaceutical ingredient |
| aPMMA | basic butylated methacrylate copolymer, Eudragit® E |
| approx. | approximately |
| AUC | area under the curve $[\mu g/mLxmin]$ |
| BCS | biopharmaceutics classification system |
| $c_{max}$ | maximum concentration |
| $c_{super}/2$ | half-value of the maximal supersaturation concentration $[\mu g/mL]$ |
| $c_s$ | saturation concentration $[\mu g/mL]$ |
| $c_t$ | concentration at time $t$ $[\mu g/mL]$ |
| CL | crospovidone |
| CMC | critical micelle concentration $[\mu g/mL]$ |
| COP | copovidone |
| DSC | differential scanning calorimetry |
| FD | felodipine |
| FF | fenofibrate |
| HME | hot-melt extrusion |
| HPLC | high performance liquid chromatography |
| HPMC | hydroxypropyl methylcellulose |
| ICH | International Conference on Harmonization |
| L/D ratio | length to diameter ratio |
| LOD | limit of detection |
| midpt | midpoint |
| n | number of samples or trials |
| n/a | not available |
| OX | oxeglitazar |

| | |
|---|---|
| PE | polyethylene |
| PEG | polyethylene glycol |
| PEO | polyethylene oxide |
| Ph.Eur. | European Pharmacopoeia |
| PM | physical mixture |
| PTFE | polytetrafluoroethylene, Teflon® |
| PVA-AA-MMA | polyvinyl alcohol-acrylic acid-methyl methacrylate copolymer |
| PVCL-PVAc-PEG | polyvinyl caprolactam-polyvinyl acetate-polyethylene glycol graft copolymer, Soluplus® |
| PVP | polyvinylpyrrolidone, povidone |
| rpm | revolutions per minute |
| SAS | supercritical antisolvent |
| SEDS | solution enhanced dispersion by supercritical fluids |
| SEM | scanning electron microscopy |
| SI | International System of Units |
| SMEDDS | self-microemulsifying drug delivery system |
| std | standard |
| $T_{degr}$ | degradation temperature |
| $T_g$ | glass transition temperature |
| $T_m$ | melting point |
| US | ultrasound |
| USAC | ultrasound-assisted compaction |
| USP | United States Pharmacopeia |
| UV | ultraviolet |
| w/w | weight in weight |
| XRD | X-ray diffraction |

# List of Tables

# List of Figures

# 1 Introduction

## 1.1 Solubility enhancement of poorly soluble drugs

### 1.1.1 Methods of solubility enhancement

The oral bioavailability of a drug, which is by definition the degree at which its active form is made available at the site of action after oral administration, is mainly dependent on the solubility of the drug in the gastrointestinal tract, its permeability through the intestinal wall and on effects of the pharmaceutical formulation. According to the biopharmaceutics classification system (BCS) class II drugs are most suitable for bioavailability enhancement through pharmaceutical formulation due to their good permeability which is only limited by their dissolution rate (Amidon et al., 1995). In the field of drug delivery system development for peroral application, the enhancement of in vivo solubility of newly developed drugs is becoming increasingly challenging as the number of innovative but poorly soluble active pharmaceutical ingredients (APIs) is rising. Various methods are available for solubility enhancement that are classified either as chemical or physical approaches.
The formation of salts or prodrugs with an enhanced solubility behavior are examples for chemical approaches. However, these are only suitable in an early stage of development as this approach will lead to fundamental changes in the substance properties.
The theoretical foundation for physical approaches to modify the solubility of a drug is the Noyes-Whitney equation (Noyes and Whitney, 1897), in this case depicted in its modified version according to Nernst and Brunner (Brunner, 1904; Nernst, 1904):

$$\frac{dc}{dt} = \frac{DA(c_s - c_t)}{Vh} \tag{1.1}$$

where $dc/dt$ is the dissolution rate, $D$ is the diffusion coefficient of the compound, $A$ is the surface area, $c_s$ is the solubility of the compound in the dissolution medium, $c_t$ is the concentration of the compound in the dissolution medium at a time $t$, $V$ is the volume of the dissolution medium and $h$ is the thickness of the diffusion layer adjoining the compound surface.
From Eq. 1.1 it can be concluded that there are various possibilities to influence the dissolution behavior of the drug: an increase of the surface area of the compound available for dissolution, for example through a reduction of the particle size or an improvement of the wetting characteristics, an improvement of the drug's solubility in the medium, an increase of the dissolution medium volume, for example, through the establishment of sink conditions and, finally, the diffusion layer thickness can be reduced. Two strategies shall be emphasized:

The modification of the compound's surface area and the alteration of the apparent solubility $c_s$ of a drug are both classified as physical approaches to dissolution behavior improvement. Examples for the methods mentioned above are listed in Table 1.1.

Table 1.1: Summary of available strategies to solubility enhancement of poorly water-soluble compounds

| | |
|---|---|
| Chemical approach | |
| Salt formation | |
| Prodrug formation | |
| Physical approach | |
| Reduction of the particle size | |
| | Milling |
| | Micronization |
| | Nanoization |
| Pre-/Solubilization | |
| | Employment of surfactants |
| | Employment of cosolvents |
| | Microemulsions |
| | Self-microemulsifying drug delivery systems SMEDDS |
| Complexation | |
| | complexing agents |
| | Inclusion complexes (e.g. cyclodextrines) |
| Solid dispersions | |
| | Eutectic mixtures |
| | Solid suspensions |
| | Solid solutions |
| Modification of the solid form | |
| | Use of metastable solid forms |
| | Use of a better soluble polymorph |
| | Cocrystals |

## 1.2 Solid dispersions

### 1.2.1 Definition and historical background

The foundation for the application of solid dispersions as a method for bioavailability enhancement of poorly soluble drugs was laid by Sekiguchi and Obi in 1961 by the introduction of eutectic mixtures as a novel method for solubility enhancement (Sekiguchi and Obi, 1961). An eutectic system is a blend of substances that are fully miscible in their molten state but only to a limited extent in their solid state. Upon cooling, the components of a mixture with

an eutectic composition crystallize out simultaneously. With any other mixture ratio, the components begin to crystallize consecutively. At a specific temperature which is referred to as the eutectic point, the liquid phase and the solid phases of the components of an eutectic mixture are in a chemical equilibrium. When a molten eutectic composition of a drug and a highly water-soluble carrier is rapidly cooled below the eutectic point, very fine and intimately mixed crystals of both substances are obtained. These very fine crystals of the API are rapidly released as the carrier dissolves in, for example, the gastrointestinal fluid. Because of the drastically increased surface area of this suspension, both the dissolution and absorption rate of the drug substance are enhanced.
Goldberg et al. pursued the subject further, suggesting that solid solutions of a drug in a carrier are superior to eutectic mixtures as the particle size is drastically reduced (Goldberg et al., 1965, 1966a,b,c). By definition, the solid solution of two substances is a homogeneous, single-phase system where one component is dissolved in the other at a molecular level and both components are present in their solid state. With a solid solution system, a maximum particle size reduction of the API is achieved. The general term solid dispersion for a dispersion of one or more active ingredients in an inert carrier or matrix at solid state was defined by Chiou and Riegelman in 1971 who also gave a detailed classification of solid solution and solid dispersion systems and a summary of manufacturing methods (Chiou and Riegelman, 1971). A short summary of this classification is given in Table 1.2.
Frequently, a single class cannot be attributed to a manufactured solid dispersion as they often consist of multiple types of solid dispersions. In that case, the dissolution behavior is a result from a combination of the influences of all present solid dispersion types.
In some publications, compound or complex formations are also classified as solid dispersion systems (Breitenbach, 2002; Ford, 1986). However, these cannot truly be regarded as solid dispersions in the classical sense as defined by Chiou and Riegelman; thus, they are not included in Table 1.2.
Traditionally, highly water-soluble carriers have been used for solid dispersion preparation as the aim was to enhance the drug's solubility. Today, water-insoluble carriers are also used for solid dispersion preparation as they offer the possibility to modify a drug's release behavior, for example, through a sustained release formulation.

Table 1.2: Summary of different solid dispersion types (Chiou and Riegelman, 1971; Ford, 1986)

| Type of solid dispersion | Drug | Carrier | Phases |
|---|---|---|---|
| Eutectic mixtures | Crystalline | Crystalline | 2 |
| Glassy suspensions | Amorphous or crystalline | Amorphous | 2 |
| Amorphous precipitation | Amorphous | Crystalline | 2 |
| Solid solutions | Molecularly dispersed | Crystalline | 1 |
| Glassy solutions | Molecularly dispersed | Amorphous | 1 |

### 1.2.2 Methods of manufacture

According to the definition by Chiou and Riegelman, solid dispersions are manufactured via the melting, melting-solvent or solvent method (Chiou and Riegelman, 1971).
With the melting method, a physical mixture of the API and the carrier is heated until it is melted. An accelerated cooling of the molten mixture is essential for the desired outcome. Stirring in an ice-bath (Sekiguchi and Obi, 1961), pouring onto a stainless steel plate (Chiou and Riegelman, 1969) or spraying onto a cooled surface (Kanig, 1964) are all documented approaches for a rapid cooling of the melt. Alternatively, the drug is dispersed in the already molten carrier and solidified by rapidly cooling the mixture. The benefit of the second approach is that the drug is exposed to relative low temperature levels. For heat-sensitive materials however, the melting method might not be suitable.
If the solvent method is used, both drug and carrier are dispersed in a common solvent. Subsequently, the solvent is removed, for example, through evaporation under vacuum. Other possibilities for the removal of the solvent that have been documented in literature are drying at elevated temperatures, lyophilization and spray-drying or the use of supercritical antisolvents (Serajuddin, 1999; Leuner and Dressman, 2000). While the solvent method offers the possibility to produce a solid dispersion of a heat-sensitive drug and a carrier with a high melting point, it might prove difficult to find a common solvent. The reason for this is that often a hydrophobic API is supposed to be incorporated into a hydrophilic carrier through solid dispersion manufacture. In addition, toxicological problems might arise from solvent residues remaining in the manufactured formulation and the use of organic solvents is generally associated with ecological problems.
The melting-solvent method is a combination of the two previously described methods.
Newer methods for the manufacture of solid dispersions include hot-melt extrusion (HME), hot spin mixing (Dittgen et al., 1995) and super critical fluid technology (Van Nijlen et al., 2003; Ghaderi et al., 1999). Furthermore, ultrasound-assisted compaction (USAC) has been proposed as another novel manufacturing method (Fini et al., 2002a,b).
As the main focus of the present work was on HME and USAC, the principles of these methods are described in separate Sections 1.3 and 1.4.

### 1.2.3 Proposed mechanisms of drug dissolution from solid dispersion systems

Although numerous publications are available on the characteristics and manufacture of solid dispersions, the properties of these systems have not yet been fully understood. This does not only concern their structure or the nature of the prevailing interactions in the system but also the dissolution mechanism leading to the observed improvements in dissolution rate and drug solubility. A summary on possible mechanisms leading to a dissolution enhancement has been given by Chiou and Riegelman (Chiou and Riegelman, 1971):

1. Particle size reduction
2. Solubilization effect resulting from the high concentrations of the carrier in the diffusion layer surrounding the solid dispersion

3. Reduced aggregation of drug particles
4. Improvement of wettability
5. Modifications to the physical form of the drug, e.g. a different polymorphic form

In 2002, Craig classified the possible dissolution mechanisms from solid dispersion systems as being either *a*) carrier-controlled or *b*) drug-controlled dissolution (Craig, 2002). The theory of the carrier-controlled dissolution mechanism was introduced in 1985 by Corrigan (Corrigan, 1985). The dissolution rate of the polymer alone was shown to be equivalent to the release rate of the drug from a drug-carrier system with a high carrier fraction. This finding was confirmed by Dubois and Ford in 1985 who investigated the release rates of various drugs from polyethylene glycol (PEG) 6000 systems. If a solid dispersion was formed by the drug and the carrier, the rate of dissolution was determined to be equivalent for all investigated drug-carrier systems regardless of the drug properties (Dubois and Ford, 1985). In the case of a drug-controlled dissolution mechanism, the release rate is mainly dependent on the properties of the drug substance (Sjökvist and Nyström, 1988; Sjökvist Saers and Craig, 1992).
It is suggested by Craig that at high drug loadings, the theory of the formation of a drug-rich layer that has been proposed by Higuchi et al. may be applied (Craig, 2002; Higuchi et al., 1965). If a polymer-rich layer is present on the solid dispersion surface which is the case, for example, at low drug loadings, carrier-controlled or drug-controlled dissolution takes place depending on the way the drug passes through the polymer layer. In the case of carrier-controlled dissolution, the drug dissolves in the polymer-rich layer. It is molecularly dispersed in the polymer layer. If a drug-controlled mechanism applies, the drug particles are released almost intact or entirely unaltered as the dissolution in the polymer-rich layer is very slow. Even so, the dissolution rate can be improved through some of the proposed mechanisms, for example, a reduction of the aggregation of the drug particles.

## 1.3 Ultrasound-assisted compaction technique

### 1.3.1 Introduction

A comprehensive review on the application of USAC in different sectors, its basic principles and the main effects on the material was published by Levina et al. (2000). In the following section, the main aspects of this technology shall be highlighted to allow a basic understanding of the process.
USAC is a tableting process that combines ultrasound (US) application with the simultaneous compaction of the material. Rodriguez et al. described an USAC machine especially for pharmaceutical usage in 1995 (Rodriguez et al., 1995).
Figure 1.1 gives a short overview of the process. There are two punches which are driven by pneumatic pistons. The material is inserted into the die and is compacted by the bottom punch which moves upwards. Piezoelectric material that is conjoined to a transducer

produces US waves via vibration. The US waves are amplified by an inserted booster and transferred onto the material through the upper punch; therefore, it is also referred to as sonotrode (Fini et al., 2002a,b). The frequency is set at 20 kHz. The starting point of US application can be set manually. In this work, the US energy application begins after a short period of precompaction of the material. Thus, a good transmission of US energy from sonotrode to the material was ensured. After the material has been poured into the Teflon® (PTFE)-lined die, the USAC process is started on the touch of a button. The process flow after start-up can be summarized as follows:

1. Lowering of sonotrode upon material; sealing of the die by applying chosen upper piston pressure
2. Lower punch moves upwards: precompaction of material while air is being pressed out of the die.
3. Further movement of lower punch upwards: compaction of material performed with a previously defined lower piston pressure
4. After a set time period, US application begins while compaction of material continues at constant pressure.
5. When the set US energy level is reached, the process is terminated; both punches stay in position.
6. Cooling time
7. Sonotrode is raised; lower punch moves back into its initial position.
8. The compact is ejected from the die by an upward movement of the lower punch.

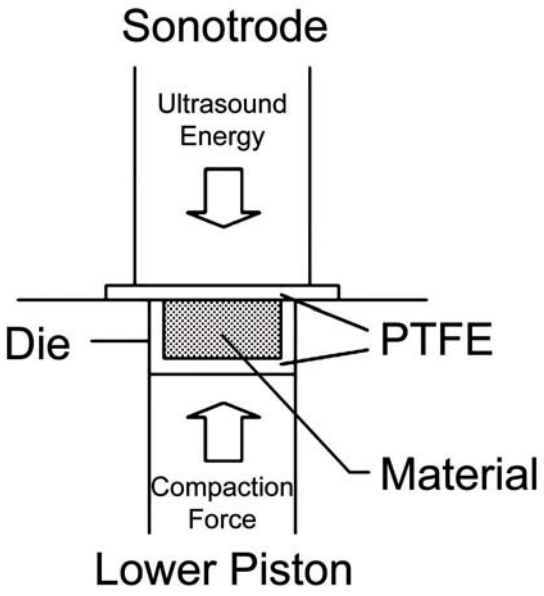


Figure 1.1: Schematic description of the USAC working principle

### 1.3.2 Effects of ultrasound-assisted compaction technique on the material

This section shall focus on the physical processes that are induced by USAC application and summarize the findings of the various publications that are available on this subject.
An overview of the effects generated by the application of US energy on solid material was given by Suslick et al. in 1987 and 1990: A particle size reduction is induced through an increase of interparticle collisions, the intercalation rate is increased, an aggregation of small-sized particles is induced, changes in the particles' surface morphology occur and local heating effects are observed (Suslick et al., 1987; Suslick and Doktycz, 1990).
The combination of pressure, heat and US as it occurs during USAC application leads to a formation of interparticulate bonds and the incorporation of the API into the thermoplastic polymer. Specific effects of US application in USAC are particle rearrangement and the supplying of energy for interparticulate bonding via partial melting and subsequent fusion of particles (Levina and Rubinstein, 2002), particle size reduction and transformation of the crystalline API into its amorphous state (Fini et al., 2009). An increase of mechanical strength of the compacts can be attributed to interparticulate bonding and leads to a decrease of the dissolution rate (Levina and Rubinstein, 2002).
USAC application was shown not to promote interactions between API and polymer on a molecular level (Sancin et al., 1999). Nevertheless, it was demonstrated that the drug is amorphized during the process and stabilized by the polymeric carrier, possibly due to an adsorption of the drug to the surface of the polymeric particles (Sancin et al., 1999).
Differences in viscosity of the material at elevated temperatures lead to an asymmetric drug distribution in the compacts (Fini et al., 2009).
Both the mechanical effects as well as the thermal effects of US application are essential for the outcome and the thermal effects were shown to predominate at higher US energies (Rodriguez et al., 1998). Hence, the properties of a USAC compact in comparison to a conventionally compacted tablet are dependent on the amount of US energy that has been delivered to the material.
Not only the amount of US energy delivered to the material, but also the moment of US energy input are crucial for the outcome (Levina and Rubinstein, 2000). As a result, the US energy is applied simultaneously with the compression force during this work.

### 1.3.3 Application of ultrasound-assisted compaction technique in the pharmaceutical sector

The literature available on the application of ultrasound for formulation development in the pharmaceutical sector is very limited. In 1993, a patent was filed by Gueret on the manufacture of so-called "pharmaceutical or cosmetic compacted powders" (Gueret, 1993). A mixture of thermoplastic (e.g. polyethylene and polyvinyl chloride) and non-thermoplastic ingredients (minerals and organic substances, for example zinc oxide and silk powder) was compacted under simultaneous US application with the aim to produce a compact with optimized solidity properties. It was demonstrated that if 5-80 % of thermoplastic material are

present in the mixture, a framework is formed which holds the non-thermoplastic material. The solid state properties were successfully optimized, resulting in a sufficiently friable but still firm compact.

Various research groups employed USAC for the manufacture of sustained- and immediate-release solid dosage forms which are shortly described in the following paragraphs.

Saettone et al. (1996) and Rodriguez et al. (1995) applied USAC for the preparation of a sustained release formulation of theophylline (30 %, 50 % or 75 % drug load), Eudragit® RL and Eudragit® RS with added talc (1 %) and magnesium stearate (1 %). The material was either conventionally compacted or US-compacted, whereby the former was only possible at drug loads of 30 %. It was shown that the preparation of sustained release formulations with high drug loads is possible via USAC, presumably due to the melting of the excipients and their subsequent coating of the API particles. Further details on the theophylline-Eudragit® RL formulation were published by Rodriguez et al. (1998).

Caraballo et al. (2000) and Millán and Caraballo (2006) investigated the effects of particle size on US-compacted tablets and their percolation threshold using potassium chloride as drug model and Eudragit® RS as polymeric carrier. It was observed that the results gained with USAC are less dependent on the particle size of the drug than the conventional compaction method. Also, it was shown that the excipient surrounds the drug resulting in a higher percolation threshold thus offering the possibility for the application of this technology for the manufacture of sustained-release formulations.

Levina and Rubinstein investigated the ultrasound-assisted compaction of ibuprofen and paracetamol with dibasic calcium phosphate dihydrate and microcrystalline cellulose (Levina and Rubinstein, 2000, 2002). It was demonstrated that the application of USAC increases tablet hardness and dissolution times of these formulations.

Ketoprofen and Eudragit® S-100 were subjected to USAC technology by Sancin et al. (1999) using drug loads of 25 %, 50 % and 75 % (w/w). A conversion of the API into its amorphous state was observed. Eudragit® S-100 reduced recrystallization of the drug. Furthermore, it was pointed out that neither changes of the hydrogen bonding of the drug nor the formation of drug-polymer associates are induced via US application. Although the authors made a suggestion on the application of USAC for solubility enhancement, it seems that this specific drug-polymer combination was not pursued further as no additional literature is available on this topic.

A high-energy US compaction was shown to improve the dissolution behavior of indomethacin as the ultrasound-compacted mixture of indomethacin and betadex ($\beta$-cyclodextrin) showed higher initial release rates than pure API, the physical mixture of the components and conventionally compacted mixture. Also, the total amount of dissolved API was improved. The reason for this dissolution enhancement is a transformation of indomethacin into its amorphous state. Furthermore, the molten API was found to form a coating on the $\beta$-cyclodextrin particles. However, similar results were obtained if the mixture was ground in a mortar (Fini et al., 1997).

If polyvinylpyrrolidone (PVP) or different kinds of PEG were employed as carriers, the dissolution rate of indomethacin was even further enhanced (Fini et al., 2002a,b). In comparison to co-evaporation as another method to manufacture solid dispersions, USAC was shown

to result in comparable dissolution profiles (Fini et al., 2002a). USAC was also employed for the formulation of ibuprofen-isomalt compacts (Fini et al., 2009). It was demonstrated that the distribution of the API in the compact is not homogeneous. Unfortunately, no dissolution studies were reported.

## 1.4 Hot-melt extrusion

### 1.4.1 Introduction

Hot-melt extrusion (HME) is the process of melting and mixing a blend of drug and carrier inside a heated barrel. The molten material is transferred through the barrel using one or two rotating screws and pressed through a die into a product of uniform shape and high density.
An extruder can be divided intro three main zones: the feeding zone, the compression zone and the metering zone (see Figure 1.2).

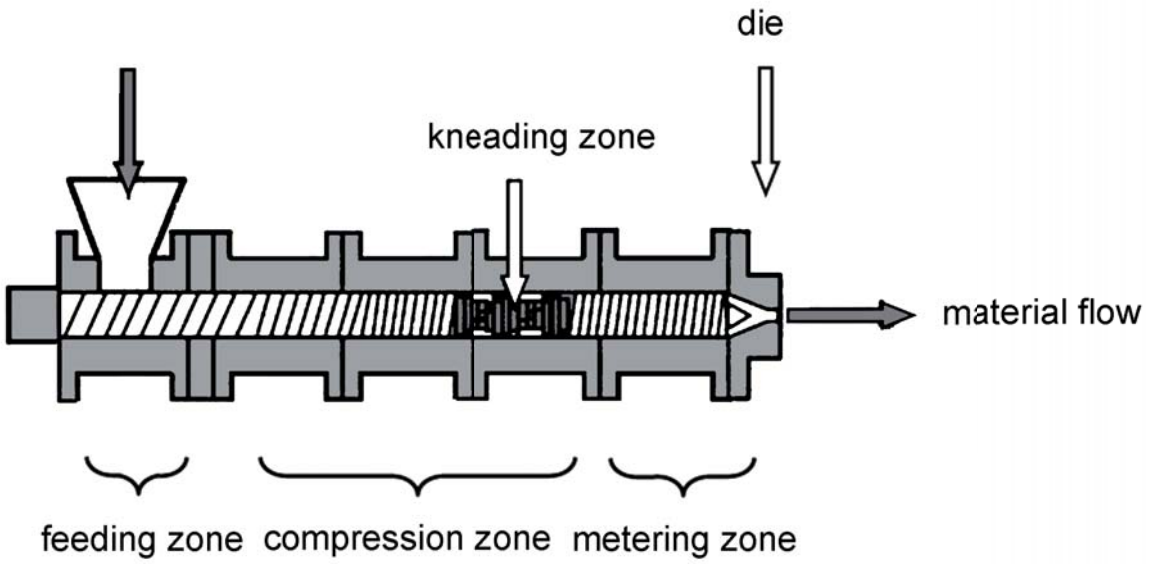


Figure 1.2: Schematic description of the HME working principle (reproduced with modifications from Nakamichi et al., 2002)

Solid material is inserted into the extruder through a feeding system. The material is gently mixed and transported to the compression zone by the conveying system which consists of one or two rotating screws. In the compression zone, the material is homogenized and compressed. Also, the main melting process takes place in this region. Kneading screw

elements may be applied to intensify the effects by an increase of shear energy introduced to the material. In the metering zone, the material is transported to the die. A build-up of pressure takes place in this section of the extruder. The main function of the metering zone is to reduce pulsating flow. Finally, the material is pressed out through the die. Downstream equipment may be connected to the system, for example, calendering, pelletizing or film-forming equipment may be used.
Coming from the plastics industry, HME was first used for pharmaceutical formulation in 1971 by El-Egakey et al. and refined in later years by various research groups (Breitenbach, 2002; El-Egakey et al., 1971; Repka et al., 2008). The advantages of HME in comparison to other solid dispersion manufacturing methods are the continuity of the process, its flexibility both in the instrument set-up and the settings of the process parameters and the wide variability of downstream equipment available. In addition, it overcomes the disadvantages of both the melting and the solvent method. Unlike the solvent method, it is a solvent-free process thus being environmentally friendly and economically efficient without the need for additional drying steps to facilitate solvent removal. In the early stages of pharmaceutical application of HME, especially the process temperatures and residence times were discussed as possible drawbacks of the technology. However, it was shown by various research groups that HME processing is even possible at lower temperatures through a modification of the extrusion equipment or through the addition of plasticizers to lower the glass transition temperature ($T_g$) thus reducing the required process temperatures (Repka and McGinity, 2000; Repka et al., 1999; Zhu et al., 2002).

### 1.4.2 Application of polymeric blends as carriers in hot-melt extrusion

The choice of the carrier plays an important role in solid dispersion formulation as the physicochemical characteristics of the carrier have a strong influence on the properties of the manufactured formulation. Various polymers have been applied in literature for hot-melt extruded formulations: PEG, PVP or sugar alcohols for immediate release and methacrylic acid copolymer (Eudragit® L 100; Evonik Roehm GmbH, Darmstadt, Germany) or ethylcellulose for sustained release solid dosage forms (Repka et al., 2008).
Crowley et al. used polyethylene oxide (PEO) for a sustained release formulation of chlorpheniramine maleate in 2002 (Crowley et al., 2002). Because of difficulties with the thermal stability of PEO, low molecular weight PEO was incorporated. Thus, the stability of the formulation was improved without significant changes to the release profile.
The application of polymeric blends as carriers offers the possibility to modulate the dissolution profile of a hot-melt extruded formulation (Coppens et al., 2006). Acetaminophen and nifedipine were used as APIs and hydroxypropyl methylcellulose (HPMC), PEO, ethylcellulose and blends of these as carriers.
Janssens et al. (2008) applied blends of PEG 6000 and HPMC as carriers for poorly water-soluble drug itraconazole. The dissolution behavior was successfully enhanced with all hot-melt extruded formulations containing the amorphous form of the drug, regardless of the carrier system. If a ternary blend of the API and excipients was used, a super-additive effect

on the dissolution profile was observed. The authors contributed this effect to the properties of PEG 6000 which is assumed to improve the wetting, inhibit recrystallization and act as a cosolvent for itraconazole.
Nollenberger et al. (2009a,b) added ethyl acrylate and methyl methacrylate copolymer dispersion (Eudragit® NE 30 D, Evonik Röhm GmbH, Darmstadt, Germany) to a mixture of aPMMA and felodipine (FD) thus stabilizing the supersaturation level of the extrudate reached in dissolution studies.
Blends of polymers were also applied as carrier for poorly water-soluble drug clotrimazole in HME (Prodduturi et al., 2007). It was pointed out that the characteristics of a hot-melt extruded film could be improved by adding another polymer with more favorable properties. In this particular case, the poor mechanical properties of a hydroxypropyl cellulose film were successfully modified through the addition of polyethylene oxide while maintaining the film's enhanced release properties.

## 1.5 Manufacture of solid dispersions using the applied drugs

### 1.5.1 Solid dispersions with fenofibrate

In the past, different methods were applied to improve the dissolution behavior and the bioavailability of fenofibrate (FF) preparations. Special emphasis was laid on developing a FF solid dosage form which may be applied independently from food uptake. Micronization (Munoz et al., 1994), stabilization of micronized FF through a coating process (Guichard et al., 2000), SMEDDS (Patel and Vavia, 2007) were all methods which were applied for optimization of FF formulations. More recently, solid dispersions were examined as another possibility to improve FF dissolution behavior. It was shown by various research groups that the solubility of FF may be enhanced via the manufacture of a solid dispersion (Sheu et al., 1994; Vogt et al., 2008). Various polymeric carriers were employed, for example copovidone (COP) and aPMMA (He et al., 2010), PVP and COP (Kanaujia et al., 2011) or polyvinyl caprolactam-polyvinyl acetate-polyethylene glycol graft copolymer (PVCL-PVAc-PEG) (Djuric and Kolter, 2010).

### 1.5.2 Solid dispersions with felodipine

Although solid dispersions of FD were successfully manufactured using various methods, for example the solvent method (Rumondor et al., 2009a,b), spin-coating method (Marsac et al., 2008) or spray-drying (Nollenberger et al., 2009b), only limited information is available on hot-melt extruded formulations with FD. The reason for this might be the documented thermal instability of FD when exposed to elevated temperatures (Marciniec and Ogrodowczyk, 2006). Nevertheless, mixtures of FD and aPMMA were successfully extruded at process temperatures of 160 °C (Nollenberger et al., 2009a; Qi et al., 2010). The dissolution rate was significantly improved with this formulation. Supersaturation stability was achieved with

the addition of 2.5-10 % of Eudragit® NE (Evonik Röhm Pharma Polymers, Darmstadt, Germany) (Nollenberger et al., 2009a).

### 1.5.3 Solid dispersions with oxeglitazar

Spray-freezing (Badens et al., 2009), co-evaporation and supercritical antisolvent (SAS) methods (Majerik et al., 2006, 2007; Majerik, 2006) were successfully employed for the manufacture of oxeglitazar (OX) solid dispersions. Drug loads of approximately 50 % (w/w) were applied. Depending on the manufacturing method and the polymeric carrier, different polymorphic forms of OX and different crystallinity indices of the samples were obtained. While the crystallinity index of solid dispersions manufactured using crystalline excipients was shown to be at approximately 60-100 %, formulations with amorphous excipients showed low degrees of crystallinity. If poloxamers 188 and 407, PEG 8000 and PVP K17 were used as polymeric excipients, the dissolution rate was improved with all of the mentioned manufacturing methods. Although the dissolution rate was reduced in dissolution medium pH 7.4 if Eudragit® E or RL were applied as polymeric carriers, it was improved in dissolution medium pH 1.2 which can be attributed to the solubility of the applied substances in these media (Majerik, 2006). Additionally, solution enhanced dispersions (SEDS) were manufactured using supercritical fluids (Majerik, 2006). No dissolution results are reported with SEDS.

# 2 Outline and aims of this work

The key objective of this work was to utilize USAC and HME for solubility enhancement of poorly water-soluble APIs.
The present work is therefore divided into three main areas of research:

1. USAC was investigated for its feasibility in solid dispersion manufacture. A main focus was to evaluate the applicability of USAC machine Sonica Lab (IMA, Bologna, Italy) in general and its suitability for dissolution enhancement (see Section 3.1). Specific aims of the part of this work which is dealing with USAC technology were:

- Application of USAC for solubility enhancement of poorly water-soluble model drug FF
- Assessment of this technology's potential for solid dispersion formation using a broad spectrum of polymeric carriers
- Examination of the dissolution performance of each formulation and a comparison of these to the untreated physical mixtures of the components and pure API powder
- Investigation of the effects of process parameters on the product
- Verification of the reproducibility of results to assess process robustness
- Evaluation of the equipment to allow the assessment of the technology's feasibility for a routine application in formulation development

2. HME was applied with the intention to manufacture solid dispersions with an improved dissolution performance. The aim was to further optimize the release performance and storage stability of the formulations. The examination of HME technology is covered in Sections 3.2-3.4 and 3.5.2 of this work. A focus was laid on the investigation of the possibilities of polymeric blends if applied as carriers. Key objectives can be summarized as follows:

- Manufacture of FF-polymer extrudates to serve as a comparison to the USAC compacts
- Application of various polymers and blends of these as carriers with the aim to enhance the solubility of the embedded poorly water-soluble APIs FF, OX and FD
- Elucidation of the influence of polymeric additives on the dissolution profile of the extrudates
- Development of extrudates with a sufficient storage stability regarding their dissolution behavior and crystallinity
- Examination of the transferability of the results from FF to the other poorly water-soluble drugs

3. A comparison of the results from HME experiments to the results that were gained with USAC technology was performed as HME is a technique for the manufacture of solid dispersions which is somewhat more established in the pharmaceutical sector. The juxtaposition of the two applied technologies and a comparison of the results to the untreated physical mixtures and marketed solid dosage forms is performed in Sections 3.5.3 - 3.5.5. Furthermore, the results are compared to other available technologies for the manufacture of solid dispersions (see Section 3.5.6).

# 3 Results and discussion

## 3.1 Ultrasound-assisted compaction technique

### 3.1.1 Introduction and objectives

USAC was introduced as a novel technique for the compaction of plastic powders by Paul and Crawford in 1981 who also described the main effects of the US application on the material. The compaction technique with ultrasonic assistance is reported to be suitable for thermoplastic materials as it promotes the fusion of the particles through local heat effects. It is especially feasible for materials with small particle sizes and if an improvement of the compact's tensile strength is desired.

In the pharmaceutical sector, only limited literature is available on this topic. USAC has been used to improve tablet hardness (Gueret, 1993) and consequently prolong the dissolution times of, for example, theophylline-Eudragit® RL and RS compacts (Rodriguez et al., 1995; Saettone et al., 1996). The technology was found to improve the dissolution profile of poorly water-soluble drugs (Fini et al., 1997, 2002a). It was postulated that a solid dispersion of the drug in the carrier is formed with indomethacin being molecularly dispersed inside PVP. The conversion of the drug into its amorphous state via USAC technique was confirmed for Ketoprofen-Eudragit® S100 mixtures. However, no evidence was found for the formation of a solid solution (Sancin et al., 1999).

The aim of this work was to investigate USAC technology in general and to verify its potential for the manufacture of solid dispersions. An evaluation of the ultrasound-assisted compaction machine Sonica Lab by IMA (Bologna, Italy) and its feasibility for dissolution behavior enhancement of poorly soluble drugs was performed.
The specific aims of this work were chosen as follows:

- Evaluation of the technology's potential for solid dispersion formation
- Investigation of the technique's feasibility for dissolution enhancement of a poorly water soluble drug
- Examination of the suitability for a broad spectrum of compounds
- Determination of crucial process parameters and the assessment of the effects of variable process parameters on the outcome
- Evaluation of the reproducibility of results and process robustness

### 3.1.2 Developing a design of experiments

The main focus of these preliminary experiments was on the characterization of the effect of variable process parameters on the outcome, and on the identification of crucial process parameters. It was an aim of this work to employ a statistical design of experiments to provide meaningful information about the USAC process and to allow for an assessment of the technology.
In the first step, influential process parameters and suitable responses were defined.

The process parameters of USAC machine Sonica Lab KU1003 that may be set by the user are: Duration or intensity of US energy, pressure of lower and upper piston, sonotrode position, die depth, compaction threshold, detachment time and cooling time.
As no active cooling is performed, the cooling time is not considered to be a determining factor. It was kept constant at 6 s throughout the trials. The same applies for the detachment time which was kept constant at 1 s.
The compaction threshold defines the pressure of the lower piston at which the US application begins. During the precompaction of the material, air is removed out of the die thus ensuring a good transmission of the US energy. The chosen setting for all experiments was 10 kg. The measurement unit differs from the usually applied SI unit for pressure: ($Pa = N/m^2 = kg/ms^2$). Hence, it is assumed that the setting "10 kg" is derived from the applied force per die area.
The die depth defines the volume of the compaction chamber and thus the amount of material applied. It was decided to leave this parameter constant at 10 mm for all trials. The sonotrode position is crucial to allow for an optimal energy transfer and sealing of the die. It is independent of the material applied and was thus not changed by the user but monitored during the experiments. The setting of the upper piston's pressure is also relevant for the US energy transfer and the sealing of the die. The importance of an optimal setting and timepoint of the application of US energy and compaction pressure is reported in literature (Rodriguez et al., 1998; Levina and Rubinstein, 2000). Thus, the intensity of US energy, the pressure of the lower and the pressure of the upper piston were defined as determining factors.

In the pharmaceutical field, any undesired variation of material characteristics affecting the quality of the product has to be avoided or minimized to guarantee a reproducibility of drug product performance.
Powdery areas on the compact's surface indicate an incomplete transition of material into its (semi-)liquid state. In that case, the applied US energy did not suffice for a complete softening or melting of the polymeric carrier or the drug. Therefore, the appearance of the compacts' surface area was set as response and monitored.
In preliminary trials, leakage of the material out of the die upon its liquefaction was observed due to an insufficient sealing of the die by the sonotrode. It has to be reduced to ensure a maximum yield and a consistent drug to polymer ratio. Thus, the amount of material leaked out of the die was defined as a response.

The formation of bubbles and the occurrence of degradation effects were also set as responses as these parameters describe undesired changes to the compacted material. The evaluation of the responses was performed on a scale from 1 to 6 where one is very good. The rating according to the assessment scale is specified in Tables 6.8 and 6.9 (pp. 117-118 of this work).

Additionally, the in-process monitoring tool Sonica View Software which is integrated into the controlling device of Sonica Lab may be used for the evaluation of the compaction process. It was not included into the statistical design of experiments as the meaning of the curve progression is not yet fully understood.
Figure 3.1 shows the in-process monitoring data curves of an aPMMA compact.

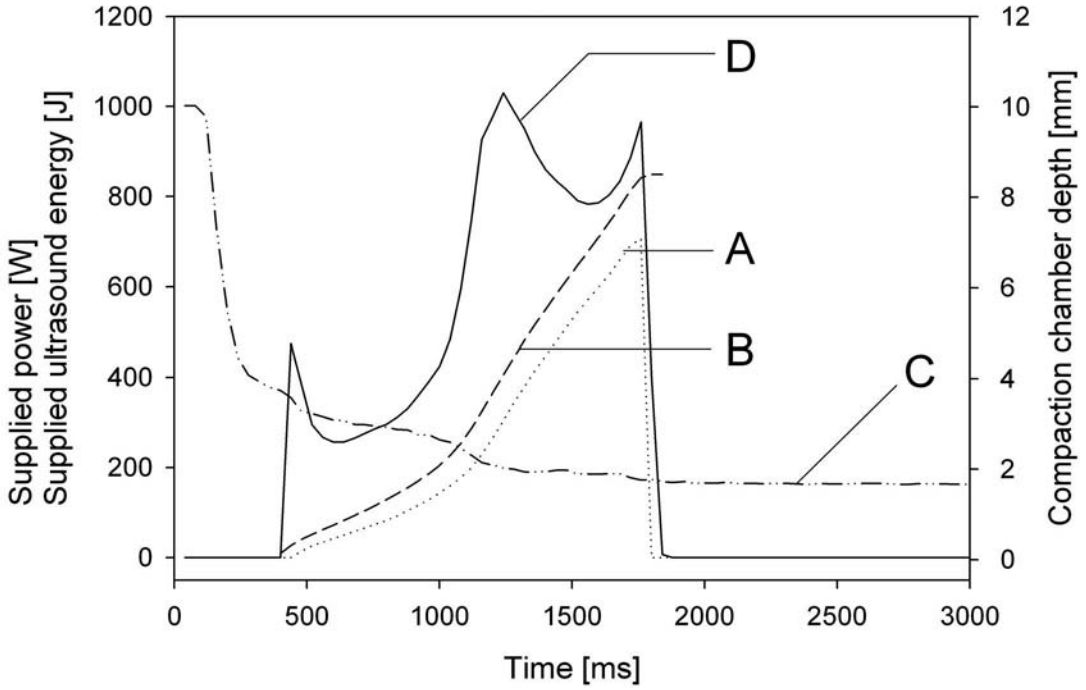


Figure 3.1: In-process monitoring of USAC process parameters with aPMMA as model substance: A) supplied US energy as calculated by Sonica Lab, B) recalculated supplied US energy, C) compaction chamber depth as measured by Sonica Lab, D) supplied power as measured by Sonica Lab. Set parameters: US energy: 700 J, pressure upper piston: 6.5 bar, pressure lower piston: 7 bar. Amount of material: 1.00 g, absolute distance sonotrode to die: 16.08 mm.

As an explanation, US energy itself is not being measured during the process. Instead, it is calculated by Sonica Lab as the time integral of the total electrical power which is delivered to the converter of the sonotrode up to a specific time (Figure 3.1 curve A). To verify these computations, a recalculation of the data was performed by manual integration (Figure 3.1 curve B). Figure 3.1 shows that the two computations are not eqivalent. This is either due to imprecise calculations of Sonica Lab or due to inaccurate data sets which are made available to the user.

During the first 300 ms, a massive decline of the compaction chamber depth (Figure 3.1 curve C) is visible which can be associated with the precompaction of the material. During precompaction, the material in the die is still able to rearrange and the air from inter-particulate spaces is pushed out of the die. With further upward movement of the lower punch, the reduction of the compaction chamber depth slows down until it reaches a constant level. At this point, no further compression of the material is possible. A correlation of compaction chamber depth (Figure 3.1 curve C) and supplied power (curve D) was observed as the power peaks and sudden decreases of the compaction chamber depth occur simultaneously. The progression of these curves was found to be associated with changes in the material characteristics:

**0-500 ms** Densification of the material by compaction alone

**500 ms** Effects of the beginning of the US application, for example an increase in particle movements

**1100-1300 ms** Transition of the material into its molten state

**1500 ms** Maximal compression of the material

**1700 ms** Effects resulting from the prolonged US application, for example leakage, gas development, degradation

Consequently, these curves have to be closely monitored during the optimization of the process to avoid undesirable effects to the material, such as degradation.

Central point settings were determined by trial and error for each substance or blend of materials. A factorial design $N = 2^3$ with a minimum of 6 central point repetitions was employed. The settings of the design of experiments are described in Section 6.2.1.2. Optimized runs were determined with statistical evaluation software Modde.

### 3.1.3 Ultrasound-assisted compaction of pure polymers

To allow for a meaningful screening, multiple polymers with differing physicochemical properties were chosen as carriers. Because the knowledge on the application of USAC is limited, polymeric carriers were used which were already successfully employed in solid dispersion manufacture and have proven to be suitable for the solubility enhancement of poorly water-soluble drugs: COP, HPMC, aPMMA and PVCL-PVAc-PEG (Leuner and Dressman, 2000; Hardung et al., 2010). Polyvinyl alcohol-acrylic acid-methyl methacrylate copolymer (PVA-AA-MMA) was also employed as an excipient because its potential for dissolution enhancement of nifedipine via USAC was reported to be superior to other polymeric carriers, including HPMC, PVP and polyvinyl alcohol (Uramatsu et al., 2007).

Exemplary results which were received when applying the optimal settings as determined by Modde software are summarized in Table 3.1.

Table 3.1: Optimized runs for the US-assisted compaction of single polymers

| | aPMMA | HPMC | PVA-AA-MMA | PVCL-PVAc-PEG |
|---|---|---|---|---|
| | 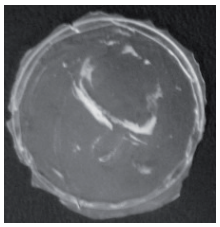 | 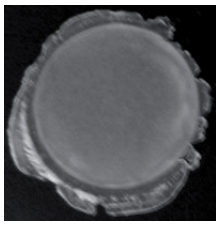 | 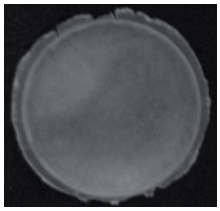 | 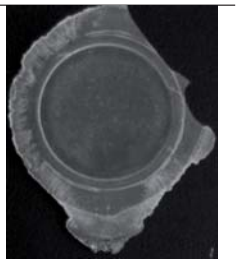 |
| Supplied US energy [J] | 707 | 1218 | 861 | 1061 |
| Pressure lower piston [bar] | 7.0 | 6.9 | 7.0 | 6.0 |
| Pressure upper piston [bar] | 6.6 | 6.1 | 6.6 | 6.0 |
| Sample weight [g] | 0.9972 | 1.4961 | 1.4979 | 1.4985 |
| Absolute distance sonotrode to die | | 16.08 | | |
| Responses | | | | |
| Surface | 3 | 2 | 2 | 2 |
| Leakage | 4 | 3 | 2 | 5 |
| Bubbles | 2 | 1 | 1 | 1 |
| Degradation | 1 | 1 | 1 | 1 |

Each polymer was observed to behave differently under USAC application.
aPMMA showed residual powder agglomerates within the compacts at any setting. Discoloration and bubble formation were avoided with the optimized settings.
With HPMC, discoloration and degradation effects were very pronounced. Even at very low energy and pressure levels resulting in compacts with a high amount of residual powder, degradation was observed. This indicates the formation of hot spots inside the die which are promoted by an inhomogeneous US energy distribution.
Discoloration at high US energy levels was also observed with PVA-AA-MMA.
No degradation was observed with PVCL-PVAc-PEG. Although all of the compacts showed some leakage, PVCL-PVAc-PEG and COP exhibited a very high amount of material leakage. Especially at high US energy levels and high lower piston pressures, the US assisted compaction of COP was automatically aborted due to an excessive amount of leakage (compact thickness $<0.5\,\mathrm{mm}$). For this reason, the design of experiments could not be completed with COP and no optimized parameters were determined. Furthermore, the handling of the COP compacts proved to be difficult due to the brittleness and stickiness of the material.
The desired outcome of 1-1-1-1 (surface-leakage-bubbles-degradation; see Section 6.2.1.2 for specifications on the rating) was not obtained with any of the polymers or applied settings.

No sweet spots were detected by the evaluation software.
Nevertheless, an important understanding of the factors' interplay was gained through these experiments. The effects of the factors US energy, pressure of the lower and pressure of the upper piston on the responses are summarized in Table 3.2.

Table 3.2: Effects of factor variations on responses when increased: +) low, ++) medium, +++) high improvement; -) low, - -) medium, - - -) high worsening of the rating. A reduction of the factor settings results in a response change into the opposite direction.

| Responses \ Factors | Ultrasound energy | Pressure lower piston | Pressure upper piston |
|---|---|---|---|
| Surface | +++ | +++ | + |
| Leakage | - - - | - - - | ++ |
| Bubbles | - - - | - - | - - |
| Degradation | - - - | - - | - - |

An increase of US energy promotes particle movement, leading to a higher rate of particle collisions. The melting of the material is induced. The formation, growth and subsequent collapse of bubbles is promoted (Doktycz and Suslick, 1990). Material leakage was also shown to be induced by an increase of US energy or time (Levina and Rubinstein, 2002).
The factors pressure lower piston and US energy were shown to be dependent on each other: If the material is tightly compressed (high pressure of the lower punch), the effect of US application is increased as particle collisions are facilitated. The interparticulate contact and the contact of the particles to the sonotrode are reduced if the pressure of the lower piston is decreased, leading to less particle-particle interactions and an insufficient US energy transmission to the material. A higher pressure of the lower piston results in an increase of leakage as the punch pushes the molten material out of the die.
If the pressure of the upper piston is increased, it was shown to result in a better sealing of the die (reduction of leakage) and a better US energy transmission.
The effect of the piston pressures on bubble formation and degradation was not as pronounced as with US energy. The conclusion has to be drawn that the desired outcome of 1-1-1-1 (surface-leakage-bubbles-degradation) cannot be reached as the responses are affected in the opposite direction by a variation of the factor settings.

In summary, the preliminary trials using five polymers with different physicochemical characteristics did not succeed in the determination of ideal process settings. A basic understanding of the effects of the influential parameters was gained from these trials.

### 3.1.4 Reproducibility of results

The design of experiments that was employed in Section 3.1.3 was also used to assess the system's reproducibility of results. The central point settings were repeated six times. Exemplary results from the trials using HPMC are depicted in Tables 3.3 and 3.4.
The settings were 1350 J for US energy and 6 bar for both lower and upper piston pressure. The amount of material used was 1.5 g accurately weighed. The sonotrode to die distance was set to 16.08 for all trials.
Tables 3.3 and 3.4 show HPMC compacts which were manufactured using the same setting. The observed degrees of degradation and leakage vary from compact to compact. Tables 3.3 and 3.4 show that the compaction time and sonotrode height values of the trials 1-6 differ without any intervention of the user. If the same amount of US energy is delivered over a varying period of time, the results will undoubtedly differ. Temperature differences within the die which might result from a change in the compaction time, for example, are assumed to induce different degrees of degradation. Accordingly, the responses leakage, bubble formation and degradation were worsened with decreasing compaction times. Unfortunately, no temperature sensors were available to monitor the temperatures prevailing in the die during the compaction process to confirm this hypothesis.
Additionally, the user does not have a sufficient control over the setting of the sonotrode to die distance. Although its setting was not changed throughout the trials, variations of the sonotrode/die distance were observed. It was shown in preliminary trials, that even small variations have a tremendous effects on the outcome (0.01 mm). As this very sensitive parameter is adjusted manually, the exact alignment of the sonotrode is very challenging.

Table 3.3: Evaluation of the reproducibility of results using central point settings for HPMC (Part 1)

| | 1 | 2 | 3 |
|---|---|---|---|
| | 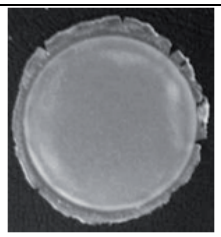 | 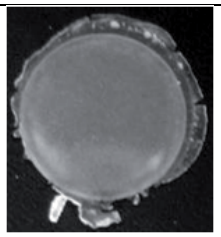 | 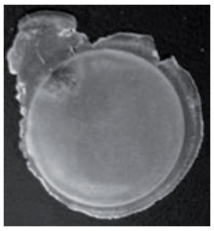 |
| Compaction time [s] | 5.20 | 4.67 | 4.34 |
| Supplied US energy [J] | 1357 | 1356 | 1356 |
| Sonotrode height [mm] | 0.31 | 0.33 | 0.35 |
| Sample weight [g] | 1.4964 | 1.4953 | 1.4944 |
| Responses | | | |
| Surface | 2 | 2 | 2 |
| Leakage | 3 | 3 | 4 |
| Bubbles | 1 | 3 | 3 |
| Degradation | 1 | 2 | 3 |

Table 3.4: Evaluation of the reproducibility of results using central point settings for HPMC (Part 2)

| | 4 | 5 | 6 |
|---|---|---|---|
| | 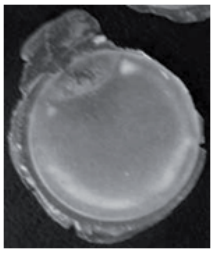 | 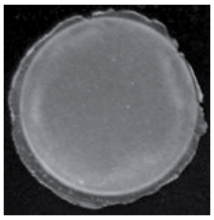 | 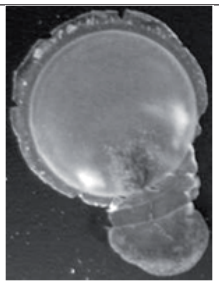 |
| Compaction time [s] | 4.78 | 5.08 | 4.22 |
| Supplied US energy [J] | 1355 | 1353 | 1353 |
| Sonotrode height [mm] | 0.36 | 0.36 | 0.36 |
| Sample weight [g] | 1.4939 | 1.4962 | 1.4906 |
| Responses | | | |
| Surface | 3 | 2 | 3 |
| Leakage | 3 | 3 | 5 |
| Bubbles | 3 | 1 | 4 |
| Degradation | 3 | 1 | 4 |

USAC results of two batches of HPMC with a different particle morphology were compared to allow for an evaluation of the batch to batch variability of the process. While batch 1 consisted mostly of equant particles (approx. 3-5 µm), the particles of batch 2 were columnar and approximately 5-10 µm in size. As the die depth was fixed, a lower amount of material had to be used for batch 2 due to its lower bulk density. Table 3.5 shows that different settings had to be applied to manufacture compacts with a similar appearance.

Table 3.5: Assessment of the batch to batch variability of the USAC process using two different batches of HPMC

| | Batch 1 | Batch 2 | |
|---|---|---|---|
| | 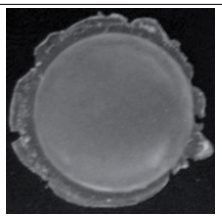 | 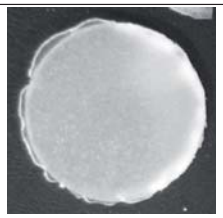 | 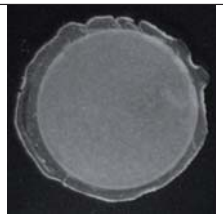 |
| Sample weight [g] | 1.4984 | 1.2527 | 1.2497 |
| Supplied US energy [J] | 1248 | 1251 | 1510 |
| Pressure lower piston [bar] | 7.0 | 7.0 | 7.0 |
| Pressure upper piston [bar] | 7.0 | 7.0 | 7.0 |
| Absolute distance sonotrode to die | 16.08 | 16.08 | 16.08 |

Although a lower amount of material is used for batch 2 compacts, the US energy has to be increased to produce a compact which is similar to the batch 1 compact shown in Table 3.5. This is in accordance to the observation made by Paul and Crawford (1981): The smaller the particles, the better the interparticulate heat transfer. Consequently, lower US energies suffice for a complete melting of the material consisting of smaller, equant particles as in HPMC batch 1.

Overall, the reproducibility of results using USAC machine Sonica Lab KU1003 in its current state is inadequate as the process is very sensitive to parameters which cannot be influenced by the user.

### 3.1.5 Ultrasound-assisted compaction of fenofibrate and various polymeric carriers

The system's robustness was shown to be insufficient for a routine application in the pharmaceutical sector. Nevertheless, the transition of a single polymer into its molten state was successful. To verify the process' potential for the manufacture of solid dispersions as it is suggested in literature, blends of a poorly water-soluble model drug and polymeric excipients were compacted using USAC technique (see Table 3.6 for the composition of FF-carrier mixtures) (Fini et al., 2009).

Table 3.6: Composition of ultrasound compacted fenofibrate (FF)-polymer blends. All data are given in weighted parts unless otherwise specified.

| Formulation | FF | COP | HPMC | PVCL-PVAc-PEG | aPMMA | PVA-AA-MMA | drug load [%] |
|---|---|---|---|---|---|---|---|
| US-A | 1 | 3 | - | - | - | - | |
| US-B | 1 | - | 3 | - | - | - | |
| US-C | 1 | - | - | 3 | - | - | 25.0 |
| US-D | 1 | - | - | - | 3 | - | |
| US-E | 1 | - | - | - | - | 3 | |

Differential scanning calorimetry (DSC) analysis was used to determine the solid state of the drug and the polymer after US-assisted compaction. The dissolution behavior of the compacts was investigated to enlighten the technology's feasibility for dissolution enhancement. FF was chosen as a model poorly water-soluble drug because its dissolution enhancement via pharmaceutical formulation using numerous manufacturing methods is well documented in literature (He et al., 2010; Sheu et al., 1994; Srinarong et al., 2009).
Blends of FF with aPMMA, COP, HPMC, PVA-AA-MMA or PVCL-PVAc-PEG with a drug load of 25 % were compacted using USAC technique as described in Section 6.2.1.3. A design of experiments was employed to identify optimal process settings for each mixture. Results are shown in Table 3.7.

Table 3.7: Optimized runs for the US-assisted compaction of FF-polymer blends using a drug load of 25 %

| | US-A | US-B | US-C | US-D | US-E |
|---|---|---|---|---|---|
| | 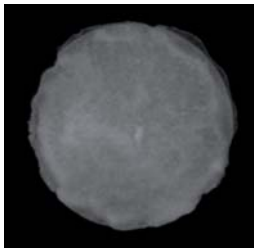 | 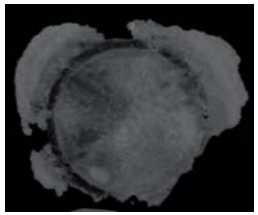 |  | 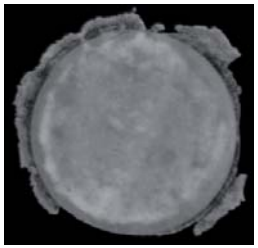 | 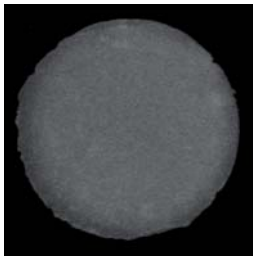 |
| Supplied US energy [J] | 282 | 787 | 772 | 248 | 416 |
| Pressure lower piston [bar] | 7.1 | 5.7 | 5.0 | 7.0 | 7.8 |
| Pressure upper piston [bar] | 7.2 | 6.3 | 5.0 | 8.0 | 8.0 |
| Sample weight [g] | 0.8260 | 1.2444 | 1.4996 | 0.9999 | 1.4965 |
| Absolute distance sonotrode to die | 16.08 | 16.08 | 16.08 | 16.08 | 16.08 |
| Responses | | | | | |
| Surface | 3 | 3 | 3 | 3 | 2 |
| Leakage | 2 | 4 | 4 | 3 | 1 |
| Bubbles | 1 | 1 | 1 | 1 | 1 |
| Degradation | 1 | 1 | 1 | 1 | 1 |

The optimization of the responses bubble formation and degradation effects was successful. As the responses surface appearance and amount of leakage are affected in the opposite direction by a variation of the factors US energy and pressure of the lower piston (see Table 3.2), no parameters resulting in an optimal outcome could be defined. When comparing the FF-polymer compacts to those manufactured using single polymers (see Tables 3.1 and 3.7), the compacts with the incorporated API were found to be neither transparent nor homogeneous in their appearance. This indicates an incomplete transition of the material into the molten state.
DSC results confirm this finding: In all DSC thermograms of USAC compacts, a melting peak of FF (melting point ($T_m$)=83.2 °C) remains visible in the first heating cycle (see Figure 3.2).

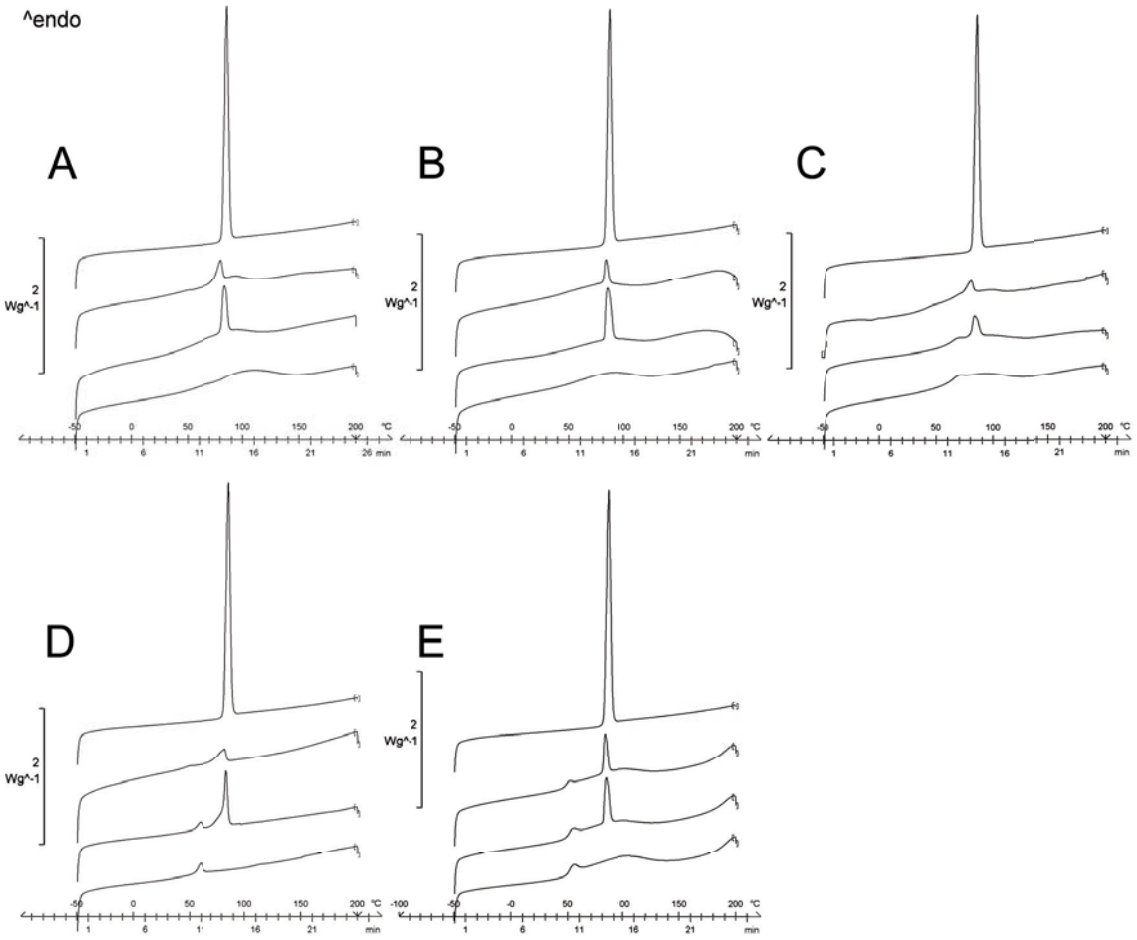


Figure 3.2: DSC thermograms of milled USAC compacts A) US-A (FF+COP), B) US-B (FF+HPMC), C) US-C (FF+PVCL-PVAc-PEG), D) US-D (FF+aPMMA), E) US-E (FF+PVA-AA-MMA; all consisting of 1+3 weighted parts of API and polymer) showing from top to bottom: pure FF, milled compact, physical mixture of the components, pure carrier

When compared to the DSC thermogram of the respective physical mixture, the amount of crystalline material is reduced as the melting peak area decreases, indicating a partial conversion of the API into its amorphous state or a partial dissolving of the API in the polymer matrix. The area under the curve of the respective thermograms was not calculated as the melting peak of FF is partially overlayed by the evaporation of water, thus falsifying the computations. Even so, US energy was shown to promote a transition of crystalline material into its amorphous state. At the same time, it was pointed out that it is not sufficient enough for a complete amorphisation of the crystalline drug substance. Due to the inhomogenic appearance of the compact it is assumed that clusters of the amorphous or crystalline drug in the polymeric carrier are present. Differences in the distribution of API and carrier in US-compacts were pointed out by Fini et al. (2009), who used Raman microscopy for the assessment. It was postulated that a low melting point of the drug results in its flowing down in between the yet unmolten carrier particles once liquefied. In the present case, an inhomogeneous appearance was found with all formulations regardless whether the melting point of FF is lower or higher than the $T_g$ of the carrier ($T_g$COP=104.9 °C, $T_g$HPMC=176.2 °C, $T_g$PVCL-PVAc-PEG=70 °C, $T_g$aPMMA=50.5 °C, $T_g$PVA-AA-MMA=69.2 °C). It has to be assumed that an asymmetric distribution of the US energy within the die is the reason for the observed effects.

The initial release from USAC compacts was improved in comparison to pure FF powder (see Figure 3.3).

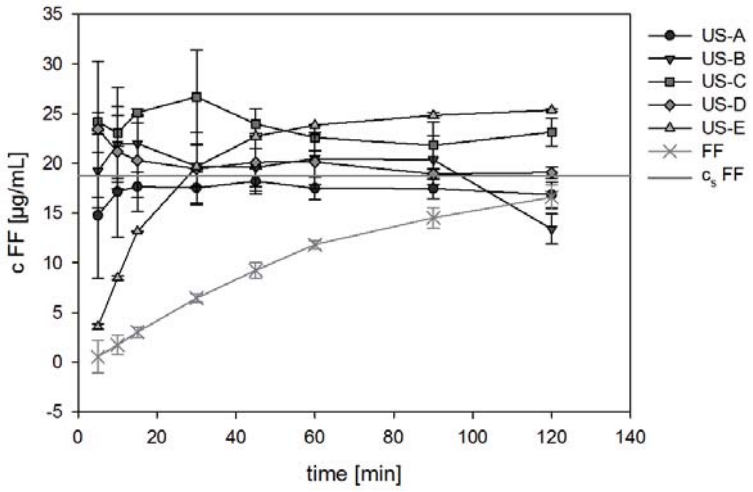


Figure 3.3: Dissolution profiles of milled USAC compacts US-A (FF+COP), US-B (FF+HPMC), US-C (FF+PVCL-PVAc-PEG), US-D (FF+aPMMA) and US-E (FF+PVA-AA-MMA; all consisting of 1+3 weighted parts of API and polymer) in comparison to pure FF powder

In comparison to pure FF after 5 min of dissolution, the released amount of API from USAC compacts was 51 times higher for formulation US-C, 47 times higher for US-D, 40 and 37 times higher for US-A and US-B compacts, respectively. The dissolved amount of FF re-

mained constantly 1 to 1.5 times above $c_s$ level for US-A - US-D compacts throughout the investigated dissolution time of 120 min. Initial release from US-E compacts was 1.5 times higher in comparison to pure FF, which is below the performance of the other US-compacted formulations and below $c_s$. After 45 min, the dissolved amount of FF from US-E compacts was equal to and after 2 h 1.2 to 1.3 times higher than with US-A - US-D.
In conclusion, the initial release rate of FF was improved by the application of USAC technology in comparison to the dissolution profile of untreated FF powder.

### 3.1.6 Effect of the polymer on the dissolution profile

To verify whether the observed enhancement of dissolution behavior (see Section 3.1.5) can be directly related to effects resulting from USAC compaction, the dissolution results of US-compacted tablets were compared to solubility studies conducted with pure FF and the respective polymeric carrier added to the dissolution medium. As can be seen in Figure 3.4, after 30 min the release from all samples but of FF with added aPMMA and of FF without additives is above saturation concentration and remains constant for 48 h.

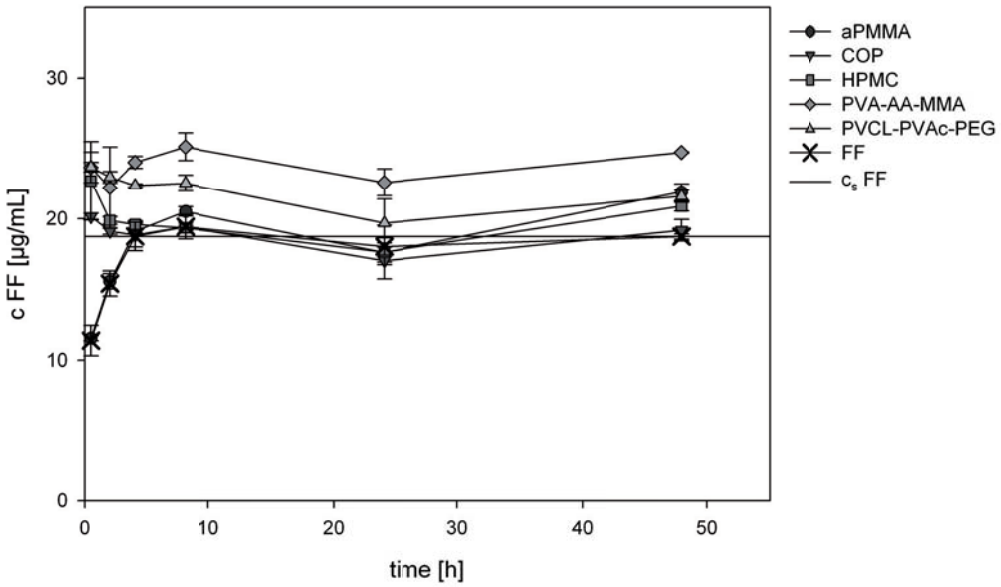


Figure 3.4: Dissolution profile of FF where the polymer was added directly to the dissolution medium

After 4 h, the release in aPMMA medium reaches the same level. The plateau values are 1.1 times above FF saturation concentration in dissolution medium with added aPMMA and HPMC, 1.2 times for PVCL-PVAc-PEG and 1.3 times for PVA-AA-MMA. The plateau values for FF in dissolution medium with added COP are equal to the release in dissolution medium without additives.

In summary, the presence of COP, HPMC, PVA-AA-MMA and PVCL-PVAc-PEG in the dissolution medium improves the initial dissolution rate of FF. The addition of aPMMA does not enhance the dissolution behavior of FF.
In comparison to the dissolution profiles of the USAC compacts, the differences of initial dissolution rate and $c_{max}$ of dissolved API are not profound for all samples but formulation US-D. In this case, USAC compaction resulted in an improvement of the initial release rate. This effect is contributed to a higher concentration of the polymer in the diffusion layer surrounding the compact leading to an intense solubilization effect by aPMMA on FF which results in an enhanced API release (Chiou and Riegelman, 1971). It can be concluded that for an enhancement of API dissolution, a sufficient concentration of aPMMA in the dissolution layer has to be ensured. For the dissolution profile enhancement that was achieved using USAC machine Sonica Lab for formulations US-A to -C and -E, even very low concentrations of the polymers in the dissolution medium are sufficient to gain similar results. Hence, it was pointed out that the impact of USAC on the dissolution behavior is negligible.

### 3.1.7 Evaluation of the equipment

The handling of the USAC machine and the setting of process parameters have proven to be challenging. For example, the compaction time and rate of US energy delivery cannot be controlled by the user. Both of these parameters have been identified to be crucial for the outcome. The distance between the sonotrode and die was pointed out to be a very sensitive parameter which is difficult to control.
The USAC machine Sonica Lab KU1003 in its present state is not only lacking sufficient user control, but also adequate process monitoring tools. For example, no monitoring of the temperatures reached in the die is possible which would be especially important for heat-sensitive materials. Additionally, the impression was raised that the computations of the supplied in-process monitoring software Sonica View lack accuracy as these values were shown to differ from re-calculations which were performed in the course of this study.
PTFE sheets were used to cover the die to prevent a direct contact of the material to the sonotrode and to improve the sealing of the die. A PTFE lining is employed to prevent the material from sticking to the die and to diminish temperature effects in critical areas of the compact. This procedure is recommended by the manufacturer and is very important for the process but it is clearly another drawback of the technology: As the PTFE sheets have to be shaped manually to fit the die using additional equipment (Teflon moulder KU1003, IMA, Bologna, Italy), the preparation of experiments is a time consuming step. For an intense application of the machine in formulation development, improvements to avoid the usage of these PTFE sheets are mandatory, for example by providing a die which is made out of a different material or which has a durable PTFE coating on its surface.
Various pharmaceutical excipients with or without the addition of an API were compacted using USAC technology. It was observed, that different process settings are required for each formulation. A statistical design of experiments was employed to identify optimal process parameters. Unfortunately, no optimal outcome was achieved with any of the recommended

settings and materials as the determining factors affect the responses in the opposite direction. With this technology, a compromise between the loss of substance through leakage, impairment of the product through degradation effects and an incomplete transition of the material into its amorphous state has to be made.

Considering all these points, the poor reproducibility of results that was observed in this work had to be expected. It was shown that this technology is offering the possibility of embedding drug into polymeric matrices as it induces a transition of the API and carrier into their (semi-)liquid state with a subsequent re-solidification of the material. An enhancement of dissolution behavior through US application could not be confirmed. The immediate release of FF from USAC compacts was reproduced with pure FF powder by adding the polymeric carrier directly to the dissolution medium.
Due to the observed drawbacks of the technology, for example insufficient user control of the process and a lack of reproducibility, it had to be concluded that USAC technology in its current state is not suitable for the manufacture of solid dispersions in the pharmaceutical sector. Unless significant improvements are made to USAC machine Sonica Lab KU1003, other methods for solubility enhancement have to be preferred.

## 3.2 Solubility enhancement of fenofibrate via hot-melt extrusion

### 3.2.1 Introduction and objectives

In the first part of this work, USAC was applied for dissolution enhancement of poorly water-soluble drug FF. The improvements of the dissolution profile were associated with the presence of the polymeric carriers. If the polymer was added directly to the dissolution medium, similar results were obtained with the untreated API as with the USAC compacts. DSC analysis of the physical mixtures confirmed the compatibility of FF and the applied polymers as a glassy solution was formed in all cases. Crystalline FF was detected in all USAC samples showing that the manufacture of a glassy solution of the components using USAC was not successful (see Section 3.1).
In order to explore whether HME technology is more suitable for the manufacture of solid dispersions, FF-polymer blends of the same composition as previously in USAC trials were extruded and their dissolution behavior and solid state properties were assessed.

Accordingly, FF was hot-melt extruded with single polymeric carriers COP, HPMC, PVCL-PVAc-PEG, aPMMA and PVA-AA-MMA using a drug load of 25 % (w/w).
Solid dispersions of FF and COP have been manufactured using HME by He et al. (2010) and Kanaujia et al. (2011). With all formulations, the solubility enhancement of FF was successful. Recrystallization of the drug during storage was observed as well as a drop of the release profile of the extrudates (Kanaujia et al., 2011). Therefore, special emphasis of the present work was laid on the stability testing of the extrudates.
He et al. (2010) applied aPMMA as carrier for FF to manufacture solid dispersions with an improved dissolution profile. The relevance of the results in vivo was verified: The bioavailability enhancement of a FF-aPMMA solid dispersion with a drug load of 20 % was demonstrated. The in vivo performance of the solid dispersion was shown to be superior to marketed product Lipanthyl® (Laboratoires Fournier S.A., Dijon, France).
PVCL-PVAc-PEG was previously applied as polymeric carrier for FF in HME by Djuric and Kolter (2010) and Linn et al. (2011). A solid solution of FF and PVCL-PVAc-PEG was produced. It was pointed out that this extrudate shows an enhanced solubility, high levels of supersaturation and a complete drug release within 1 h of dissolution in vitro (Djuric and Kolter, 2010). The relevance of the results was verified in vivo as the bioavailability was enhanced in comparison to pure FF powder (Djuric and Kolter, 2010; Linn et al., 2011). In comparison to the physical mixture of FF and PVCL-PVAc-PEG, the solid solution was of a similar effectivess concerning the bioavailability enhancement in vivo (Linn et al., 2011).
The application of HPMC in HME is documented in literature. For example, HPMC was successfully used as carrier for itraconazole by Verreck et al. (2003). A stable, amorphous solid dispersion with an improved dissolution rate of the API was obtained.
PVA-AA-MMA has also been applied as carrier for solid dispersion systems (Uemura et al.; Uramatsu et al., 2007). An improvement in the dissolution rate and the maximum concen-

tration of dissolved API was observed for hot-melt extruded formulations of nifedipine and PVA-AA-MMA in comparison to solid dispersions with PVP or polyvinyl alcohol. It has to be pointed out, that these hot-melt extruded formulations were not manufactured using a twin screw extruder as in our case. Instead, extrusion plastometer Melt Indexer P-101 (Toyoseiki Co, Japan) was used which consists of a heated barrel, a die orifice and a piston to push the molten material through the die. In contrast to a hot-melt extruder, there are no screws. Usually, an extrusion plastometer is applied for the determination of the melt mass flow rate (MFR) and melt volume flow rate (MVR) of resins. Uramatsu et al. (2007) propose the use of an extrusion plastometer to predict the results of a twin screw extruder-HME process with the benefit of a small sample amount needed. It is unclear whether these results are transferable as kneading elements as they are commonly applied in hot-melt extrusion processes using twin screw extruders are missing.

After the HME of FF using single polymers as carriers, the application of polymeric blends was investigated. Mixtures of polymers were reported to offer the possibility to optimize the mechanical properties of the manufactured extrudate (Prodduturi et al., 2007). Furthermore, polymeric blends were shown to modulate the dissolution behavior of the extrudates (Coppens et al., 2006; Janssens et al., 2008; Papageorgiou et al., 2008). The aim of the present work was to further investigate the possibilities of polymeric blends as carriers for HME. It was a goal of these experiments to allow for an assessment of the feasibility of polymeric blends for dissolution enhancement and improvements concerning the extrudates' storage stability in comparison to the respective single polymeric formulations.
FF was thus extruded using blends of COP, HPMC and PVCL-PVAc-PEG as carriers.

### 3.2.2 Hot-melt extrusion of fenofibrate with single polymeric carriers

FF was extruded with COP, HPMC, PVCL-PVAc-PEG, aPMMA and PVA-AA-MMA as single polymeric carriers to serve as a comparison for the formulations manufactured using USAC technology. The composition of the API-polymer blends for HME was equivalent to the USAC blends to enable an effective evaluation of the methods. In all cases, one weighted part of FF was added to three weighted parts of the polymeric carrier prior to the extrusion, resulting in a drug load of 25 % (w/w) (see Table 3.8).

Table 3.8: Composition of FF-single polymer extrudates that served as a comparison to USAC compacts. Data are given in weighted parts unless otherwise specified.

| Formulation | FF | COP | HPMC | PVCL-PVAc-PEG | aPMMA | PVA-AA-MMA | drug load [%] |
|---|---|---|---|---|---|---|---|
| FF-A | 1 | 3 | - | - | - | - | |
| FF-B | 1 | - | 3 | - | - | - | |
| FF-C | 1 | - | - | 3 | - | - | 25.0 |
| FF-J | 1 | - | - | - | 3 | - | |
| FF-K | 1 | - | - | - | - | 3 | |

An immediate release was determined for FF-COP formulation FF-A as the $c_{max}$ was reached after 10 min of dissolution (see Figure 3.5). The concentration of dissolved FF detected at this sampling point was 227 µg/mL which equates 78 % of total API. At $c_{max}$, the concentration is 12.1 times above $c_s$.

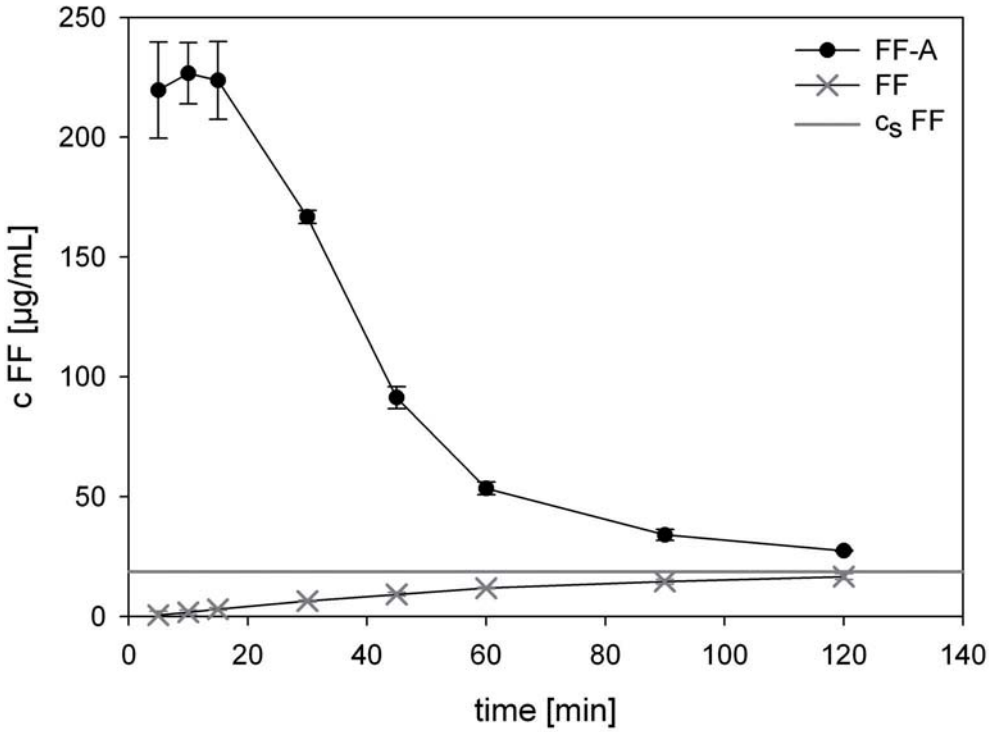


Figure 3.5: Dissolution profile of FF-A pellets (FF+COP = 1+3 weighted parts) in comparison to pure FF

However, it was discovered that the supersaturation level is not stable with formulation FF-A as the concentration has dropped down to 4.9 times above $c_s$ after 45 min of dissolution. After 120 min of dissolution, the amount of dissolved FF has dropped down to 1.4 times above $c_s$. Overall, the solubility of FF was significantly improved with COP as single polymeric carrier.
From DSC results it can be concluded that no crystalline API is present in the hot-melt extruded formulation of FF and COP (FF-A) as no melting peak was detected in the first heating cycle (see Figure 3.6).This indicates the formation of a dispersion of the amorphous drug in the amorphous polymer. Only one glass transition was detected for FF-A extrudate ($T_g$=39.1,°C, first heating cycle), lying in between the individual glass transitions of the drug ($T_g$=-18.5 °C, second heating cycle) and carrier ($T_g$=104.9 °C, second heating cycle). Therefore, it can be concluded that a one-phase system is present (O'Donnell and Williams III, 2009).

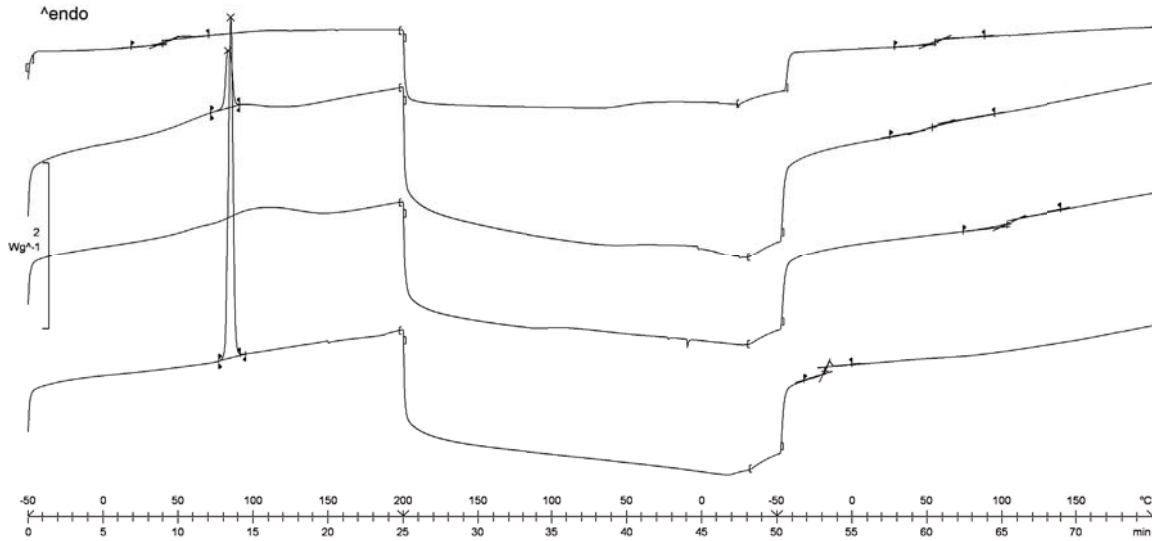


Figure 3.6: DSC thermogram of FF-A extrudate (FF+COP = 1+3 weighted parts) showing from top to bottom: pellets, physical mixture, carrier, pure FF

X-ray diffraction (XRD) analysis showed that both drug and polymer are present in their amorphous form in the hot-melt extruded formulation FF-A (see Figure 3.7) while crystalline FF was detected in the physical mixture of the components. It is assumed that a molecular dispersion of the drug in the polymer is present, forming a glassy solid solution.

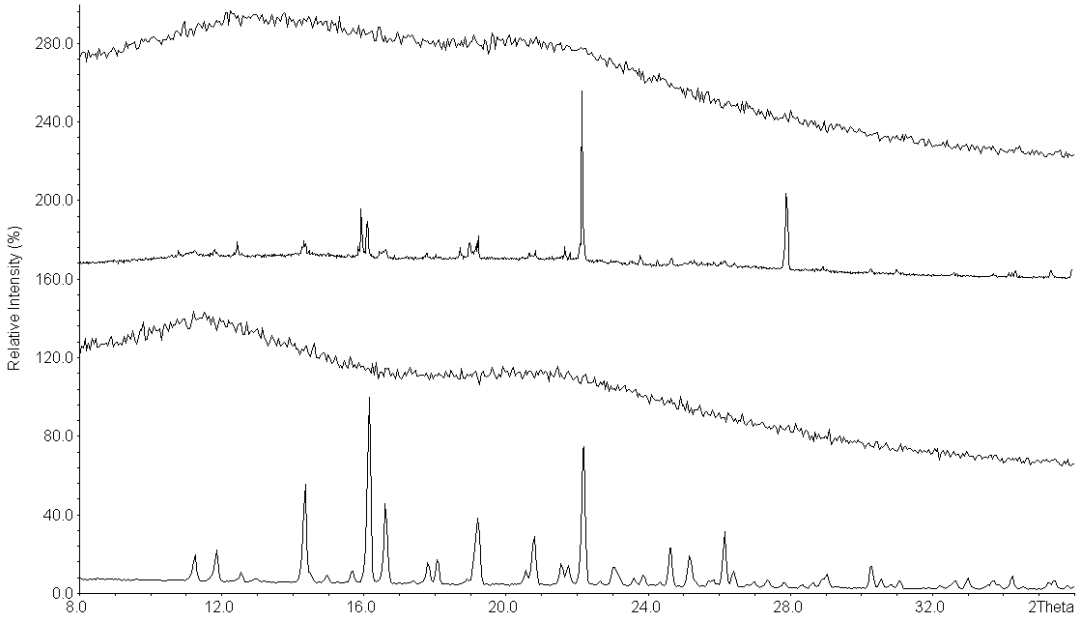


Figure 3.7: XRD patterns of FF-A extrudate (FF+COP = 1+3 weighted parts), physical mixture of the components, carrier and pure FF (from top to bottom)

With FF-HPMC formulation FF-B, $c_{max}$ was reached after 30 min of dissolution. At that sampling point, 80 µg/mL of FF were dissolved, resulting in a dissolved amount of 28% of total API and a supersaturation of 4.3 (see Figure 3.8).

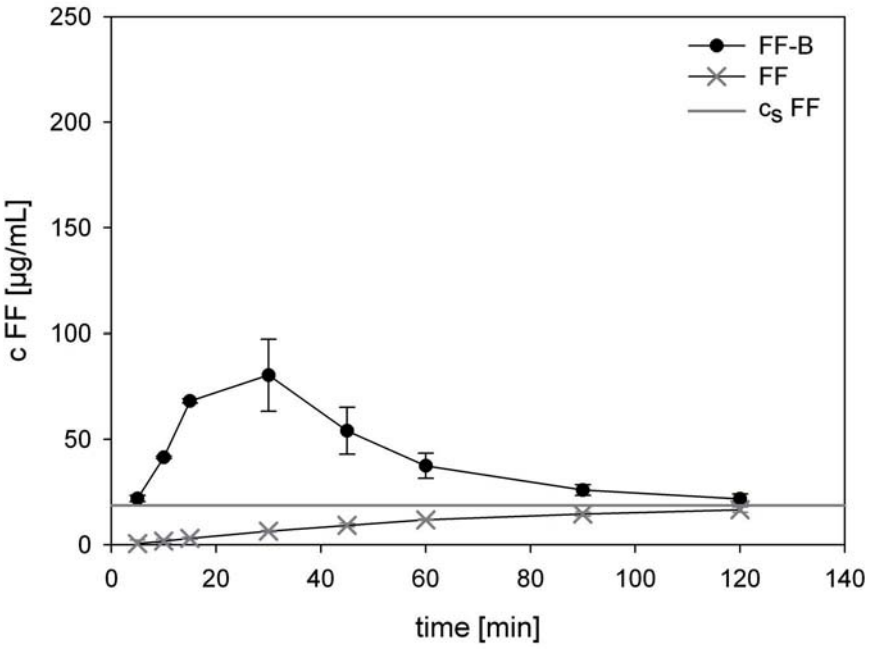


Figure 3.8: Dissolution profile of FF-B pellets (FF+HPMC = 1+3 weighted parts) in comparison to pure FF

Commonly, HPMC is applied for the manufacture of controlled release solid dosage forms with a sustained release profile, as this excipient swells due to the absorption of water thus forming a gel layer which acts as a diffusion barrier. The drug release from HPMC matrix systems is reported to be diffusion and erosion controlled (Tu et al., 2010). The initial release rate was enhanced with poorly water soluble drug itraconazole when hot-melt extruded using HPMC as carrier (Verreck et al., 2003; Six et al., 2003). Similarly, the initial dissolution rate was enhanced with FF-HPMC extrudates in comparison to pure FF. The initial dissolution rate of FF-COP formulation FF-A was superior to FF-B (see Figures 3.5 and 3.8).
As with FF-A extrudate, no crystalline API was detected in FF-B pellets using XRD analysis (see Figure 3.34). The physical mixture of the components was shown to contain crystalline FF. Only the first heating cycle of the DSC analysis of formulation FF-B was taken into consideration. The reason for this decision was the degradation of the carrier HPMC at higher measuring temperatures (browns at 190-200 °C, chars at 225-230 °C; Harwood, 2003). Unfortunately, the measuring range could not be adjusted to lower temperatures as the glass transition temperature of the carrier was very high ($T_g$=175.4 °C). It can be assumed that a glassy dispersion is formed as both components were shown to be present in their amorphous form during the first heating cycle since no melting peak was detected (see Figure 3.9).

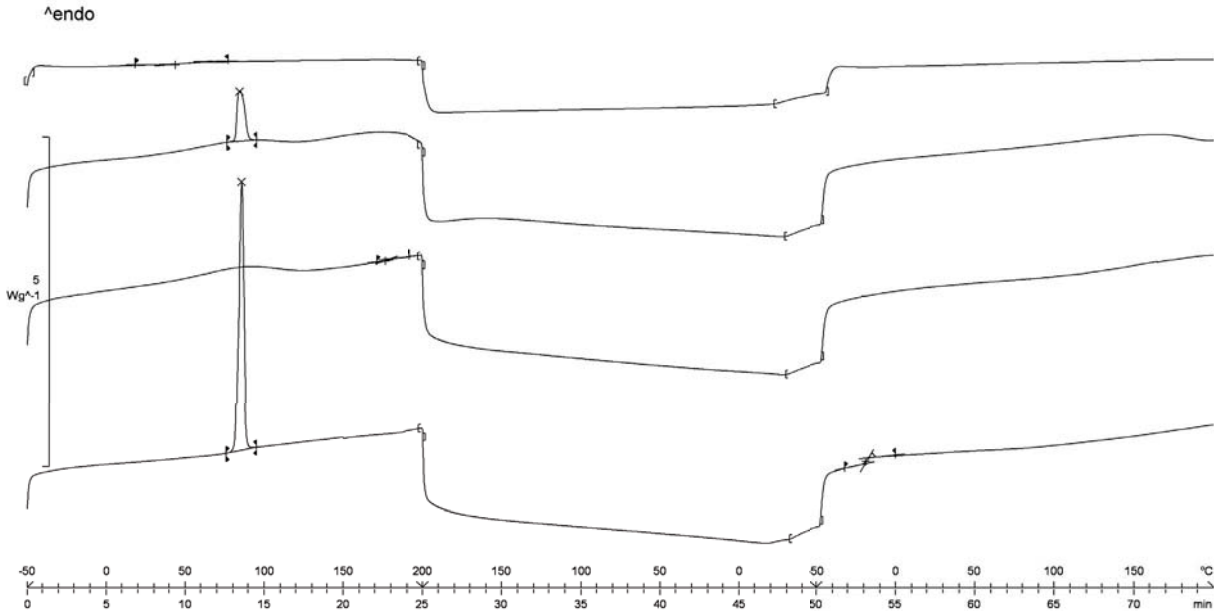


Figure 3.9: DSC thermogram of FF-B extrudate (FF+HPMC = 1+3 weighted parts) with the following data displayed from top to bottom: pellets, physical mixture, carrier, pure FF

The maximum concentration of dissolved API reached with FF-PVCL-PVAc-PEG formulation FF-C was 138 µg/mL after 60 min of dissolution (see Figure 3.10).

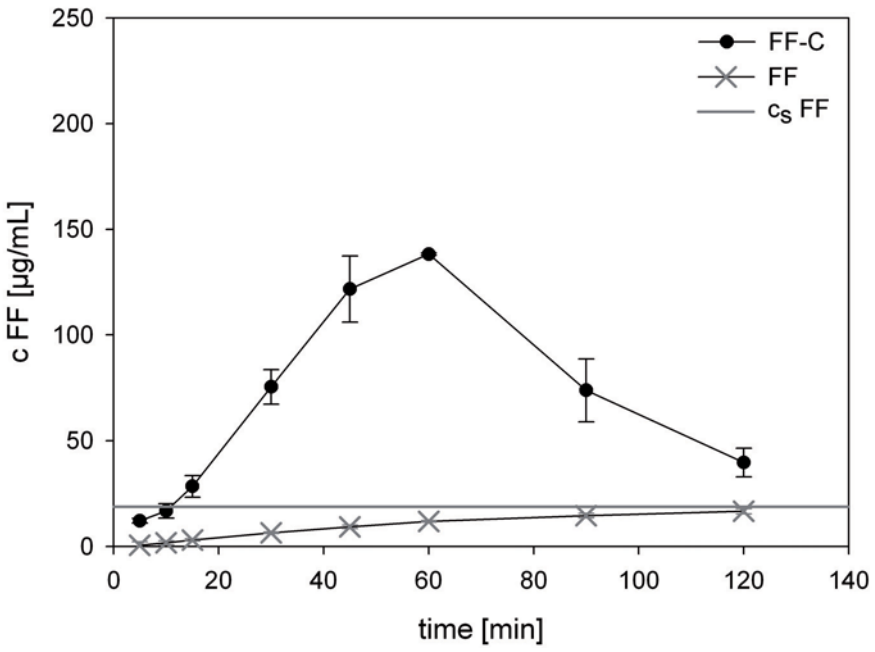


Figure 3.10: Dissolution curve of FF-C pellets (FF+PVCL-PVAc-PEG=1+3 weighted parts) in comparison to pure FF

This corresponds to 48 % of total API and is 7.4 times above saturation level. Again, the dissolution profile of poorly water-soluble drug FF was successfully enhanced via HME.
For formulation FF-C, the same conclusion can be derived from its DSC thermogram as with the other manufactured single polymeric extrudates of FF in which COP or HPMC are applied as carriers (FF-A, FF-B): No crystalline API is present in any of the extrudates directly after manufacture. The $T_g$ of the mixture ($T_g$=40.2 °C, first heating cycle) which is in between the $T_g$ values of the individual components ($T_g$ FF=-18.5 °C, second heating cycle; $T_g$ carrier=70 °C) indicates the presence of a molecular dispersion in the FF-C pellets (see Figure 3.11).

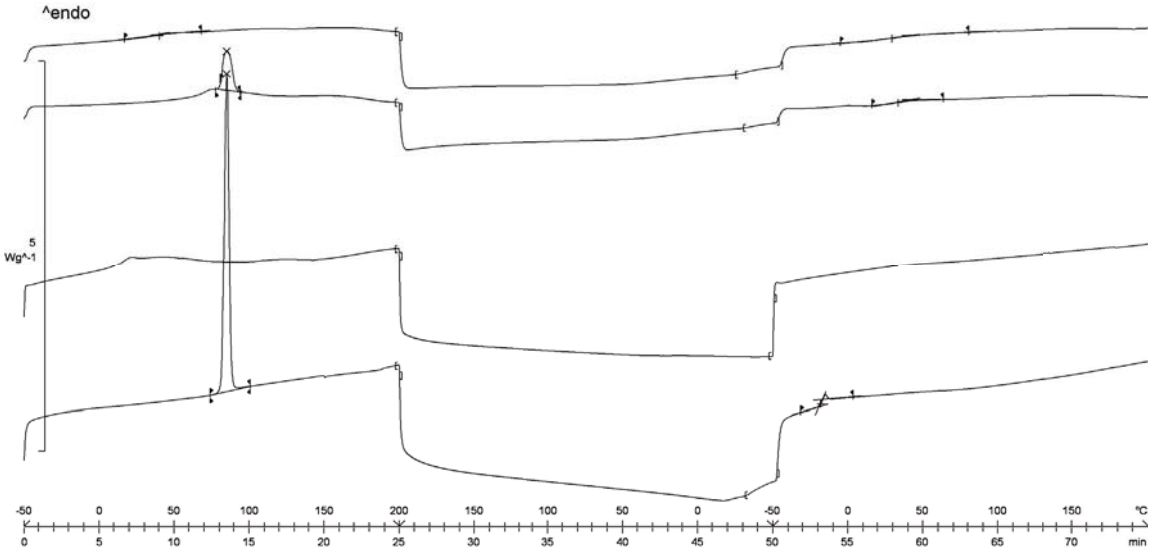


Figure 3.11: DSC thermogram of FF-C extrudate (FF+PVCL-PVAc-PEG = 1+3 weighted parts) with the following data displayed from top to bottom: pellets, physical mixture, carrier, pure FF

It has to be pointed out that no clear $T_g$ was detected from the analysis of PVCL-PVAc-PEG, most likely due to an overlaying of the polymers' glass transition by the water evaporation curve, so the literature data were used as a reference (Technical Information Soluplus).

In summary, an immediate release was observed with formulation FF-A while a sustained release dissolution profile was determined for formulations FF-B and FF-C. With all three formulations, the initial dissolution rate was increased through HME in comparison to untreated FF powder. Supersaturation could be maintained for at least 105 min. However, the level of supersaturation was not stable for any of the three formulations. It is concluded that the release profile of the extrudates FF-A, FF-B and FF-C is carrier-controlled.

HME was also performed with aPMMA and PVA-AA-MMA as carriers FF to be compared with the corresponding USAC formulations. These extrudates consist of one weighted part FF and three weighted parts aPMMA (FF-J) or PVA-AA-MMA (FF-K), respectively, to ensure full comparability to the USAC compacts (see Table 3.8).

As the $T_g$ of the extruded formulation with aPMMA was below room temperature (see Figure 3.12), there were insurmountable difficulties with the down-processing of the extruded material. For example, the pelletizing of the strand has proven to be impossible as the FF-J strand remained flexible even after cooling down to room temperature. Therefore, the strand had to be cut manually.

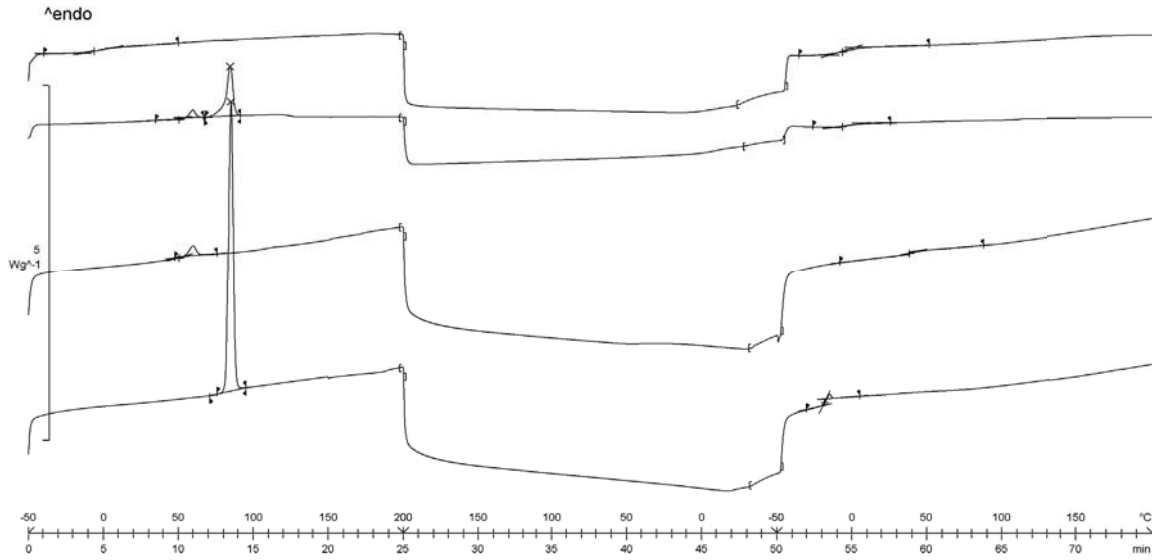


Figure 3.12: DSC thermogram of FF-J extrudate (FF+aPMMA = 1+3 weighted parts) with the following data displayed from top to bottom: pellets, physical mixture, carrier, pure FF

DSC thermograms of this formulation show that the API is present in its amorphous form in the pellets (see first heating cycle in Figure 3.12). The formation of a molecular, amorphous dispersion of FF in the carrier due to the previously described $T_g$ shift is confirmed. Because of the encountered difficulties, no XRD analysis was performed with FF-J. The same applies for storage stability testing: The trials had to be aborted due to a fusion of the still flexible strands or pellets within 24 h after manufacture of the extrudate.
Nevertheless, the solubility enhancement of FF via HME was successful with aPMMA as carrier: After 5 min of dissolution, a concentration of 157.6 µg/mL was detected for FF-J pellets (see Figure 3.13). This value equals an amount of 54 % of total API and is 8.4 times above saturation level. The high variation of the results is a consequence of the instant release of the pellets and their differing sizes as the strand was cut manually.
Although a successful application of aPMMA as a carrier for dissolution enhancement using HME is reported in literature for a variety of drugs, including indomethacin (Liu et al., 2010), FD (Nollenberger et al., 2009a,b) and FF (He et al., 2010), this formulation approach was not pursued further due to the described challenges concerning both the manufacture as well as the analysis of the extrudate. It is unclear whether similar problems were observed by He et al. (2010) who consider aPMMA a suitable carrier for HME of FF.

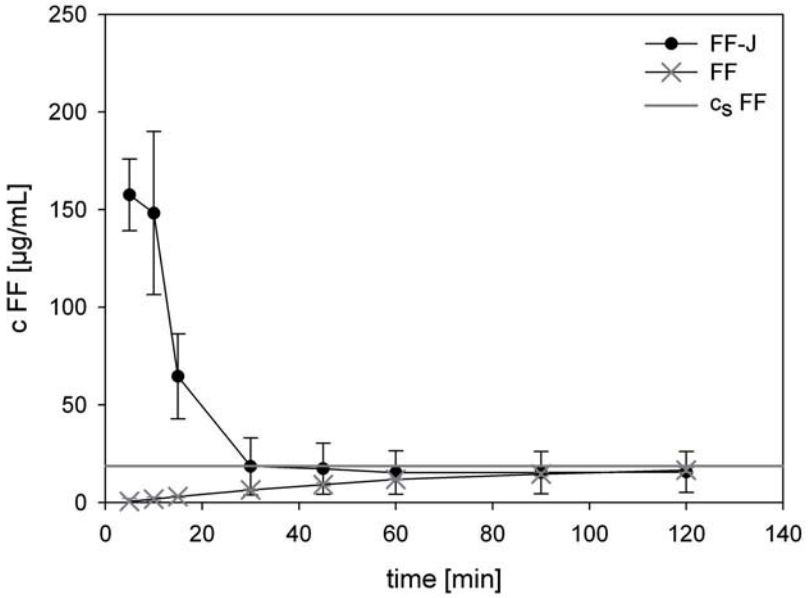


Figure 3.13: Dissolution profile of FF-J extrudate (FF+aPMMA = 1+3 weighted parts) in comparison to pure FF

When PVA-AA-MMA was used as carrier for FF (FF-K), a thermal decomposition of the polymer and a volume expansion of the extrudate was observed at process temperatures from 90-180 °C. No uniform and smooth melt was obtained with any of the applied process settings (see Figure 3.14).

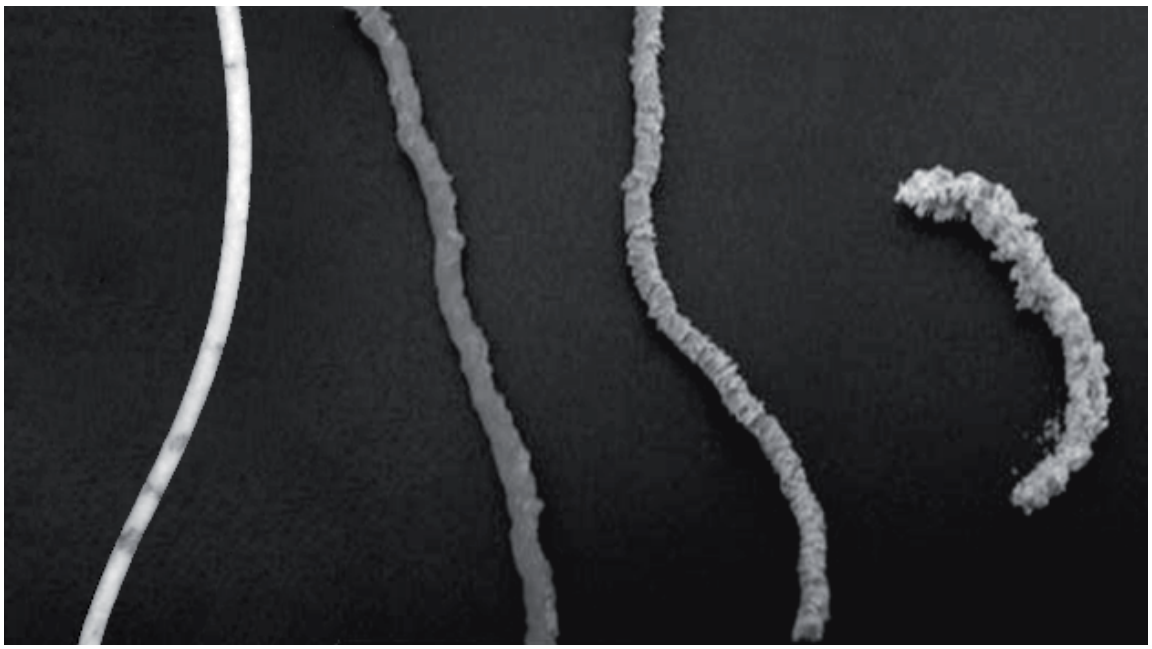

Figure 3.14: Strands of formulation FF-K (FF+PVA-AA-MMA = 1+3 weighted parts) extruded at process temperatures 90, 120, 150 and 180 °C (from left to right)

The dissolution behavior of FF is even worsened through its incorporation into PVA-AA-MMA (see Figure 3.15).
Figure 3.16 shows that the API is not fully transformed into its amorphous state as crystalline FF was detected in formulation FF-K (first heating cycle).

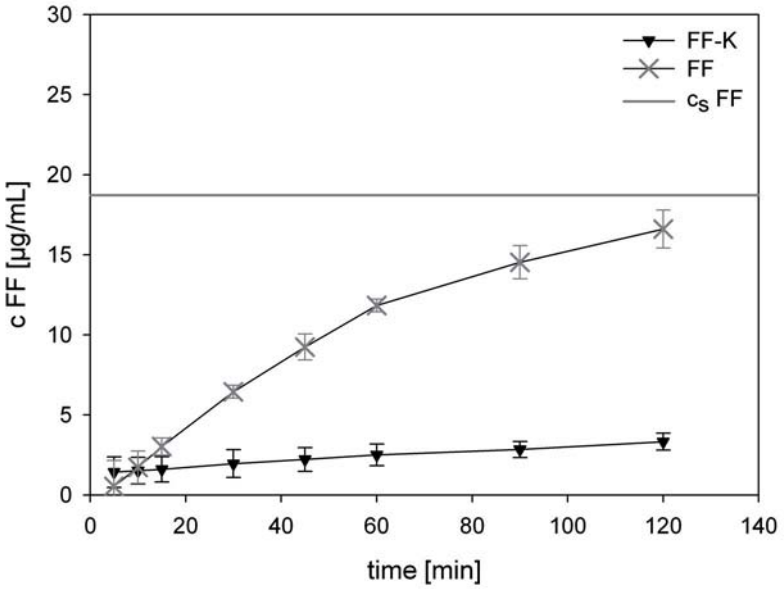


Figure 3.15: Dissolution profile of FF-K extrudate (FF+PVA-AA-MMA = 1+3 weighted parts) in comparison to pure FF

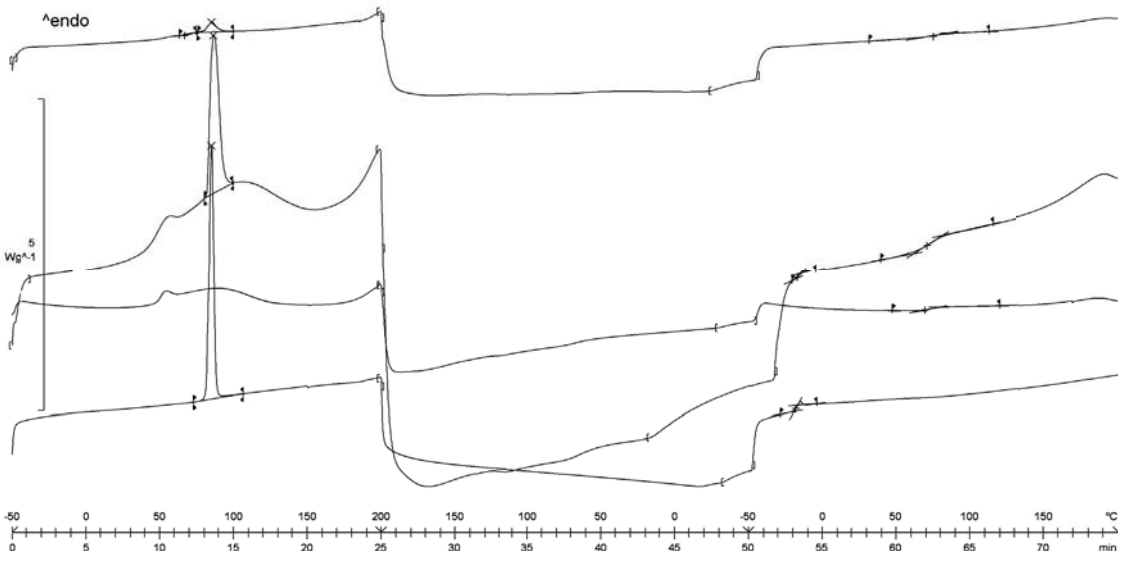


Figure 3.16: DSC thermogram of FF-K extrudate (FF+PVA-AA-MMA = 1+3 weighted parts) with the following data displayed from top to bottom: pellets, physical mixture, carrier, pure FF

The glass transition temperature which was detected in the second heating cycle of FF-K pellets equates the $T_g$ value of the pure carrier. As no $T_g$ shift was detected, it is assumed that a glassy suspension of the crystalline drug in the amorphous carrier is formed resulting in a two phase system. The same applies to the DSC results of the physical mixture.
No degradation of PVA-AA-MMA was detected when heating the extruded samples or untreated physical mixtures of the components to up to 200 °C in DSC analysis. This is in accordance to the manufacturer's information: PVA-AA-MMA is reported to be stable to up to 230 °C (Characteristization of Povacoat).
It must be concluded that PVA-AA-MMA is not suitable as a carrier for HME using the applied conditions, possibly due to high shear rates leading to local increases of the process temperature within the extruder (Breitenbach, 2002). As the application of a screw design which includes kneading elements was reported to induce a rise of shearing rates, a modification of the screw set-up might facilitate the manufacture of a PVA-AA-MMA extrudate. On the contrary, the application of kneading elements is a key factor for the transformation of a crystalline drug into its amorphous state and for the manufacture of solid dispersions with an enhanced dissolution behavior (Nakamichi et al., 2002; Crowley et al., 2007).
Processability and dissolution behavior of the FF-PVA-AA-MMA blend might also be improved using additional excipients, for example by lowering the required process temperatures. However, the use of additional excipients would result in formulations that differ from the USAC compact composition. Thus, the comparability of the results would be affected. Due to these reasons, this approach was not pursued further.

### 3.2.3 Milling of the extrudates

The manufactured extrudates of a poorly water-soluble drug and a carrier are usually milled prior to dissolution testing (Repka et al., 2008). Capsules are filled with the milled extrudate or the milled extrudate is pressed into a tablet. Sometimes, further excipients are added after milling of the extrudate, for example disintegrants (Djuric and Kolter, 2010; Lakshman et al., 2008).
By milling of the extruded strand, the manufacture of a final solid oral dosage form is facilitated as the uniformity of the drug content of the single-dose preparation can be better controlled. Additionally, the particle size is reduced by milling, leading to an increased surface area available for dissolution. According to the modified Noyes-Whitney equation (see Eq. 1.1 on page 1), an increased surface area results in an increased dissolution rate. Hence, the bioavailability of the extrudates might be further enhanced if they are milled.
In the present work, the FF-single polymer extrudates were milled to ensure comparable testing conditions to the USAC trials: Due to the size of the USAC compacts (die diameter = 25 mm) which is not deemed suitable for an application of one compact as a single-dose preparation, milling of the USAC formulations was performed. The pellet diameter of hot-melt extruded formulations was approximately 1-2.5 mm, depending on the polymeric carrier (see Section 3.2.5 for details on die diameter and pellet sizes of the formulations). The pellet length was set to 1.5 mm (see Section 6.2.1.4). In contrast to the large USAC

compacts (compact diameter 2.5 cm), the small sized pellets offer the possibility of a direct encapsulation. To evaluate the effect of the milling process on the physicochemical properties of the component, the dissolution performance and the results from the analysis of the physical state of the milled and unmilled extrudates were compared.
Figure 3.17 shows the dissolution profiles of the pelletized extrudates FF-A, FF-B and FF-C, while Figure 3.18 depicts the dissolution profiles of the milled extrudates.

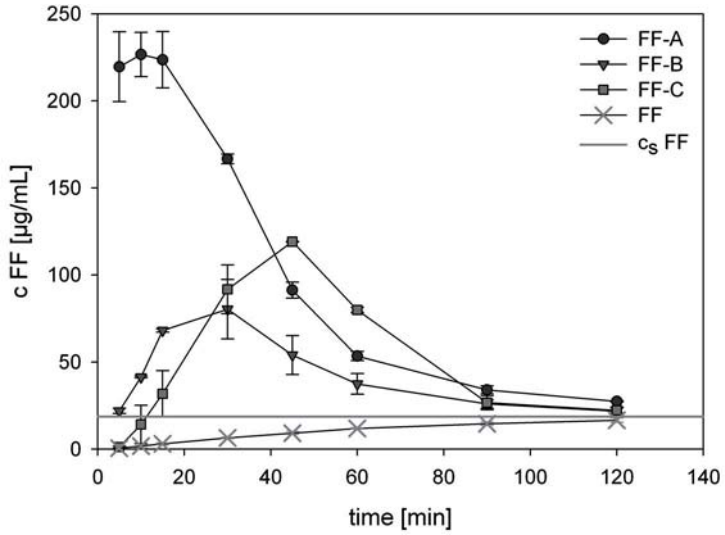


Figure 3.17: Dissolution profiles of pelletized extrudates FF-A (FF+COP), FF-B (FF+HPMC) and FF-C (FF+PVCL-PVAc-PEG; all consisting of 1+3 weighted parts of API and polymer)

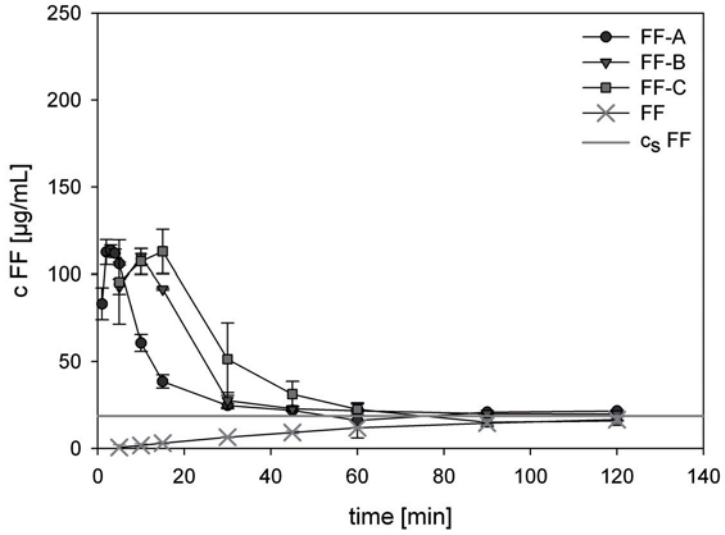


Figure 3.18: Dissolution profiles of milled extrudates FF-A (FF+COP), FF-B (FF+HPMC) and FF-C (FF+PVCL-PVAc-PEG; all consisting of 1+3 weighted parts of API and polymer)

The release profiles of milled and pelletized extrudates differ considerably. With FF-A - FF-C pellets, the dissolution characteristics of the polymeric carrier have a strong influence on the release profile (see Section 3.2.2).
For all three milled extrudates, an instant release is observed: A $c_{max}$ value of 110-113 µg/mL is reached within 15 min of dissolution with the milled FF-A, FF-B and FF-C sample. The increase of the initial dissolution rate of milled FF-B and FF-C samples can be contributed to the particle size reduction which is induced by the milling procedure. The $c_{max}$ value of dissolved FF is increased for FF-HPMC formulation FF-B through milling. However, considering the high variation of the process (see standard deviations depicted in Figure 3.18), the improvement through milling has to be regarded as negligible.
For formulations FF-A and FF-C, $c_{max}$ is reduced by 113 µg/mL and 25 µg/mL, respectively. Regardless of the different physicochemical properties of the polymeric carriers applied which lead to a different release performance of the pelletized extrudates, the dissolution profiles of the milled extrudates can be considered equivalent. Although a sixfold supersaturation was detected for the milled extrudates, it has to be concluded that the positive effect of the HME process is at least partially annulled through the milling procedure.
Furthermore, XRD results of milled and pelletized extrudate indicate that the applied milling process induces a recrystallization of the API, possibly leading to instabilities that might further diminish the dissolution performance of stored extrudates (see Figure 3.19). A complete loss of the dissolution enhancement within 4 weeks of storage due to a recrystallization of FF in FF-COP extrudates was previously reported by Kanaujia et al. (2011).
Considering these results, the extrudates are not milled in further trials to allow a better differentiation of the influence of the carrier(s) on the dissolution profile of the API.

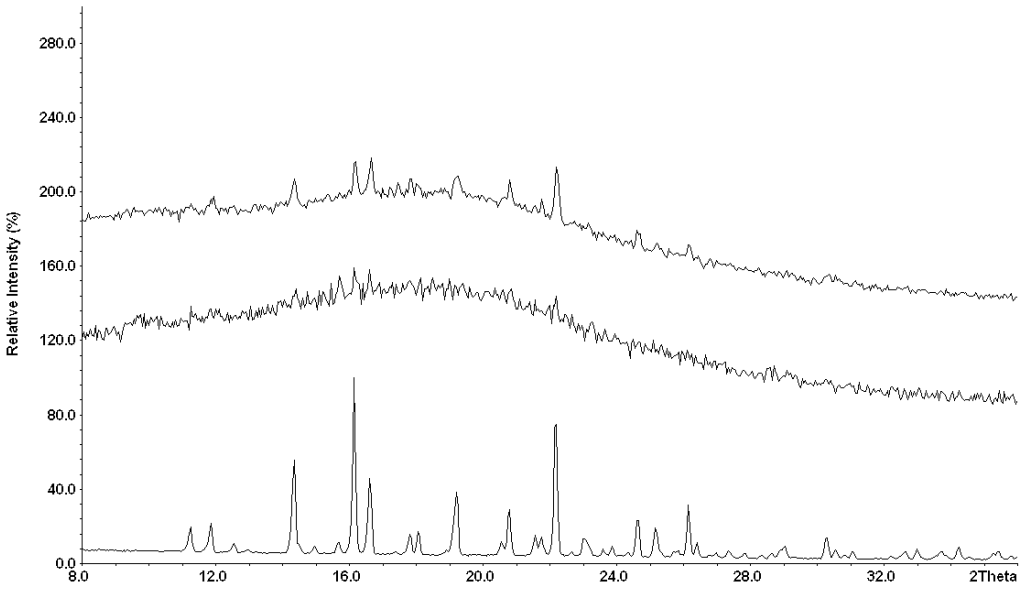


Figure 3.19: XRD pattern of milled FF-C extrudate (FF+PVCL-PVAc-PEG = 1+3 weighted parts) in comparison to FF-C pellets with the following data displayed from top to bottom: milled extrudate, pellets, pure FF

### 3.2.4 Content uniformity of the extrudates

From the results described in Section 3.2.3, it was concluded that milling of FF extrudates promotes undesired effects. It was shown that by pelletizing the extruded strand, these undesired effects are avoided. Regarding a future application of the pelletized extrudate as a single-dose preparation, the content uniformity of the pellets requires verification.
Two different pelletized extrudates were analyzed for their API content to verify the homogeneity of the extrudates: pelletized FF-A extrudate (FF+COP = 1+3 weighted parts) and FF-G extrudate (FF+COP+PVCL-PVAc-PEG = 1+3+1.5 weighted parts).
Evaluation of the results was performed according to European Pharmacopoeia (Ph.Eur.) specifications by calculation of the Acceptance Value $AV$ (see Section 6.2.2.10) using the following equation:

$$AV = |M - \overline{X}| + ks \tag{3.1}$$

with $M$ being 101.5 % by Ph.Eur. definition as the average content $\overline{X}$ of the pellets was determined to be >101.5 % of the targeted value (103.45 % for formulation FF-A and 103.76 % for FF-G; see Tables 3.9 and 3.10). $k$ is the acceptability constant which is defined as 2.4 for n=10 by the Ph.Eur. Nine pellets were assessed for their drug content in the present work. The difference coming from using $k = 2.4$ is considered to be negligible. $s$ is the standard deviation which was calculated to be 1.87 % for FF-A and 1.97 % for FF-G.

Table 3.9: Evaluation of the content uniformity of FF-A pellets (FF+COP=1+3 weighted parts; Target content: 25.00 %)

| Sample | Weight [mg] | FF content [mg/Pellet] | FF content [%/Pellet] | FF content [% of target value] |
|---|---|---|---|---|
| FF-A 1 | 5.58 | 1.41 | 25.27 | 101.08 |
| FF-A 2 | 4.02 | 1.02 | 25.37 | 101.49 |
| FF-A 3 | 4.11 | 1.07 | 26.03 | 104.14 |
| FF-A 4 | 4.93 | 1.27 | 25.76 | 103.04 |
| FF-A 5 | 4.06 | 1.05 | 25.86 | 103.45 |
| FF-A 6 | 3.88 | 0.99 | 25.52 | 102.06 |
| FF-A 7 | 3.26 | 0.85 | 26.07 | 104.29 |
| FF-A 8 | 3.24 | 0.84 | 25.93 | 103.70 |
| FF-A 9 | 3.60 | 0.97 | 26.94 | 107.78 |
| Average | 4.08 | 1.05 | 25.86 | 103.45 |
| Standard deviation | 0.72 | 0.17 | 0.47 | 1.87 |

Table 3.10: Evaluation of the content uniformity of FF-G pellets (FF+COP+PVCL-PVAc-PEG=1+3+1.5 weighted parts; Target content: 18.18 %)

| Sample | Weight [mg] | FF content [mg/Pellet] | FF content [%/Pellet] | FF content [% of target value] |
|---|---|---|---|---|
| FF-G 1 | 4.30 | 0.81 | 18.84 | 103.62 |
| FF-G 2 | 3.68 | 0.70 | 19.02 | 104.63 |
| FF-G 3 | 4.34 | 0.82 | 18.89 | 103.93 |
| FF-G 4 | 3.46 | 0.63 | 18.21 | 100.15 |
| FF-G 5 | 4.58 | 0.87 | 19.00 | 104.49 |
| FF-G 6 | 3.46 | 0.65 | 18.79 | 103.33 |
| FF-G 7 | 4.58 | 0.90 | 19.65 | 108.09 |
| FF-G 8 | 3.64 | 0.68 | 18.68 | 102.76 |
| FF-G 9 | 3.69 | 0.69 | 18.70 | 102.86 |
| Average | 3.97 | 0.75 | 18.86 | 103.76 |
| Standard deviation | 0.44 | 0.09 | 0.36 | 1.97 |

Both formulations meet the criteria as the calculated $AV$ is below the maximum allowed acceptance value of 15.0: 6.4 with FF-A and 7.0 with FF-G.
Hence, the uniformity of drug content of the analyzed extrudates was confirmed. As the process conditions are similar for the remaining API-polymer mixtures, it is assumed that the results are transferable to the other extrudates.

### 3.2.5 Influence of the die diameter on pellet size and release characteristics of extrudates

While the pellet length is equivalent for all formulations as the same setting of the pelletizing equipment is chosen throughout the studies (1.5 mm, see Section 6.2.1.4), a varying diameter of the hot-melt extruded strand was observed. The reason for this are the different viscosities of the polymeric carriers when in their molten state.
A low viscosity was observed for COP and PVCL-PVAc-PEG formulations which leads to the formation of strands with a small diameter (approx. 1.5 mm with a 3 mm die orifice, see Table A.1). With HPMC as single carrier, the mixture was relatively firm upon extrusion out of the die, resulting in pellet diameters of approximately 2.5 mm (see Table 3.11).

Table 3.11: Pellet sizes of formulation FF-B (FF+HPMC=1+3 weighted parts) extruded with die diameters 1 mm and 3 mm

| Pellet properties | Die diameter 1 mm | | | Die diameter 3 mm | | |
|---|---|---|---|---|---|---|
| | Diameter [mm] | Length [mm] | Weight [mg] | Diameter [mm] | Length [mm] | Weight [mg] |
| Mean value | 0.9228 | 1.5518 | 1.3618 | 2.5114 | 1.3754 | 8.1796 |
| Standard deviation | 0.0234 | 0.0316 | 0.1025 | 0.1332 | 0.1201 | 0.9525 |

Previously, the methods of solubility enhancement were discussed using the modified Noyes-Whitney equation which describes the rate of dissolution (see Section 1.1, Eq. 1.1). The influence of the particle size on the dissolution behavior of a solid sample is shown by this equation: With an increasing surface area, the dissolution rate is enhanced and vice versa. An increase of the pellet size reduces the surface area available for dissolution as the weighed sample amount which is applied in dissolution trials remains the same.
To enlighten the effect of the differing pellet sizes on the dissolution profiles, HME of FF-HPMC formulation FF-B was performed using two different die diameters: 1 mm and 3 mm. The samples were then submitted to dissolution trials and their dissolution profiles were compared.
Both the initial release rate as well as the $c_{max}$ value were increased if the pellet diameter was reduced (see Figure 3.20). With FF-B pellets produced using the 1 mm die diameter, the pellet size was decreased by 63 %. The dissolved amount of API after 5 min of dissolution was increased by 20.3 µg/mL which corresponds to an increase by 76 %. The $c_{max}$ value is increased by 38.4 µg/mL (+ 31 %).

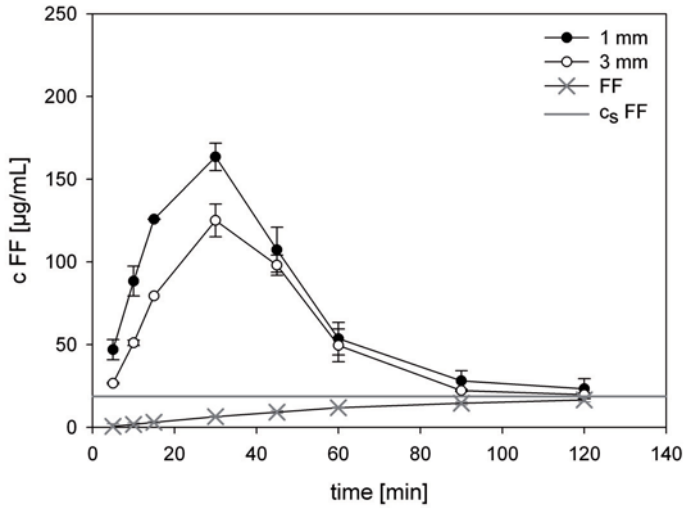


Figure 3.20: Release profile of formulation FF-B (FF+HPMC=1+3 weighted parts) extruded with die diameters 1 mm and 3 mm

The influence of the pellet diameter on its release profile was thus confirmed. However, this effect has to be taken into regard only if the release profiles of extrudates with HPMC as single carrier are compared to the other formulations as the latter are of equivalent size.

### 3.2.6 Hot-melt extrusion of fenofibrate with mixtures of polymeric carriers

Since the release mechanism of FF from the extrudates with a single polymer as carrier was shown to be carrier-controlled (see Section 3.2.2), the attempt was made to enhance the dissolution behavior of the extruded formulations through a modification of the polymeric carrier.

Given that the highest $c_{max}$ values were reached with COP as carrier (formulation FF-A), this mixture was chosen as the starting point. Due to the unstable supersaturation of this hot-melt extruded system, the main effort was laid on its stabilization.
The application of polymers with different physicochemical characteristics and different dissolution profiles in a polymeric blend as carrier for HME with a positive effect on the mechanical properties and the dissolution behavior of the extrudate has been described previously in literature (Coppens et al., 2006; Prodduturi et al., 2007; Janssens et al., 2008).
The aim of this work was to further investigate the opportunities this approach offers for pharmaceutical formulation and its feasibility for the optimization of the dissolution profile of a FF-COP extrudate (formulation FF-A, FF+COP≡1+3). It was examined whether an addition of the precipitation inhibiting agent HPMC to the API-carrier blend prior to extrusion delays the concentration decrease after $c_{max}$ as its supersaturation prolonging effect was demonstrated both in in vitro and in vivo studies (He, 2009).
PVCL-PVAc-PEG was chosen as the second additional polymer due to its solubilizing properties, possibly leading to a stabilization or even a further improvement of the supersaturation level of formulation FF-A.
Varying amounts of these polymeric additives were applied (see Table 3.12 for the composition of the extrudates).

Table 3.12: Composition of FF extrudates with a polymeric blend as carrier. Data are given in weighted parts unless otherwise specified.

| Formulation | FF | COP | HPMC | PVCL-PVAc-PEG | drug load [%] |
|---|---|---|---|---|---|
| FF-D | 1 | 3 | 0.6 | - | 21.7 |
| FF-E | 1 | 3 | 1 | - | 20.0 |
| FF-F | 1 | 3 | - | 1 | 20.0 |
| FF-G | 1 | 3 | - | 1.5 | 18.2 |
| FF-H | 1 | 3 | 1 | 1 | 16.7 |

The dissolution results that were gained with the polymeric blends as carriers were evaluated with regard to the initial dissolution rate, the $c_{max}$ and the level of supersaturation and its stability. For a better assessment, dissolution and precipitation rates were estimated using linear regression. The time period above the half-value of the supersaturation concentration of each extrudate was used for a better comparison of the stability of the supersaturation.
With all formulations where polymeric blends were applied as carrier for FF, the initial dissolution rate decreased when compared to the release profile of formulation FF-A. PVCL-PVAc-PEG was shown to reduce the initial dissolution rate to a greater extent than HPMC if applied in a polymeric blend (see calculated values for formulations FF-F and FF-G in Table 3.13).

Table 3.13: Initial dissolution rates, decrease rates, $c_{max}$ and the time period above the half-value of the supersaturation concentration were used for the comparison of the dissolution profiles of polymeric blend extrudates to the single polymeric extrudates and pure FF powder.

| Formulation | | Dissolution rate [µg/mL] | Decrease rate [µg/mL] | $c_{max}$ [µg/mL] | Time above $c_{super}/2$ [min] |
|---|---|---|---|---|---|
| Single polymers | FF-A | 47.0 | -4.0 | 227 | 25 |
| | FF-B | 4.4 | -1.6 | 80 | 50 |
| | FF-C | 2.6 | -1.4 | 138 | 60 |
| Polymeric blends | FF-D | 8.4 | -1.6 | 141 | 80 |
| | FF-E | 9.1 | -1.8 | 145 | 80 |
| | FF-F | 6.7 | -2.3 | 212 | 70 |
| | FF-G | 3.8 | -1.5 | 187 | 100 |
| | FF-H | 2.7 | -1.5 | 153 | >90 |
| Pure API | FF | 0.2 | - | - | - |

The more additional polymer was used, the more pronounced was the reduction of the dissolution rate, especially if all three polymers were used as carriers simultaneously (formulation FF-H). After 5 min of dissolution, the formulations with HPMC as additional polymer are 7.5 times above $c_s$ (FF-D and FF-E, see Figures 3.21 and 3.22) while the release from formulation FF-A was shown to be 12.1 times above $c_s$ at that sampling point.

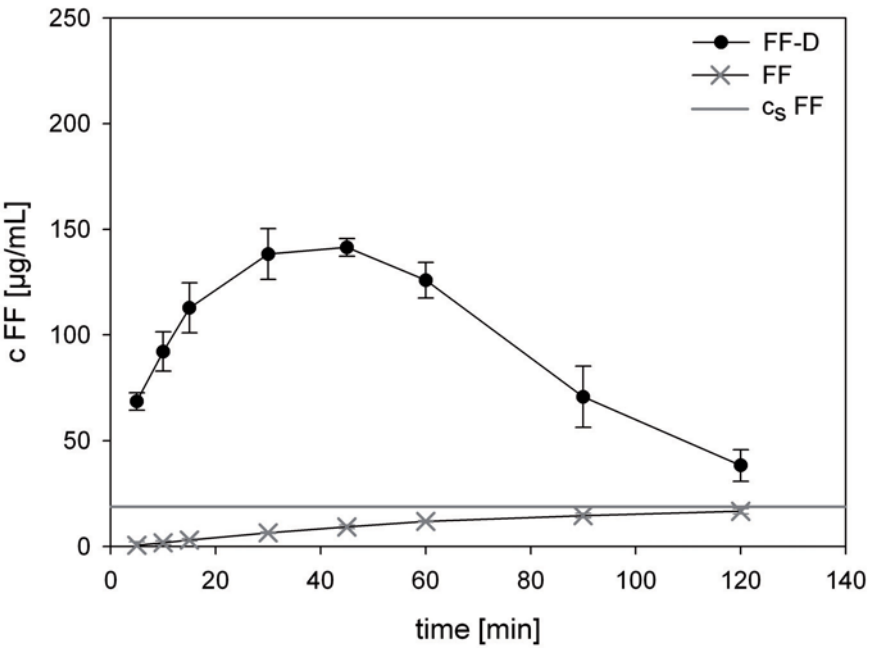


Figure 3.21: Dissolution profile of hot-melt extruded formulation FF-D (FF+COP+HPMC = 1+3+0.6 weighted parts) in comparison to pure FF

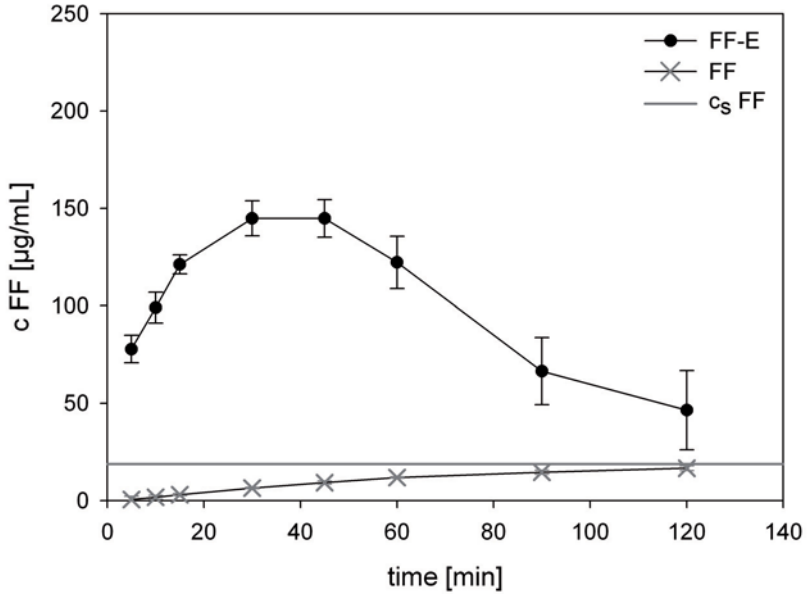


Figure 3.22: Dissolution profile of hot-melt extruded formulation FF-E (FF+COP+HPMC = 1+3+1 weighted parts) in comparison to pure FF

With PVCL-PVAc-PEG as additional carrier, the dissolved amount of FF does not exceed $c_s$ within 5 min of dissolution (formulations FF-F and FF-G, see Figures 3.23 and 3.24). Hence, the initial release rate was reduced by the addition of HPMC and to an even greater extent by the addition of PVCL-PVAc-PEG.

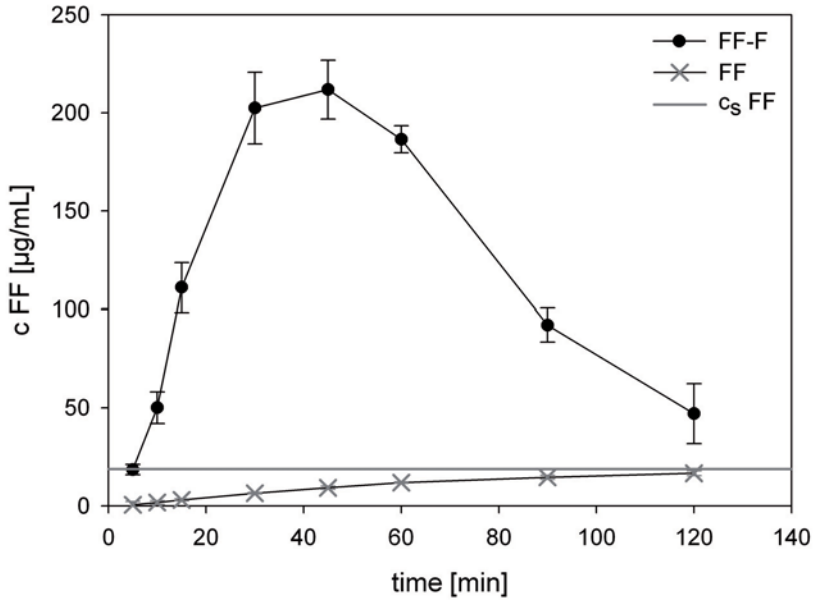


Figure 3.23: Dissolution profile of hot-melt extruded formulation FF-F (FF+COP+PVCL-PVAc-PEG = 1+3+1 weighted parts) in comparison to pure FF

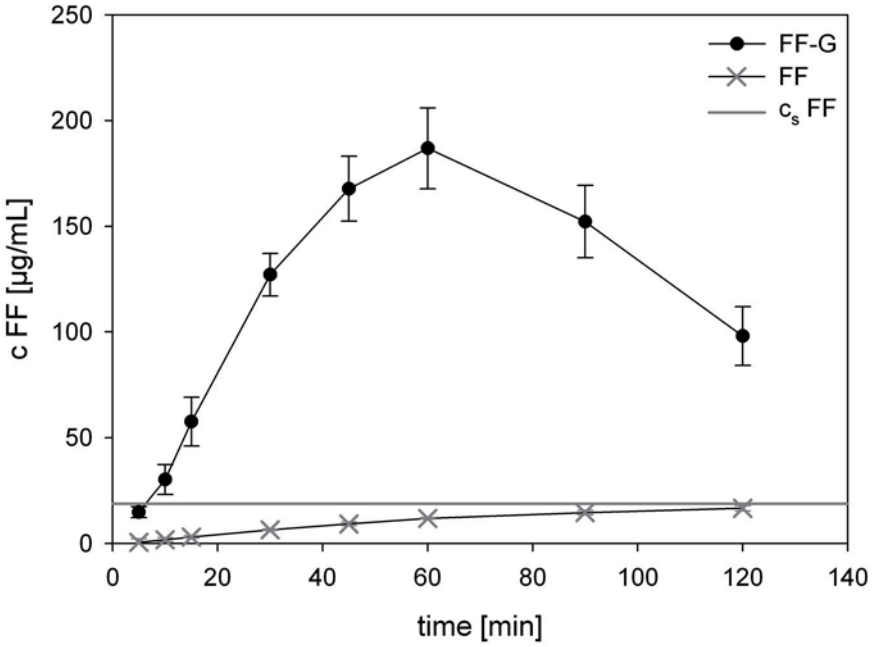


Figure 3.24: Dissolution profile of hot-melt extruded formulation FF-G (FF+COP+PVCL-PVAc-PEG=1+3+1.5 weighted parts) in comparison to pure FF

Also, the maximum concentration of dissolved FF was reduced: with FF-A, $c_{max}$ was at 227 µg/mL after 10 min of dissolution, 212 µg/mL after 45 min with FF-F, 187 µg/mL after 60 min with FF-G, 153 µg/mL after 60 min with FF-H, 145 µg/mL after 30 min with FF-E and 141 µg/mL after 45 min of dissolution with FF-D (see Table 3.13). In short, the higher the amount of the additional polymer, the lower the $c_{max}$ value, except if a blend of COP and HPMC was applied as carrier as in this case, the applied fraction of HPMC seemingly did not alter $c_{max}$.
The stability of the supersaturation was improved if additional polymers were added to the mixture of FF and COP. While the dissolved amount of FF remained for 25 min above half of the respective maximum supersaturation concentration with FF-A, this time interval was extended with formulations FF-D - FF-G to 70-100 min. With formulation FF-H, which is a combination of FF, COP, HPMC, PVCL-PVAc-PEG (1+3+1+1 weighted parts), a decrease of the API concentration was also observed after $c_{max}$. The half-value of the maximal supersaturation concentration $[\mu g/mL]$ ($c_{super}/2$) was not reached within the investigated dissolution time of 120 min, the time period above $c_{super}/2$ is thus longer than 90 min (see Figure 3.25).

The decrease rates after $c_{max}$ were improved regardless whether HPMC or PVCL-PVAc-PEG were used in the polymeric blend, but to a greater extent with HPMC. Possibly, this can be contributed to the recrystallizing inhibiting effect of HPMC (Zhang and Zhou, 2009).

To summarize the results, the dissolution profile of the hot-melt extruded formulation is mainly influenced by the main carrier, in this case COP. The shape of the dissolution curve,

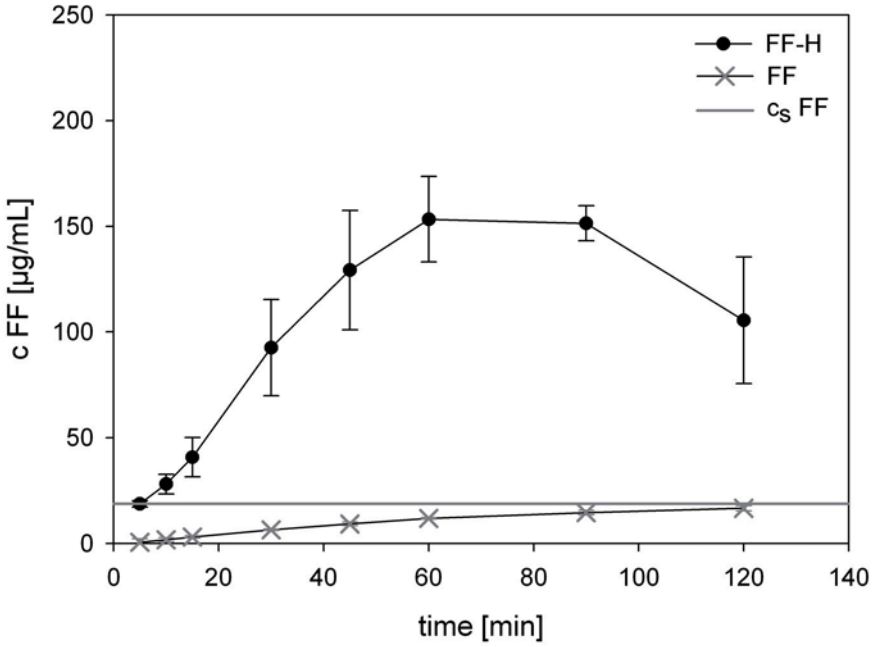


Figure 3.25: Dissolution profile of hot-melt extruded formulation FF-H (FF+COP+PVCL-PVAc-PEG+HPMC = 1+3+1+1 weighted parts) in comparison to pure FF

including the initial dissolution rates and precipitation rates, is influenced by the polymeric additives. The larger the fraction of HPMC or PVCL-PVAc-PEG, the more pronounced is the difference to the dissolution profile of the single polymeric FF-COP formulation FF-A. These findings are in accordance to literature data: While COP extrudates are reported to fully dissolve after approximately 20 min in pH 1.1 medium, it takes approximately 1 h for PVCL-PVAc-PEG extrudates (Kolter et al., 2010). HPMC forms a gel layer due to an absorption of water upon contact with the dissolution medium and subsequent swelling. Diffusion and erosion controlled drug release from HPMC matrix systems takes place (Tu et al., 2010). Nevertheless, an enhancement of the initial release rates of poorly water-soluble APIs was observed with HPMC-based extrudates (Six et al., 2003; Verreck et al., 2003).

XRD analysis showed that all components in the formulations FF-D to FF-H are present in their amorphous state directly after hot-melt extrusion while crystalline API was detected in the untreated physical mixtures. DSC data confirm these findings as no melting peaks indicating the presence of crystalline material in the pellets were detected in the first heating cycle. X-ray diffractograms are shown in Section A.6 of the Appendix.
In all physical mixtures of FF and the polymeric blends, a melting peak was detected in the first heating cycle. It can be clearly attributed to the API (see Tables A.3 and A.5 in the Appendix for $T_g$ and $T_m$ values).
With formulation FF-D, $T_g$ of the extrudate was determined to be 45.9 °C (see Figure 3.26).

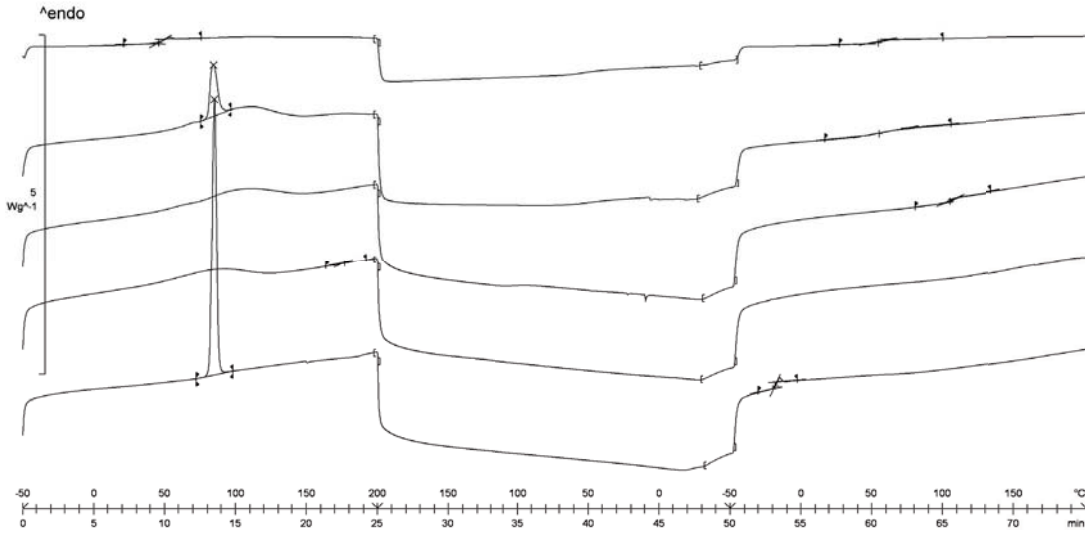


Figure 3.26: DSC thermogram of FF-D extrudate (FF+COP+HPMC = 1+3+0.6 weighted parts) with the following data displayed from top to bottom: pellets, physical mixture, COP, HPMC, pure FF

A single $T_g$ lying intermediate between the values of the individual components ($T_g$FF= -18.5 °C, $T_g$COP=104.9 °C, $T_g$HPMC=176.2 °C) indicates the formation of a glassy solid solution for both physical mixture (second heating cycle) and extrudate (first heating cycle). The same conclusion can be drawn if the fraction of HPMC in the polymer blend is increased as in formulation FF-E: The $T_g$ of the extrudate is at 47.8 °C (see Figure 3.27).

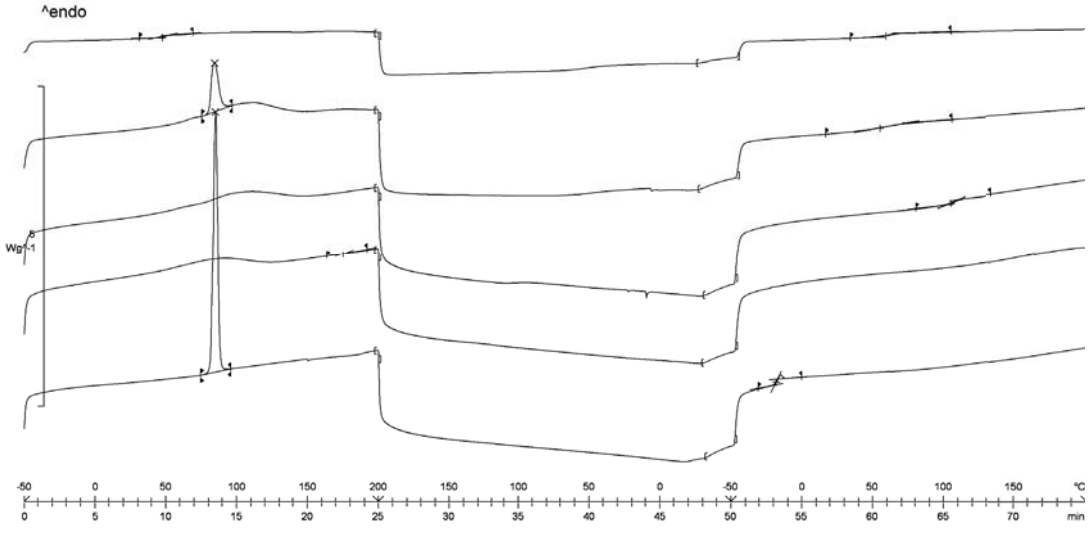


Figure 3.27: DSC thermogram of FF-E extrudate (FF+COP+HPMC = 1+3+1 weighted parts) with the following data displayed from top to bottom: pellets, physical mixture, COP, HPMC, pure FF

With hot-melt extruded formulations FF-F and FF-G, a single glass transition was detected in the first heating cycle at 39.3 and 43.8 °C, respectively (see Figure 3.28 and Figure 3.29).

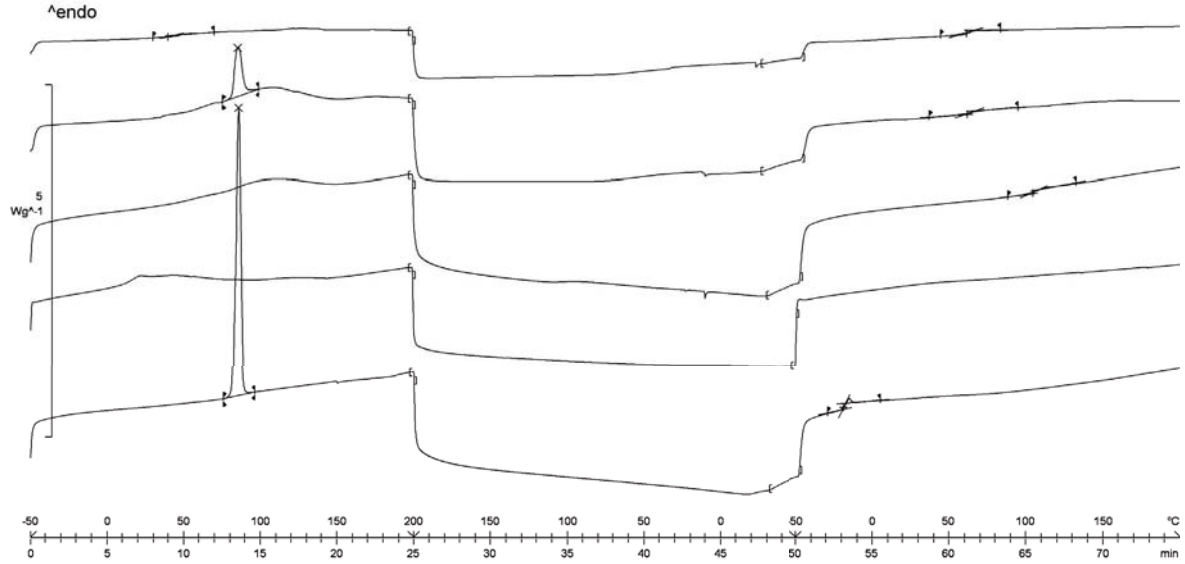


Figure 3.28: DSC thermogram of FF-F extrudate (FF+COP+PVCL-PVAc-PEG = 1+3+1 weighted parts) with the following data displayed from top to bottom: pellets, physical mixture, COP, PVCL-PVAc-PEG, pure FF

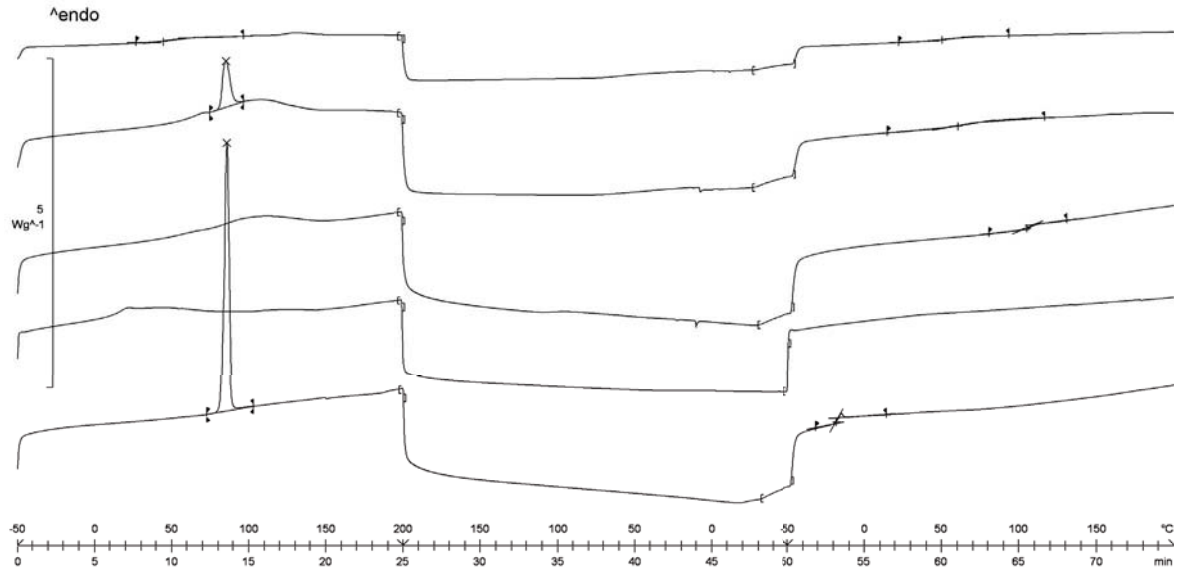


Figure 3.29: DSC thermogram of FF-G extrudate (FF+COP+PVCL-PVAc-PEG = 1+3+1.5 weighted parts) with the following data displayed from top to bottom: pellets, physical mixture, COP, PVCL-PVAc-PEG, pure FF

Although no glass transition was detected for PVCL-PVAc-PEG in any of the samples (extrudate, blend or single component), it is known from the available literature that the $T_g$ is at approximately 70 °C. Again, the single glass transitions of the extrudates are intermediate between the glass transitions of the single components. Therefore, it is assumed that a molecular dispersion of the drug in the polymeric blend is present in the extrudates FF-F and FF-G, thus forming a glass solution.
Figure 3.30 shows a DSC thermogram of FF-H (FF+COP+HPMC+PVCL-PVAc-PEG≡ 1+3+1+1) with a single glass transition of the extrudate at 47.7 °C. In accordance to the previously described hot-melt extruded FF formulations, it can be concluded that a glassy solution of the API and all three polymers is formed.

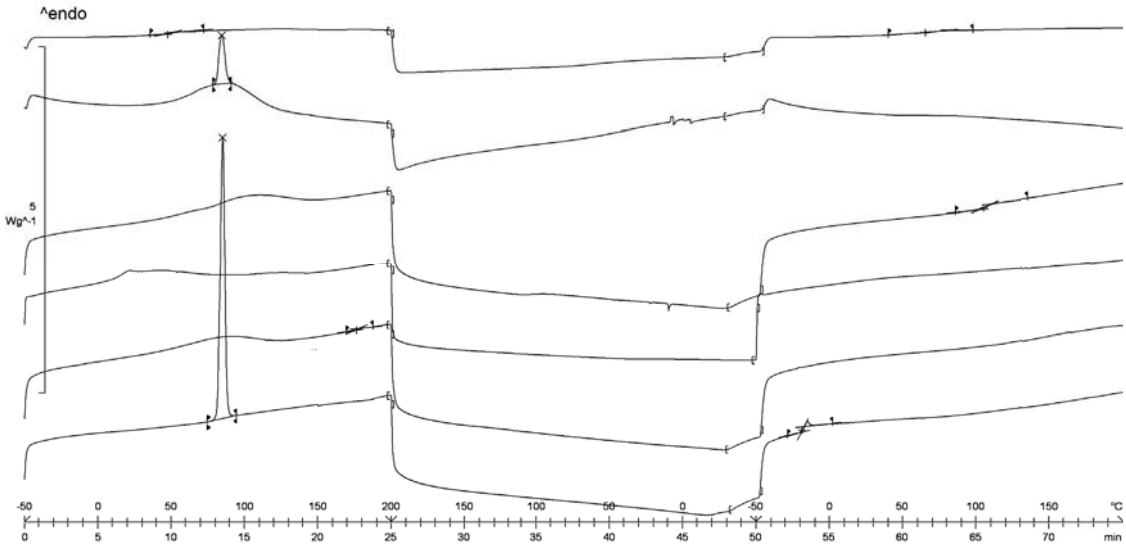


Figure 3.30: DSC thermogram of FF-H extrudate (FF+COP+PVCL-PVAc-PEG+HPMC = 1+3+1+1 weighted parts) with the following data displayed from top to bottom: pellets, physical mixture, COP, PVCL-PVAc-PEG, HPMC, pure FF

In summary, amorphous glassy solutions of FF and carriers were formed with all compositions of the drug and polymers FF-D to FF-H. The dissolution rate of all polymeric blend extrudates was reduced in comparison to the single polymeric FF-COP extrudate FF-A due to the dissolution properties of the polymeric additives PVCL-PVAc-PEG and HPMC. Even so, a remarkable improvement of the dissolution profile in comparison to pure FF powder was shown. The decrease rate after $c_{max}$ which is a measure for the precipitation rate of the API was successfully reduced by the application of additional polymers. The stability of the supersaturation level was improved with increasing amounts of HPMC and/or PVCL-PVAc-PEG in the polymeric blend.
In conclusion, the modification of the composition of the polymeric carrier is a suitable method to improve the release profile of a hot-melt extruded formulation. If the dissolution properties of the additional polymers after their extrusion are known beforehand, predictions on the dissolution behavior of the formulation can be made.

### 3.2.7 Effect of an additional polymer in the dissolution medium on the supersaturation stability of fenofibrate extrudate

Although a supersaturation was achieved with all manufactured extrudates FF-A to FF-H, the level of supersaturation was not stable for any of the extrudates even if the stability was improved by applying polymeric blends as carriers. Due to precipitation processes, the API did not dissolve completely (100 % ≡ 290 µg/mL of dissolved API).
HPMC is a known recrystallization inhibitor in dissolution media (He, 2009). It was successfully applied as an additive to the dissolution medium with the aim to facilitate a stabilization of the supersaturation level of a celecoxib-aPMMA extrudate: A hot-melt extruded, amorphous dispersion of the drug in the carrier with high initial supersaturation levels and a subsequent drop of the concentration due to a recrystallization of the drug was submitted to dissolution experiments applying HPMC as an additive to the dissolution medium. The precipitation of the drug was successfully delayed (Albers et al., 2009).
Adding HPMC to the FF-carrier mixture prior to the extrusion improves the stability of the supersaturation level (see Section 3.2.6). Even so, a decrease of the supersaturation level was observed within 120 min of dissolution time. To evaluate the external stabilizing effect of HPMC as it was observed by Albers et al. (2009), 145 mg of HPMC were added to 500 mL of dissolution medium and conditioned at 37 °C for approximately 1 h prior to adding the hot-melt extruded FF-COP formulation FF-A. Contrary to the results reported for the celecoxib-aPMMA extrudate, no stabilizing effect of HPMC was observed as the dissolution profiles of FF-A using the dissolution medium with or without additives exhibit no significant difference (see Figure 3.31).

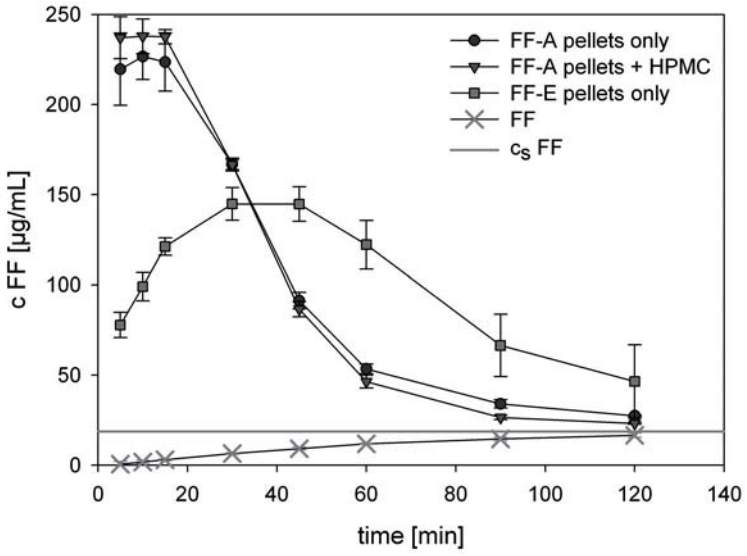


Figure 3.31: Dissolution profiles of FF-A (FF+COP = 1+3 weighted parts) extrudates with or without the addition of HPMC to the dissolution medium in comparison to FF-E extrudate (FF+COP+HPMC = 1+3+1 weighted parts)

If the respective amount of HPMC is added to the FF-COP mixture prior to the extrusion, the release profile of the extrudate is altered: The decrease of the initial release rate of the sample in comparison to FF-A extrudate can be contributed to a slower erosion of HPMC in contrast to a fast dissolution of COP. The supersaturation levels that are reached with formulation FF-E remain below the levels reached with FF-A. Nevertheless, it is clearly shown that the recrystallization of the drug is delayed if HPMC is employed as additional carrier as in formulation FF-E.
Referring to the mechanism of carrier-controlled drug dissolution from solid dispersion systems as proposed by Craig (2002), it is concluded that the formation of a polymer-rich layer surrounding the pellet surface is essential for an effect of additional polymers on the dissolution performance of the manufactured glassy solution. If HPMC is added to the dissolution medium, the concentration of this recrystallization inhibiting agent in the polymer-rich layer is not sufficient for a stabilizing effect on the supersaturation level. A positive effect of HPMC on the supersaturation stability was pointed out if added prior to the hot-melt extrusion.

### 3.2.8 Storage stability of fenofibrate extrudates

It was observed that the dissolution performance of all FF extrudates but formulation FF-B (FF-HPMC extrudate; API-polymer ratio = 1+3 weighted parts) decreases with increasing storage times. Exemplarily, the dissolution profile of FF-COP formulation FF-A is shown in Figure 3.32. For the dissolution profiles of formulations FF-B to FF-H see the Appendix Section A.1.

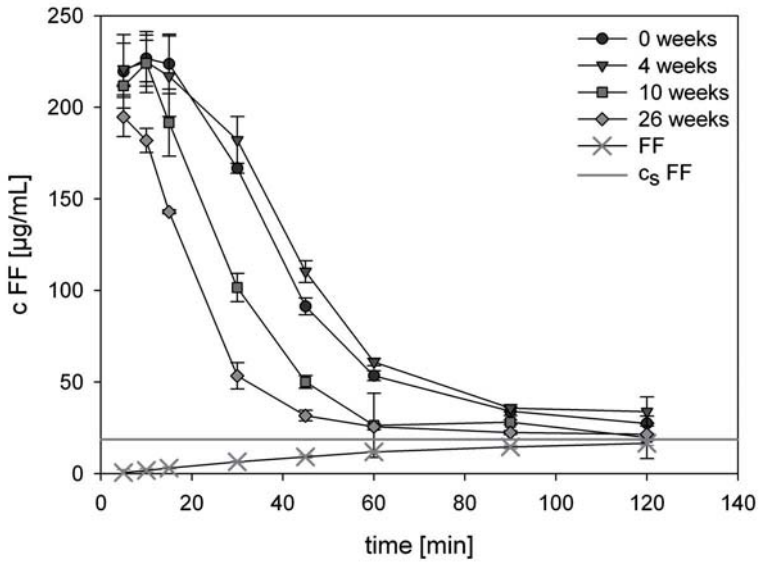


Figure 3.32: Dissolution profiles of formulation FF-A pellets (FF+COP = 1+3 weighted parts) stored at 25 °C /60 % rH for 0, 4, 10 and 26 weeks

XRD and DSC methods were applied to determine whether this behavior can be contributed to changes in the solid state of the extruded formulations. It was shown with XRD analysis that no recrystallization of FF is occurring in FF-COP (1+3 weighted parts) formulation FF-A while FF recrystallizes if HPMC (FF-B) or PVCL-PVAc-PEG (FF-C) are used as carrier, after 10 weeks and 26 weeks of storage, respectively (see Figures 3.33 - 3.35).

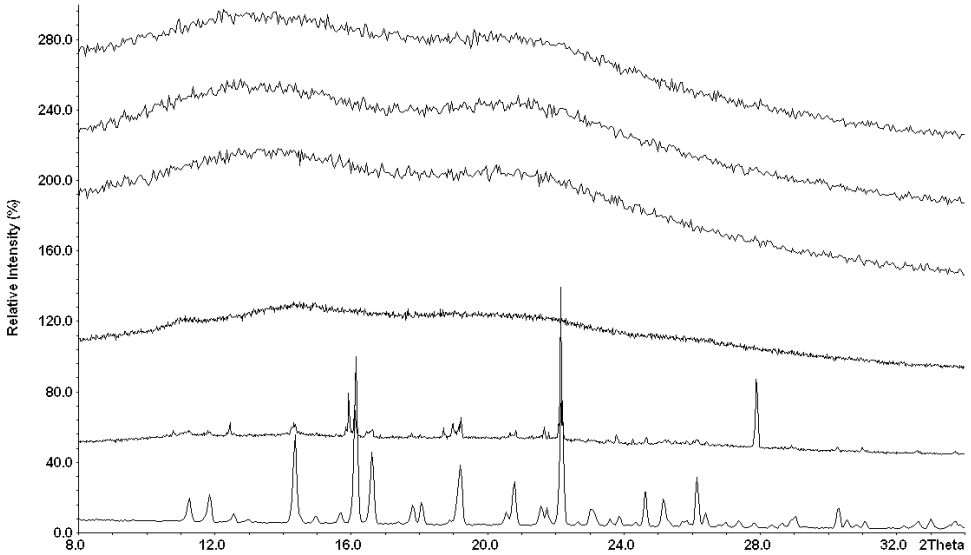


Figure 3.33: XRD pattern of FF-A extrudate (FF+COP = 1+3 weighted parts) with the following data displayed from top to bottom: pellets after 0, 4, 10 and 26 weeks of storage at 25 °C /60 % rH, physical mixture, pure FF

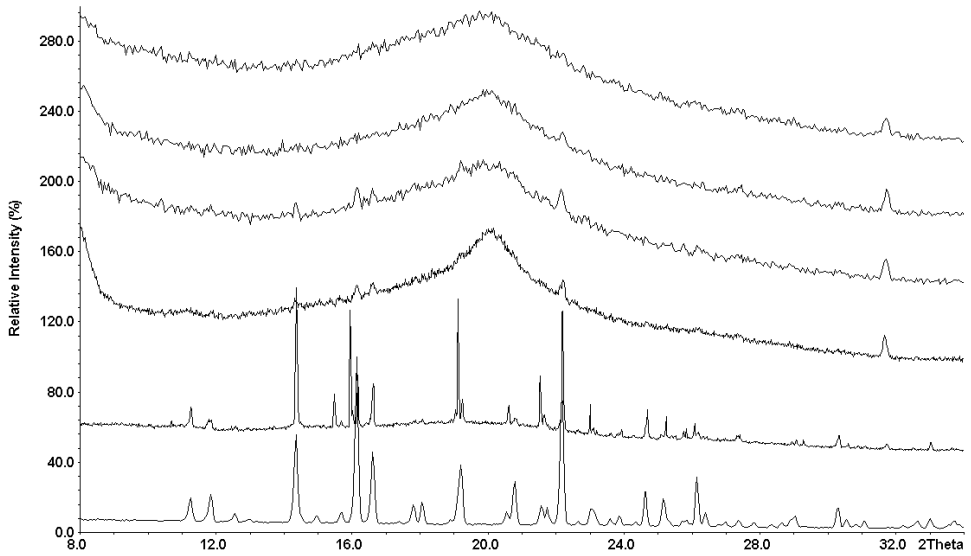


Figure 3.34: XRD pattern of FF-B extrudate (FF+HPMC = 1+3 weighted parts) with the following data displayed from top to bottom: pellets after 0, 4, 10 and 26 weeks of storage at 25 °C /60 % rH, physical mixture, pure FF

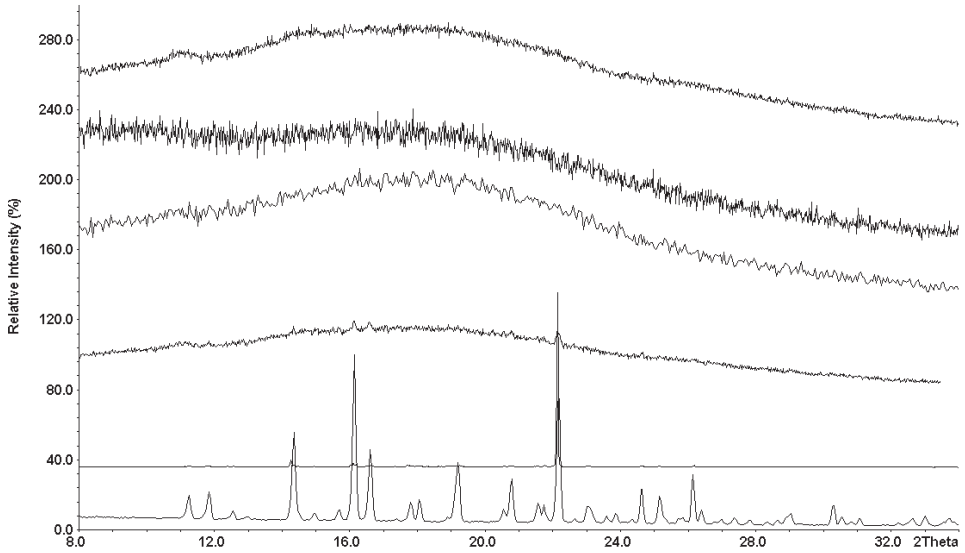


Figure 3.35: XRD pattern of FF-C extrudate (FF+PVCL-PVAc-PEG = 1+3 weighted parts) with the following data displayed from top to bottom: pellets after 0, 4, 10 and 26 weeks of storage at 25 °C /60 % rH, physical mixture, pure FF

In the thermograms of FF-B and FF-C, a small endothermic event is detected at approximately 80 °C after 10 weeks of storage, possibly indicating a recrystallization of FF within 10 weeks at 25 °C /60 % rH (see Figures 3.36 and 3.37).

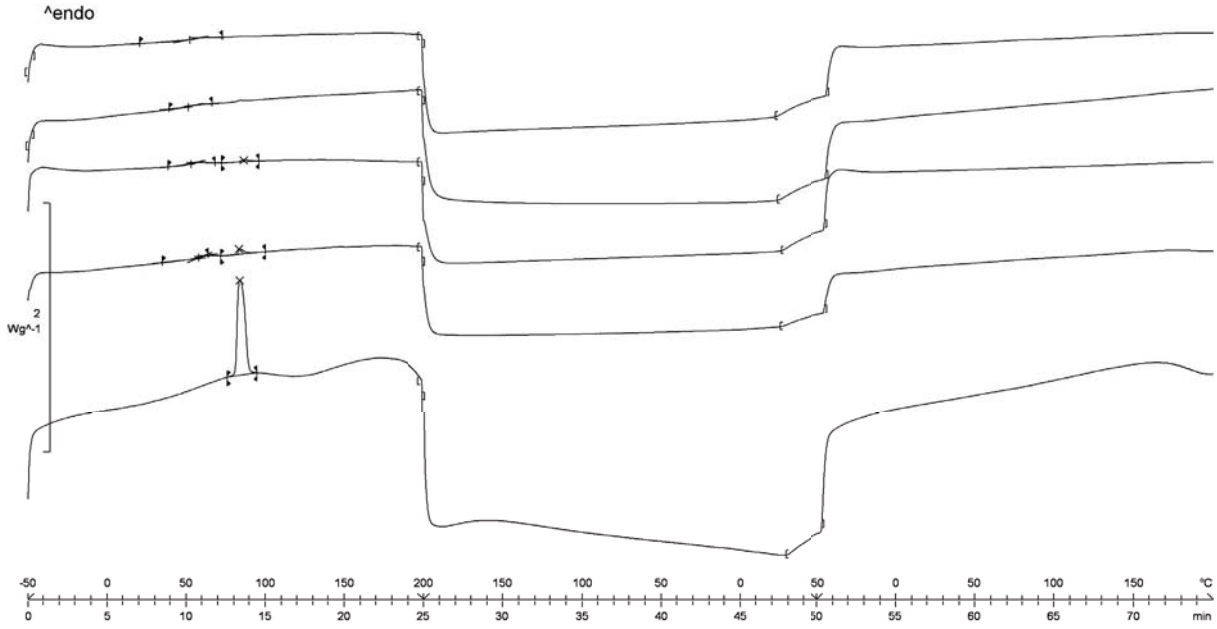


Figure 3.36: DSC thermogram of FF-B extrudate (FF+HPMC = 1+3 weighted parts) with the following data displayed from top to bottom: pellets after 0, 4, 10 and 26 weeks of storage at 25 °C /60 % rH, physical mixture

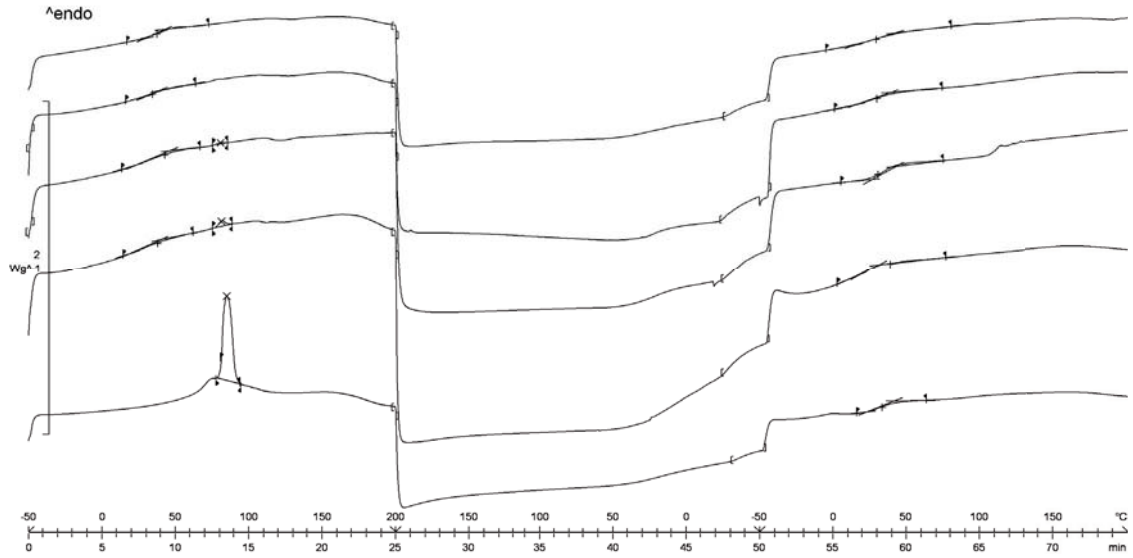


Figure 3.37: DSC thermogram of FF-C extrudate (FF+PVCL-PVAc-PEG = 1+3 weighted parts) with the following data displayed from top to bottom: pellets after 0, 4, 10 and 26 weeks of storage at 25 °C /60 % rH, physical mixture

In contrast, no crystalline FF was detected in any of the formulations where COP is employed as carrier regardless of the analytical method employed (see Figures 3.33 and 3.38 for XRD and DSC stability data of FF-A and Sections A.6 and A.10 of the Appendix for stability data of formulations FF-D to FF-H).

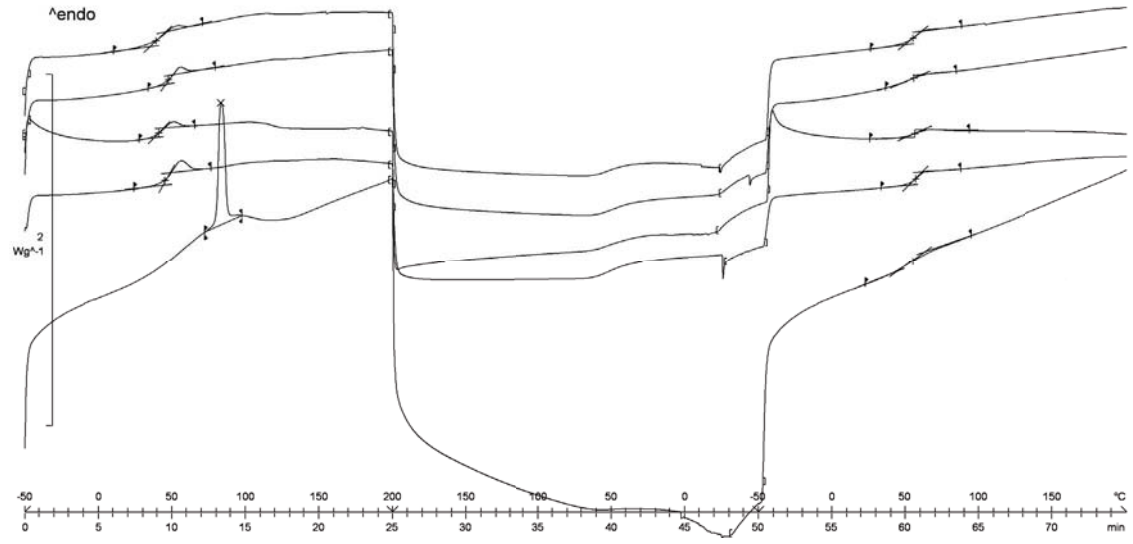


Figure 3.38: DSC thermogram of FF-A extrudate (FF+COP = 1+3 weighted parts) with the following data displayed from top to bottom: pellets after 0, 4, 10 and 26 weeks of storage at 25 °C /60 % rH, physical mixture

It can be concluded that extrudates FF-A and FF-D to FF-H remain amorphous throughout the storage time of 26 weeks or that the crystallinity content remains below the limit of detection (LOD) of both XRD and DSC. These results can be contributed to the recrystallization inhibiting effect of COP in solid dispersions (Matsumoto and Zografi, 1999; Zhang and Zhou, 2009).
The glass transition temperatures of all pellets which were detected using DSC remain in the range of 40-50 °C throughout the investigated storage time. It is therefore concluded that although a recrystallization of the API is occurring in hot-melt extruded formulations FF-B and FF-C, the amorphous part of the drug forms a glass solution with the carrier(s) while the recrystallized part of the API forms a glassy suspension with the carrier(s).

In summary, the drop of the release profiles with increasing storage times cannot be contributed to a recrystallization of the API. These findings are in accordance to the observations of Lloyd et al. (1999) who pointed out that the dissolution profile of a carrier-controlled system is independent of the drug properties. Instead, the system is strongly influenced by changes of the carrier properties (Craig, 2002). As a matter of fact, it was noted that in some of the DSC thermograms a relaxation peak was detected (see Figures 3.38 and A.30 - A.34 of the Appendix). This endothermic event at $T_g$ during the first heating cycle suggests a physical aging of the polymeric carrier(s) that occurs during the storage period. As this relaxation peak was only observed if COP was employed as carrier for FF, this aging is attributed to this polymer. Aging of the polymer affects its molecular mobility and might lead to changes of its water permeability and dissolution rate (Guo et al., 1991; Graeser, 2009). The change of the dissolution profile with increasing storage times which is shown by all extrudates with COP as carrier is in agreement with this hypothesis.

Karl-Fischer titration was used to determine whether also an increasing humidity content of the extrudates is responsible for the change of the dissolution performance. It was shown that the water content of the extrudates is continuously increasing during storage. While the water content of the extrudates was 0.4 % - 1.1 % directly after manufacture, it has increased to up to 2.2 % after 26 weeks of storage (see Table 3.14).

Table 3.14: Water content of extrudates after 0, 4 and 26 weeks of storage in PE double pouches at 25 °C /60 % rH (see Table 6.7 for the extrudates' composition)

| Formulation | water content [%] | | |
|---|---|---|---|
| | 0 weeks | 4 weeks | 26 weeks |
| FF-A | 0.6 | 1.7 | 1.9 |
| FF-B | 1.0 | - | - |
| FF-C | 0.4 | 0.8 | 1.3 |
| FF-D | - | - | 2.2 |
| FF-E | - | - | 1.9 |
| FF-F | - | - | 1.9 |
| FF-G | 1.1 | 1.8 | 2.2 |
| FF-H | - | - | 1.7 |

Unfortunately, the data sets are not complete as the analytical method was not available at all times. Even so the extrudates' tendency to absorb water during storage becomes clear from the depicted data. A more thorough analysis of the humidity content of all extrudates will have to be performed to allow for a definite conclusion about the absorptive power.
It was examined whether the drop of the release profile which was the most pronounced with FF-COP-PVCL-PVAc-PEG formulation FF-G (1+3+1.5 weighted parts) can be avoided if the storage conditions are optimized. For this reason, the release characteristics of a sample stored in polyethylene (PE) double pouches and a sample stored under humidity protection in Activ®-Vials were compared. Two formulations were assessed: FF-COP extrudate FF-A (API to polymer ratio = 1+3 weighted parts) and FF-G extrudate.
The humidity content was shown to decrease from 0.6 % to 0.4 % and from 1.1 % to 0.6 % for formulation FF-A and FF-G, respectively, after 4 weeks of storage in Activ®-Vials (see Table 3.15). If the samples were stored in PE double pouches, the water content of the samples increased to 1.7-1.8 % for formulation FF-A and FF-G, respectively.

Table 3.15: Water content of extrudates after 0 and 4 weeks of storage in Activ®-Vials or PE double pouches at 25 °C /60 % rH

| Formulation | water content [%] | | |
|---|---|---|---|
| | 0 weeks | 4 weeks (PE double pouches) | 4 weeks (Activ®-Vials) |
| FF-A | 0.6 | 1.7 | 0.4 |
| FF-G | 1.1 | 1.8 | 0.6 |

The polymeric desiccant sleeve inside the Activ®-Vials not only absorbs water from the surrounding air inside the container, but also from the pellets leading to a reduction of the humidity content. Active drying of the formulation takes place. For FF-A, no effect on the dissolution profile was observed if stored for 4 weeks (see Figure 3.39).

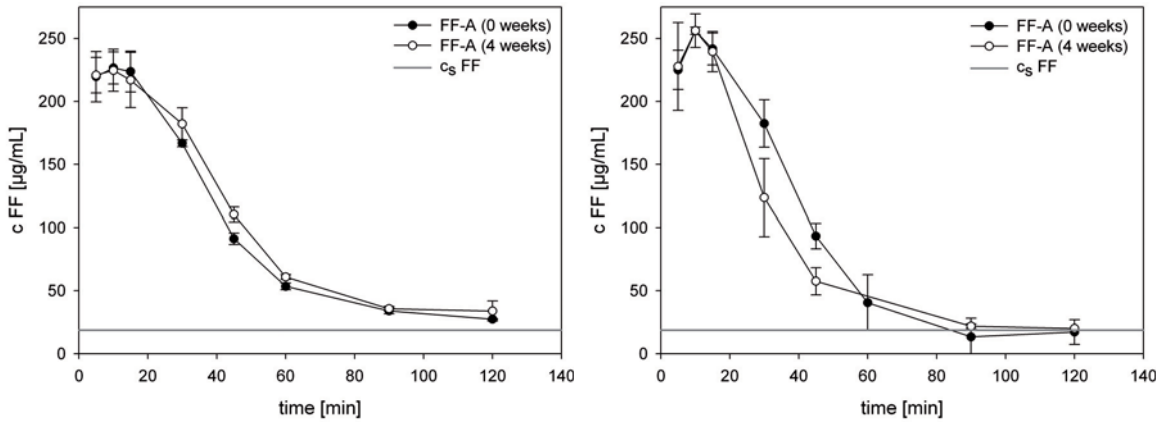


(a) PE double pouches (b) Activ®-Vials

Figure 3.39: Dissolution profiles of FF-A pellets (FF+COP≡1+3) before and after 4 weeks of storage at 25 °C /60 % rH in a) PE double pouches or b) Activ®-Vials

It is possible that the influence of the water content becomes more pronounced with increasing storage times as the dissolution profile was similar for FF-A samples stored for 0 and 4 weeks, regardless of the packaging material, while a decrease was observed with samples that were stored for 10 weeks or longer (see Figure 3.32 on page 55). With formulation FF-G, it was demonstrated that an increase of the humidity content does indeed have an influence on the release behavior of the solid dispersion formulation (see Figure 3.40).

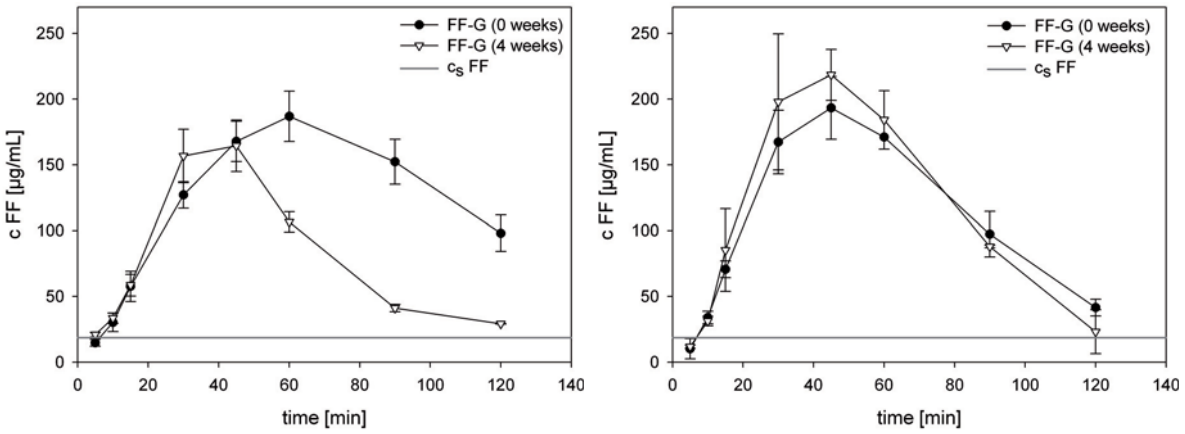


(a) PE double pouches (b) Activ®-Vials

Figure 3.40: Dissolution profiles of FF-G extrudate (FF+COP+PVCL-PVAc-PEG = 1+3+1.5 weighted parts) before and after 4 weeks of storage at 25 °C /60 % rH in a) PE double pouches or b) Activ®-Vials

The plasticizing effect of water is assumed to reduce polymer-polymer and drug-polymer interactions in solid dispersions, especially with hydrophilic polymers, possibly influencing the dissolution profile of the manufactured extrudates (Vasanthavada et al., 2004; Wypych, 2004a,b, pp.2-5 and 280-281). Depending on the applied drug and the polymer or polymeric blend used as carrier, the influence of the humidity content will vary as the interactions will differ. No correlation of the amount of absorbed water and the $T_g$ value of the extrudates which is usually associated with its plasticizing effect was determined using DSC (see Table A.5 of the Appendix).
It was successfully pointed out that the observed decrease of the dissolution performance with increasing storage times can be contributed to multiple processes taking place within the extrudates:

- a recrystallization of the API as it was observed for HPMC and PVCL-PVAc-PEG formulations FF-B and FF-C,
- a relaxation of the polymeric carrier which was detected for COP fomulations resulting in a change of the physical and/or chemical properties of the polymer and
- an increasing humidity content of the extrudates which can be avoided by an optimization of the packaging material.

## 3.3 Solubility enhancement of oxeglitazar via hot-melt extrusion

### 3.3.1 Introduction and objectives

The dissolution behavior of poorly water-soluble drug FF was successfully improved through HME. Amorphous one-phase systems were manufactured with all investigated FF-carrier formulations but FF-PVA-AA-MMA (see Section 3.2). Difficulties concerning the stability of the supersaturation and storage stability were encountered. Modifications of the carrier composition and packaging were shown to improve the stability of the dissolution profile.
FF is a compound with a low melting point ($T_m$=81.4 °C). It has a plasticizing effect on the polymeric carrier. To investigate the transferability of the results gained with FF onto extrudates using a drug with different physicochemical characteristics, OX was employed as second API ($T_m$=158.2 °C).
Solid dispersions with OX were successfully manufactured using various methods, for example spray-freezing and co-evaporation (see also Section 1.5.3) (Badens et al., 2009; Majerik et al., 2006, 2007). The application of HME is not reported in the available literature. Therefore, the aim of this work was not only to investigate the transferability of FF results to OX, but especially the suitability of HME for solubility enhancement of OX in general. Special emphasis was laid upon the miscibility of the components and the classification of the present solid dispersion system after extrusion.
While FF is a neutral compound, OX is an acidic substance. Due to its acidic character, the solubility of OX in acidic media or water is too low and in media pH>6.4 too good to enable the monitoring of changes in the dissolution behavior which are induced by the method of manufacture and to detect differences between the various formulations (see Table 3.16). For these reasons, instead of Ph.Eur. hydrochloric acid medium pH 1.2 as in the case of FF, Ph.Eur. phosphate buffer solution pH 6.4 was chosen for OX to ensure a discriminatory dissolution method. The applied quality control method does not consider in vivo conditions.

Table 3.16: Solubility of oxeglitazar in various media at 37 °C (data are partly derived from Majerik (2006) and Majerik et al. (2007))

| Solvent | Solubility [µg/mL] |
|---|---|
| Hydrochloric acid medium pH 1.2 | - |
| Purified water | 3.0 |
| Phosphate buffer solution pH 6.4 + 0.1 % polysorbate 80 | 38.1 |
| Phosphate buffer solution pH 6.8 | 68.3 |
| Phosphate buffer solution pH 6.8 + 0.1 % polysorbate 80 | 71.9 |
| Phosphate buffer solution pH 7.2 | 180.9 |
| Phosphate buffer solution pH 7.4 | 240.1 |
| Phosphate buffer solution pH 8.0 | 683.9 |

### 3.3.2 Hot-melt extrusion of oxeglitazar with single polymeric carriers

To investigate the transferability of the results from HME trials with FF as API, OX was extruded using the same carriers COP, HPMC and PVCL-PVAc-PEG. Accordingly, the formulations in which only one polymeric carrier is applied are abbreviated with OX-A, OX-B and OX-C (see Table 3.17 for their composition).

Table 3.17: Composition of OX-single polymer extrudates that served as a comparison to the corresponding FF extrudates. Data are given in weighted parts unless otherwise specified.

| Formulation | OX | COP | HPMC | PVCL-PVAc-PEG | drug load [%] |
|---|---|---|---|---|---|
| OX-A | 1 | 3 | - | - | |
| OX-B | 1 | - | 3 | - | 25.0 |
| OX-C | 1 | - | - | 3 | |

Different from the FF extrudates, the initial release rate of OX was not enhanced via HME, but reduced. Nevertheless, the overall dissolution performance of formulations OX-A and OX-B was improved as the release from both formulations exceeds $c_s$ within 30 min of dissolution (see Figures 3.41 and 3.42). Formulation OX-A reaches $c_{max}$ after 60 min.

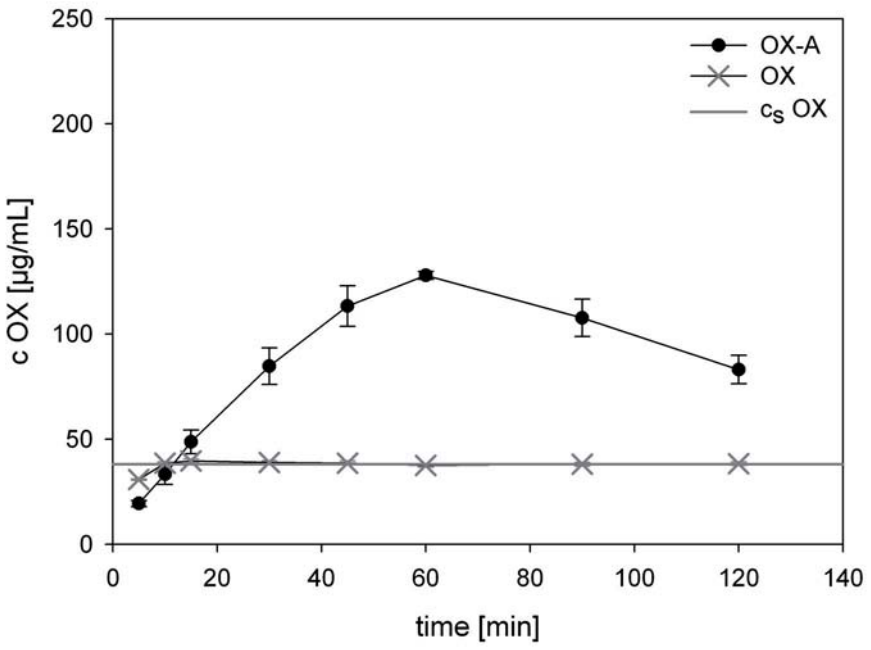


Figure 3.41: Dissolution profile of OX-A pellets (OX+COP = 1+3 weighted parts) in comparison to pure OX

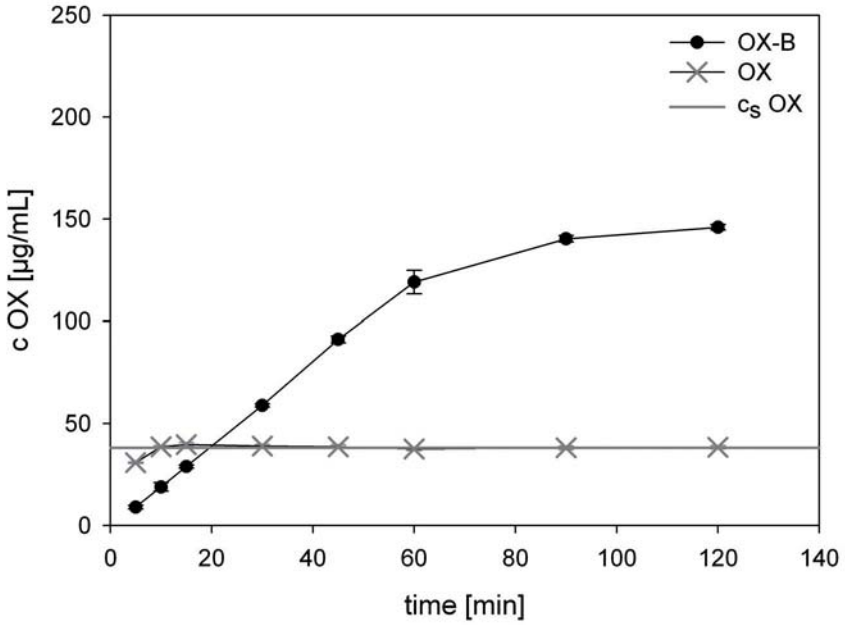


Figure 3.42: Dissolution profile of OX-B pellets (OX+HPMC = 1+3 weighted parts) in comparison to pure OX

At this sampling point, 128 µg/mL of OX are dissolved, resulting in a dissolved amount of 44 % of total API. After $c_{max}$ which is 3.4 times above saturation level, the concentration of dissolved API decreases. It has to be assumed that a recrystallization of OX is occurring in the dissolution medium (see Figure 3.41). No $c_{max}$ is reached with OX-B within 120 min. At the last sampling point (120 min), the OX concentration was 146 µg/mL which corresponds to 50 % of dissolved API and is 3.8 times above $c_s$ (see Figure 3.42).
It was derived from the manufacturer's information that PVCL-PVAc-PEG exhibits an instant release profile when applied as excipient in HME (Kolter et al., 2010). Furthermore, it is documented that PVCL-PVAc-PEG improves drug solubility by forming micelles. The CMC is reported to be 7.6 µg/mL (Technical Information Soluplus). As the amount of PVCL-PVAc-PEG per OX-C sample is 435 mg, a concentration of 870 µg/mL of PVCL-PVAc-PEG in the dissolution vessel would be reached in the case of a complete dissolution of the sample which exceeds the specified CMC by far. Even if the total concentration of the excipient in the vessel is too low to reach CMC due to a slow dissolution rate of the pellet, the local concentration of dissolved PVCL-PVAc-PEG in the diffusion layer surrounding the pelletized extrudate is expected to reach CMC level. Hence, an improvement of the dissolution performance of OX was expected for hot-melt extruded formulation OX-C.
Contrary to these expectations, the amount of OX that was released from OX-C pellets within 120 min of dissolution reached only half of the saturation concentration. In fact, the dissolution performance of the untreated OX powder without any additives is superior to hot-melt extruded formulation OX-C. After 120 min of dissolution, release from OX-C is 18 µg/mL which corresponds to 6 % of total API while 38 µg/mL are reached with pure OX (13 % of total API; see Figure 3.43).

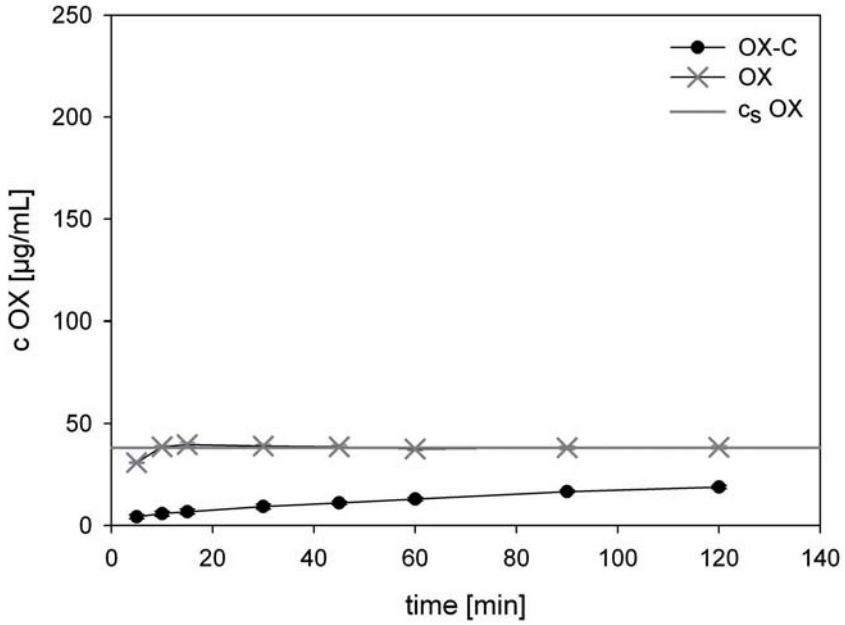


Figure 3.43: Dissolution profile of OX-C pellets (OX+PVCL-PVAc-PEG≡1+3) in comparison to pure OX

When comparing the data to the manufacturer's information, it becomes clear that without further processing of the extrudates, for example by milling, the dissolution rate of PVCL-PVAc-PEG is drastically decreased: For instance, the dissolution time of COP extrudates in pH 6.8 medium is reported to be 21 min while a PVCL-PVAc-PEG extrudate needs 1 h 35 min to dissolve completely (Kolter et al., 2010). As shown above, these findings were confirmed with OX-C pellets (OX+PVCL-PVAc-PEG = 1+3 weighted parts). A further processing of the extrudate might improve the APIs dissolution behavior. However, as the aim of this work was to evaluate HME technology and its potential for solubility enhancement of poorly water-soluble APIs in general, the investigation of various and, possibly, time-consuming down-processing methods was not within the scope of the study.

From XRD diffractograms it is derived that all components are present in their amorphous form after the extrusion (see Figure 3.44 for exemplary XRD data of formulation OX-A, XRD diffractograms of OX-B and -C are assessed in more detail in Section 3.3.8).
DSC analysis confirmed these results as no melting peak was detected with any of the OX extrudates (see Figure 3.45 for exemplary DSC data of formulation OX-A, DSC thermograms of OX-B and -C are assessed in more detail in Section 3.3.8). The glass transition temperature of the pure API was determined to be at approximately 40 °C (see Table A.3). For the physical mixtures of OX-A (OX+COP≡1+3) and OX-B (OX+HPMC≡1+3), a melting peak of the drug was found in the first heating cycle. No melting peak was observed with the physical mixture of OX-C (OX+PVCL-PVAc-PEG≡1+3), however, a small endothermic event was detected at approximately 160 °C which can be associated with the melting of the crystalline API.

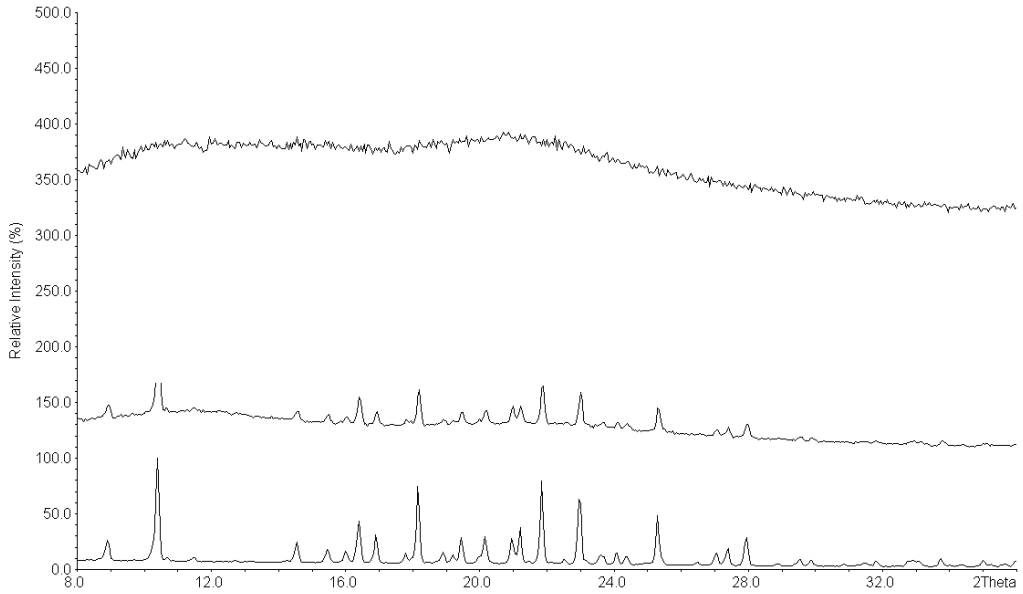


Figure 3.44: XRD pattern of OX-A extrudate (OX+COP≡1+3) with the following data displayed from top to bottom: OX-A pellets, physical mixture, pure OX

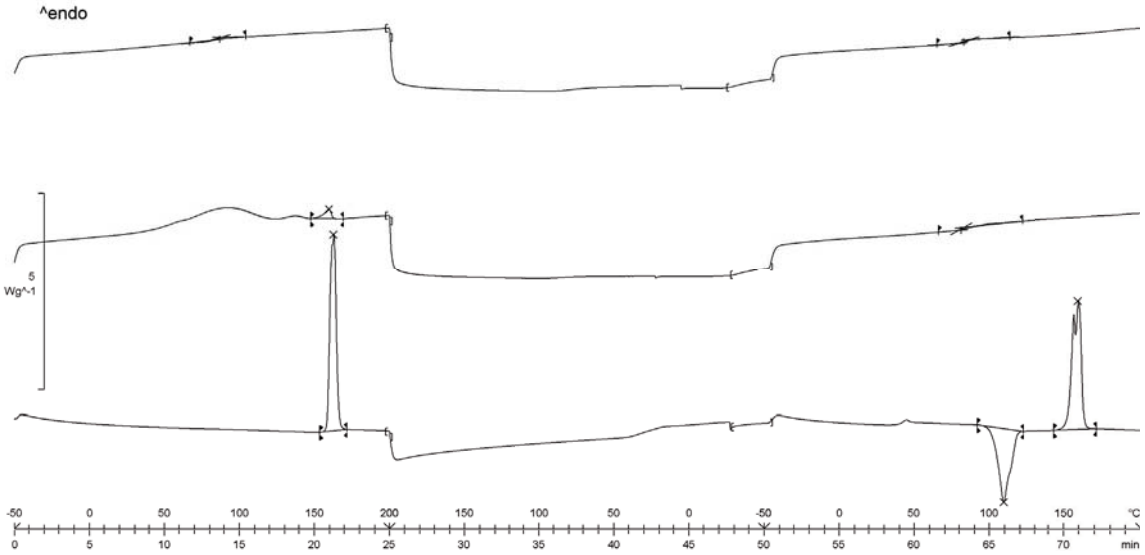


Figure 3.45: DSC thermogram of OX-A extrudate (OX+COP = 1+3 weighted parts) with the following data displayed from top to bottom: OX-A pellets, physical mixture of the components, pure OX

With hot-melt extruded formulation OX-A, $T_g$ of the extrudate is at 87 °C which is intermediate between the glass transition temperatures of the API and the carrier, indicating a one phase system of the drug and the carrier. The second heating cycle of both the extrudates and their physical mixtures of formulations OX-A and OX-B shows that a formation of a

one-phase system of OX and COP or HPMC is possible: Only one $T_g$ at approximately 80 °C was detected for OX-A samples, and one $T_g$ at approximately 70 °C for formulation OX-B (see Table A.6). It is thus concluded that the API is molecularly dispersed in the amorphous carrier forming a glassy solution.
With formulation OX-C however, a lower value for $T_g$ was determined in the first heating cycle. It is at approximately 40 °C, indicating a glass transition of the pure API. With PVCL-PVAc-PEG alone, no clear $T_g$ could be determined via DSC analysis as it is overlaid by, most likely, the evaporation of water. Thus it is possible that no $T_g$ was observed for the polymeric carrier, although a two phase system is present in the extrudate. The second heating cycle of both OX-C extrudate and its physical mixture showed a glass transition temperature at approximately 60 °C indicating the presence of a one phase system. It was thus shown that a glassy solution is possible with OX and PVCL-PVAc-PEG. However, it was not obtained by the applied HME process.

### 3.3.3 Hot-melt extrusion of oxeglitazar with mixtures of polymeric carriers

Polymeric mixtures were used as carriers for OX to investigate the transferability of the results gained with the drug FF to a drug with different physicochemical properties. Another aim was to determine whether the dissolution behavior and especially the initial release rate of OX formulations with PVCL-PVAc-PEG as carrier would be improved by applying polymeric blends.
The composition of the polymeric blends is shown in Table 3.18.

Table 3.18: Composition of OX extrudates with polymeric blends as carrier that served as a comparison to the corresponding FF extrudates. Data are given in weighted parts unless otherwise specified.

| Formulation | OX | COP | HPMC | PVCL-PVAc-PEG | drug load [%] |
|---|---|---|---|---|---|
| OX-D | 1 | 3 | 1 | - | 20.0 |
| OX-E | 1 | 3 | - | 1 | 20.0 |
| OX-F | 1 | 3 | 1 | 1 | 16.7 |

The dissolution profiles of PVCL-PVAc-PEG formulations OX-E (OX+COP+PVCL-PVAc-PEG≡1+3+1) and OX-F (OX+COP+HPMC+PVCL-PVAc-PEG≡1+3+1+1) are depicted in Figures 3.46 and 3.47.

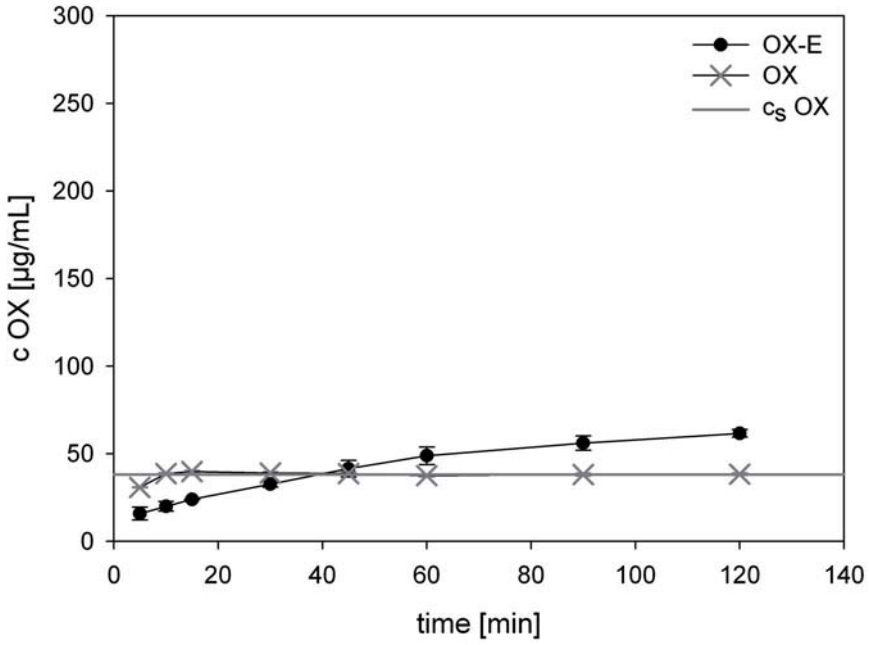


Figure 3.46: Dissolution profile of hot-melt extruded formulation OX-E (OX+COP+PVCL-PVAc-PEG = 1+3+1 weighted parts)

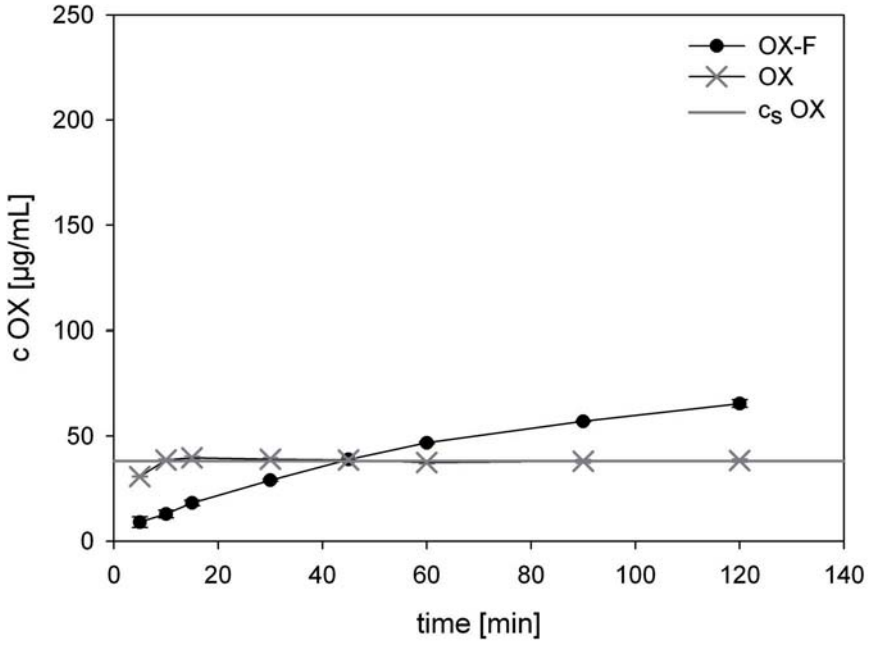


Figure 3.47: Dissolution profile of hot-melt extruded formulation OX-F (OX+COP+HPMC+PVCL-PVAc-PEG = 1+3+1+1 weighted parts)

Again, the initial release rates are reduced through the addition of PVCL-PVAc-PEG if compared to the pure API or the corresponding extrudates without added PVCL-PVAc-PEG

(see Figure 3.41 with the dissolution data for OX-COP formulation OX-A and Figure 3.48 for OX-COP-HPMC formulation OX-D). No $c_{max}$ is reached with either of the two PVCL-PVAc-PEG extrudates within the dissolution time of 120 min. The detected concentration maximum at the 120 min sampling point is 61.6 µg/mL with OX-E (OX+COP+PVCL-PVAc-PEG≡1+3+1) and 65.5 µg/mL with OX-F (OX+COP+HPMC+PVCL-PVAc-PEG ≡1+3+1+1). These values exceed $c_s$ by a factor of 1.6 and 1.7 for OX-E and OX-F, respectively. 21 % of total API are dissolved after 120 min of dissolution testing with OX-E and 23 % with OX-F. These results confirm the findings observed with OX and single polymeric carriers described in Section 3.3.2.

In summary, the dissolution performance of OX during the first 45-120 min of dissolution is drastically reduced if PVCL-PVAc-PEG is used as single or additional carrier as the released amount of OX remains below $c_s$ and the level of the pure API.
For the OX extrudate with a blend of the polymers COP and HPMC as carriers as in OX-D (OX+COP+HPMC = 1+3+1 weighted parts), a super-additive effect was observed (see Figure 3.48). The initial release rate of hot-melt extruded formulation OX-D (OX+COP+HPMC≡1+3+1) was superior to the release rates of both formulations OX-A (OX+COP ≡1+3) and OX-B (OX+HPMC≡1+3), in which only one of the two polymers is applied as carrier. With OX-D extrudate, the dissolved amount of OX is already at $c_s$ level at the first sampling point (5 min) while in the case of OX-A, $c_s$ is exceeded after 10 min of dissolution and in the case of OX-B after 15 min of dissolution. OX-D reaches $c_{max}$ after 45 min. At this sampling point, 191 µg/mL of OX were dissolved which corresponds to 66 % of total API and is 5.0 times above $c_s$ (see Figure 3.48).

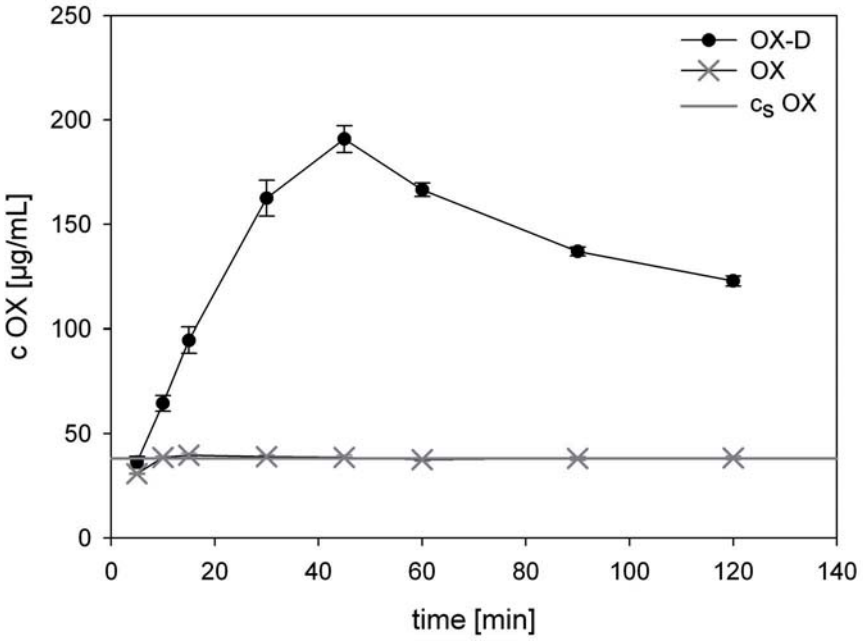


Figure 3.48: Dissolution profile of hot-melt extruded formulation OX-D (OX+COP+HPMC = 1+3+1 weighted parts)

As described in Section 3.3.2, the $c_{max}$ value for OX-A was determined to be 128 µg/mL while no $c_{max}$ was obtained for OX-B within 120 min.
Regarding the shape of the dissolution curves of the extrudates with single polymeric carriers and the extrudates with the polymeric blend of COP and HPMC as carrier, it can be stated that the overall curve progression is primarily influenced by COP as the main carrier (COP:HPMC ratio = 3:1). Due to the stabilizing function of HPMC, $c_{max}$ is increased. At the same time, it does not have an influence on the decrease rate after $c_{max}$ as these are approximately equivalent. Apparently, the amount of HPMC that is applied in formulation OX-D is not sufficient for a reduction of the recrystallization rate of the API.

In analogy to the results described in Section 3.3.2, no crystalline API was detected in the pelletized extrudates using XRD and DSC analysis. However, it has to be pointed out that no distinct melting peak in the first heating cycle was detected with the physical mixtures of formulations OX-D and OX-F although crystalline material is present in this blend. With formulation OX-E, a small endothermic event was found at approximately 160 °C, indicating the presence of an OX melting peak. Due to these findings, XRD had to be employed to verify the results. As the LOD of this method was quite high for crystalline OX (2-5 % of API may go undetected as is shown in Section C.1 of the Appendix), the presence of small amounts of crystalline API in the hot-melt extruded formulations cannot be excluded.
In the first heating cycle of hot-melt extruded formulation OX-D (OX+COP+HPMC≡1+3 +1), a single glass transition was detected at 84.4 °C (see Figure 3.49). Comparing the results to the second heating cycle of the physical mixture of the components ($T_g$=87.3 °C), these findings point to a formation of a glassy solution with formulation OX-D.

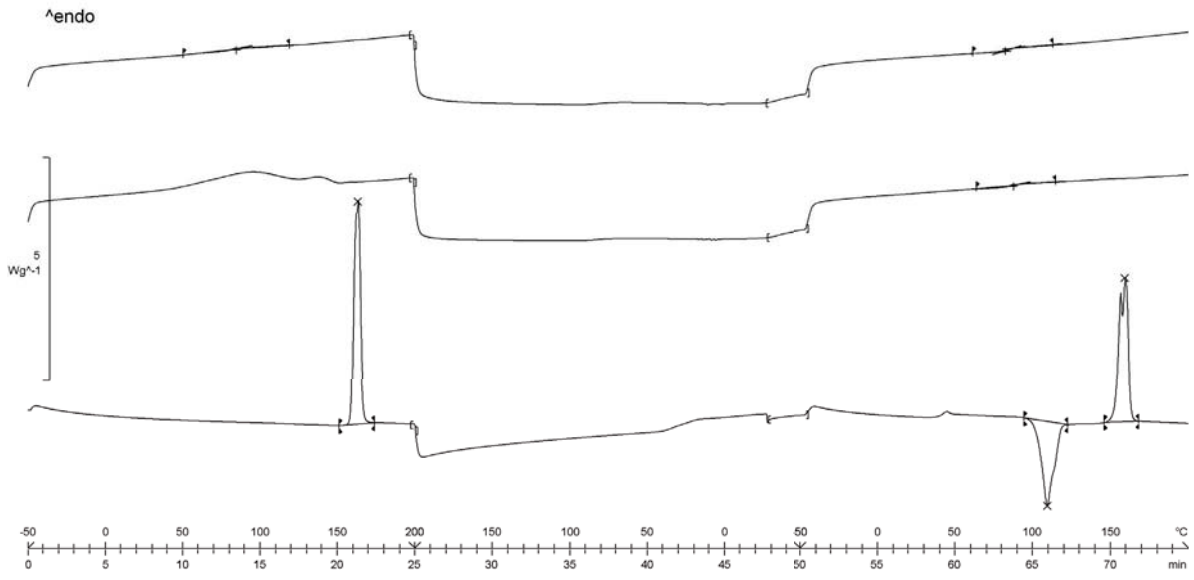


Figure 3.49: DSC thermogram of OX-B extrudate (OX+COP+HPMC = 1+3+1 weighted parts) with the following data displayed from top to bottom: pellets, physical mixture, pure OX

In the thermogram of hot-melt extruded formulation OX-E (OX+COP+PVCL-PVAc-PEG ≡1+3+1), one glass transition was detected at 74.9 °C which indicates the formation of a glassy solution (see Figure 3.50).

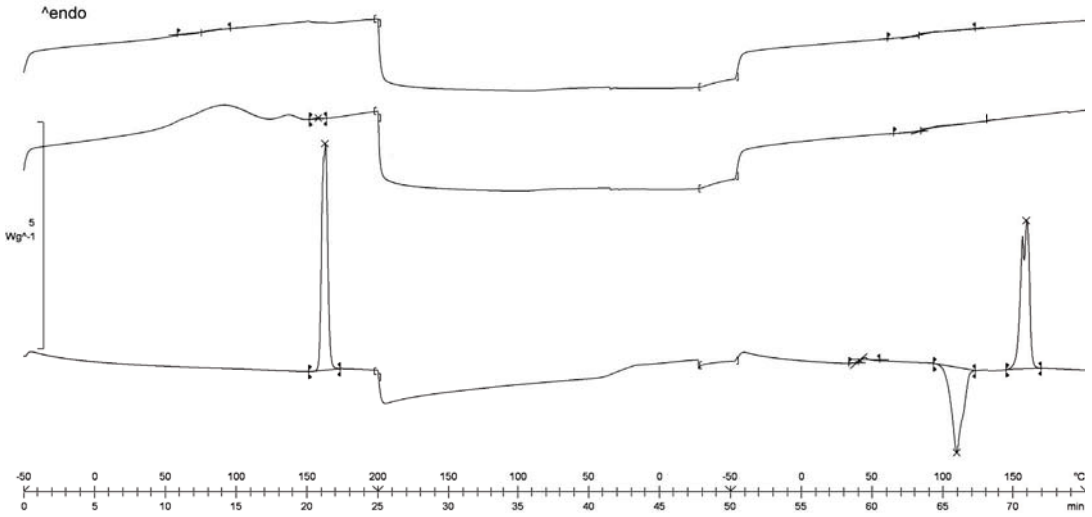


Figure 3.50: DSC thermogram of OX-E extrudate (OX+COP+PVCL-PVAc-PEG = 1+3+1 weighted parts) with the following data displayed from top to bottom: pellets, physical mixture, pure OX

With formulation OX-F, no definite conclusions can be drawn as the DSC thermogram is very vague: No clear glass transition was found in the first heating cycle (see Figure 3.51).

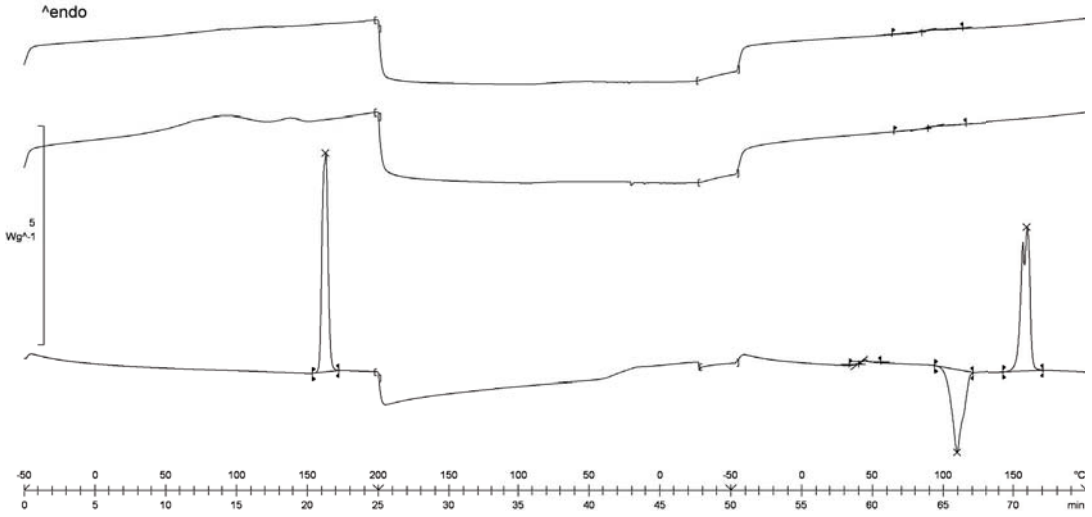


Figure 3.51: DSC thermogram of OX-F extrudate (OX+COP+HPMC+PVCL-PVAc-PEG = 1+3+1+1 weighted parts) with the following data displayed from top to bottom: pellets, physical mixture, pure OX

Due to the encountered difficulties with the detection of crystalline OX using DSC and with the high LOD level of XRD analysis in the case of OX, the system that is present after extrusion cannot be precisely defined using these analytical methods.

The $T_g$ values determined in the second heating cycle indicate that the formation of a glassy solid solution with these carriers is possible: For OX-D and OX-E extrudates, the $T_g$ was at approximately 82 °C and at approximately 84 °C for OX-F. The $T_g$ values that were determined for the physical mixtures of the components were in the range of 84 - 89 °C.

It was demonstrated that the results gained by HME of FF are not fully transferable to OX as different systems are present in the extrudate leading to a different dissolution performance. However, it was confirmed that the release from both FF and OX extrudates is carrier-controlled resulting in a dissolution performance of the drug that depends on the dissolution behavior of the carrier(s).

### 3.3.4 Variation of the COP:HPMC ratio in oxeglitazar extrudates

The COP to HPMC ratio was varied to investigate further the effects observed with formulation OX-D (see Section 3.3.3). The main aim was to further enlighten the super-additive effect of these two polymers when applied in a polymeric blend.
Polymeric blends were applied as carriers for solid dispersion systems with the aim to modify the release behavior by Papageorgiou et al. (2008) who used PVP, HPMC and the poorly water-soluble drug fluconazole. The polymer:polymer ratio showed a strong influence on the dissolution profile. In the present work, the reason for the observed super-additive effect may be the difference in drug load of the extrudates as binary formulations contain 25 % of OX and ternary formulations 20 %. The formation of a drug-rich layer at higher drug loadings might be promoted, thus opposing the carrier-controlled drug dissolution mechanism which predominates at lower drug loadings (Craig, 2002). Therefore, another focus of these experiments was to determine whether the super-additive effect is contingent on a specific composition of the polymer blend (see Table 3.19 for the composition of the extrudates). Dissolution results of the extrudates are shown in Figure 3.52.

Table 3.19: Composition of OX extrudates with a varying COP:HPMC ratio. Data are given in weighted parts unless otherwise specified.

| Formulation | OX | COP | HPMC | drug load [%] |
|---|---|---|---|---|
| OX-G | 1 | 4 | - | |
| OX-D | 1 | 3 | 1 | |
| OX-H | 1 | 2 | 2 | 20.0 |
| OX-J | 1 | 1 | 3 | |
| OX-K | 1 | - | 4 | |

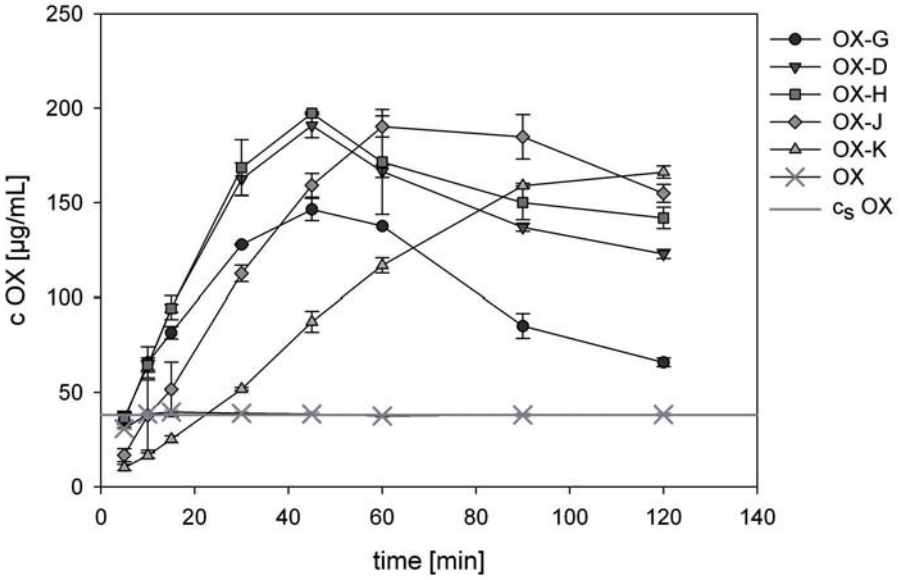


Figure 3.52: Dissolution profiles of OX extrudates where the ratio COP:HPMC was varied as follows: 4:0 (OX-G), 3:1 (OX-D), 1:1 (OX-H), 1:3 (OX-J) and 0:4 (OX-K)

Formulation OX-G (COP:HPMC≡4:0) reaches $c_{max}$ after 45 min of dissolution: At this sampling point, 146 µg/mL of API are dissolved which corresponds to 50 % of total API and is 3.8 times above $c_s$. Formulation OX-K (COP:HPMC≡0:4) does not reach $c_{max}$ within 120 min of dissolution. 166 µg/mL are detected at the last sampling point (120 min) giving an amount of 57 % of dissolved API and a 4.4-fold supersaturation. These results are in accordance with the findings of the single polymeric extrudates OX-A (OX+COP≡1+3) and OX-B (OX+HPMC≡1+3) described in Section 3.3.2.
The $c_{max}$ values of the polymeric blend extrudates are comparable: 191 µg/mL, 197 µg/mL and 190 µg/mL are reached with formulations OX-D, OX-H and OX-J, respectively. Supersaturation levels of 5.0 - 5.2 are reached. All three hot-melt extruded formulations exhibit a super-additive effect. With formulations OX-D (COP:HPMC≡3:1) and OX-H (COP:HPMC≡1:1), $c_{max}$ is reached after 45 min of dissolution, whereas it is reached after 60 min with OX-J (COP:HPMC≡1:3). At the last sampling point, the concentration of dissolved OX has dropped down to 66 µg/mL for OX-G, 122 µg/mL for OX-D, 142 µg/mL for OX-H and 156 µg/mL for formulation OX-J.
It is shown in Figure 3.52 that the super-additive effect of the OX-polymeric blend extrudate is independent of the polymer to polymer ratio as the $c_{max}$ values not only of OX-D but also of OX-H and OX-J are higher than those of the single polymer formulations OX-G and OX-K. At the same time, it was demonstrated that the curve shape is mainly influenced by the predominant polymer of the blend: If the amount of HPMC exceeds the amount of COP, the curve shape approaches the curve shape of the formulation where no COP is applied (formulation OX-K) and vice versa. Accordingly, $c_{max}$ is delayed if the amount of HPMC in the polymeric blend is higher than the amount of COP. The higher the fraction of HPMC, the more stable the supersaturation level after $c_{max}$. Again, this may be contributed to the recrystallization inhibiting effect of this excipient (Zhang and Zhou, 2009).

The dependency of the dissolution profile on the carrier composition was confirmed. The influence of the polymer:polymer ratio on the release profile was lower than in the case of fluconazole-PVP-HPMC solid dispersions (Papageorgiou et al., 2008).
From DSC and XRD studies it is derived that no crystalline API is present in hot-melt extruded formulations OX-G - OX-K (see Figures 3.53 and 3.54).

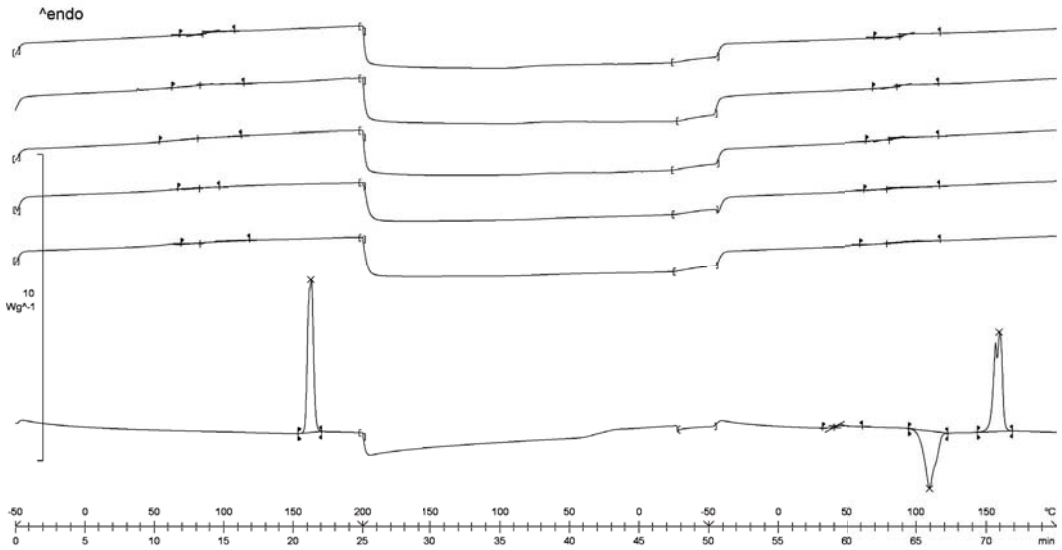


Figure 3.53: DSC thermograms of OX extrudates where the COP:HPMC ratio was varied showing from top to bottom: OX-G (COP:HPMC≡4:0), OX-D (3:1), OX-H (1:1), OX-J (1:3), OX-K (0:4), pure OX

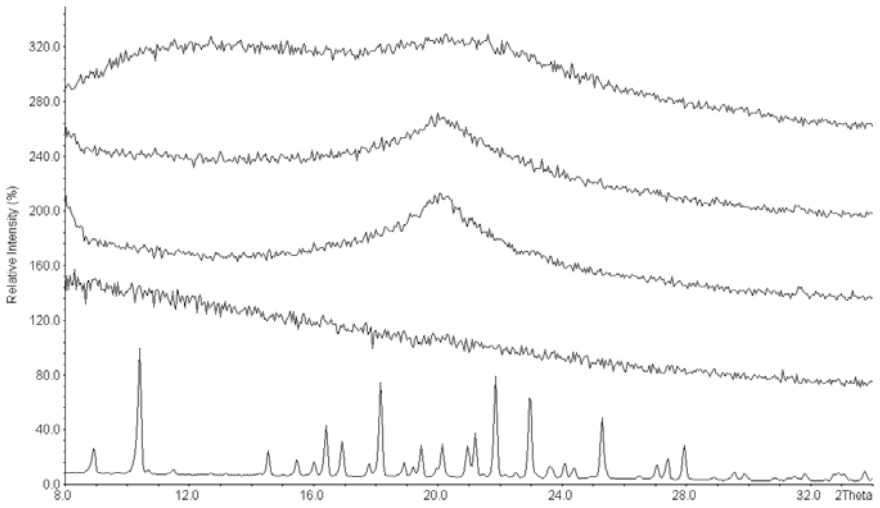


Figure 3.54: XRD patterns of OX extrudates where the COP:HPMC ratio was varied showing from top to bottom: OX-G (COP:HPMC≡4:0), OX-D (3:1), OX-H (1:1), OX-J (1:3), OX-K (0:4), pure OX

The single glass transition that was detected in the first heating cycle of OX-G, OX-D and OX-H - OX-K extrudates indicates the formation of a one-phase system regardless of the carrier composition. Hence, the differing dissolution performance of the extrudates can be associated to the dissolution behavior of the carrier which is mainly dependent on the predominant polymer. It has to be assumed that not only the dissolution behavior of the polymeric components but also the grade of their miscibility and polymer-polymer interactions are crucial for the observed release profile of the extrudates and, especially, for the super-additive effect of the COP-HPMC carrier.

### 3.3.5 24 h dissolution profiles of oxeglitazar extrudates

Because the maximum concentration was not reached within 120 min for all OX-formulations but OX-A (OX+COP≡1+3) and OX-D (OX+COP+HPMC≡1+3+1), 24 h dissolution trials were performed under otherwise equivalent testing conditions (see Sections 3.3.2 and 3.3.3 for all results from 120 min dissolution studies).
The release profiles of formulations OX-A - OX-F which were previously observed during 120 min dissolution trials were confirmed. Again, the maximum concentration is reached after 60 min of dissolution testing with OX-A and the amount of dissolved OX decreases from this sampling point onward until it reaches a concentration of 53 µg/mL after 24 h. This value corresponds to a dissolved amount of 18 % of OX and is 1.4 times above saturation level (see Figure 3.55).

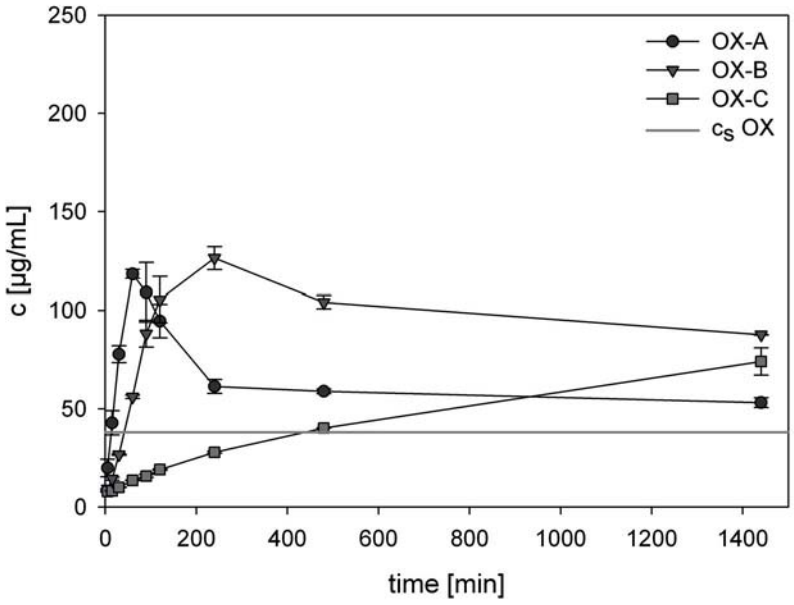


Figure 3.55: 24 h release profiles of OX-A (OX+COP), OX-B (OX+HPMC) and OX-C (OX+PVCL-PVAc-PEG; all ≡1+3) extrudates

The same applies for OX-B (OX+HPMC≡1+3): $c_{max}$ is reached after 240 min and the concentration decreases after this sampling point. After 24 h, 88 µg/mL of OX are dissolved which corresponds to 30 % of total API and is 2.3 times above $c_s$ (see Figure 3.55). The super-additive effect which was observed in 120 min dissolution trials was verified. The $c_{max}$ is reached after 60 min with OX-D extrudate and drops down to 74 µg/mL which corresponds to 25 % of total API and is 1.9 times above $c_s$ level (see Figure 3.56).

To summarize these results, supersaturation was maintained for at least 20 h for hot-melt extruded formulations OX-A, OX-B and OX-D, depending on the initial release rate.
To assess the stability of the supersaturation level, the time interval from $c_{max}$ to half of the respective maximum supersaturation concentration was evaluated. For formulations OX-A and OX-D, the time interval was determined to be approximately 120 min. With formulation OX-B, however, this concentration was not reached within the monitored period of 24 h making the time interval longer than 22 h. This outstanding stability of the supersaturation level that was pointed out for OX-B can be contributed to the recrystallization inhibiting effect of HPMC during dissolution if applied as single polymeric carrier (Zhang and Zhou, 2009).
If PVCL-PVAc-PEG was applied as single or additional carrier, no $c_{max}$ was detected within 24 h. It was shown for all formulations with PVCL-PVAc-PEG that the released amount of OX from the pelletized extrudates surpasses $c_s$ within the investigated period of time. The dissolved amount of OX exceeds $c_s$ after 60 min with formulation OX-F, after 90 min with OX-E and after 480 min with OX-C (see Figures 3.55 and 3.56).

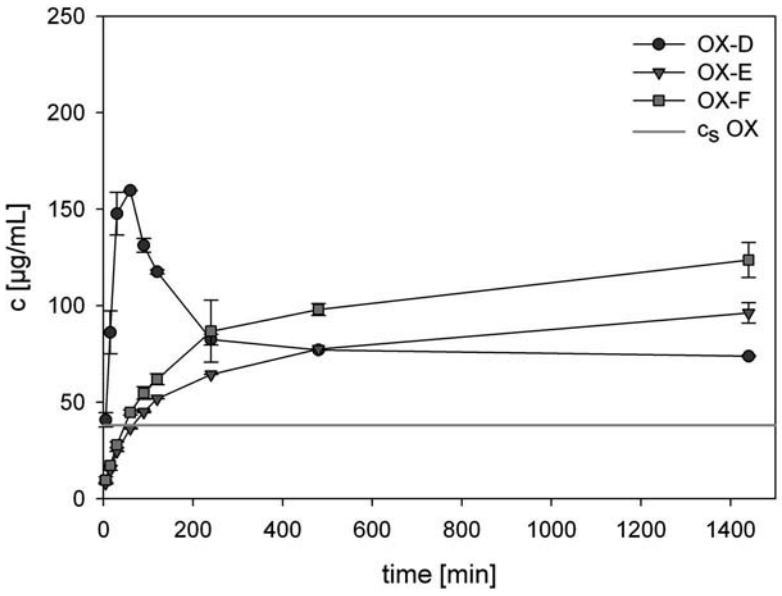


Figure 3.56: 24 h release profiles of OX-D (OX+COP+HPMC), OX-E (OX+COP+PVCL-PVAc-PEG, both ≡1+3+1) and OX-F (OX+COP+HPMC+PVCL-PVAc-PEG≡1+3+1+1) extrudates

It was thus shown that with increasing PVCL-PVAc-PEG amounts, the release rate from the extrudates is reduced. The reason for this is the slow dissolution rate of the extruded polymer PVCL-PVAc-PEG which leads to drastically reduced initial release rates of the API (Kolter et al., 2010).

### 3.3.6 Addition of a disintegrant to oxeglitazar extrudates with PVCL-PVAc-PEG as carrier

For all extrudates with PVCL-PVAc-PEG as single or additional carrier, very slow initial release rates were observed (see Sections 3.3.2 - 3.3.5). It is assumed that the API is entrapped in PVCL-PVAc-PEG extrudates due to the slow dissolution rate of the extruded polymer. Additional trials were performed using crospovidone (CL) as an additive to examine whether its application leads to an increase of the initial release of the API from the hot-melt extruded formulation due to its pronounced disintegrative properties (see Table 3.20 for the composition of the extrudates).
CL was added to the API-polymer mixture prior to extrusion with the intention to promote the disintegration of the pellets as it swells once it comes in contact with water. The dissolution enhancement of different poorly water-soluble drugs by the incorporation of various superdisintegrants, including CL, into a solid dispersion system is well documented in literature (Chowdary and Rao, 2000; Aly et al., 2005). The incorporation of the superdisintegrant into the solid dispersion was shown to be superior to a physical mixture of both (Srinarong et al., 2009).

Table 3.20: Composition of OX-PVCL-PVAc-PEG extrudates with added superdisintegrant CL. Data are given in weighted parts unless otherwise specified.

| Formulation | OX | PVCL-PVAc-PEG | CL | drug load [%] |
|---|---|---|---|---|
| OX-CL 1 | 1 | 2.6 | 0.4 | 25.0 |
| OX-CL 2 | 1 | 2.2 | 0.8 | |

The release from OX-CL 1 and 2 extrudates can be considered equivalent to the dissolution profile of the respective extrudate without the addition of the superdisintegrant (see Figure 3.57). Interestingly, all of these extrudates are outperformed by the physical mixture of the components and even the pure API (both without the addition of CL).
This provides evidence that the intention to have the disintegrant function as a spacer between the polymer particles and to enhance the release rate of OX via swelling and the acceleration of pellet disintegration has failed. It is very likely that the PVCL-PVAc-PEG which is molten during the extrusion process forms a coating layer around API and CL particles thus preventing the swelling of CL and the release of OX (Serajuddin, 1999).

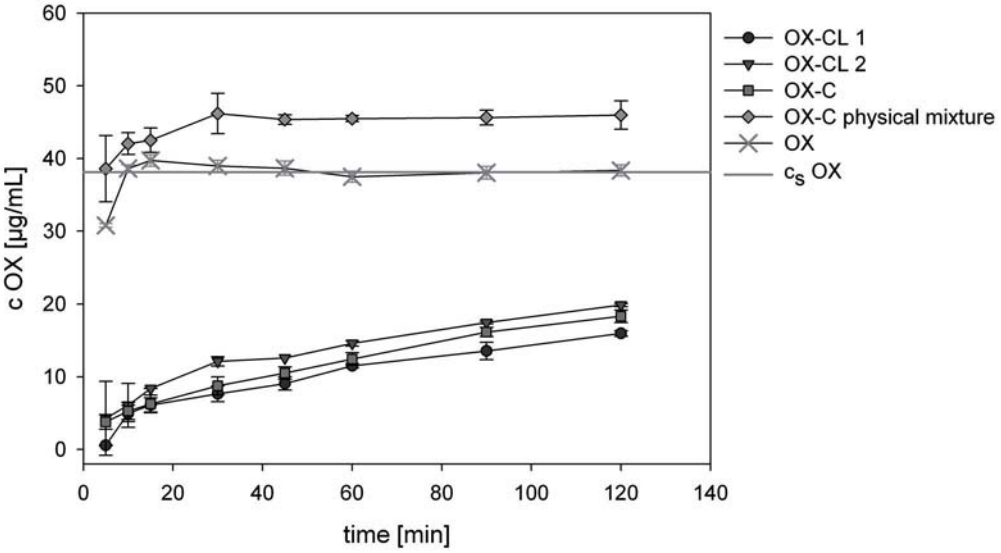


Figure 3.57: Dissolution profiles of formulations OX-CL 1 and 2 in comparison to the superdisintegrant-free formulation OX-C (OX+PVCL-PVAc-PEG = 1+3 weighted parts) and the untreated physical mixture of OX-C

To allow for CL functioning as a disintegrant, a further down-processing of the extrudate would be necessary, for example through milling, and the addition of this excipient would have to be to the milled extrudate instead. It was pointed out in Section 3.2.3 that milling of the hot-melt extruded formulations diminishes the positive influence of the polymeric carriers on the dissolution profile of the API. In this case however, a break-up of the polymeric structures is desirable as the manufacture of an immediate release formulation is intended. The release profile of the milled extrudate has to be compared to the release profile of solid dispersions gained with other manufacturing methods to clarify which of these methods results in a superior dissolution performance. However, these investigations go beyond the scope of this work and were therefore not pursued further.

When comparing the results that were gained with hot-melt extruded formulations of OX to those gained with the FF formulations as described in Section 3.2, the dissolution results of PVCL-PVAc-PEG-FF with or without further additives are very striking: In contrary to the OX results, the dissolution performance of FF-PVCL-PVAc-PEG extrudates is very good as it reaches supersaturation levels of up to 11 times in the case of FF-F which is a FF-COP-PVCL-PVAc-PEG formulation (API to polymer ratio≡1+3+1 weighted parts). It has to be remembered however, that FF does not only have a lower $T_m$ than OX thus lowering the $T_g$ of the hot-melt extruded mixture and promoting molecular mobility within the extrudate. Furthermore, FF acts as a plasticizer leading to an increase of the possible chain movement and polymer flexibility. The mechanisms of action of a plasticizer have been discussed by Sears and Darby (1982) and Cadogan and Howick (2000). The plasticizing properties of FF are a possible reason why the release of the API is improved in the case of FF-PVCL-PVAc-PEG extrudates but not with OX-PVCL-PVAc-PEG extrudates.

### 3.3.7 Surface morphology of oxeglitazar extrudates as monitored with scanning electron microscopy

Differences of surface morphology of OX extrudates before and after exposure to the dissolution medium were analyzed using scanning electron microscopy (SEM). The aim was to assess the different release behavior of OX extrudates and, possibly, find proof for the assumption that the API is trapped within the slowly dissolving PVCL-PVAc-PEG pellet (formulation OX-C). Therefore, two extrudates were compared: formulation OX-A (OX+COP≡1+3) which shows an improved dissolution behavior in comparison to the pure API and formulation OX-C (OX+PVCL-PVAc-PEG≡1+3) for which a decrease of the initial release rate was observed.
The surface of both hot-melt extruded strands was observed to be smooth and without crystalline residues. Due to the brittleness of the strand which was observed for formulation OX-A, small extrudate fragments are present on the pellet surface (see Section A.12 of the Appendix for SEM photographs of the strands prior to dissolution).
After the exposure to the dissolution medium for 2 or 10 min, crystals were observed with both hot-melt extruded formulation OX-A and OX-C (see Figures 3.58 and 3.59).

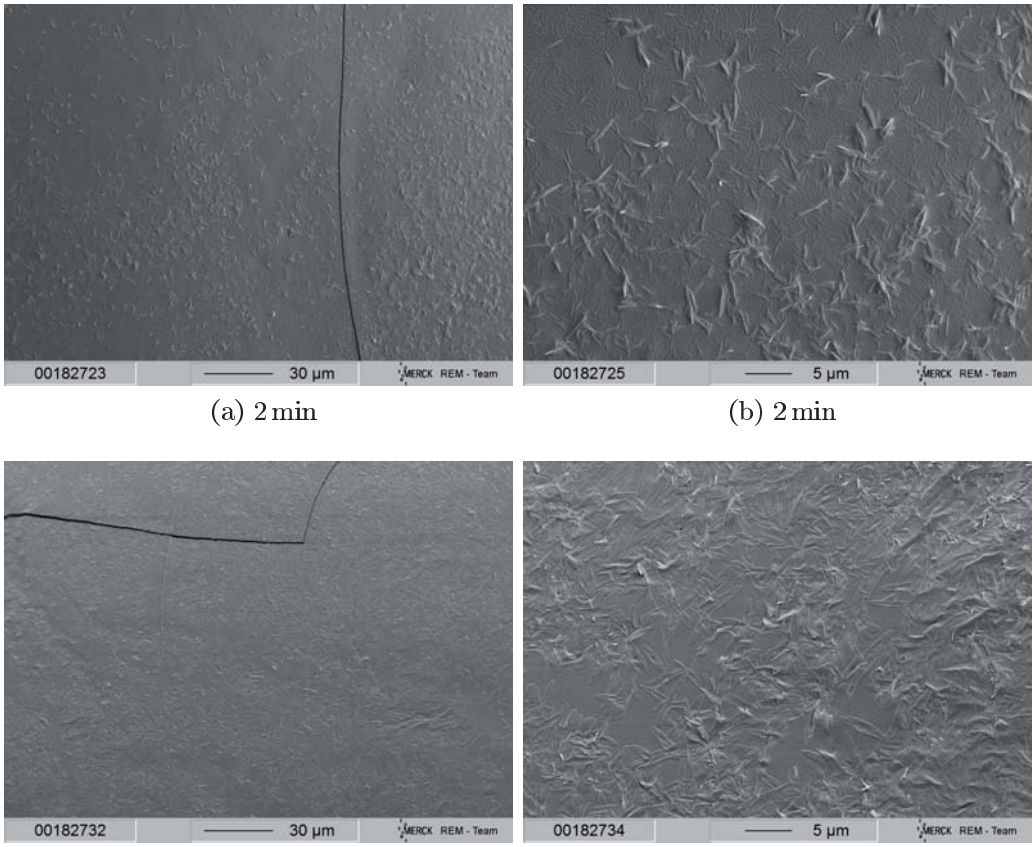


(a) 2 min (b) 2 min

(c) 10 min (d) 10 min

Figure 3.58: SEM images of OX-A pellets after exposure to the dissolution medium

It is important to point out that the recrystallization of the formerly amorphous API on the pellet surface was very likely induced during the drying procedure that was a part of the sample preparation for SEM analysis (see Section 6.2.2.9). This change of the solid state during the drying process was desirable as it enables the visualization of the OX distribution on the pellet surface.
Formulation OX-A shows a homogeneous distribution of small sized crystals on its surface after 2 min in the dissolution medium, whereas formulation OX-C exhibits crystalline clusters on its surface. It could be postulated that the overall distribution of API is not homogeneous in OX-C extrudates. However, after 10 min in dissolution medium, the outer surface of the OX-C extrudates was softened enough so a thin layer could be removed with forceps. Evenly distributed crystals become visible underneath (see Figure 3.60). Therefore, it must be concluded that the API distribution is similar for all extrudates. When the extrudate gets into contact with the dissolution medium, the embedded drug is released. In this case, the release is carrier-controlled. With formulation OX-C, the carrier-controlled dissolution is very slow so only a limited amount of API has come to the surface and recrystallized. In contrary, the physicochemical characteristics of the carrier COP allow a faster release so the presence of the drug on the OX-A surface was shown to be pervasive.

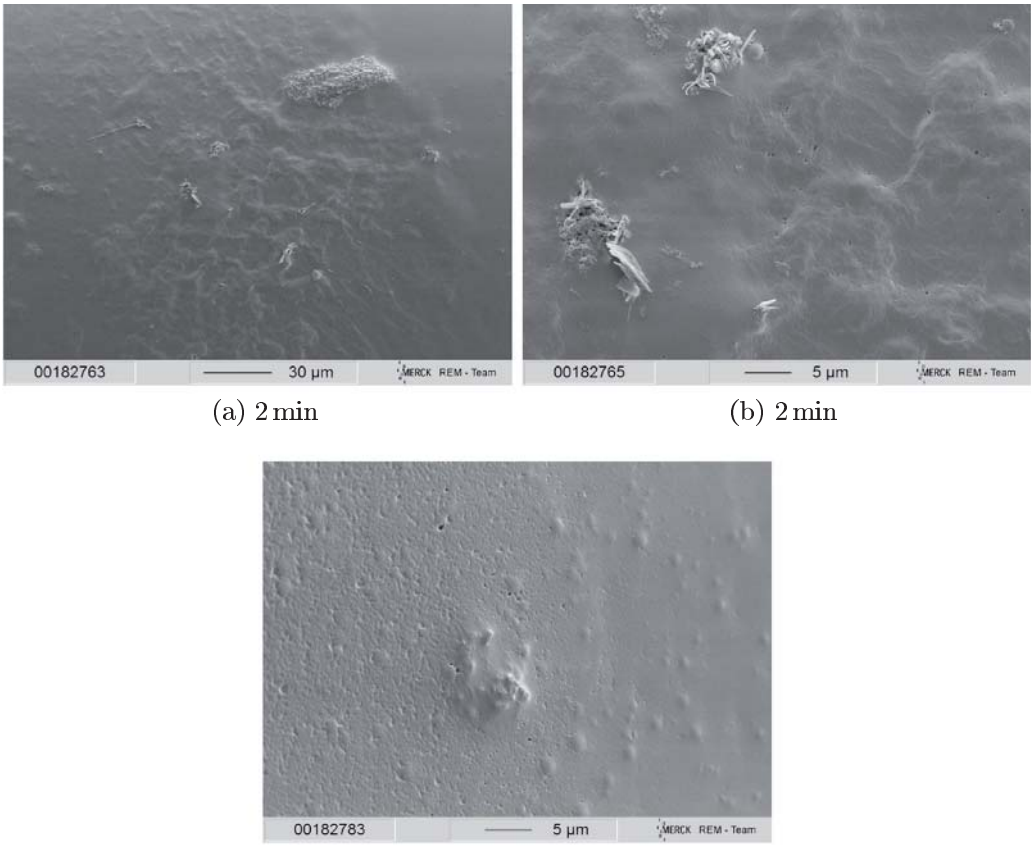


(a) 2 min (b) 2 min

(c) 10 min

Figure 3.59: SEM images of OX-C pellets after exposure to the dissolution medium

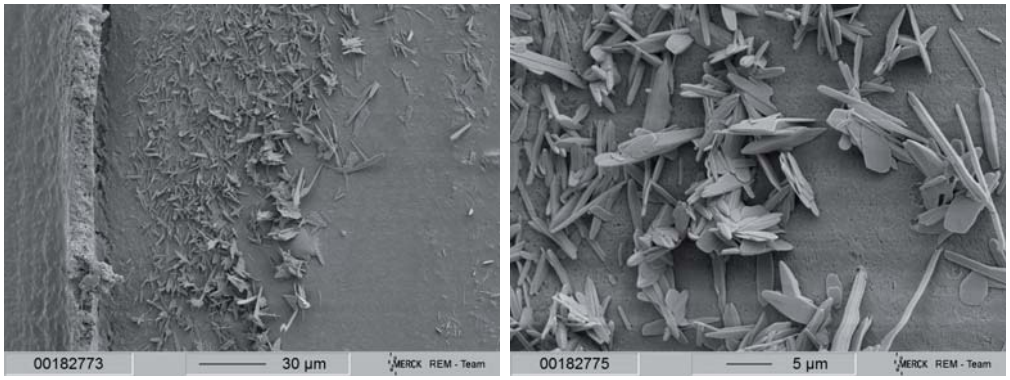


(a) (b)

Figure 3.60: SEM images of OX-C after 10 min in the dissolution medium with the outer layer of the pellet surface removed

### 3.3.8 Storage stability of oxeglitazar extrudates

Of the series OX-A to OX-F, only OX-A (OX+COP≡1+3), OX-B (OX+HPMC≡1+3) and OX-D (OX+COP+HPMC≡1+3+1) showed a significant improvement of the release profile of the API within 120 min of dissolution time. Therefore, the storage stability under long-term storage conditions (25 °C /60 % rH) was determined only for these three formulations. Over the investigated storage period of 10 weeks, the dissolution performance of the formulations OX-A, OX-B and OX-D remained stable (see Figure 3.61 on exemplary results for OX-A extrudate and Figures A.9 - A.10 of the Appendix for the remaining data).

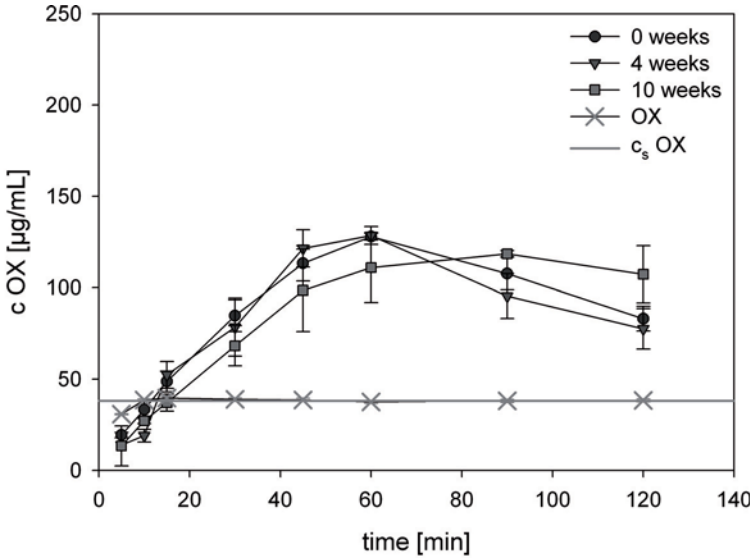


Figure 3.61: Dissolution profiles of OX-A pellets (OX+COP = 1+3 weighted parts) stored for 0, 4 and 10 weeks at 25 °C /60 % rH

Furthermore, no conversion of the amorphous API into its crystalline state was observed with XRD or DSC analysis (see Figure 3.62 on exemplary results for OX-A extrudate and Figures A.20 - A.22 of the Appendix for the remaining data).
Again, it was pointed out that the results are not fully transferable from FF to OX extrudates. Although all extrudates that were assessed for their storage stability were present as a glassy solution, the dissolution performance of FF extrudates decreased with increasing storage times while the performance of OX extrudates was not affected. It is assumed that the differing physicochemical properties of these drugs which lead to different drug-polymer interactions and the plasticizing effect of FF are a reason for the different storage stabilities.

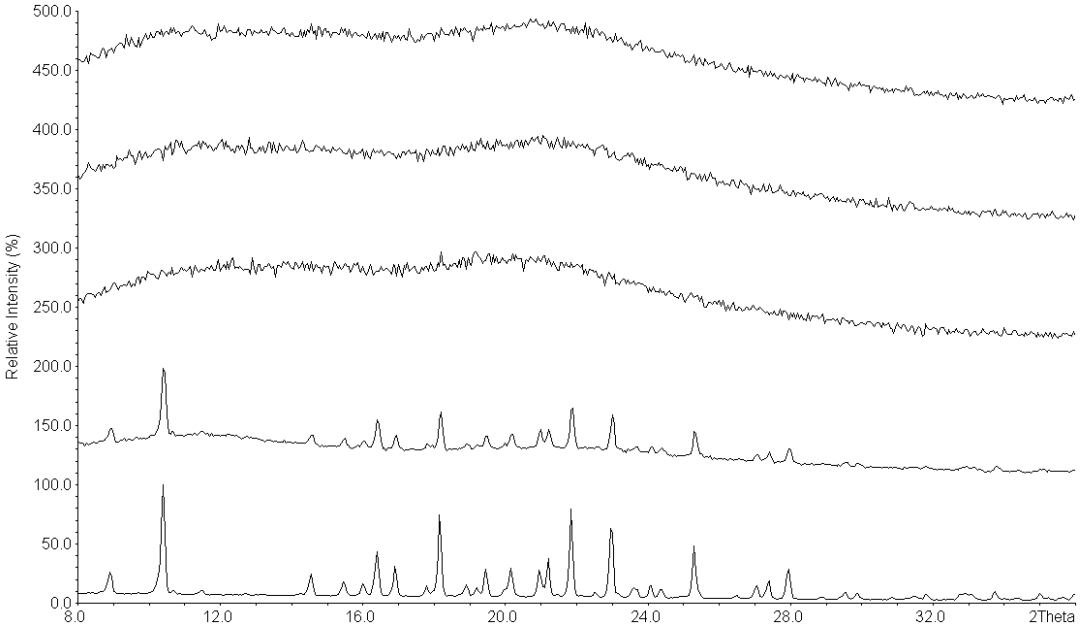


Figure 3.62: XRD patterns of OX-A extrudates (OX+COP = 1+3 weighted parts), depicting from top to bottom the following data: pellets after 0, 4 and 10 weeks of storage at 25 °C /60 % rH, physical mixture, pure OX

# 3.4 Solubility enhancement of felodipine via hot-melt extrusion

## 3.4.1 Introduction and objectives

Hot-melt extrusion (HME) was successfully applied for the dissolution enhancement of poorly water-soluble drug FF with different polymers and mixtures of these as carriers (see Section 3.2). The transferability of the results was investigated using OX which is also a poorly water-soluble API. While with both APIs, the formation of a single phase glassy solid solution was successful, differences in the dissolution behavior of the extrudates were observed: The initial release rate was improved with all FF formulations with COP, HPMC and/or PVCL-PVAc-PEG as carriers, whereas it was reduced with the corresponding OX extrudates. Especially if PVCL-PVAc-PEG was used as main or additional polymeric carrier, the released amount of OX from extrudates remained for 45-480 min below the concentration levels gained with pure API. This was contributed on the one hand to a reduced dissolution rate of PVCL-PVAc-PEG after extrusion and on the other hand to the low $T_g$ and the plasticizing effect of FF which is not given in the case of OX (see Section 3.3). Furthermore, the chemical properties of the two APIs differ, for example, FF is a neutral substance while OX has an acidic functional group.
To investigate whether the results gained with FF are transferable onto yet another drug and to verify the drawn conclusions, FD was employed as API. It is a weak base with a pH independent solubility and a melting point in the same range as OX: $T_m$FD=145.1 °C (see Table 6.2 for a comparison of the physicochemical properties of the three APIs).
Special attention was paid to the thermal instability of FD as it might be a problem of the HME process (Marciniec and Ogrodowczyk, 2006). For the assessment of possible degradation resulting from the manufacturing process, high performance liquid chromatography (HPLC) analysis was performed according to Ph.Eur. specifications with ultraviolet (UV) detection at 254 nm. The chosen wavelength for quantitative FD detection via HPLC was 362 nm.

A successful manufacture of solid dispersions of FD and aPMMA via HME is reported by Nollenberger et al. (2009a) and Qi et al. (2010). No degradation effects at process temperatures of up to 160 °C were reported by these research groups. It has to be pointed out that the HPLC analysis was performed at 362 nm where degradation products of FD may remain undetected (Nollenberger et al., 2009a).

## 3.4.2 Hot-melt extrusion of felodipine with single polymeric carriers

To ensure a full comparability to the FF and OX extrudates with single polymers as carriers, blends of FD and COP, HPMC and PVCL-PVAc-PEG were manufactured using the same composition of drug and carrier as with the other two APIs (see Table 3.21).

Table 3.21: Composition of FD-single polymer extrudates that served as a comparison to the corresponding FF and OX extrudates. Data are given in weighted parts unless otherwise specified.

| Formulation | FD | COP | HPMC | PVCL-PVAc-PEG | drug load [%] |
|---|---|---|---|---|---|
| FD-A | 1 | 3 | - | - | |
| FD-B | 1 | - | 3 | - | 25.0 |
| FD-C | 1 | - | - | 3 | |

Although the saturation concentration of FD in Ph.Eur. hydrochloric acid medium pH 1.2 + 0.1 % polysorbate 80 is higher than the one of FF ($c_s$FD = 44.2 µg/mL; $c_s$FF = 18.7 µg/mL; see Table D.7 of the Appendix), the dissolution results of hot-melt extruded FD formulations stay well below the results gained with FF extrudates (see Figure 3.63).

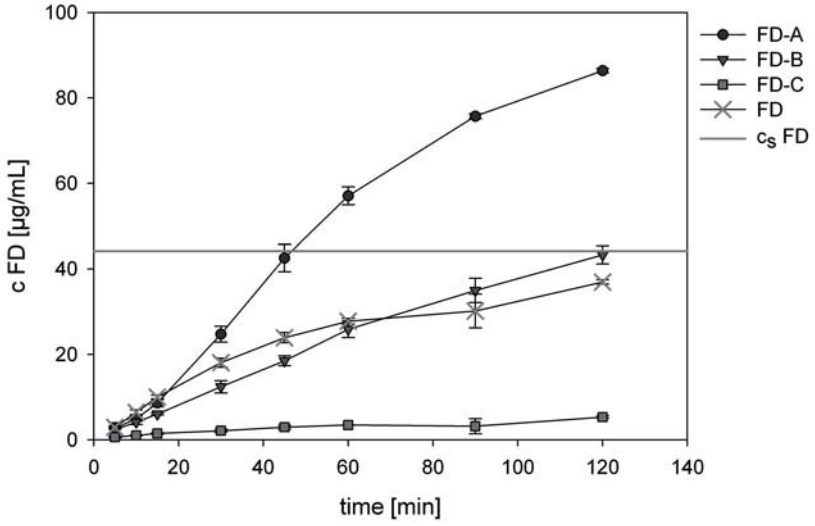


Figure 3.63: Dissolution profiles of hot-melt extruded formulations FD-A (FD+COP), FD-B (FD+HPMC) and FD-C (FD+PVCL-PVAc-PEG; all consisting of 1+3 weighted parts of API and polymer)

FD-A (FD+COP≡1+3) is the only formulation which exceeds $c_s$ within 120 min of dissolution time. Release from none of the hot-melt extruded FD formulations reaches $c_{max}$ within the investigated time.
With FD-A extrudate, the dissolved amount of FD is above $c_s$ after 45 min of dissolution. After 120 min, 86.4 µg/mL are dissolved, resulting in a 2-fold supersaturation. At this sampling point, 30 % of total API are dissolved.
FD concentrations of 43.3 µg/mL and 5.3 µg/mL are reached with FD-B (FD+HPMC≡1+3) and FD-C (FD+PVCL-PVAc-PEG≡1+3), respectively, after 120 min. While FD-B is at saturation level at this sampling point, FD-C remains far below this level as only 1.8 % of total

API are dissolved. Even with unprocessed FD powder, 37.0 µg/mL of FD are dissolved after 120 min, which is 6.9 times superior to FD-C.

No crystalline FD was detected with any of the formulations FD-A - FD-C using XRD (LOD=1 %) and DSC (LOD=1-5 %, depending on the carrier). Hence, the API is converted into its amorphous state. Exemplary DSC and XRD data for FF-A pellets are shown in Figures 3.64 and 3.65 (see Sections A.9 and A.5 of the Appendix for the remaining data).

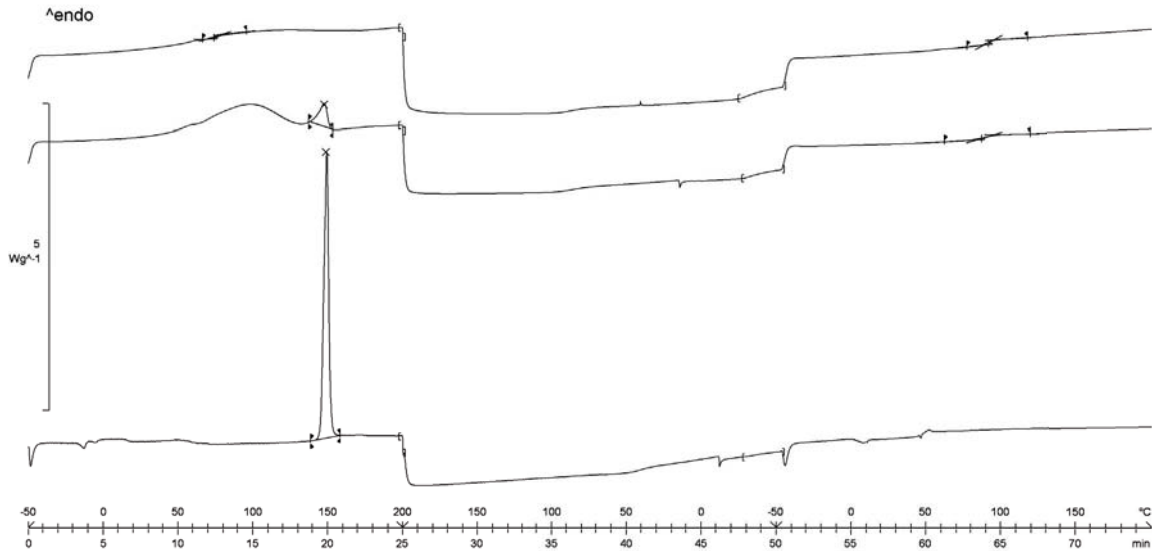


Figure 3.64: DSC thermogram of FD-A extrudate (FD+COP≡1+3) with the following data displayed from top to bottom: pellets, physical mixture, pure FD

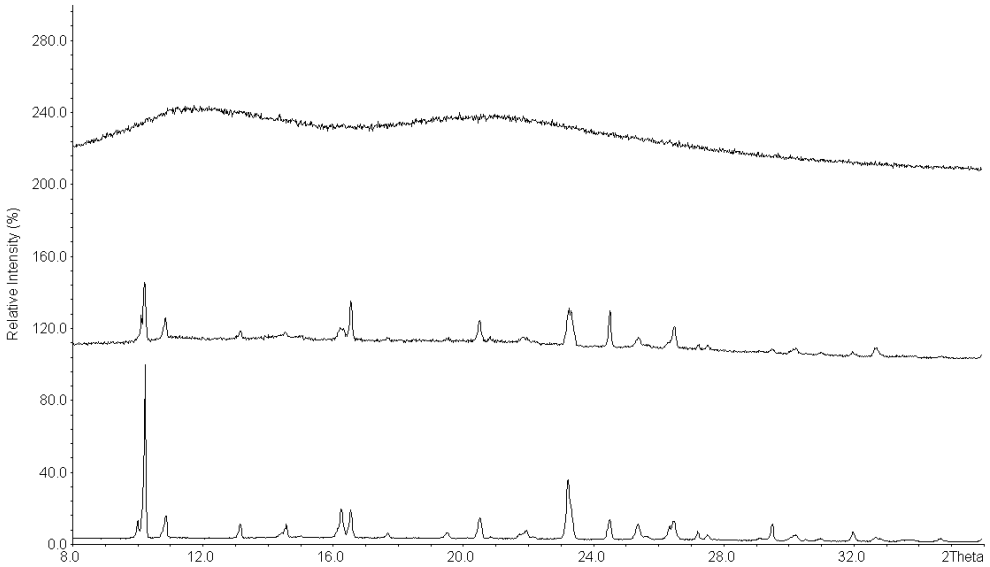


Figure 3.65: XRD pattern of FD-A extrudate (FD+COP≡1+3) with the following data displayed from top to bottom: pellets, physical mixture, pure FD

From the DSC thermograms it can be concluded that one-phase systems are present in the FD extrudates, indicating the presence of a glassy solution, as only one glass transition was detected for all hot-melt extruded single-polymeric formulations of FD.

According to the manufacturer's information, COP needs approximately 17 min until dissolution in buffer medium pH 1.1 and is therefore classified as an instant release carrier (Kolter et al., 2010). In our case, $c_{max}$ is reached after 10 min with formulation FF-A, after 60 min with formulation OX-A and not within 120 min of dissolution time with formulation FD-A. In all three formulations, glassy one-phase systems were detected via DSC analysis. XRD analysis confirmed the amorphous state of the samples. From these results it seems reasonable to assume that either the differences in glass transition temperatures of the extrudates ($T_g$ FF-A =39.1 °C; $T_g$ FD-A = 73.8 °C; $T_g$ OX-A =86.6 °C) or the different structural and physicochemical properties of the APIs leading to different drug-polymer interactions are the reason for the observed variability in the dissolution performance of the manufactured extrudates. Further research will have to be conducted to verify this assumption.

### 3.4.3 Hot-melt extrusion of felodipine with mixtures of polymeric carriers

Poorly water-soluble drug FD was hot-melt extruded with blends of COP, HPMC and PVCL-PVAc-PEG in analogy to the previously performed trials with FF or OX (see Sections 3.2 and 3.3). Table 3.22 shows the composition of FD extrudates.

Table 3.22: Composition of FD extrudates with polymeric blends as carrier that served as a comparison to the corresponding FF and OX extrudates. Data are given in weighted parts unless otherwise specified.

| Formulation | FD | COP | HPMC | PVCL-PVAc-PEG | drug load [%] |
|---|---|---|---|---|---|
| FD-D | 1 | 3 | 1 | - | 20.0 |
| FD-E | 1 | 3 | - | 1 | 20.0 |
| FD-F | 1 | 3 | 1 | 1 | 16.7 |

The dissolution performance as well as the physical state of the extrudates was analyzed to allow for an evaluation of the manufacturing method and the transferability of the results from one API to the other.
As was already observed with FD extrudates using only one polymer as carrier, the application of PVCL-PVAc-PEG diminishes the dissolution performance (see Figure 3.66).

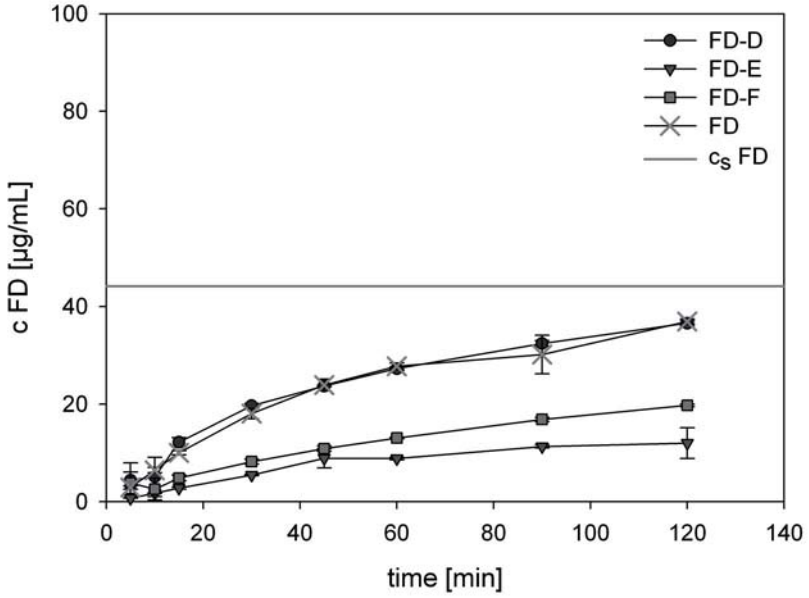


Figure 3.66: Dissolution profiles of hot-melt extruded formulations FD-D (FD+COP+HPMC≡1+3+1), FD-E (FD+COP+PVCL-PVAc-PEG≡1+3+1) and FD-F (FD+COP+HPMC+PVCL-PVAc-PEG≡1+3+1+1)

While 36.6 µg/mL are dissolved after 120 min of dissolution with formulation FD-D which is a FD-COP-HPMC extrudate (1+3+1), only 19.7 µg/mL and 12.0 µg/mL are reached with FD-F (FD+COP+HPMC+PVCL-PVAc-PEG≡1+3+1+1) and FD-E (FD+COP+PVCL-PVAc-PEG≡1+3+1), respectively. As was observed with single polymeric PVCL-PVAc-PEG-FD formulation FD-C (see Section 3.4.2), the release performance of FD-E and FD-F extrudates which contain PVCL-PVAc-PEG as an additional carrier is inferior to the dissolution profile of pure FD powder. None of the three formulations exceed $c_s$ within the investigated time. Again, no $c_{max}$ was reached within 120 min of dissolution (see Figure 3.66).

HPLC analysis showed no degradation products of FD in the pelletized extrudates. It is concluded that the applied process temperatures of up to 160 °C (see Table 6.11) do not induce a thermal degradation of the API.

XRD and DSC analysis were applied to investigate the physical state of the API and to classify the solid dispersion system which is present in the extrudate. No crystalline API was detected via XRD in FD extrudates with multiple polymers. These results were confirmed by DSC thermograms (see Figures 3.67 and 3.68 for exemplary data on formulation FD-D and Sections A.9 and A.5 of the Appendix for the remaining data).
The first heating cycle of the DSC analysis showed one single $T_g$ for formulations FD-D, FD-E and FD-F, indicating the formation of a glassy one-phase system ($T_g$ FD-D = 80.4 °C; $T_g$ FD-E = 53.5 °C;$T_g$ FD-F = 57.9 °C).

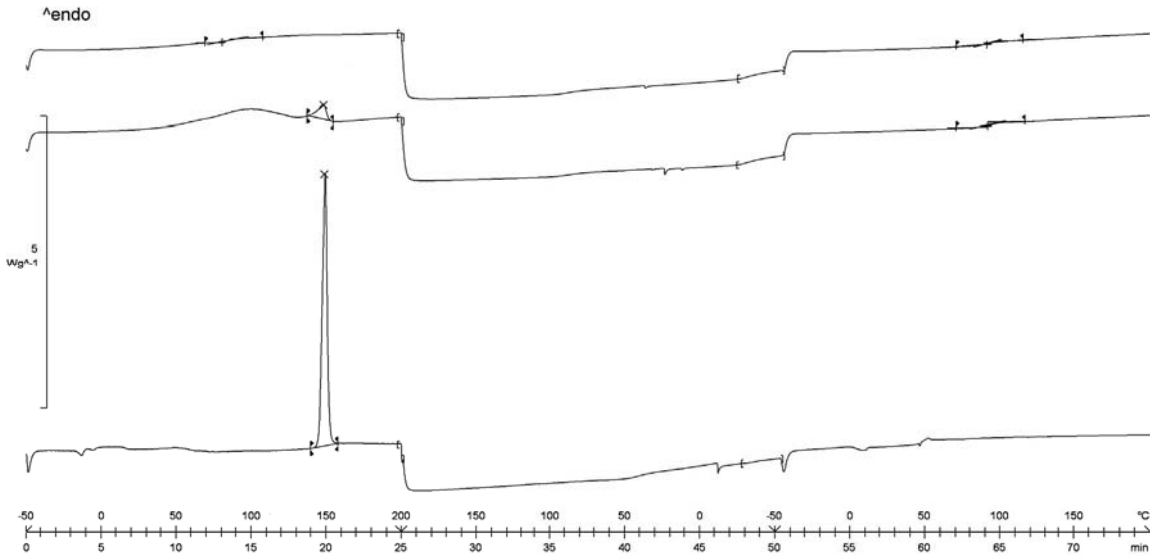


Figure 3.67: DSC thermogram of FD-D extrudate (FD+COP+HPMC≡1+3+1) with the following data displayed from top to bottom: pellets, physical mixture, pure FD

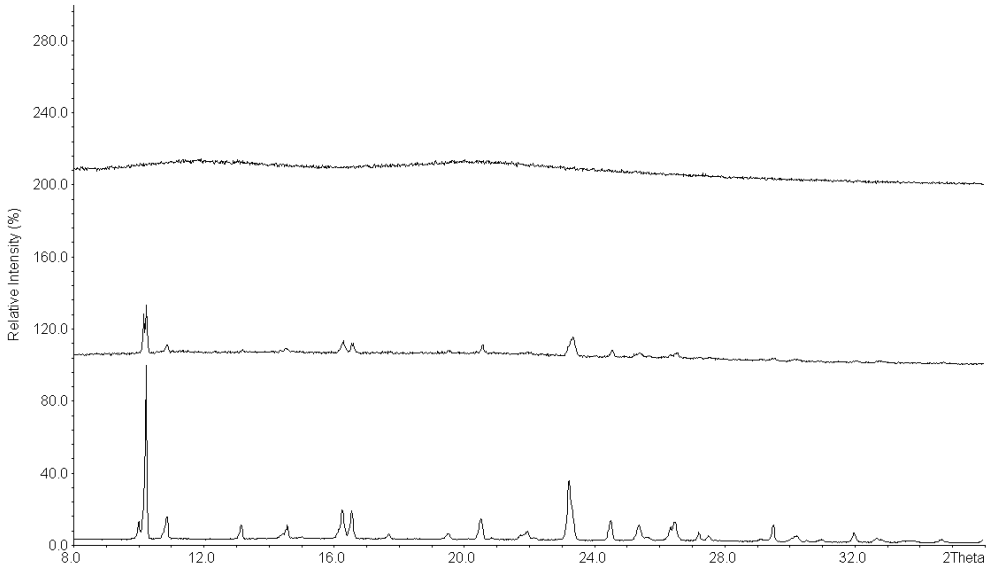


Figure 3.68: XRD pattern of FD-D extrudate (FD+COP+HPMC≡1+3+1) with the following data displayed from top to bottom: pellets, physical mixture, pure FD

It has to be pointed out that the glass transitions in the first heating cycle are not very distinct. It is possible that their evaluation is falsified by water evaporation as it was observed with all COP extrudates. Consequently, the second heating cycle was consulted to give evidence whether the formation of a single phase system is possible with the applied

compounds: One single $T_g$ in the range of 85 - 90 °C was observed for FD-D - FD-F extrudates thus confirming the previously discussed results. A glassy solution of the amorphous drug in the polymeric carrier is present.

From DSC and XRD results, the formation of a molecular dispersion of FD in the carrier(s) was confirmed.
Nevertheless, it was shown that neither an improvement of the initial release rate nor an overall enhancement of the dissolution performance is achieved through HME of FD with any of the selected polymeric blends as carrier using the given process conditions.

### 3.4.4 24 h dissolution profiles of felodipine extrudates

None of the FD formulations reached $c_{max}$ within 120 min, regardless whether a single carrier system was used or if a polymeric blend was applied as carrier (see Sections 3.4.2 and 3.4.3). For this reason, 24 h dissolution trials were performed to monitor the dissolution profile of FD pellets over an extended period of time.
Figure 3.69 shows the release profiles of hot-melt extruded FD formulations.

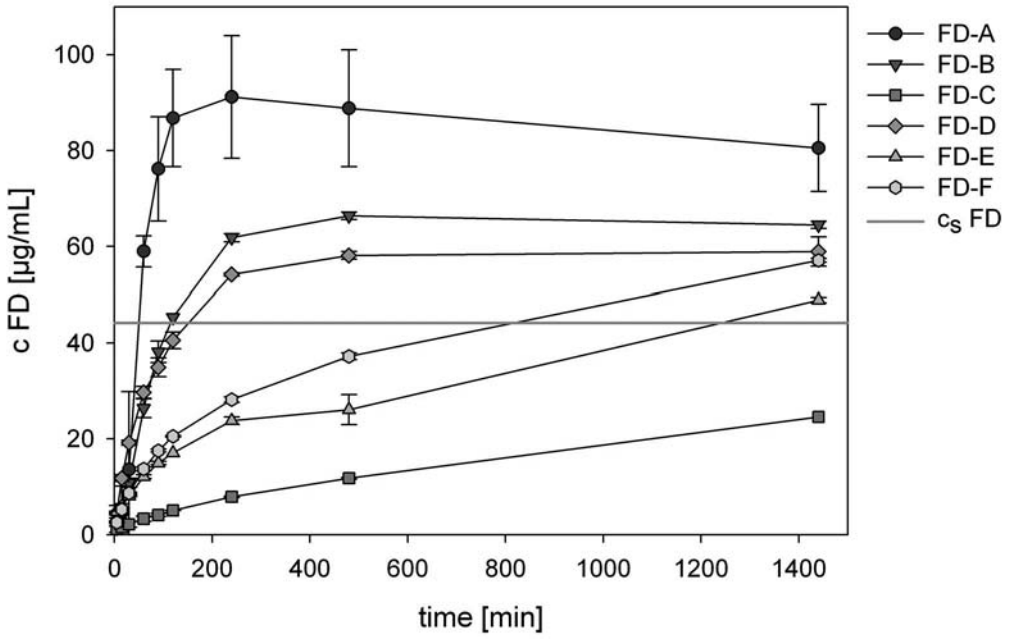


Figure 3.69: 24 h dissolution profiles of hot-melt extruded FD formulations FD-A (FD+COP), FD-B (FD+HPMC), FD-C (FD+PVCL-PVAc-PEG), FD-D (FD+COP+HPMC), FD-E (FD+COP+PVCL-PVAc-PEG) and FD-F (FD+COP+HPMC+PVCL-PVAc-PEG; see Tables 3.21 and 3.22 for the composition of the extrudates)

Formulation FD-A (FD+COP≡1+3) reaches $c_{max}$ after 240 min of dissolution. At $c_{max}$, 91.2 µg/mL are dissolved which equals 31 % of total API and is 2.1 times above saturation concentration. From this point onward, the dissolved amount of FD slowly decreases, indicating a recrystallization of the drug.
Release from HPMC formulations FD-B (FD+HPMC≡1+3) and FD-D (FD+COP+HPMC ≡1+3+1) was shown to reach a plateau value after 8 h of dissolution. The amount of dissolved API is approximately 65 µg/mL and 59 µg/mL for formulations FD-B and FD-D, respectively. The formulations are stable over 24 h of dissolution time, as no decrease of the drug concentration was observed. It is therefore concluded that HPMC acts as a recrystallization inhibiting agent in the dissolution medium (He, 2009). This effect was previously observed for hot-melt extruded FF and OX formulations; however, the stabilizing effect was not as pronounced as with FD extrudates because the concentration of dissolved drug begun to decrease within 45 min for FF extrudates and within 240 min for OX extrudates.
If PVCL-PVAc-PEG was applied as single carrier as in FD-C, the amount of dissolved FD did not exceed saturation concentration for 24 h. Even at the last sampling point, the concentration has reached only half of the $c_s$ level: 24.6 µg/mL are dissolved (8.5 % of total API).
The initial release rate was also reduced if PVCL-PVAc-PEG was applied as additional carrier as in FD-E and FD-F extrudate. After 24 h, the dissolved API exceeded $c_s$: 48.9 µg/mL were detected for FD-E and 57.1 µg/mL for FD-F. It is expected that further FD will be released from FD-PVCL-PVAc-PEG pellets if the dissolution time is even more prolonged. However, considering the situation in vivo, these results are deemed irrelevant for a future application as solid oral dosage form, which is why the trials were not pursued further.

The overall dissolution performance of FD pellets is reminiscent of the release profile of OX pellets: While a dissolution enhancement was observed with COP and HPMC formulations, as these were shown to exceed saturation concentration within 120 min of dissolution, no improvement of the dissolution profile was observed if PVCL-PVAc-PEG was applied as carrier. A glassy solution of the amorphous drug in the polymeric carrier is present with all three APIs FD, FF and OX except in the case of a PVCL-PVAc-PEG-OX extrudate.
It is concluded that the different physicochemical properties of FF and FD or OX, for example the molecular structure, and the low melting point of FF result in different drug-polymer and polymer-polymer interactions. The plasticizing effect of FF is assumed to result in a faster initial release rate of FF-PVCL-PVAc-PEG extrudates, while it is very slow for FD and OX extrudates with the same carrier. Both COP and HPMC and mixtures of these were shown to enhance the dissolution behavior of all applied drugs, even if the initial dissolution rate differs. As is postulated by Craig (2002), the release rate of the drug is dependent on the dissolution rate of the polymeric carrier which is modified by the drug's influence on the drug-polymer and polymer-polymer interactions.

## 3.5 Evaluation of results

### 3.5.1 Influence of the drug content on the release characteristics of the extrudates

A main objective of this work was to investigate the effect of the carrier on the dissolution profile of hot-melt extruded formulations. Different polymers and blends of these were applied as carriers. The polymer to polymer ratio within the carrier blend was varied to assess the effect of the carrier composition on the release profile.
In the present case, all of the extrudates containing COP, HPMC and/or PVCL-PVAc-PEG as carrier for poorly water-soluble drugs FF, FD and OX but the binary mixture of PVCL-PVAc-PEG and OX were solid solution systems with the amorphous drug molecularly dispersed within the amorphous polymer. These systems showed a carrier-controlled dissolution mechanism with the drug release being dependent on the dissolution behavior of the carrier and independent from the properties of the drug (see Sections 3.2 - 3.4 for results). In literature, it is documented, that the dissolution profile may also be dependent on the applied drug loads (Albers, 2008; Craig, 2002). As drug loads ranging from 16.7 - 25 % are applied during the experiments, the influence of the drug content on the dissolution profile of the extrudates has to be investigated. Figure 3.70 shows exemplary dissolution data of COP-OX and HPMC-OX extrudates with a drug load of 20 and 25 %.

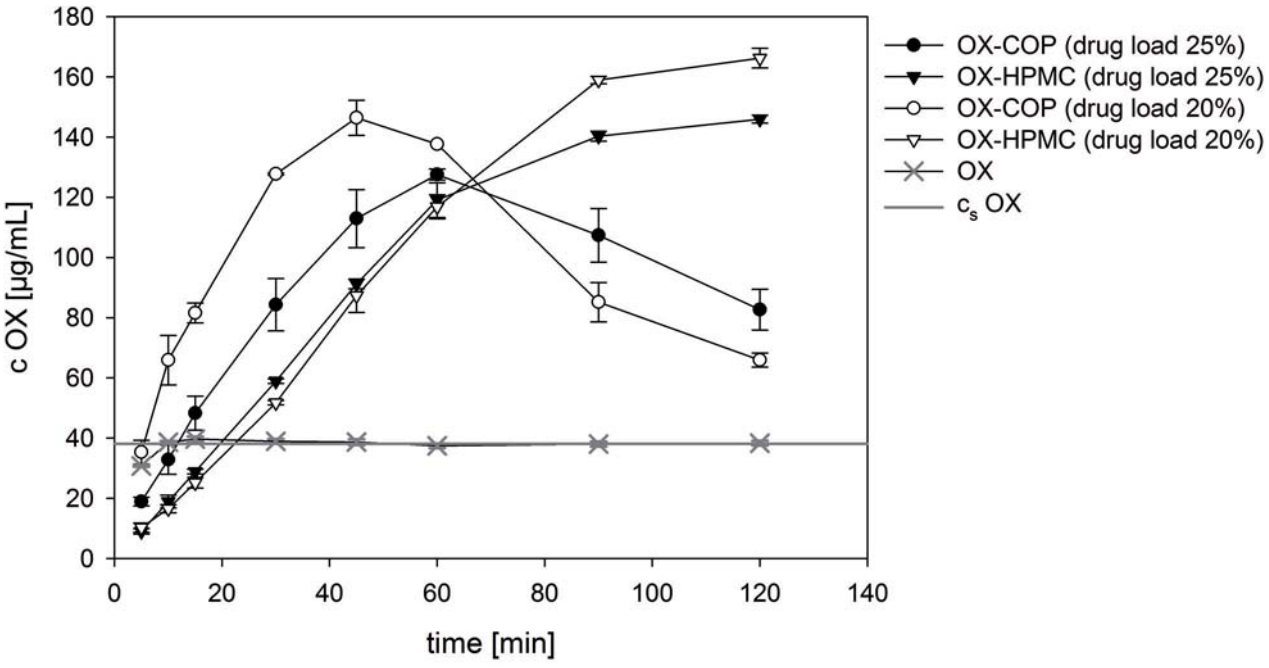


Figure 3.70: Comparison of the dissolution profiles of OX extrudates with COP and HPMC as carriers using drug loads of 20 and 25 %

Both the initial dissolution rate as well as the reached maximum concentration of dissolved drug are influenced by the drug content of the extrudates. The initial dissolution rate was shown to be lowered by increasing drug contents due to drug-polymer interactions (Corrigan, 1985). The effects of the solid dispersion composition on the dissolution processes in the surface-adjacent region are also discussed by Ford (1986) who pointed out precipitation and aggregation processes in this area which are influenced by the drug loading. Similar processes are assumed to affect the dissolution profiles of the extrudates manufactured in the course of this work. For this reason, the initial dissolution rates as well as the $c_{max}$ values reached by extrudates which are compared are not only influenced by their carrier composition, but also by the different amounts of drug they contain.
In Section 3.3.4, the variation of the drug load is discussed as a determining factor for the observed super-additive effect of the ternary blend of COP, HPMC and OX. Although it is shown that the initial dissolution rate and the reached $c_{max}$ values are increased with decreasing drug contents, the shapes of the dissolution curves remain equivalent. Consequently, special emphasis was laid on the comparison of the dissolution curve progression resulting from different carrier compositions throughout this work.

### 3.5.2 Comparison of hot-melt extruded formulations

Three different poorly water-soluble drugs were hot-melt extruded using the same selection of polymeric carriers: COP, HPMC and PVCL-PVAc-PEG. All of these carriers were shown to be suitable for the improvement of bioavailability of various APIs via solid dispersion manufacture (Leuner and Dressman, 2000; Linn et al., 2011). Successful dissolution enhancement of the three applied model drugs FD, FF and OX using different techniques for solid dispersion manufacture is documented in literature (Majerik et al., 2007; Nollenberger et al., 2009a; He et al., 2010). The main difference between the FD, OX and FF formulations are the different structural and physicochemical properties of the drugs as the applied carriers remain the same and the process conditions can be considered equivalent.
In the present work, it is shown that the dissolution profile differs from formulation to formulation. Both the initial dissolution rate and the maximum achieved concentration differ considerably (see Figures 3.71 and 3.72).
For all FF formulations using COP, HPMC and/or PVCL-PVAc-PEG as carrier, the dissolution performance was enhanced via HME. The more polymers were applied simultaneously in the carrier blend, the lower was the initial dissolution rate, especially if PVCL-PVAc-PEG was applied as additional carrier (see Figure 3.72).

The initial dissolution rate of all OX extrudates but the ternary formulation of OX, COP and HPMC (API to polymer ratio≡1+3+1) was reduced in comparison to the dissolution behavior of pure OX powder due to a slow dissolution of the extruded carrier (see Figure 3.72). The initial dissolution rate of OX extrudates using PVCL-PVAc-PEG as main or additional carrier is especially low. Nevertheless, the overall dissolution performance was improved with all OX extrudates as the release from all formulations exceeds $c_s$ within the investigated dissolution time (see Section 3.3 for the respective data).

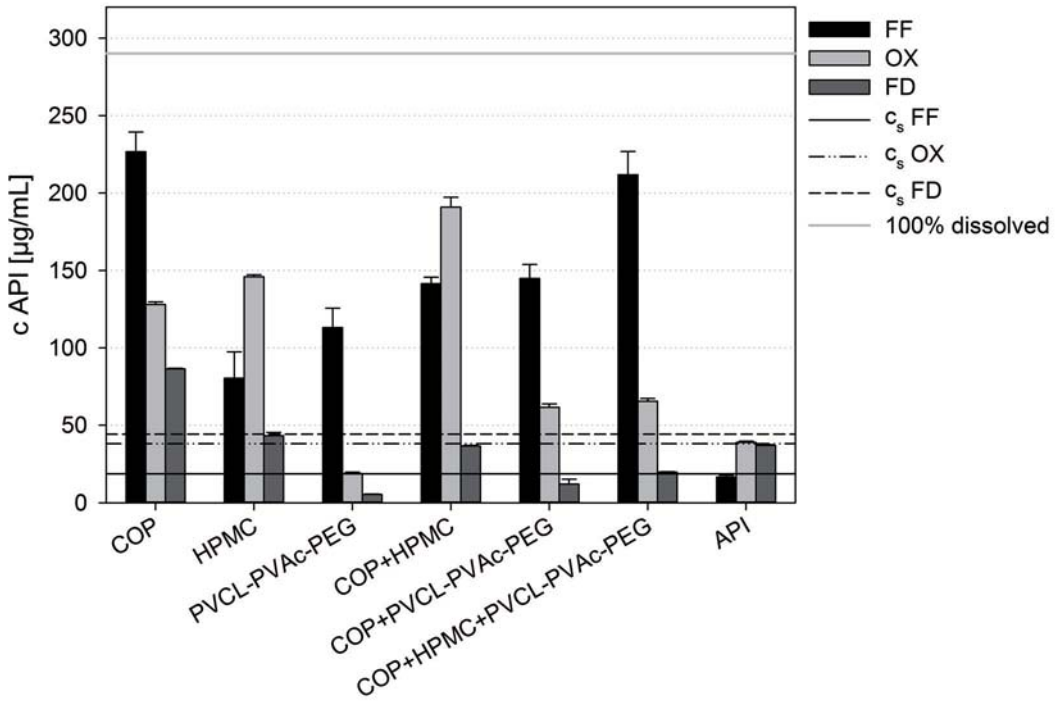


Figure 3.71: Maximum concentration levels reached with FF, OX and FD extrudates using the following carriers: COP (API+COP≡1+3 weighted parts), HPMC (1+3), PVCL-PVAc-PEG (1+3), COP+HPMC (1+3+1), COP+PVCL-PVAc-PEG (1+3+1) and COP+HPMC+PVCL-PVAc-PEG (1+3+1+1) in comparison to the untreated API powder

Although the enhancement of the maximum diluted amount of OX using PVCL-PVAc-PEG as polymeric carrier in HME was successful, this drug-carrier system is not suitable for the manufacture of instant release solid oral dosage forms under the applied conditions.
A super-additive effect was observed with hot-melt extruded OX-COP-HPMC blends as the detected $c_{max}$ was higher than the corresponding single polymer extrudates' $c_{max}$ values (see Figure 3.71). Furthermore, the initial dissolution rate was improved with the ternary mixture of OX, COP and HPMC after its extrusion (see Figure 3.72). No super-additive effect was determined for the corresponding formulations of FD and FF. In literature, a similar effect was observed by Janssens et al. (2008) who applied PEG and HPMC as carriers for itraconazole. The dissolution behavior of ternary dispersions was shown to be superior to binary dispersions of the drug in the carrier(s). Crystalline API was detected in the itraconazole-PEG solid dispersion which is a possible reason for the poor dissolution performance of this formulation. In our case, all OX extrudates were amorphous. It must be assumed that the super-additive effect is specific for this drug-carrier composition.

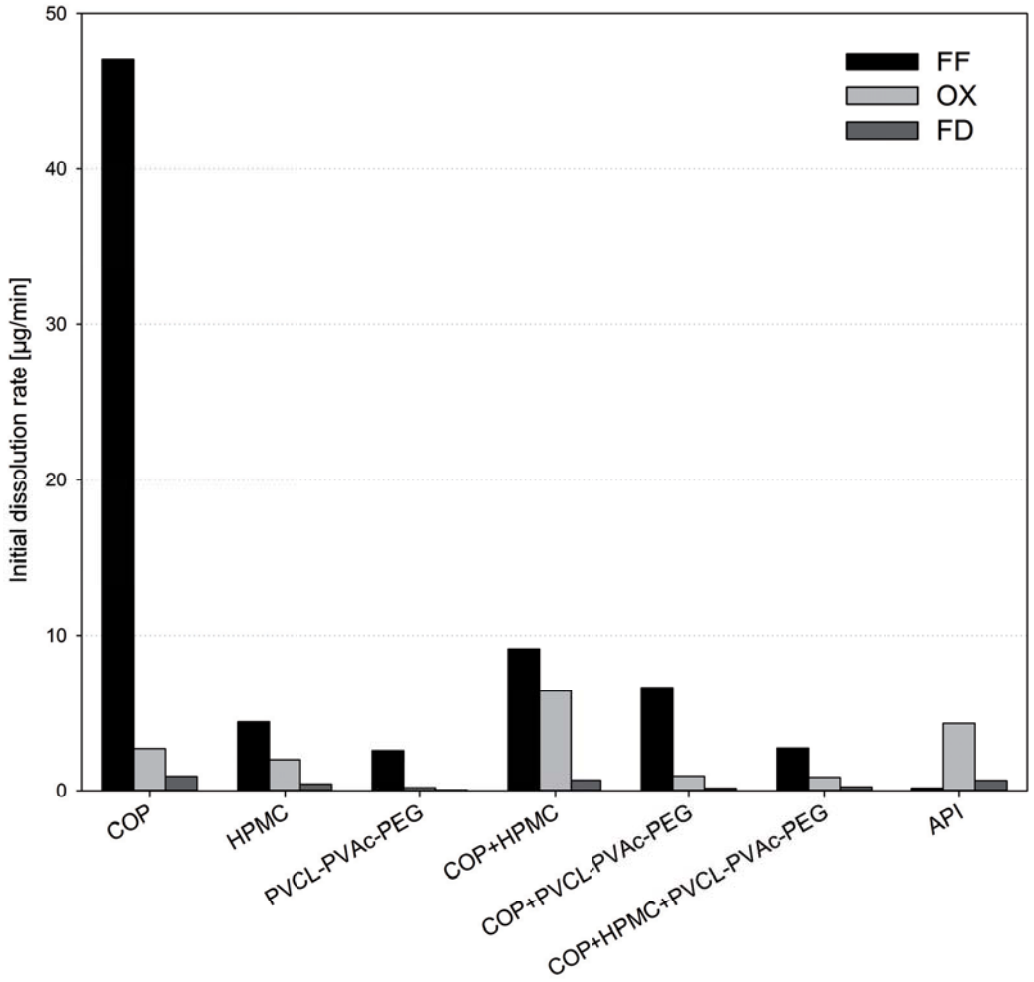


Figure 3.72: Initial dissolution rates of FF, OX and FD extrudates using the following carriers: COP (API+COP≡1+3 weighted parts), HPMC (1+3), PVCL-PVAc-PEG (1+3), COP+HPMC (1+3+1), COP+PVCL-PVAc-PEG (1+3+1) and COP+HPMC+PVCL-PVAc-PEG (1+3+1+1) in comparison to untreated API powder

With the exception of the single polymeric formulation FD+COP (≡1+3), the FD extrudates' dissolution performance within 120 min of dissolution time was equal to or worse than the dissolution profile of pure FD powder (see Figures 3.71 and 3.72). It was demonstrated that the application of PVCL-PVAc-PEG as main or additional carrier reduces the initial dissolution rate of FD. All formulations but the binary dispersion of FD and PVCL-PVAc-PEG exceed $c_s$ within 24 h of dissolution (see Section 3.4.4 for the respective data).

All extrudates with the depicted carrier compositions were found to be amorphous if analyzed directly after their manufacture. It has to be assumed that either the solid dispersion system which is formed during the extrusion process or the drug-polymer interactions within

the extrudate differ depending on the applied drug, thus leading to a different dissolution performance.
For FF extrudates, the presence of a single phase glassy dispersion of the amorphous FF in the carrier(s) was confirmed using DSC analysis. The glass transition temperatures of the extrudates containing FF were relatively low, ranging from 40 - 53 °C. Due to the plasticizing properties of FF, the polymer-polymer interactions in the extrudates are modified, possibly leading to a better release profile in comparison to the other APIs.
It was shown for OX extrudates that an amorphous, single phase system is present with single polymeric extudates OX+COP (API+carrier≡1+3) and OX+HPMC (≡1+3) as well as with the polymeric blend extrudates of OX+COP+HPMC (≡1+3+1) and OX+COP +PVCL-PVAc-PEG (≡1+3+1) as only one $T_g$ in the range of 50-90 °C was detected. With the OX formulation using PVCL-PVAc-PEG as carrier (API+carrier≡1+3), the glass transition of the pure drug was detected in the first heating cycle, indicating a two-phase system of the amorphous drug in the amorphous carrier. It was thus shown that a glassy suspension is present. No distinct glass transition was detected in the first heating cycle of the quaternary OX formulation (OX+COP+HPMC+PVCL-PVAc-PEG≡1+3+1+1), but it was shown in the second heating cycle of the corresponding physical mixture that the formation of a one-phase system is possible.
Only one single $T_g$ (50-80 °C) was detected for all FD extrudates, indicating a glassy dispersion of the amorphous drug in the amorphous carrier. The observed glass transitions for FD formulations using blends of COP and HPMC or COP, HPMC and PVCL-PVAc-PEG as carrier are not very distinct as they are partially overlaid by the evaporation of water.

In summary, the formulations with the carrier(s) COP, PVCL-PVAc-PEG, COP+PVCL-PVAc-PEG and COP+HPMC+PVCL-PVAc-PEG show the same trend in their dissolution profiles: Best results are achieved with FF, the second highest values with OX and the lowest $c_{max}$ levels were reached with FD (see Figure 3.71). In contrast to FF and FD extrudates where the highest initial release rates and $c_{max}$ values were reached with COP as carrier, the maximum concentration values reached with HPMC or the blend of COP and HPMC as carrier for OX were superior to those gained with COP. However, different dissolution media were applied to ensure a discriminatory testing method for each API thus prohibiting a direct comparison of dissolution results gained with OX extrudates to the results obtained with FF or FD extrudates.
From DSC results it can be concluded that the dispersion profiles of the drugs in the carrier(s) are equivalent as glassy solutions are formed in all cases but in the case of OX-PVCL-PVAc-PEG extrudate which is a glassy suspension as a two-phase system was detected. Hence, it has to be assumed that the super-additive effect of the OX-COP-HPMC formulation (≡1+3+1) is a result of substance-specific properties, for example drug-polymer interactions which are not reproduced with FF or FD.
In conclusion, it can be stated that the release behavior of all manufactured extrudates is mainly controlled by the polymeric carrier. In the case of a carrier-controlled dissolution mechanism, changes of the carrier properties affect the dissolution profile of the hot-melt extruded samples, for example through a variation of the polymeric blend or through undesired

storage effects as the absorption of water or an aging of the polymer, all of which applies to the manufactured extrudates (Corrigan, 1985; Dubois and Ford, 1985; Craig, 2002). Since substance-specific properties were shown to have an influence on the dissolution behavior as well, a definite conclusion on the dissolution mechanism of the manufactured extrudates cannot be drawn. The observed dissolution profiles are assumed to be a result of a combination of a carrier-controlled dissolution mechanism and drug-polymer specific interactions. It was demonstrated that the dissolution curves of ternary or quaternary formulations lie intermediate between the dissolution curves of the binary dispersions of the drug in a single polymer. Predictions can be made on the dissolution performance of formulations with a polymeric blend as carrier previous to their manufacture if the dissolution behavior of the hot-melt extruded single carriers is known beforehand. However, the dissolution performance of the extruded formulations is not solely determined by the dissolution profile of the extruded polymeric carrier. It has to be emphasized that the differences of the analyzed extrudates' dissolution profiles arise on the one hand from the plasticizing properties of FF and on the other hand from PVCL-PVAc-PEG's slow dissolution rate. The release profiles are not only influenced by the applied carrier system, but also by the physicochemical properties of the drug as, for example, the plasticizing properties of FF strongly improve the dissolution performance. This assumption has to be verified by the use of a plasticizing agent as an additional excipient in FD or OX extrudates.
Overall, the application of polymeric blends as carriers offers the possibility to fit the extrudate's release profile to one's needs as the dissolution curves of extrudates with polymeric blends were shown to lie intermediate between the dissolution curves of the respective extrudates with only one of the polymers as carrier. Unfortunately, the results are not fully transferable from one API to the other due to substance-specific interactions. Limited knowledge of the release mechanisms and present drug-polymer or polymer-polymer interactions limits the possibility to predict the dissolution profile of polymeric blend extrudates without information about the single carrier extrudates' dissolution performance.

### 3.5.3 Comparison of the applied manufacturing methods

Two different technologies for solid dispersion manufacture were applied: the novel USAC technique and the somewhat more established HME. Blends of FF and one of the polymers COP, HPMC, PVCL-PVAc-PEG, aPMMA and PVA-AA-MMA with a drug to polymer ratio of 1+3 weighed parts (corresponds to a drug load of 25 %) were either US-compacted or hot-melt extruded. The solid formulations were then assessed for their physical state to verify the technologies' suitability for solid dispersion manufacture. Furthermore, their dissolution profiles were compared to allow for an evaluation of the two methods.
In all USAC formulations, crystalline API was detected, indicating an incomplete transition of the material into its amorphous state (see Section 3.1.5 for results). A glassy suspension of the partially crystalline drug in the amorphous carrier is formed. The presence of crystalline and amorphous clusters of the drug within the compact is assumed. These results are in accordance to the observations made by Sancin et al. (1999) who used a different poorly

water-soluble model drug with a low melting point, ketoprofen ($T_g$=94-97 °C; European Pharmacopoeia), for the assessment of USAC technology and was also not successful in the manufacture of a glassy solution.
With all FF extrudates but the one using PVA-AA-MMA as polymeric carrier, the manufacture of a glassy solution of the drug in the carrier was successful using hot-melt extrusion. Crystalline API was detected in the FF-PVA-AA-MMA extrudate and the presence of a two-phase system was confirmed by DSC analysis, indicating the formation of a glassy suspension of the crystalline drug in the amorphous and partially degraded carrier (see Section 3.2.2 for results).
Maximum dissolution enhancement is to be expected from a molecular dispersion of the drug in the carrier as it is present in hot-melt extruded FF formulations with COP, HPMC, PVCL-PVAc-PEG and aPMMA (Goldberg et al., 1965).
When comparing the dissolution data of the formulations manufactured either using USAC or HME, the superiority of the hot-melt extruded formulations' dissolution profile was confirmed (see Figure 3.73 and Table 3.23).

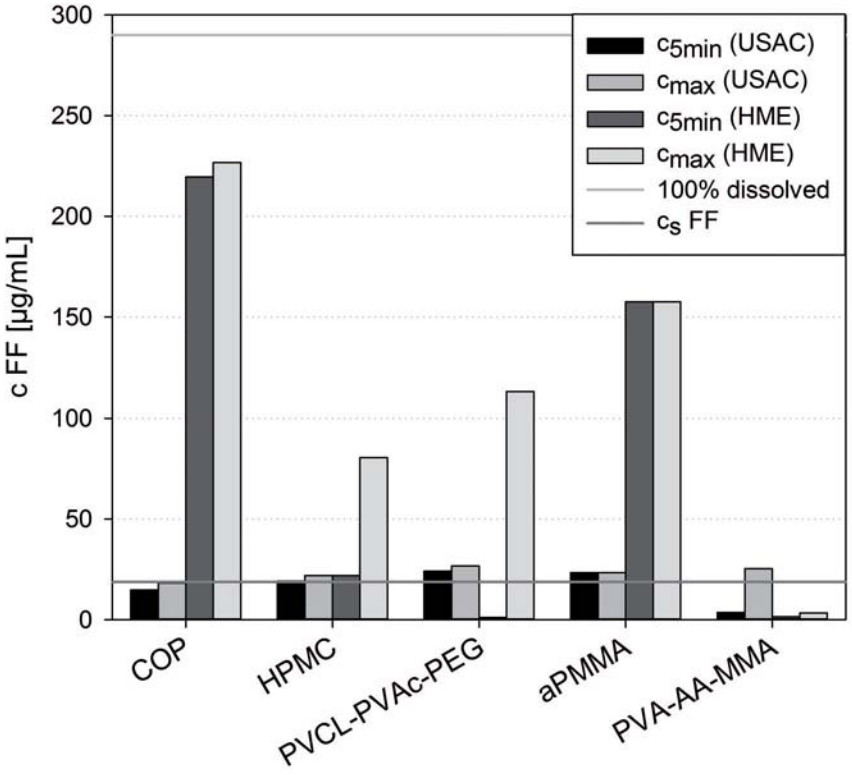


Figure 3.73: Comparison of FF formulations produced via USAC and HME showing the dissolved amount of FF after 5 min ($c_{5min}$) and $c_{max}$ values observed within 120 min of dissolution time

Table 3.23: Comparison of USAC and HME technology using the AUC values derived from dissolution profiles of either US-compacted or hot-melt extruded formulations (FF to carrier ratio≡1+3 weighted parts)

| Carrier | AUC values [µg/mLmin] | |
|---|---|---|
| | USAC | HME |
| COP | 2007 | 10426 |
| HPMC | 2241 | 4905 |
| PVCL-PVAc-PEG | 2698 | 6486 |
| aPMMA | 2269 | 3355 |
| PVA-AA-MMA | 2481 | 281 |
| untreated FF | 1227 | |

If COP or aPMMA are used as carriers, the dissolved amount of FF after 5 min of dissolution is approximately 8-12 times higher for the pelletized formulations. In contrast, the dissolved amount from FF-HPMC extrudates and US compacts is approximately equal and from PVCL-PVAc-PEG or PVA-AA-MMA pellets it is lower than the release from the respective compacts after 5 min of dissolution. This is due to the slow dissolution of PVCL-PVAc-PEG which is improved by milling of the compacts while the extrudates are pelletized. As is described in the Section 3.2.3, it was decided not to mill the hot-melt extruded strand because of unfavorable effects of the milling process on the extrudates. Unlike from the pelletized extrudates, the US compacts are too large for a possible application as single dosage form. Milling is thus mandatory for the USAC formulations. The slow initial release from FF-PVA-AA-MMA pellets is associated with the degradation of the carrier during the extrusion process.
Calculations of the area under the curve [$\mu g/mLxmin$] (AUC) values of the formulations demonstrate the enhancing effect of HME technology: the AUC of hot-melt extruded FF formulations using COP, HPMC or PVCL-PVAc-PEG as carrier are 2.2 - 5.2 times superior to the corresponding USAC compact. The FF-aPMMA formulation is improved by 1.5 times if processed via HME. Due to the incompatibility of PVA-AA-MMA with the high temperatures prevailing during the HME process, the dissolution profile is enhanced only if the formulation is compacted using USAC technology.
Regardless of the applied technique, the initial dissolution rate, $c_{max}$ as well as the AUC are improved in comparison to the untreated API with the exception of FF-PVA-AA-MMA extrudate.
From the assessed formulations' dissolution profiles and solid state characteristics it is concluded that HME is especially suitable for the manufacture of homogeneous solid dispersion systems with an enhanced release behavior. Especially if the drawbacks of the USAC technology in its current state are taken into consideration, for example insufficient process control by the user, scarce and seemingly inaccurate process monitoring tools, difficult and time-consuming operation of the USAC machine and, most importantly, an unsatisfactory reproducibility of results, the application of HME has to be preferred.

### 3.5.4 Comparison to untreated physical mixtures

The formulations manufactured by USAC or HME were compared to their untreated physical mixtures of the respective drug and carrier(s) in order to identify the impact of the manufacturing process on the material characteristics. Consequently, the physical mixture of each API-carrier combination which was used in the course of the present study was assessed for its physical state and dissolution behavior.
The DSC thermograms and XRD diffractograms demonstrated the unchanged, crystalline state of the API in the physical blend of the components (see Sections 3.1 - 3.4). In contrast, a partial or complete conversion of the API into its amorphous form was determined for both the US-compacted as well as for the hot-melt extruded material.
Figures 3.74 - 3.77 show the dissolution profiles of either USAC compacted, hot-melt extruded or untreated formulations of FD, FF, OX and the polymers COP, HPMC, PVCL-PVAc-PEG, aPMMA and PVA-AA-MMA applied as single polymeric carriers or as a blend. Through the application of HME, the release profile of all FF formulations was enhanced. As can be seen in Figure 3.74, the initial dissolution rate as well as the maximum concentration of dissolved FF was higher with all extruded formulations in comparison to the corresponding physical mixtures.

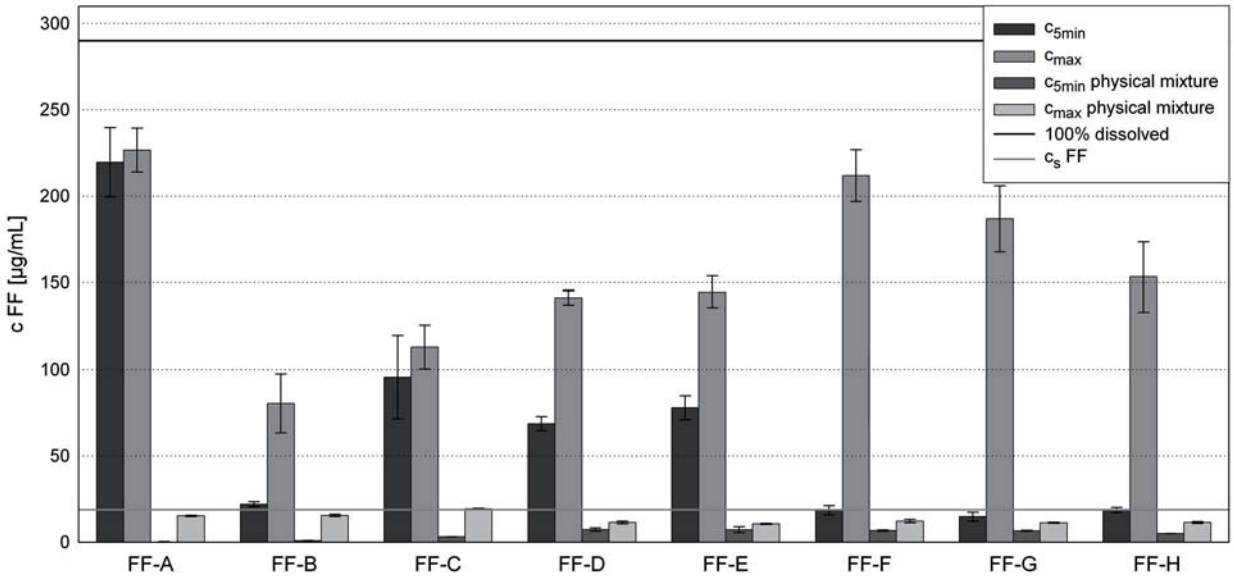


Figure 3.74: Dissolution profiles of FF pellets and untreated physical mixtures

While the physical mixtures did not reach the supersaturation level, $c_s$ was exceeded with all hot-melt extruded formulations of FF within 5 to 15 min of dissolution. It was pointed out that the concentrations reached with the physical mixtures with PVCL-PVAc-PEG as main carrier are consistently above the results gained with pure FF due to its solubilizing effect (Technical Information Soluplus). For example, the release level of the physical mixture

of the formulation FF-C is consistently 3 µg/mL above the pure APIs dissolution profile. Formulations FF-A, FF-B and FF-D to FF-H can be considered equivalent to the release profile of pure FF powder. For all OX extrudates, the dissolved amount of API after 5 min of dissolution was reduced in comparison to the untreated physical mixture, pointing out a slow initial dissolution rate. While the $c_{max}$ value of the physical blends was at saturation level, it exceeded $c_s$ with all hot-melt extruded formulations but the one using PVCL-PVAc-PEG as single polymeric carrier (OX-C) (see Figure 3.75). This is due to a slow dissolution rate of the extruded polymeric carrier (Kolter et al., 2010).

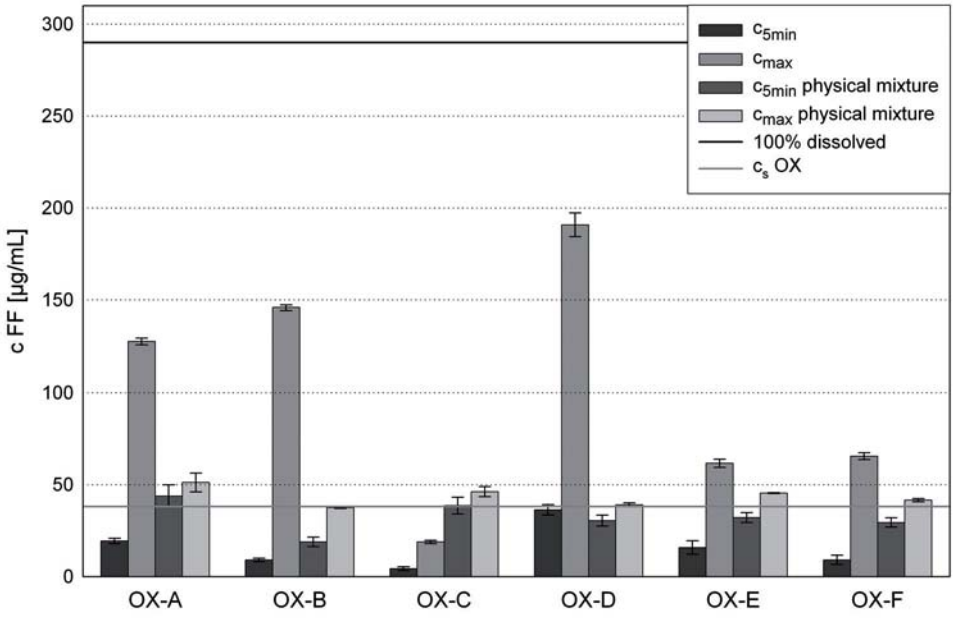


Figure 3.75: Dissolution profiles of OX pellets and untreated physical mixtures

With FD pellets, the initial dissolution rate was not improved in comparison to the corresponding physical mixtures (see Figure 3.76). Only the FD-COP extrudate (FD-A) showed enhanced maximum concentration levels. Hot-melt extruded formulations with HPMC as single polymeric carrier (FD-B) or as an additive to a polymeric blend (FD-D) were equivalent to their physical mixtures. PVCL-PVAc-PEG is clearly not suitable for a dissolution enhancement of FD using the applied method, as both the initial dissolution rate as well as the $c_{max}$ values were below those achieved with the untreated blend of the components.
In summary, the results gained with one poorly water-soluble model API cannot be transferred onto another. Although all hot-melt extruded FF formulations were superior to their physical mixtures, the $c_{max}$ values were improved only with five out of six OX extrudates and the initial dissolution rates were reduced for all but one OX formulation in comparison to the corresponding physical mixtures. With FD as model API, the initial dissolution rate was lowered for all extrudates and the maximum dissolved amount of FD was improved only with one out of six extrudates.

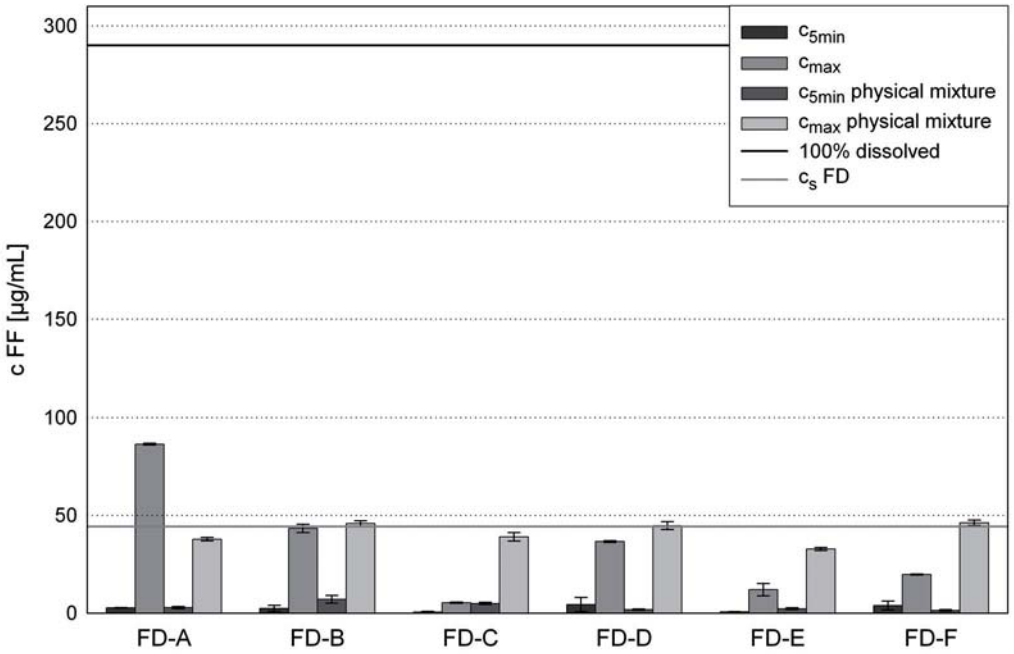


Figure 3.76: Dissolution profiles of FD pellets and untreated physical mixtures

If USAC technology was applied for the manufacture of solid dispersion systems, only the initial dissolution rate was improved in comparison to the untreated blend of the components (see Figure 3.77).

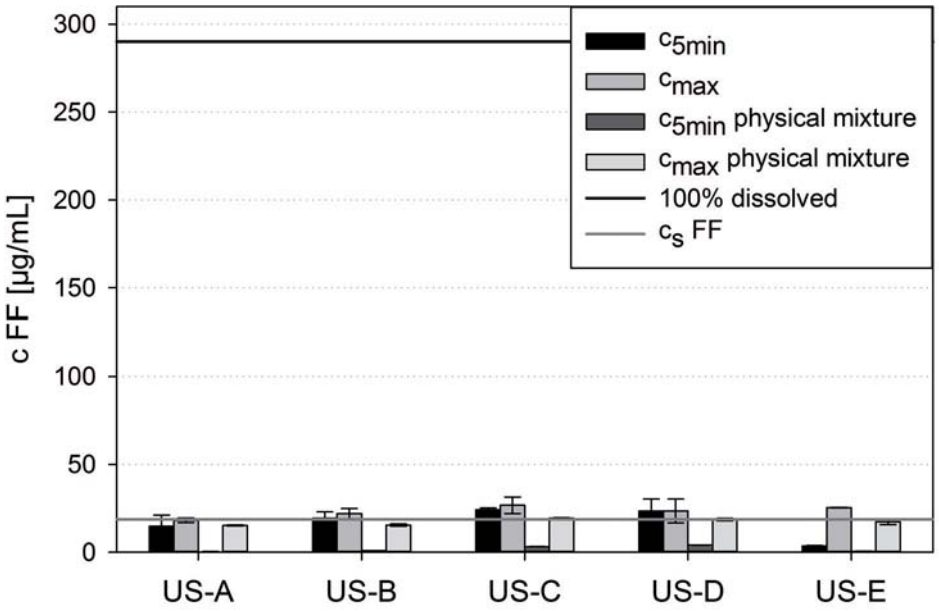


Figure 3.77: Comparison of US-compacted FF formulations to physical mixtures

As crystalline API is present in all manufactured compacts, an improvement of the initial dissolution rate was not expected (McGinity et al., 1984; Craig et al., 1999). The observed effect may be contributed to an intensified contact of API to the carrier which is induced by the melting and subsequent solidification during the USAC process thus improving the wettability. The importance of the initial dissolution rate on the bioavailability in vivo is discussed by Sato et al. (1981). Due to a fast recrystallization in the aqueous dissolution medium which is induced by crystalline fractions of the API within the compact, the dissolved amount of FF does not exceed saturation concentration (Haleblian and McCrone, 1969).

### 3.5.5 Comparison to marketed solid dosage forms

For a better assessment of the observed changes to the dissolution profiles of the applied model drugs induced by USAC or HME technology, the results were compared to the performance of marketed solid oral dosage forms containing the same API.
For FF, there are numerous products available on the market, for example sustained-release preparations or formulations containing micronized or nanosized API. The marketed FD solid oral dosage forms show all a sustained-release profile while the intention of the present work was to manufacture immediate release formulations. Hence, the FD extrudates and originators are incommensurable.
Until now, no formulations containing OX have been marketed.
Therefore, the juxtaposition of the extrudates and originators was performed only with FF. Lipidil®, which contains micronized FF, Lipidil-Ter®, which contains micronized FF dispersed upon a hydrophilic PVP matrix, and Lipidil 145 ONE®, which is a nanoparticulate FF formulation, were chosen as comparators for FF pellets.
As can be seen in Figure 3.78, the initial dissolution rate of the analyzed comparators differs.

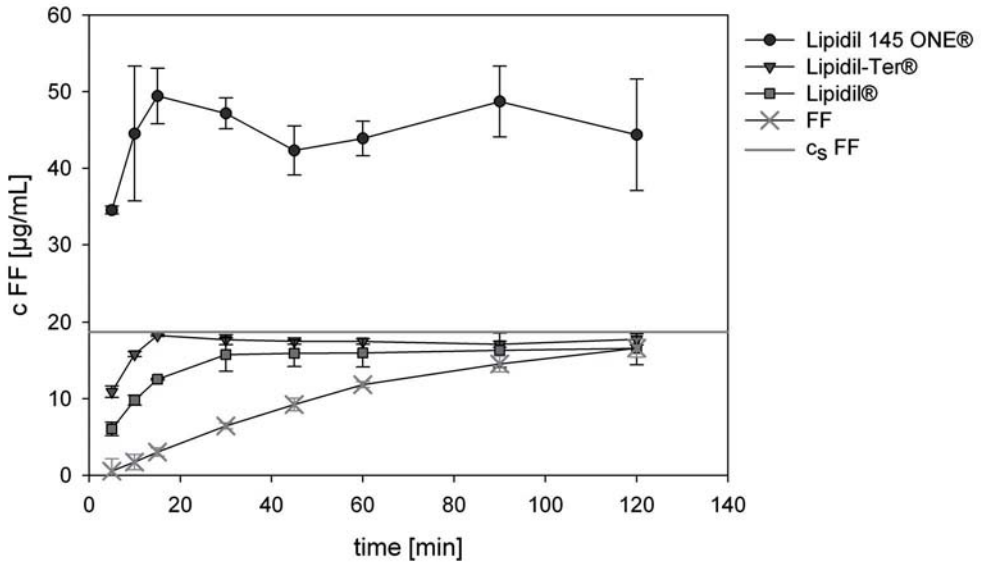


Figure 3.78: Dissolution profile of originators in comparison to pure FF powder

With Lipidil®, a dissolved amount of 6.1 µg/mL of FF is reached after 5 min of dissolution. The initial dissolution rate is enhanced with Lipidil-Ter®. Lipidil 145 ONE® is the only one of the three investigated comparators whose FF release exceeds the saturation concentration under the experimental conditions.
Difficulties were encountered with the nanoparticulate formulation as the detected amount of FF in the samples strongly depends upon the pore size of the filters used as is shown in Figure 3.79 where two syringe filters with differing pore sizes are compared. As the term "nanoparticle" is usually associated with particles smaller than 400 nm in the pharmaceutical sector, it is assumed that both dissolved FF and nanoparticulate FF are detected via HPLC analysis if filters with 0.45 µm pore size are applied. If filters with a 0.2 µm pore size are used, the nanoparticulate FF is partially or completely removed from the sample, thus leading to lower detected concentration values (see Figure 3.79).

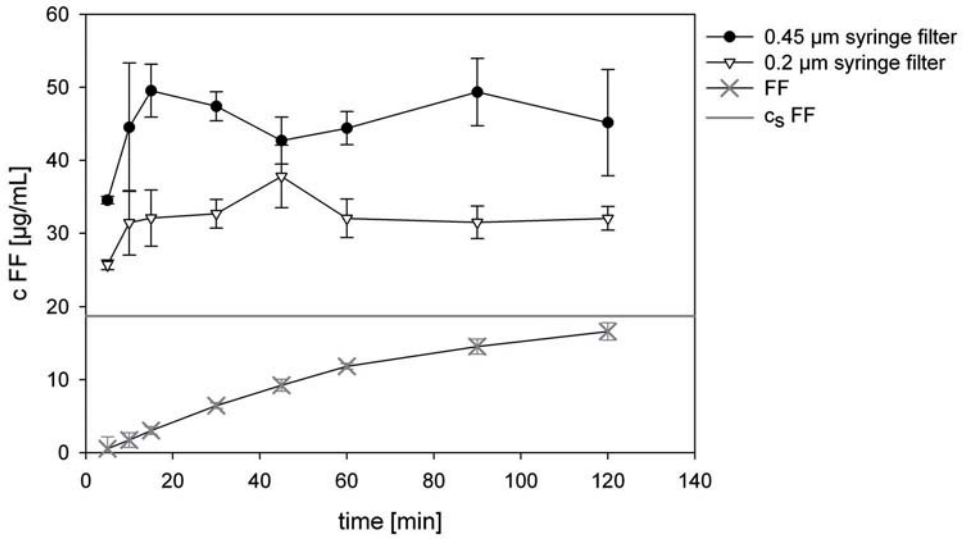


Figure 3.79: Dissolution profile of nanoparticulate originator product using two different syringe filter pore sizes

It was chosen not to remove the nanosized particles through filtration as it has to be assumed that these are essential for the in vivo performance of the originator. Therefore, syringe filters with a pore size of 0.45 µm were used for all samples.
The maximum concentrations of dissolved FF reached with the comparators within 120 min of dissolution testing are 17 µg/mL with Lipidil® and Lipidil-Ter® and 49 µg/mL with Lipidil 145 ONE®.
All of the hot-melt extruded FF formulations exceed saturation concentration within 15 min or less. The $c_{max}$ values were 80-227µg/mL, depending on the applied carrier(s). It was thus demonstrated, that hot-melt extruded FF formulations are superior to the analyzed marketed solid dosage forms regarding the maximum concentration of dissolved API. With Lipidil 145 ONE®, the supersaturation level was stable over time, in contrast to the manufactured extrudates where the dissolved amount of drug decreased due to recrystallization effects.

### 3.5.6 Comparison to other available methods for solid dispersion preparation

To allow an evaluation of the results achieved using HME and various single polymers or polymeric blends as carriers for different poorly water-soluble model drugs, their dissolution performance and storage stability were compared to literature data. As there are numerous manufacturing methods available for solid dispersion formulation, these other techniques were also included in the assessment.
The results of the dissolution studies in the quoted literature are mostly given in % of the total amount of drug applied to the dissolution medium. For a better comparison, the absolute concentrations of the dissolved drug in the medium were calculated from the available data and are given in µg/mL.

In the present work, the initial dissolution rate of FF was successfully enhanced using HME. Supersaturation levels of up to 12.1 times were detected, followed by a decrease of the dissolved amount of FF due to recrystallization effects. The stability of the supersaturation was improved if additional polymers were added to the API-polymer blend prior to the extrusion. During storage at 25 °C/60 % rH, recrystallization was observed with HPMC and PVCL-PVAc-PEG but not with COP due to its recrystallization inhibiting effect. With increasing storage times, the dissolution performance decreased for all formulations but the one with HPMC as single carrier due to a rising humidity content of the pellets.
Kanaujia et al. (2011) used HME to manufacture COP-FF and PVP-FF extrudates. Directly after manufacture, 30 % of the drug dissolved resulting in a concentration of 60 µg/mL. After 4 weeks of storage, crystallinity was detected in both samples and the dissolution profile was equivalent to pure API. In our case, up to 78 % of the drug were dissolved (COP-FF) which equals a concentration of 227 µg/mL. The performance of the extrudates was superior to pure FF powder throughout the investigated storage time of 26 weeks. It must be emphasized that Kanaujia et al. (2011) milled the extrudates prior to analysis and storage testing. Milling was observed to induce recrystallization and to modify the dissolution behavior (see Section 3.2.3). Under the employed storage conditions (40 °C/75 % rH) this might affect the dissolution performance within storage times as short as 4 weeks.
He et al. (2010) applied aPMMA and COP as carriers for FF using HME. Approximately 55-85 % of FF were dissolved. No decrease of the concentration level due to precipitation effects was observed within 120 min of dissolution time. Instead of polysorbate 80, sodium dodecyl sulfate was employed as an additive to the dissolution medium to facilitate wetting. As a result, the dissolved amount of FF from untreated API powder reached 30 %. With polysorbate, only 6.5 % of the drug dissolved. The absolute concentration of dissolved API could not be calculated as the applied volume of the dissolution medium is not known. The dissolution peformance of the COP-FF extrudate manufactured in the course of this work is approximately 12 times superior to the pure API powder, while it is only 2 times superior in the case of the COP-FF extrudates manufactured by He et al. (2010). Again, the extrudates were milled prior to the dissolution testing. The presence of crystalline FF within the milled solid dispersions was confirmed.
FF solid dispersion systems were also investigated by Sheu et al. (1994). The melting method was employed to incorporate FF within PEG. Depending on the crystallinity of the sample,

the initial dissolution rate varied. 100 % of drug dissolution was achieved with most formulations. The resulting concentration of the drug in the dissolution medium is 111 µg/mL. However, as 900 mL of an ethanolic solution were used as dissolution medium, the results are not comparable to the data of the present work.
Lyophilization was used to manufacture FF solid dispersions with PVP, hydroxypropylbetadex (hydroxypropyl-$\beta$-cyclodextrin), inulin, PEG or mannitol as carrier by Srinarong et al. (2009). Different methods to incorporate superdisintegrants into the solid dispersion system were investigated. Depending on the carrier, superdisintegrant and incorporation method, the dissolution profile was enhanced to up to 60-100 % of dissolved drug. A sample amount equivalent to 48 mg of FF was added to 1000 mL of dissolution medium resulting in concentrations of 29-48 µg/mL of dissolved API. Sink conditions were employed for dissolution testing resulting in a poor comparability of these results to the present work.
The fusion method was employed using PEG as carrier for FF by Law et al. (2003). The manufacturing of eutectic mixtures of the components was observed to reduce the particle size of the API and to improve the dissolution profile in comparison to the untreated FF powder. The dissolution behavior was not affected by storage.
Vogt et al. (2008) compared different techniques for bioavailability enhancement of FF. Cogrinding and spray-drying of FF with lactose enhanced the dissolution profile of the drug, while the analyzed originators were equivalent to the untreated API powder. In coground mixtures, the drug remained in its crystalline state while a conversion to the amorphous state was induced by the spray-drying process. The amorphous formulations of lactose and FF showed a similar dissolution profile to the COP-FF extrudate: the $c_{max}$ value of, in this case, 60 % of dissolved drug was reached within 10 min of dissolution, followed by a subsequent decrease of the supersaturation level due to recrystallization processes. At $c_{max}$, the spray-dried FF-lactose formulation reached a concentration of 40 µg/mL of dissolved API. Cogrinding resulted in slower initial dissolution rates and stable concentration levels, but the dissolved amount of FF did not exceed the saturation level.
As a conclusion, the dissolution profile of FF may be enhanced by different techniques for solid dispersion manufacture. The dissolution performance and storage stability of the formulation is strongly dependent on the carrier type and the physical state of the API.

The HME method used to enhance the dissolution behavior of FD in this work, was successful with COP as carrier. 30 % of the total amount of drug were dissolved after 120 min of dissolution which equals a concentration of 86.4 µg/mL. If the binary mixture of HPMC and FD or the ternary mixture of both and COP was hot-melt extruded, the dissolution was equivalent to the untreated API powder for approximately 120 min. The saturation level was exceeded by FD-COP pellets after 45 min and by FD-HPMC and FD-COP-HPMC pellets after 2-4 h. With PVCL-PVAc-PEG as carrier, the dissolution performance was well below the level of the untreated drug for at least 8 h. All of the extrudates were amorphous one-phase systems (see Section 3.4).
HME of FD and aPMMA was compared to a spray-drying method by Nollenberger et al. (2009b). To stabilize the supersaturation level, an ethyl acrylate and methyl methacrylate

copolymer dispersion (Eudragit® NE 30 D) was added to the blend. With both manufacturing methods, an amorphous solid dispersion was obtained. Approximately 80 % of the drug were dissolved within 10 min of dissolution time which equals a concentration of 16 µg/mL. No decrease of the dissolved amount of FD due to recrystallization processes was observed within 60 min of dissolution time. These results are seemingly superior to those gained in the course of the present work. However, higher $c_{max}$ levels were reached with FD extrudates using COP and/or HPMC as carriers. A drug load as low as 10 % (w/w) was used by Nollenberger et al. (2009b), and only a sample amount corresponding to 10 mg was used for dissolution experiments. In the present case, 145 mg were applied. The drug loads of the manufactured solid dispersions were 16.7 - 25 %. It is reported that lower drug loadings facilitate carrier-controlled dissolution behavior (Craig, 2002). A high surplus amount of the drug in the dissolution sample results in high drug loadings in the boundary layer of the pellets, promoting a faster recrystallization rate and reducing the initial dissolution rate. Even so, the concentration levels of the hot-melt extruded FD formulations using COP and/or HPMC as carrier are higher than those reached with aPMMA. It is assumed that both the suitability of the drug-carrier composition as well as the different testing conditions lead to the observed differences in the dissolution performance of the FD solid dispersions. It is very probable that if Nollenberger et al. had applied a higher sample amount, the dissolved amount of FD would also have surpassed saturation concentration.

Alonzo et al. (2011) prepared solid dispersions of FD and PVP or HPMC as carriers using the solvent method. The obtained solid dispersions were cryomilled prior to analysis. At 10 % drug loading, the dissolved amount of drug reached concentration levels of approximately 30-90 µg/mL. The higher the sample amount, the more pronounced the supersaturation and the subsequent drop of the dissolution curve. Crystalline submicron particles were detected via dynamic light scattering approximately 5 min after the start of the dissolution experiments which correlates with the concentration decrease. These nanosized particles were shown to add up to the concentration of dissolved FD which was determined via UV analysis. As their size increases due to recrystallization processes, the detected amount of the drug decreases. HPMC was shown to reduce the particle growth in contrast to PVP. When a drug load of 50 % was used, the maximum concentrations remained at the same level as pure amorphous FD. It is concluded that the dissolution is drug-controlled at high drug loadings, without a beneficial effect of the polymeric carrier. In the present case, these findings were not confirmed, as none of the FD extrudates showed an immediate release profile.

The solvent evaporation method was applied by Konno et al. (2008), who used PVP, HPMC and HPMC acetate succinate as carrier for FD. Supersaturation levels of up to 5 times were observed. With HPMC as carrier, 2-5 µg/mL of FD dissolved, depending on the applied drug to polymer ratio. With FD-HPMC extrudates, a concentration of 43.3 µg/mL was reached within 120 min of dissolution time. It has to be pointed out that Konno et al. applied USP simulated intestinal fluid pH 6.8 as dissolution medium, while in the present case hydrochlorid acid medium pH 1.2 was used.

The observed differences between the literature data and the results of the FD extrudates are contributed to the different testing conditions, the applied manufacturing method or, as

was demonstrated in Section 3.2.3, to effects induced by the milling of the samples which was performed by both Alonzo et al. (2011) and Konno et al. (2008).

Similar results to those gained with FD were observed with OX extrudates. While the dissolution performance was enhanced with COP and HPMC or the mixture thereof as carrier(s), reaching $c_{max}$ values of 44-66 % (128-191 µg/mL) within 120 min of dissolution time, the dissolution rate was drastically reduced with PVCL-PVAc-PEG. A glass transition in the range of pure OX was detected in the binary extrudate of PVCL-PVAc-PEG and OX, indicating a two-phase system which is a possible reason for the poor dissolution performance of this formulation. A substance specific super-additive effect with the hot-melt extruded ternary blend of OX, COP and HPMC was observed.
Unfortunately, no literature data on hot-melt extruded systems containing OX are available for comparison.
Solid dispersions of OX were prepared using various technologies, for example spray-freezing and supercritical antisolvent (SAS) methods (Badens et al., 2009; Majerik et al., 2006, 2007; Majerik, 2006). Different polymers were applied as carriers: aPMMA, ammonio methacrylate copolymer (Eudragit® RL), poloxamers 188 and 407, PEG and PVP.
With SAS technology, crystalline residues were detected via XRD, the amount depending on the polymeric carrier. If spray-freezing was used for solid dispersion manufacture, the blend of PVP and OX was amorphous. The dissolved amount of OX after 5 min varied from approximately 30 %-100 % of the total amount of the drug, resulting in concentrations of 15-50 µg/mL (Badens et al., 2009). In the present case, all OX formulations but the one using a blend of HPMC and COP as carrier were below the saturation concentration after 5 min of dissolution time, which equals a diluted amount of OX lower than 13 %. Even so, up to 38.1 µg/mL of FD were dissolved at this sampling point. In contrast to the solid dispersions produced using HME technology, the application of SAS and spray freezing results in samples with an increased surface area which facilitates a fast initial release of the drug. It must be emphasized that the dissolution studies with hot-melt extruded samples were performed using pH 6.4 medium while the results from literature were gained using pH 7.4 medium. In the latter, the $c_s$ of OX is approximately 4 times higher than with pH 6.4 medium. Possibly, the dissolution profiles would be equivalent if the same medium was applied.

To summarize the results, the dissolution enhancement of FF extrudates surpassed the results documented in literature as higher supersaturation levels were reached. Further research has to be conducted to improve the stability of the supersaturation level and to verify the significance of the results in vivo. Although the $c_{max}$ values reached with FD and OX extrudates were comparable or even superior to some of the literature data, other techniques for the manufacture of solid dispersions have to be preferred for FD and OX as the initial dissolution rate was lower.
It was observed that the dissolution profile of the solid dispersions is dominated by the release behavior of the carrier system. Especially PVCL-PVAc-PEG was shown to be not suitable as a carrier for an immediate release dosage form due to its slow dissolution rate after applying HME. The application of different polymers as carriers for FD and OX might improve the performance of the extrudates.

# 4 Summary

Solid dispersions are a promising approach for controlled release drug delivery systems as both the bioavailability enhancement of poorly water-soluble drugs as well as the sustained release of water-soluble drugs are possible to optimize their in vivo performance.
Different methods for the manufacture of solid dispersion systems have been introduced in literature. In the present work, two methods are compared: hot-melt extrusion and ultrasound-assisted compaction technique. Various carrier systems and drugs with different physicochemical properties are applied to investigate the feasibility of the technologies for pharmaceutical formulation. The formulations are compared to the corresponding untreated physical blends of the components regarding their solid state structure and dissolution behavior to assess the effect of the manufacturing technique.

Ultrasound-assisted compaction technique improves the initial dissolution rate of fenofibrate, a poorly water-soluble model drug. The crystalline API is partially converted into its amorphous state. The enhancement of the initial dissolution rate may be contributed to various factors, for example, the improved solubility of the amorphous compound, a particle size reduction resulting in an increased surface area, improved wettability of the drug substance and drug-carrier interactions. As equivalent results can be achieved if the polymers are added directly to the dissolution medium, the dissolution enhancement is attributed to an improved wettability of the drug.
Because there is little knowledge on the ultrasound-assisted compaction process itself, the technology is also assessed based on its handling by the user and the reproducibility of the results to allow an evaluation of its feasibility for an application in the pharmaceutical sector. A statistical design of experiments is employed to investigate the effect of the process parameters on the results.
Difficulties are encountered in the determination of process parameters which result in an optimal outcome. The process is very sensitive to the smallest changes of settings, for example of the position of the sonotrode. Additionally, the delivery of ultrasound energy is inhomogeneous. There is no or only insufficient user control of these parameters available. Furthermore, the duration of ultrasound energy delivery which is identified as a crucial parameter cannot be set by the user. The variable factors ultrasound energy, pressure of the lower piston and pressure of the upper piston affect the defined responses in the opposite direction: While the surface appearance, an indicator for the grade of the compounds' conversion, is improved if the factors are increased, the responses leakage of material out of the die, degradation and bubble formation are worsened. There are no settings which result in a satisfactory outcome. A strong influence of the material characteristics on the process is observed leading to a batch to batch variability.

Due to an insufficient reproducibility of results, the application of the technology cannot be recommended in its current state in the pharmaceutical formulation development and/or production. Improvements in homogeneity of energy delivery, process monitoring, user control and amount of leakage are mandatory for an acceptable performance and a future application in the pharmaceutical sector.

The polymers COP, HPMC and PVCL-PVAc-PEG are well suitable as carriers for hot-melt extruded formulations of fenofibrate. All three extrudates are amorphous one-phase systems with the drug molecularly dispersed in the polymer and a carrier-controlled dissolution mechanism. The enhancement of the initial dissolution rate and the maximum concentration level achieved are dependent on the applied carrier system. Supersaturation levels of up to 12.1 times are reached which are not stable due to recrystallization processes. The application of blends of polymers as carriers reduces the decrease rate after $c_{max}$. All extrudates with COP as carrier remain amorphous throughout the investigated storage time of 26 weeks due to its recrystallization inhibiting effect. Because of water absorption and polymer relaxation, the overall dissolution performance decreases with increasing storage times which can be avoided through an optimization of the packaging.
If oxeglitazar is used as API, the initial dissolution rate of the extrudates is below that of the untreated drug, with the exception of the ternary blend of COP, HPMC and oxeglitazar. In contrast to the other extrudates, the formulation of PVCL-PVAc-PEG and oxeglitazar does not form a molecularly dispersed solid solution of the drug in the carrier. Instead, an amorphous two-phase system is present. The dissolved amount of oxeglitazar remains for 8 hours below saturation concentration. With the ternary mixture of COP, HPMC and oxeglitazar, a substance-specific super-additive effect is observed: While the dissolution curves of the remaining extrudates with polymeric blends as carriers are in between the curves of the extrudates with the corresponding single polymers as carrier, higher concentration levels are reached with the ternary extrudate. No changes are observed after storage, presumably due to higher glass transition temperatures of the hot-melt extruded systems which are considerably above those of the corresponding fenofibrate extrudates.
With felodipine as API, the dissolution profile is enhanced with COP as single carrier. If HPMC or PVCL-PVAc-PEG are used as single or additional polymeric carriers, the dissolution is equivalent (HPMC) or lower (PVCL-PVAc-PEG) than that of the pure drug although molecularly disperse systems are present in all cases.

Out of the two investigated methods only hot-melt extrusion is a suitable technology to manufacture solid dispersions with an improved dissolution behavior. The dissolution profile of the extrudates can be influenced by adding polymers with differing physicochemical characteristics. Predictions on the dissolution behavior of the extrudates with polymeric blends as carriers can be made if there is knowledge on the dissolution profiles of the corresponding single polymeric extrudates. Due to substance-specific effects, the results are not transferable from drug to drug. Even so, the data are promising as the release behavior of the manufactured extrudates can be easily modified and readily adapted to one's needs.
Further research will have to be conducted to verify the concept and the relevance of the results in vivo.

# 5 Zusammenfassung

Feste Dispersionen sind ein vielversprechender Ansatz zur Herstellung von Drug Delivery-Systemen mit kontrollierter Wirkstofffreisetzung, da sie sowohl die Bioverfügbarkeit schlecht wasserlöslicher Arzneistoffe verbessern als auch die Freisetzung gut wasserlöslicher Arzneistoffe verzögern können und so deren in vivo Verhalten optimieren.
Verschiedene Herstellungsmethoden wurden in der Literatur vorgestellt. In der vorliegenden Arbeit werden zwei Technologien miteinander verglichen: Schmelzextrusion und Ultraschall gestützte Verpressung (USAC). Verschiedene Trägersysteme und Arzneistoffe mit unterschiedlichen physikochemischen Eigenschaften werden untersucht, um die Einsatzmöglichkeit im pharmazeutischen Bereich zu überprüfen. Die Struktur der hergestellten Systeme und deren Freisetzungsverhalten werden mit den physikalischen Mischungen der Komponenten verglichen, um den Einfluss der Formulierung zu bestimmen.

Durch USAC wird die initiale Freisetzungsrate von Fenofibrat, einem schlecht wasserlöslichen Modellarzneistoff, verbessert. Eine teilweise Umwandlung vom kristallinen in den amorphen Zustand tritt auf. Verschiedene Faktoren können eine Verbesserung der Freisetzung bewirken: die bessere Löslichkeit der amorphen Substanz, eine durch die Verringerung der Partikelgröße induzierte Oberflächenvergrößerung, verbesserte Benetzbarkeit sowie Arzneistoff-Polymer Wechselwirkungen. Vergleichbare Ergebnisse werden bei einer Polymerzugabe zum Freisetzungsmedium erreicht; daher wird davon ausgegangen, dass vor allem eine verbesserte Benetzbarkeit des Arzneistoffs eine Rolle spielt.
Da bislang nur wenig über den USAC-Prozess bekannt ist, wird auch die Handhabung und Reproduzierbarkeit der Ergebnisse beurteilt, um die Anwendung dieser Technologie in der pharmazeutischen Formulierungsentwicklung und Produktion zu bewerten. Mittels statistischer Versuchsplanung wird der Einfluss der verschiedenen Prozessparameter untersucht.
Die Einstellung der Prozessparameter, um ein optimales Ergebnis zu erhalten, gestaltet sich schwierig. Der Prozess reagiert auf kleinste Veränderungen, zum Beispiel der Position der Sonotrode, überaus sensitiv. Außerdem wird die Ultraschallenergie nicht homogen übertragen. Die Kontrolle dieser Parameter durch den Anwender ist nicht oder nur unzureichend möglich. Ebenso kann die Dauer der Ultraschallapplizierung, die essentiell für den Prozess ist, nicht eingestellt werden. Die Prozessparameter Ultraschallenergie, Unterstempeldruck und Sonotrodendruck beeinflussen die Zielgrößen in entgegengesetzter Richtung: Während sich eine Erhöhung der Einflussgrößen positiv auf die Zielgröße Aussehen der Oberfläche, die einen Rückschluss auf den Umwandlungsgrad der Komponenten zulässt, auswirkt, werden die Zielgrößen Austreten des Materials aus der Matrize, Zersetzung und Blasenbildung dadurch negativ beeinflusst. Es gibt keine Einstellung, die für alle Zielgrößen optimale Ergebnisse liefert. Zusätzlich ist der Prozess stark abhängig von den Eigenschaften des verwendeten

Materials: Die Verwendung unterschiedlicher Polymerchargen macht eine Anpassung der Prozessparameter notwendig, um vergleichbare Ergebnisse zu erhalten.
Eine ausreichende Reproduzierbarkeit der Ergebnisse für einen Einsatz dieser Technologie in Formulierungsentwicklung oder Produktion ist nicht gegeben. Eine homogene Ultraschallenergiezufuhr sowie Verbesserungen der Prozessüberwachung, der Benutzerkontrolle und eine Verminderung der austretenden Materialmenge sind für eine akzeptable Leistung und eine zukünftige Anwendung im pharmazeutischen Bereich zwingend erforderlich.

Die Polymere COP, HPMC, PVCL-PVAc-PEG sind für eine Freisetzungsverbesserung von Fenofibrat mittels Schmelzextrusion geeignet. Es liegen einphasige, molekulardisperse feste Lösungen mit einem Träger-kontrollierten Freisetzungsmechanismus vor. Abhängig von der Trägersubstanz wird die initiale Freisetzungsrate unterschiedlich stark erhöht, ebenso die maximale Konzentration des Arzneistoffes in Lösung. Eine bis zu 12.1-fache Übersättigung wird erreicht, die aufgrund von Rekristallisationsprozessen nicht stabil ist. Der Einsatz von polymeren Mischungen reduziert die Geschwindigkeit des Konzentrationsabfalls.
Alle COP-Extrudate bleiben aufgrund des rekristallisationsinhibierenden Effekts der Trägersubstanz über einen Zeitraum von 26 Wochen amorph. Die Absorption von Wasser und Relaxationseffekte vermindern die Freisetzungserhöhung mit zunehmender Lagerdauer; dieser Entwicklung kann durch eine Optimierung des Packmittels entgegengewirkt werden.
Wird der ebenfalls schwer wasserlösliche Arzneistoff Oxeglitazar verwendet, so ist die initiale Freisetzungsrate der Extrudate der des reinen Arzneistoffs unterlegen, mit Ausnahme der ternären Mischung von COP, HPMC und Oxeglitazar. PVCL-PVAc-PEG-Oxeglitazar-Extrudate bilden im Gegensatz zu den übrigen Formulierungen keine molekulardisperse feste Lösung, sondern ein amorphes Zwei-Phasen-System. Die freigesetzte Menge bleibt für einen Zeitraum von 8 Stunden unterhalb der Sättigungskonzentration. Ein substanzspezifischer superadditiver Effekt für die tertiäre Mischung von COP, HPMC und Oxeglitazar tritt auf: Während die Freisetzungskurven der übrigen Extrudate mit Polymermischungen als Träger intermediär zwischen den Kurven der Einzelpolymer-Extrudate liegen, wird hier eine höhere maximale Konzentration erreicht. Eine Veränderung während der Lagerzeit wird nicht beobachtet, vermutlich aufgrund der höheren Glasübergangstemperaturen dieser Systeme.
Lediglich das Freisetzungsprofil von COP-Felodipin-Extrudaten ist verbessert. Gegenüber dem reinen Arzneistoff ist die Freisetzung der übrigen Extrudate vergleichbar (HPMC) oder verringert (PVCL-PVAc-PEG), obwohl auch hier molekulardisperse Systeme vorliegen.

Von den beiden untersuchten Technologien ist lediglich die Schmelzextrusion geeignet, um feste Dispersionen mit einem verbesserten Freisetzungsverhalten herzustellen. Das Freisetzungsprofil der Extrudate kann durch den Zusatz von Polymeren mit unterschiedlichen Eigenschaften optimiert und vorhergesagt werden, wenn das Freisetzungsprofil der Einzelpolymer-Extrudate bekannt ist. Die Ergebnisse sind aufgrund von substanzspezifischen Effekten nicht von Arzneistoff auf Arzneistoff übertragbar. Nichtsdestotrotz sind die Erkenntnisse dieser Arbeit vielversprechend, da gezeigt wird, dass das Freisetzungsprofil der Extrudate leicht beeinflusst und an spezifische Anforderungen angepasst werden kann.
Weitere Untersuchungen sind notwendig, um das Konzept und die Relevanz der Ergebnisse in vivo zu überprüfen.

# 6 Experimental part

## 6.1 Materials

### 6.1.1 Active pharmaceutical ingredients

Poorly water-soluble drugs were chosen as testing substances as the aim of this work was to evaluate various formulation techniques with respect to their potential for bioavailability enhancement (see Table 6.1). The physicochemical properties of the used drug substances are summarized in Table 6.2. The chemical structures of the APIs are shown in Figure 6.1.

Table 6.1: Drugs used for the manufacture of solid dispersions

| Substance | Abbreviation | Source |
|---|---|---|
| Felodipine | FD | Zhejiang Supor Pharmaceuticals, Zhejiang, China |
| Fenofibrate | FF | Smruthi Organics, Solapur, India |
| Oxeglitazar | OX | Merck Santé, Lyon, France |

Table 6.2: Physicochemical properties of investigated drugs. Data are partially derived from Blaschek et al. (2002), Meng et al. (2009), Majerik (2006) and Diez et al. (1991)

| | FD | FF | OX |
|---|---|---|---|
| Molecular weight [g/mol] | 384.3 | 360.8 | 314.4 |
| Melting point [°C] | 145 | 80-81 | 153 |
| Solubility in water at 25°C | 0.5 µg/mL (Blaschek et al., 2002) | 0.1 µg/mL (Meng et al., 2009) | 1.64 µg/mL (Majerik, 2006) |
| Solubility in water at 37°C | 1.2 µg/mL (Blaschek et al., 2002) | n/a | 3.0 µg/mL (Majerik, 2006) |
| logP | 3.86 (Diez et al., 1991) | 5.24 (Blaschek et al., 2002) | 4.8 |
| $pk_a$ | $< 1$ (Blaschek et al., 2002) | - | 4.9 (Majerik, 2006) |
| Indication | antihypertensive | hypolipidemic, hypotriglyceridemic | antidiabetic, hypoglycemic, hypotriglyceridemic |

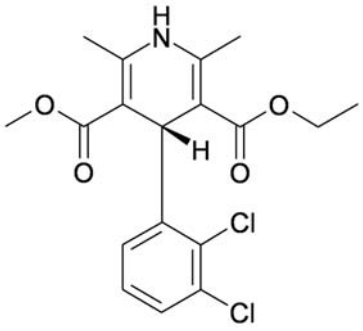


(a) Felodipine

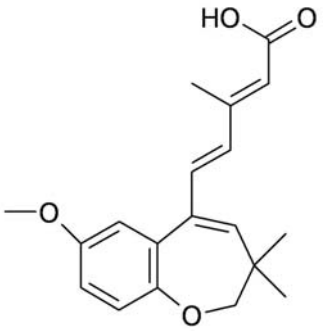


(b) Oxeglitazar

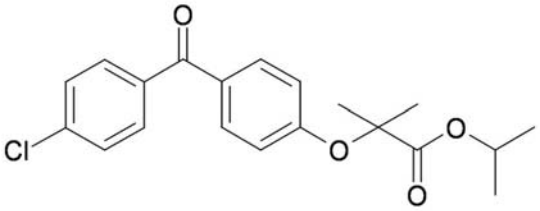


(c) Fenofibrate

Figure 6.1: Chemical structures of investigated drugs

### 6.1.2 Polymeric carriers

The applied polymeric carriers and their physicochemical properties are summarized in Tables 6.3 and 6.4. The chemical structures of the polymers are shown in Figure 6.2.

According to the Ph.Eur., the ratio of dimethylaminoethyl methacrylate groups to butyl methacrylate groups to methyl methacrylate groups in aPMMA is approximately 2:1:1.

The HPMC type used is substitution type 2910 as defined in Ph.Eur. Accordingly, the percentage of methoxy groups is approximately 29 % and of hydroxy groups approximately 10 %. The viscosity of the applied HPMC is 5 mPa s.

Table 6.3: Polymers applied as carriers in the solid dispersion manufacturing process

| Substance | Trade name | Source |
|---|---|---|
| aPMMA | Eudragit® E PO | Evonik Röhm Pharma Polymers, Darmstadt, Germany |
| COP | Kollidon® VA 64 | BASF, Ludwigshafen, Germany |
| HPMC | Methocel® E5 Premium LV | Colorcon, Idstein, Germany |
| PVA-AA-MMA | Povacoat® Type MP | Daido Chemical, Osaka, Japan |
| PVCL-PVAc-PEG | Soluplus® | BASF, Ludwigshafen, Germany |

Table 6.4: Physicochemical properties of applied polymeric substances

| Substance | Molecular weight [g/mol] | $T_g$ [°C] | $T_{degr}$ [°C] | Solubility [°C] | CMC [mg/L] |
|---|---|---|---|---|---|
| aPMMA | 150000 | 48 | >200 | soluble in gastric fluid; swells above pH 5.0; practically insoluble in water | - |
| COP | 40000-70000 | 110 | 230 | all hydrophilic solvents | - |
| HPMC | 10000-1500000 | 146 | 225 | cold water | - |
| PVA-AA-MMA | approx. 40000 | 73 | 220 | water | - |
| PVCL-PVAc-PEG | 90000-140000 | 70 | >250 | water; precipitation at approx. 40°C | 7.6 |

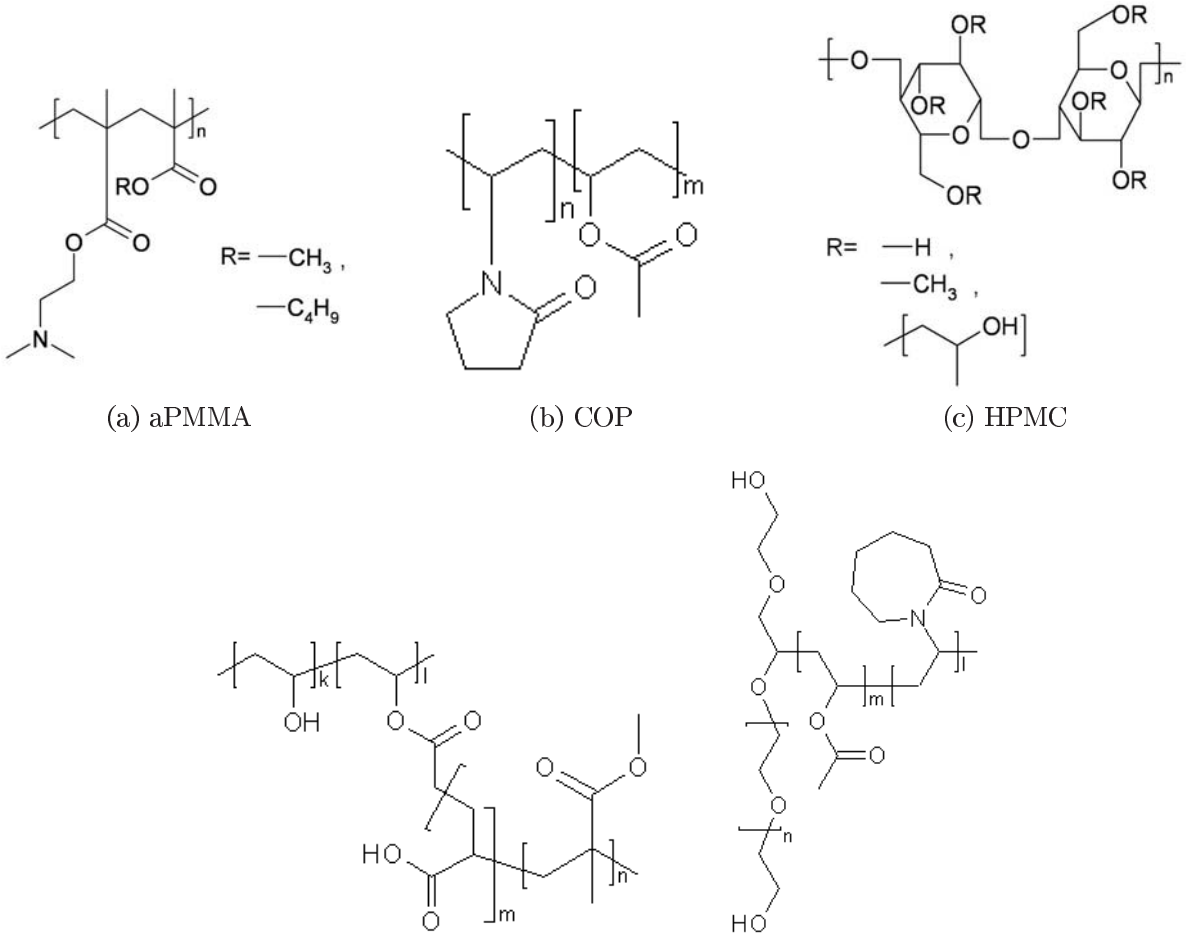


(a) aPMMA (b) COP (c) HPMC

(d) PVA-AA-MMA (e) PVCL-PVAc-PEG

Figure 6.2: Chemical structures of applied polymeric carriers

### 6.1.3 Other

Chemicals and reagents that were used for analysis or manufacture of the investigated formulations are listed in Table 6.5.

Table 6.5: Chemicals used for the analysis of the manufactured solid dispersions

| Substance | Trade name | Purity | Source |
|---|---|---|---|
| Acetic acid 100 % | | Ph.Eur. | Merck KGaA, Darmstadt, Germany |
| Acetonitrile | Acetonitril LiChrosolv® | Gradient grade, Ph.Eur. | Merck KGaA, Darmstadt, Germany |
| Hydrochloric acid 25 % | | Ph.Eur. | Merck KGaA, Darmstadt, Germany |
| Crospovidone | Kollidon® CL | Ph.Eur. | BASF SE, Ludwigshafen, Germany |
| Methanol | Methanol LiChrosolv® | Gradient grade, Ph.Eur. | Merck KGaA, Darmstadt, Germany |
| Phosphoric acid 85 % | | Ph.Eur. | Merck KGaA, Darmstadt, Germany |
| Polysorbate 80 | Tween® 80 | Ph.Eur. | Merck KGaA, Darmstadt, Germany |
| Potassium phosphate | | Ph.Eur. | Merck KGaA, Darmstadt, Germany |
| Purified water | | Ph.Eur. | - |
| Sodium chloride | | Ph.Eur. | Merck KGaA, Darmstadt, Germany |
| Sodium hydroxide 1 mol/L | | Ph.Eur. | Merck KGaA, Darmstadt, Germany |

## 6.2 Methods

### 6.2.1 Manufacturing methods

#### 6.2.1.1 Preparation of physical mixtures

The respective model drug, one or more carrier polymers and any additional excipients were weighted according to Tables 6.6 and 6.7 and blended for 15 min using shaker-mixer Turbula® T2C (Willy A. Bachofen AG Maschinenfabrik, Basel, Switzerland). Of each mixture, a batch size of 500 - 750 g was prepared. If one single polymeric carrier was used, the ratio drug to polymer equals 1+3 (weighted parts) which corresponds to a drug load of 25 % (w/w). These mixtures were then either ultrasound-compacted, hot-melt extruded or analyzed directly.

Table 6.6: Composition of ultrasound compacted FF-polymer blends. All data are given in weighted parts unless otherwise specified.

| Formulation | FF | COP | HPMC | PVCL-PVAc-PEG | aPMMA | PVA-AA-MMA | drug load [%] |
|---|---|---|---|---|---|---|---|
| US-A | 1 | 3 | - | - | - | - | |
| US-B | 1 | - | 3 | - | - | - | |
| US-C | 1 | - | - | 3 | - | - | 25.0 |
| US-D | 1 | - | - | - | 3 | - | |
| US-E | 1 | - | - | - | - | 3 | |

Table 6.7: Composition of hot-melt extruded drug-polymer blends. All data are given in weighted parts unless otherwise specified.

| Formulation | API | COP | HPMC | PVCL-PVAc-PEG | aPMMA | PVA-AA-MMA | CL | drug load [%] |
|---|---|---|---|---|---|---|---|---|
| FD-A | 1 | 3 | - | - | - | - | - | 25.0 |
| FD-B | 1 | - | 3 | - | - | - | - | 25.0 |
| FD-C | 1 | - | - | 3 | - | - | - | 25.0 |
| FD-D | 1 | 3 | 1 | - | - | - | - | 20.0 |
| FD-E | 1 | 3 | - | 1 | - | - | - | 20.0 |
| FD-F | 1 | 3 | 1 | 1 | - | - | - | 16.7 |
| FF-A | 1 | 3 | - | - | - | - | - | 25.0 |
| FF-B | 1 | - | 3 | - | - | - | - | 25.0 |
| FF-C | 1 | - | - | 3 | - | - | - | 25.0 |
| FF-D | 1 | 3 | 0.6 | - | - | - | - | 21.7 |
| FF-E | 1 | 3 | 1 | - | - | - | - | 20.0 |
| FF-F | 1 | 3 | - | 1 | - | - | - | 20.0 |
| FF-G | 1 | 3 | - | 1.5 | - | - | - | 18.2 |
| FF-H | 1 | 3 | 1 | 1 | - | - | - | 16.7 |
| FF-J | 1 | - | - | - | 3 | - | - | 25.0 |
| FF-K | 1 | - | - | - | - | 3 | - | 25.0 |
| OX-A | 1 | 3 | - | - | - | - | - | 25.0 |
| OX-B | 1 | - | 3 | - | - | - | - | 25.0 |
| OX-C | 1 | - | - | 3 | - | - | - | 25.0 |
| OX-D | 1 | 3 | 1 | - | - | - | - | 20.0 |
| OX-E | 1 | 3 | - | 1 | - | - | - | 20.0 |
| OX-F | 1 | 3 | 1 | 1 | - | - | - | 16.7 |
| OX-G | 1 | 4 | - | - | - | - | - | |
| OX-H | 1 | 1 | 1 | - | - | - | - | 20.0 |
| OX-J | 1 | 1 | 3 | - | - | - | - | |
| OX-K | 1 | - | 4 | - | - | - | - | |
| OX-CL 1 | 1 | - | - | 2.6 | - | - | 0.4 | 25.0 |
| OX-CL 2 | 1 | - | - | 2.2 | - | - | 0.8 | |

#### 6.2.1.2 Design of experiments

A statistical design was developed to allow an evaluation of influential parameters and the USAC machine itself. Using a $2^3$ factorial design, correlations of settings of process parameters and outcome were to be found and optimal settings were to be defined.

US energy and the pressure of lower and upper piston were defined as factors. The fraction of powdery material remaining after USAC treatment, the amount of material which has leaked out of the die, the formation of bubbles and degradation effects, detected by discoloration, were set as responses and evaluated on a scale from 1 to 6 where 1 is very good (see Tables 6.8 and 6.9). Accordingly, the optimal outcome is identified as follows: surface appearance = 1, leakage of material = 1, formation of bubbles = 1, degradation = 1.

HPLC analysis was applied to detect whether degradation of FF is induced via US application. The degradation of the polymeric carrier was detected optically.

Central point settings were determined by feasibility trials.

The statistical designs of experiments were generated and evaluated with Modde v8.0 (Umetrics, Umeå, Sweden).

Table 6.8: Specifications for the evaluation of USAC compacts

| Responses | Rating | | | | | |
|---|---|---|---|---|---|---|
| | 1 | 2 | 3 | 4 | 5 | 6 |
| Surface appearance | Glassy, transparent | Powdery residues $<\frac{1}{4}$ of compact surface | Powdery residues on $\frac{1}{4}-\frac{1}{2}$ of compact surface | Powdery residues on $\frac{1}{2}$ of compact surface | Powdery residues on $>\frac{1}{2}$ of compact surface | No or negligible glassy areas |
| Leakage of material | None | Rim width $\leq$ 1 mm | Rim width 1 - 5 mm | Rim width 0.5 - 1 cm | Rim width >1cm and compact height >0.5 mm | Maximal (compact height < 0.5mm) |
| Formation of bubbles | None | 1 - few ($\ll\frac{1}{8}$ of compact) | Multiple ($<\frac{1}{4}$ of compact) | Several (approx. $\frac{1}{4}$ of compact) | Several ($\frac{1}{4}-\frac{1}{2}$ of compact) | Many ($>\frac{1}{2}$ of compact), surface is affected |
| Degradation | None | Isolated ($<0.1\,cm^2$) | Multiple ($<0.5\,cm^2$) | Several ($<\frac{1}{8}$ of compact) | $\frac{1}{8}-\frac{1}{4}$ of compact is affected | $>\frac{1}{4}$ of compact is affected |

Table 6.9: Graphical illustration of USAC compact evaluation. Photographs of USAC compacts consisting of HPMC are rated according to Table 6.8 and inserted into the present Table 6.9 according to their rating.

| Responses | Rating 1 | 2 | 3 | 4 | 5 | 6 |
|---|---|---|---|---|---|---|
| Surface appearance |  |  |  |  |  |  |
| Leakage |  |  |  |  |  |  |
| Formation of bubbles |  |  |  |  |  |  |
| Degradation |  |  |  |  |  |  |

#### 6.2.1.3 Ultrasound-assisted compaction technique

The ultrasound-tableting machine Sonica Lab KU1003 by IMA, Bologna, Italy was used for USAC trials (see Figure 6.3).

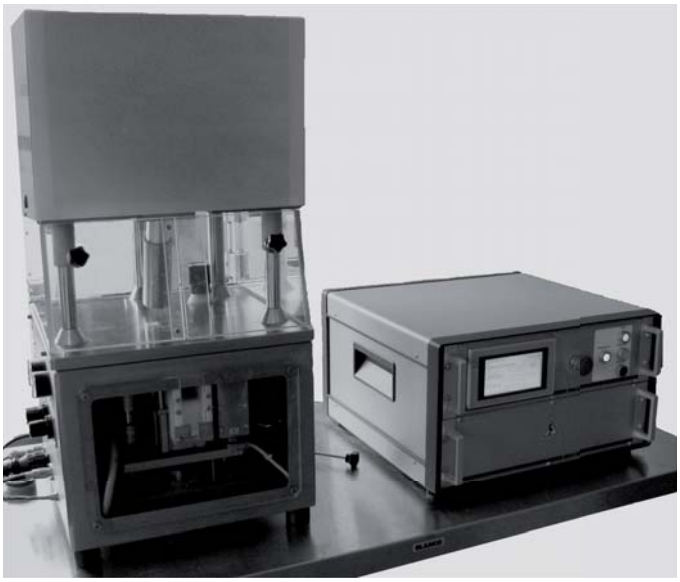

(a) Compacting device of Sonica Lab KU1003 (left) and its control and power supply device (right)

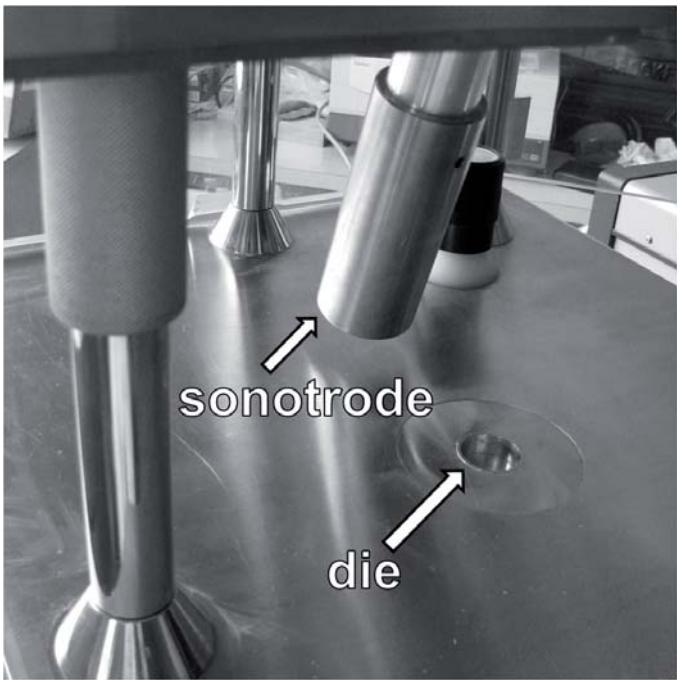


(b) Close-up on sonotrode and die of Sonica Lab KU1003

Figure 6.3: Ultrasound-tableting machine Sonica Lab KU1003

PTFE sheets were used to line and cover the die. The die diameter was 25 mm and the compaction chamber depth was set to 10 mm resulting in a die volume of 4.91 $cm^3$. Different amounts of material were used for each substance or API-polymer blend as the material was poured into the compaction chamber and allowed to settle freely. The amount of material was limited by its bulk density and the compaction chamber volume.
Process parameters were set according to Table 6.10. In-process monitoring of the USAC process was performed using Sonica View software (IMA, Bologna, Italy).

Table 6.10: Settings as chosen for design of experiments using pure polymers and FF-polymer blends 1+3 (weighted parts)

| | | US energy [J] | Pressure lower piston [bar] | Pressure upper piston [bar] | Amount of material [g] | Absolute distance sonotrode/die |
|---|---|---|---|---|---|---|
| COP | -1 | 750 | 5,4 | 5.9 | 0.83 | 16.08 |
| | 0 | 850 | 6.4 | 6.9 | | |
| | +1 | 950 | 7.4 | 7.9 | | |
| HPMC | -1 | 1200 | 4.5 | 5 | 1.5 | 16.08 |
| | 0 | 1350 | 6 | 6 | | |
| | +1 | 1500 | 7.5 | 7 | | |
| PVCL-PVAc-PEG | -1 | 850 | 5 | 5 | 1.5 | 16.08 |
| | 0 | 1050 | 6 | 6 | | |
| | +1 | 1250 | 7 | 7 | | |
| aPMMA | -1 | 700 | 4.5 | 5 | 1.00 | 16.08 |
| | 0 | 900 | 6 | 6 | | |
| | +1 | 1100 | 7.5 | 7 | | |
| PVA-AA-MMA | -1 | 750 | 4.5 | 5 | 1.5 | 16.08 |
| | 0 | 950 | 6 | 6 | | |
| | +1 | 1150 | 7.5 | 7 | | |
| US-A | -1 | 280 | 5.5 | 6 | 0.83 | 16.08 |
| | 0 | 430 | 6.5 | 7 | | |
| | +1 | 580 | 7.5 | 8 | | |
| US-B | -1 | 510 | 6 | 5 | 1.25 | 16.08 |
| | 0 | 710 | 7 | 6 | | |
| | +1 | 910 | 8 | 7 | | |
| US-C | -1 | 400 | 5 | 5 | 1.5 | 16.08 |
| | 0 | 600 | 6 | 6 | | |
| | +1 | 800 | 7 | 7 | | |
| US-D | -1 | 150 | 5 | 6 | 1.00 | 16.08 |
| | 0 | 300 | 6 | 7 | | |
| | +1 | 450 | 7 | 8 | | |
| US-E | -1 | 450 | 6 | 5.5 | 1.5 | 16.08 |
| | 0 | 650 | 7 | 6.5 | | |
| | +1 | 850 | 8 | 7.5 | | |

#### 6.2.1.4 Hot-melt extrusion

Co-rotating twin screw extruder PRISM PharmaLab 16 (Thermo Fisher Scientific, Karlsruhe, Germany) with a screw diameter of 16 mm and a length to diameter ratio (L/D ratio) of 40:1 was used for hot-melt extrusion. A screw configuration with two kneading zones was used throughout the studies (see Figure 6.4). The barrel is divided into ten zones allowing a full variability in the barrel set-up. Barrel zone 1 is the feeding zone and cannot be heated. The temperature of the die plate is also defined by the user. To ensure an efficient degassing of the molten material, venting ports were applied in barrel zones 5 and 10. A vacuum pump was connected to the zone 10 venting port. For all extrudates, the chosen setting was −0.5 bar.

As the applied components exhibit different physicochemical characteristics, the hot-melt extrusion process parameters were adjusted such that a semisolid, transparent strand suitable for down-processing was obtained with each API-polymer mixture (see Table 6.11). While the screw speed was slightly varied because of different processabilities of the API-polymer mixtures, the feeding rate was kept constant at 0.4 kg/h for all formulations. The standard diameter of the applied die was 3 mm. For trials with a reduced die hole size, a die with a die hole diameter of 1 mm was used. After the extrusion of the molten mixture through the die hole, the strand was air-cooled on a conveyer belt (Pharma 16 mm air cooled conveyor belt) and pelletized into pellets with a set length of 1.5 mm (Pharma 16 mm Varicut pelletizer; both Thermo Fisher Scientific, Karlsruhe, Germany).

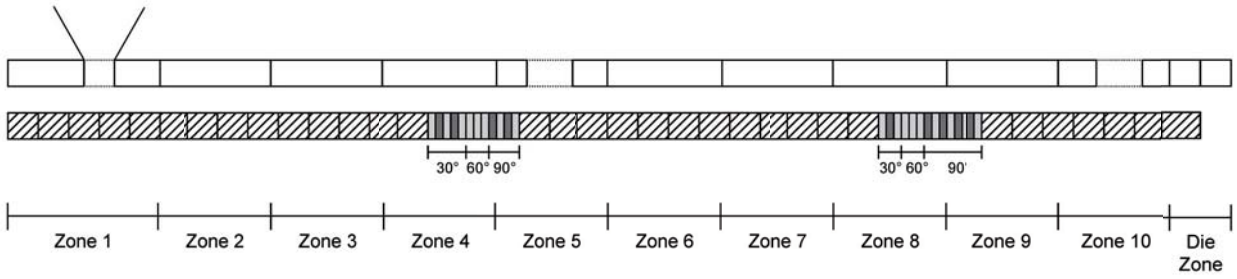


Figure 6.4: Configuration of the extruder barrel and screws. Hatched areas represent conveying elements, light gray and dark gray areas represent kneading elements with a 0 °and 90 °offset, respectively. Kneading elements are aligned to result in kneading areas with displayed advance angles.

#### 6.2.1.5 Milling

USAC compacts or hot-melt extruded pellets were milled using ultra centrifugal mill ZM 100 (Retsch, Haan, Germany). The chosen setting was 14.000 rpm. A ring sieve with 0.5 mm trapezoid holes and a 12 teeth-rotor were used.

Table 6.11: Hot-melt extrusion process settings

| Formulation | Barrel zone temperature [°C] | | | | | | | | | | screw speed [rpm] | feed rate [kg/h] |
|---|---|---|---|---|---|---|---|---|---|---|---|---|
| | 2 | 3 | 4 | 5 | 6 | 7 | 8 | 9 | 10 | die | | |
| FD-A | 50 | 120 | 150 | 150 | 150 | 150 | 150 | 150 | 150 | 150 | 100 | 0.4 |
| FD-B | 50 | 120 | 145 | 150 | 150 | 150 | 160 | 160 | 155 | 150 | 150 | 0.4 |
| FD-C | 60 | 120 | 145 | 150 | 150 | 150 | 160 | 160 | 155 | 150 | 100 | 0.4 |
| FD-D | 50 | 120 | 145 | 150 | 150 | 150 | 150 | 150 | 150 | 150 | 100 | 0.4 |
| FD-E | 50 | 120 | 145 | 150 | 150 | 150 | 150 | 150 | 150 | 150 | 100 | 0.4 |
| FD-F | 50 | 120 | 145 | 150 | 150 | 150 | 150 | 150 | 150 | 150 | 100 | 0.4 |
| FF-A | 60 | 100 | 110 | 110 | 110 | 110 | 110 | 110 | 110 | 105 | 75 | 0.4 |
| FF-B | 90 | 150 | 165 | 165 | 165 | 165 | 165 | 165 | 165 | 165 | 150 | 0.4 |
| FF-C | 50 | 100 | 115 | 115 | 115 | 115 | 115 | 115 | 115 | 115 | 100 | 0.4 |
| FF-D | 60 | 110 | 125 | 135 | 135 | 135 | 135 | 135 | 135 | 135 | 150 | 0.4 |
| FF-E | 60 | 110 | 145 | 150 | 150 | 150 | 150 | 150 | 150 | 150 | 150 | 0.4 |
| FF-F | 60 | 100 | 110 | 115 | 115 | 115 | 115 | 115 | 115 | 110 | 100 | 0.4 |
| FF-G | 60 | 100 | 110 | 115 | 115 | 115 | 115 | 115 | 115 | 110 | 100 | 0.4 |
| FF-H | 60 | 100 | 125 | 135 | 135 | 135 | 135 | 135 | 135 | 130 | 100 | 0.4 |
| OX-A | 50 | 120 | 145 | 150 | 150 | 150 | 150 | 150 | 150 | 150 | 100 | 0.4 |
| OX-B | 90 | 150 | 165 | 165 | 165 | 165 | 165 | 165 | 165 | 165 | 150 | 0.4 |
| OX-C | 60 | 120 | 145 | 150 | 150 | 150 | 150 | 150 | 150 | 150 | 100 | 0.4 |
| OX-D | 50 | 120 | 145 | 150 | 150 | 150 | 150 | 150 | 150 | 150 | 100 | 0.4 |
| OX-E | 50 | 120 | 145 | 150 | 150 | 150 | 150 | 150 | 150 | 150 | 100 | 0.4 |
| OX-F | 50 | 120 | 145 | 150 | 150 | 150 | 150 | 150 | 150 | 150 | 100 | 0.4 |
| OX-CL 1 | 60 | 120 | 145 | 150 | 150 | 150 | 150 | 150 | 150 | 150 | 100 | 0.4 |
| OX-CL 2 | 60 | 120 | 145 | 150 | 150 | 150 | 150 | 150 | 150 | 150 | 100 | 0.4 |

## 6.2.2 Analytical methods

### 6.2.2.1 Stability testing

Stability testing was performed according to International Conference on Harmonization (ICH) Guideline "Stability testing of new drug substances and products Q1A(R2)" to assess the effects of temperature, humidity and time on the product. The samples were stored in PE double pouches under long-term storage conditions (25 °C /60 % rH) for 4, 10 and 26 weeks. To assess the effect of humidity onto the dissolution performance of the extrudates, some of the samples were stored under moisture protection in Activ®-Vials (CSP Technologies, Auburn, AL, USA).

### 6.2.2.2 Saturation concentration

For determination of the saturation concentration $c_s$ of each API in the dissolution medium, a shake-flask method was used.
A surplus amount of 200 mg of pure API powder was added to 50 mL of dissolution medium. Hydrochloric acid medium pH 1.2 according to Ph.Eur. was used as dissolution medium for FF and FD. Ph.Eur. phosphate buffer solution pH 6.4 was used for OX. 0.1 % of polysorbate 80 were added to the dissolution media to ensure sufficient wetting. The trials were conducted over a time period of 48 h at a shaking rate of 95 $min^{-1}$. At set time points, a sample volume of 2 mL was drawn through a 10 µm PE filter (Poroplast®, Durst Filtertechnik, Besigheim-Ottmarsheim, Germany) attached to a stainless steel cannula (Erweka, Heusenstamm, Germany) and then filtered through a 0.45 µm syringe filter (Spartan® 30, Whatman, Dassel, Germany). The first milliliter of filtered sample was discarded. Sampling times were 0, 0.5, 2, 4, 8, 24 and 48 h. The samples were diluted 1:1 with acetonitrile and analyzed via HPLC. All solubility studies were performed in triplicate.
When the polymer was added directly to the dissolution medium for comparison, 43.5 mg of polymer were used to establish similar conditions as in the dissolution studies with United States Pharmacopeia (USP) apparatus 2 as described in section 6.2.2.3.

### 6.2.2.3 Dissolution studies

For dissolution studies with USP apparatus 2 (DT 80, Erweka, Heusenstamm, Germany), 500 mL of dissolution medium were conditioned at 37.0±0.5 °C. Ph.Eur. hydrochloric acid medium pH 1.2 was used as dissolution medium for FF and FD while for OX, phosphate buffer solution pH 6.4 according to Ph.Eur. was applied. 0.1 % of polysorbate 80 were added to the media to ensure sufficient wetting conditions. Weighted samples corresponding to 145 mg of API were used. PE filters (Poroplast®, Durst Filtertechnik, Besigheim-Ottmarsheim, Germany) with a pore size of 10 µm were attached to the manual sampling manifold (Erweka, Heusenstamm, Germany) to reduce the draw-in of larger particles into syringes (Omnifix®, B. Braun Melsungen, Melsungen, Germany). At set time points, sam-

ple volumes of 3 mL were withdrawn and filtered through a 0.45 µm syringe filter (Spartan® 30, Whatman, Dassel, Germany). The first milliliter of filtered sample was discarded. The removed sample volume was substituted with the same amount of tempered dissolution medium. Sampling times were 0, 5, 10, 15, 30, 45, 60, 90 and 120 min. For FD and OX, additional trials were conducted with sampling times 0, 5, 15, 30, 60, 90, 120, 240, 480, 1440 min to monitor the dissolution behavior over a time period of 24 hours.
In some dissolution experiments for FF-COP extrudates, a second polymer was added directly to the dissolution medium. The amount of added HPMC or PVCL-PVAc-PEG corresponded to the amount given in Table 6.7, e.g. 145 mg of the additional polymer HPMC and a sample amount of 580 mg of FF-A pellets was used to be comparable to FF-B extrudates. For comparator products Lipidil-Ter® (drug content 160 mg FF) and Lipidil® (drug content 200 mg FF), 552 mL and 690 mL of dissolution medium were used, respectively.
The samples were diluted 1:1 with acetonitrile and analyzed via HPLC. All dissolution studies were performed in triplicate. Solid dispersions might lead to a temporary supersaturation of the dissolution medium. Non-sink conditions were applied as they allow a better differentiation of solid dispersion formulations and comparison of the degree of supersaturation reached.

Dissolution rates and decrease rates of the samples were calculated by linear regression using SigmaPlot Software Version 10 (Systat Software, San Jose, CA, USA).

To monitor changes of surface morphology after exposition to the dissolution medium, several pellets were released under the test conditions given above. The pellets were removed after 2 or 10 min from the dissolution vessel and washed with purified water. Several samples were dried at room temperature, while others were dried using Moisture Analyzer MA 30 (Sartorius, Goettingen, Germany). With Moisture Analyzer MA 30, the pellets were placed separately on an aluminum pan and heated up to 130 °C. Total drying time was 1-2 min (until no further mass loss). The samples were then further analyzed as described in Section 6.2.2.9.

#### 6.2.2.4 High pressure liquid chromatography

The amount of dissolved API in dissolution and saturation concentration studies was determined via HPLC analysis using a Merck-Hitachi LaChrom system equipped with a pump L-7100, autosampler L-7200, column oven L-7300, UV-VIS detector L-7420 and a Merck-Hitachi interface L-7000 (Hitachi High-Technologies, Tokyo, Japan). For each API, a specific method was applied (see Table 6.12). Typical chromatograms of the APIs are shown in Figure 6.5. HPLC method validation was performed: Linearity was verified over a concentration range of 1 µg/mL to 1 mg/mL and the precision of the method was confirmed.

Table 6.12: HPLC analysis parameters as chosen for each of the investigated APIs. Mobile phase composition is given in % (v/v).

| | FD | FF | OX |
|---|---|---|---|
| mobile phase A | 20 % methanol<br>40 % acetonitrile<br>40 % phosphate buffer pH 3.0 | 70 % acetonitrile<br>30 % water pH 2.5 acidified with phosphoric acid | 10 % acetonitrile<br>90 % acetic acid 0.2 % |
| mobile phase B | - | - | 90 % acetonitrile<br>10 % acetic acid 0.2 % |
| gradient settings | isocratic | isocratic | time [min] / A [%] / B [%]<br>0 / 80 / 20<br>1 / 80 / 20<br>16 / 20 / 80<br>17 / 20 / 80<br>17.1 / 80 / 20<br>20 / 80 / 20 |
| column type | LiChroCART® 125-4 LiChrospher® 100 RP-18 5µm | LiChroCART® 250-4 Superspher® 100 RP-18 5µm | LiChroCART® 125-4 LiChrospher® 60 RP select B 5µm |
| flow rate [mL/min] | 1.5 | 2 | 2 |
| column temperature [°C] | 40 | 50 | 40 |
| detection wavelength [nm] | 362 | 286 | 255 |
| injection volume [µL] | 5 | 5 | 5 |
| elution time [min] | 3.9 | 5.4 | 9.9 |
| solvent for standard solutions | mobile phase | mobile phase | 65 % acetonitrile<br>35 % water |
| reference | modified Ph.Eur. method | modified Ph.Eur. method | - |

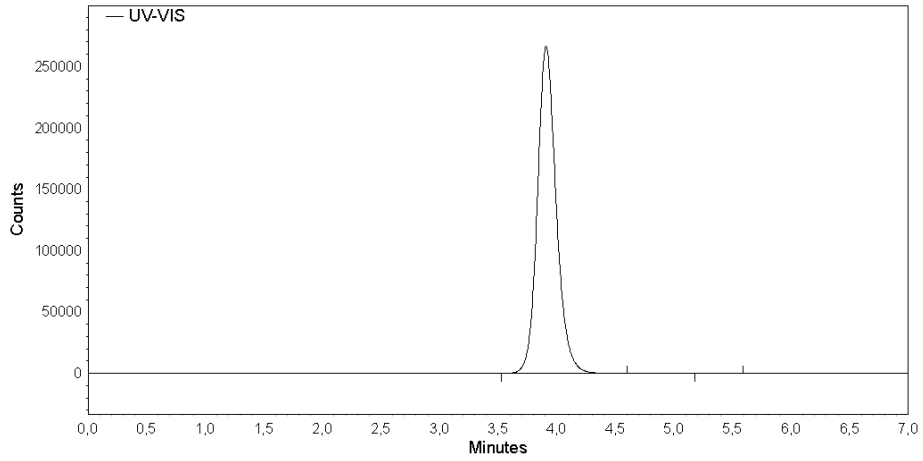


(a) Felodipine

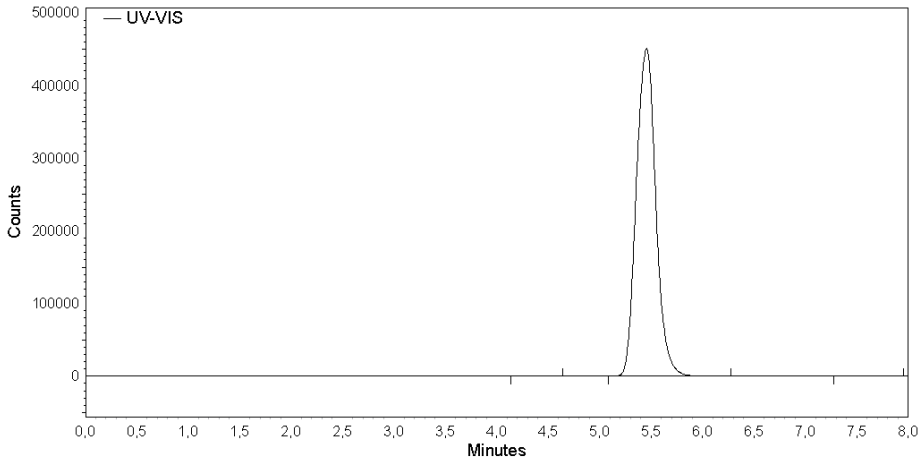


(b) Fenofibrate

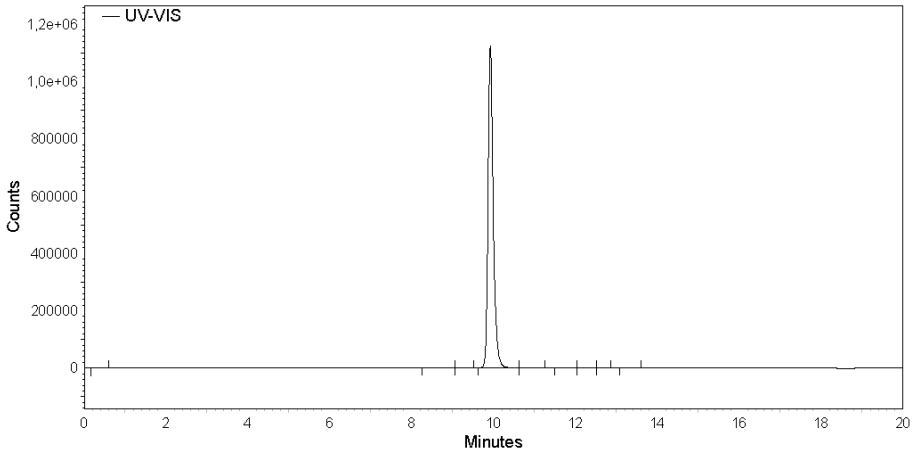


(c) Oxeglitazar

Figure 6.5: Typical chromatograms of a) felodipine, b) fenofibrate and c) oxeglitazar

#### 6.2.2.5 Differential scanning calorimetry

About 10-15 mg of sample in a 100 µL aluminum pan were measured with DSC 821e (Mettler-Toledo, Giessen, Germany) at a scan rate of 10 K/min and a nitrogen gas flow of 50 mL/min. A temperature range of −50 to 200 °C was used. The measurement was conducted in duplicate.

#### 6.2.2.6 X-ray diffraction

The analysis of the physical state of the API in pelletized extrudates, milled USAC compacts and the physical mixtures was performed using transmission diffractometer StadiP (STOE & Cie, Darmstadt, Germany).
The diffractometer was equipped with a Ge(111) monochromator and Cu K$\alpha$ radiation. A generator accelerating voltage of 40 kV and a plate current of 40 mA were applied. Measurement was conducted in the $2\theta$-range from 1-64.95° with a step size of 0.05° and a dwelling time of 15 s.

#### 6.2.2.7 Particle size analysis

A Mastersizer 2000 with a Hydro 2000SM sample dispersion unit (Malvern Instruments, Worcestershire, United Kingdom) was used to determine the particle size distribution of the APIs via laser light diffraction. About 200 mg of sample were added to 5 mL of silicone oil. The stirring rate was 2000 rpm. Each sample was scanned 50 times with a single measurement time of 7.5 s. Values of all measurements were then averaged.

#### 6.2.2.8 Karl-Fischer titration

The water content of the pelletized extrudates was determined using the Karl-Fischer oven method. Samples were analyzed directly after the extrusion and after the removal from storage at set time points using Oven Sample Processor 774 and KF Coulometer 756 (Metrohm, Filderstadt, Germany). About 100 mg of sample were accurately weighed into a glass vial, sealed and heated up to 120 °C. The water released during the heating procedure is transferred through a hollow needle into the Karl-Fischer cell and quantified through coulometric titration. Lactose monohydrate 1 % was used as standard. The measurement was conducted in duplicate.

#### 6.2.2.9 Scanning electron microscopy

Scanning electron microscope LEO 1530 Gemini (Carl Zeiss NTS, Oberkochen, Germany) was used to analyze the surface morphology of the extrudates and pure API. Samples were fixed on aluminum specimen mounts using adhesive conductive tabs and sputter-coated with

10 nm platinum (Emitech K575; Emitech, Ashford, Kent, England). The SEM analysis was conducted in a high vacuum environment (2 x $10^{-6}$ mbar) with an accelerating voltage of 5 kV. Magnifications from 20x to 5000x were used for analysis.

#### 6.2.2.10 Content uniformity of extrudates

The homogeneity of the API content in the extrudates was assessed using HPLC. A total amount of n=9 pellets was analyzed. Each pellet was separately weighed and dissolved in 10.0 mL of mobile phase which was prepared according to Section 6.2.2.4. The sample was stirred for 30 min to ensure a complete dissolution of the pelletized extrudate. HPLC analysis was performed according to Section 6.2.2.4.
The results were evaluated according to Ph.Eur. specifications (Section 2.9.40 Uniformity of dosage units).

# 7 Appendix

## A Characterization of extrudates

### A.1 Dissolution profiles of fenofibrate extrudates

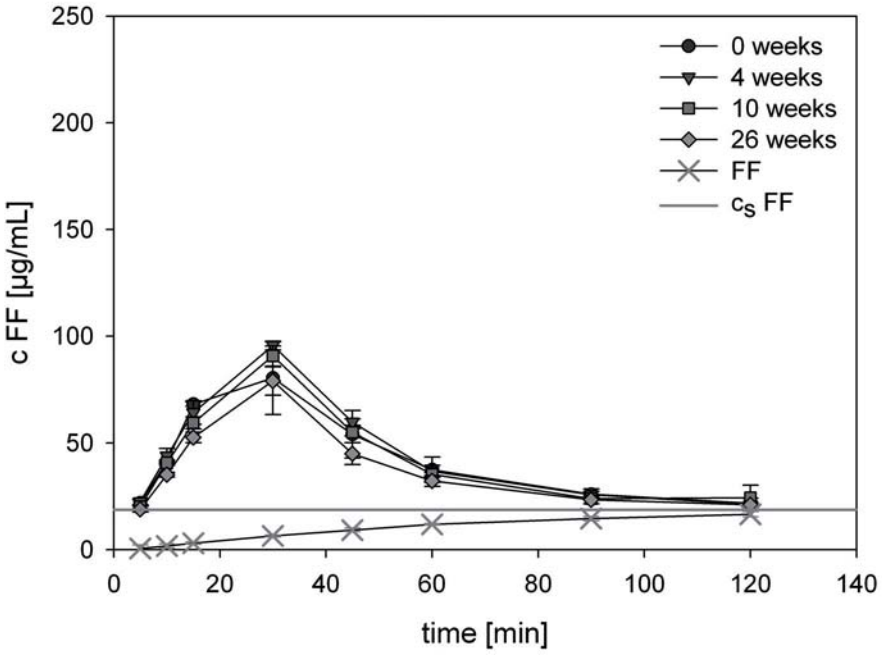


Figure A.1: Dissolution profiles of formulation FF-B pellets stored at 25 °C /60 % rH for 0, 4, 10 and 26 weeks

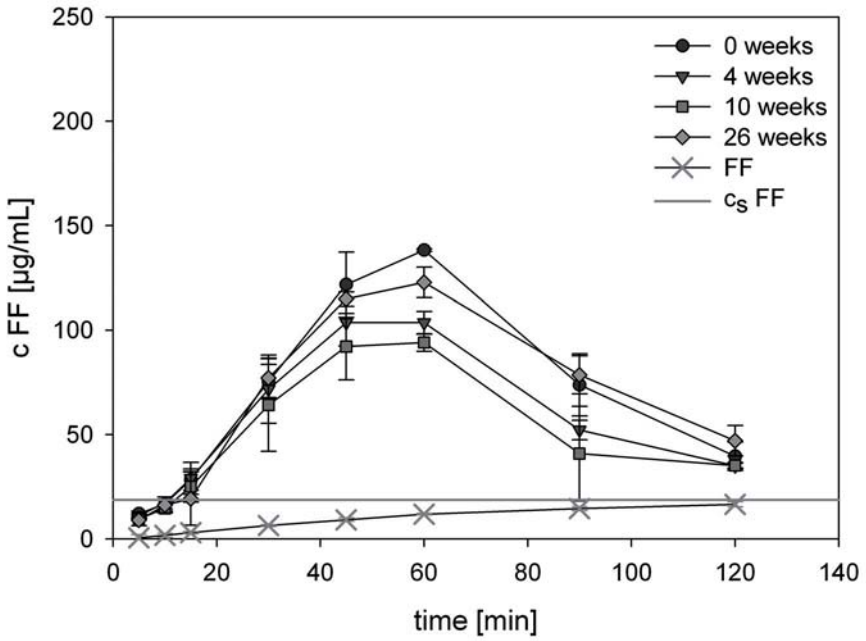


Figure A.2: Dissolution profiles of formulation FF-C pellets stored at 25 °C /60 % rH for 0, 4, 10 and 26 weeks

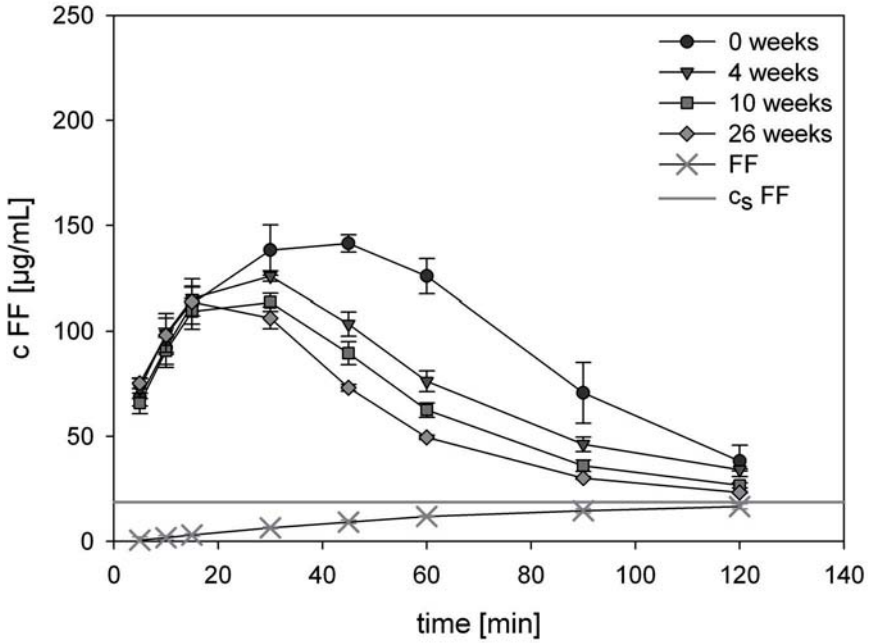


Figure A.3: Dissolution profiles of formulation FF-D pellets stored at 25 °C /60 % rH for 0, 4, 10 and 26 weeks

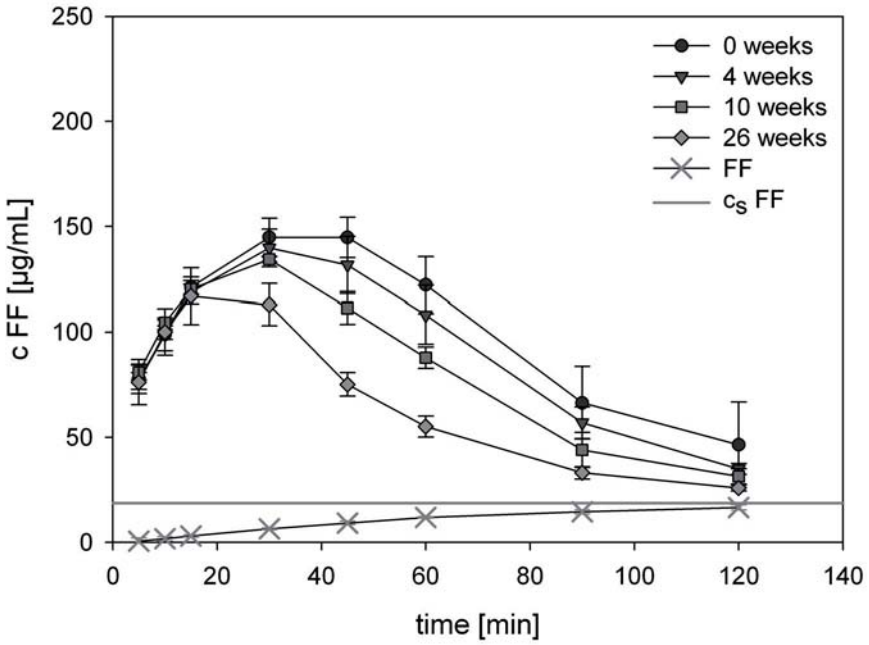


Figure A.4: Dissolution profiles of formulation FF-E pellets stored at 25 °C /60 % rH for 0, 4, 10 and 26 weeks

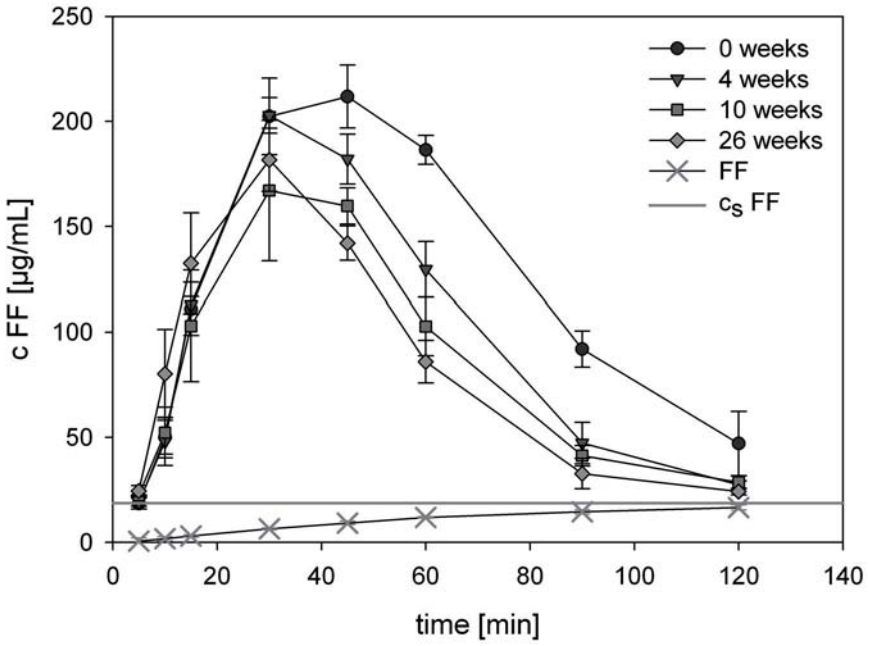


Figure A.5: Dissolution profiles of formulation FF-F pellets stored at 25 °C /60 % rH for 0, 4, 10 and 26 weeks

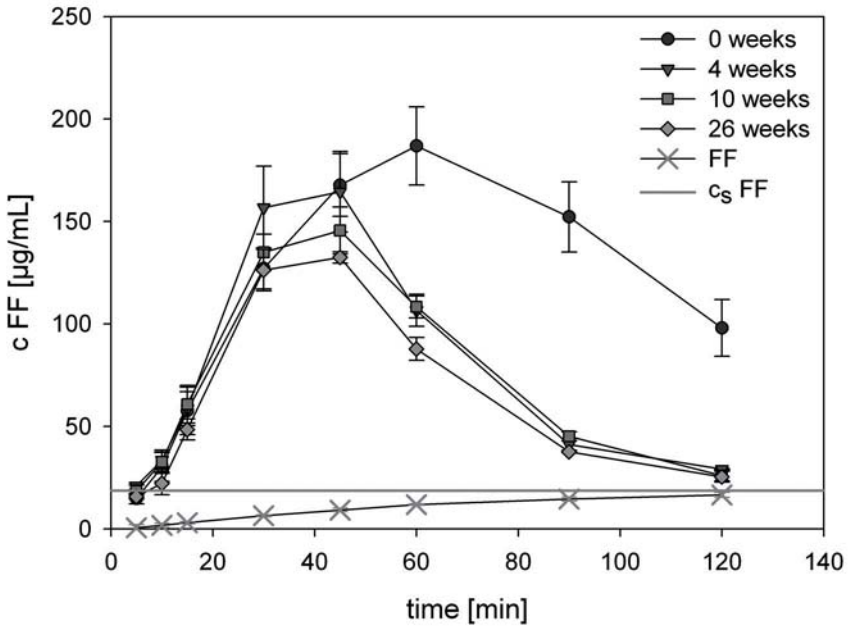


Figure A.6: Dissolution profiles of formulation FF-G pellets stored at 25 °C /60 % rH for 0, 4, 10 and 26 weeks

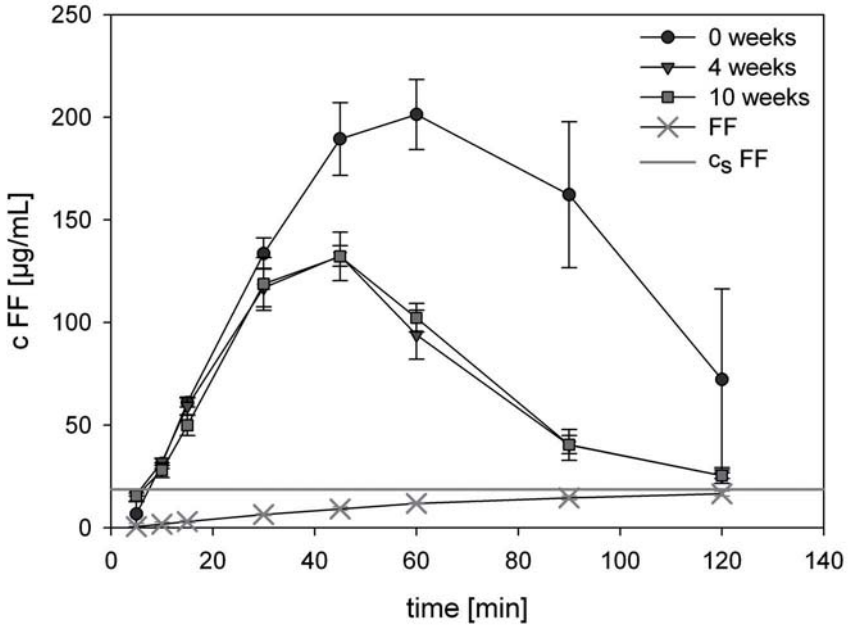


Figure A.7: Dissolution profiles of formulation FF-G pellets stored at 25 °C /60 % rH for 0, 4 and 10 weeks (repetition of trial)

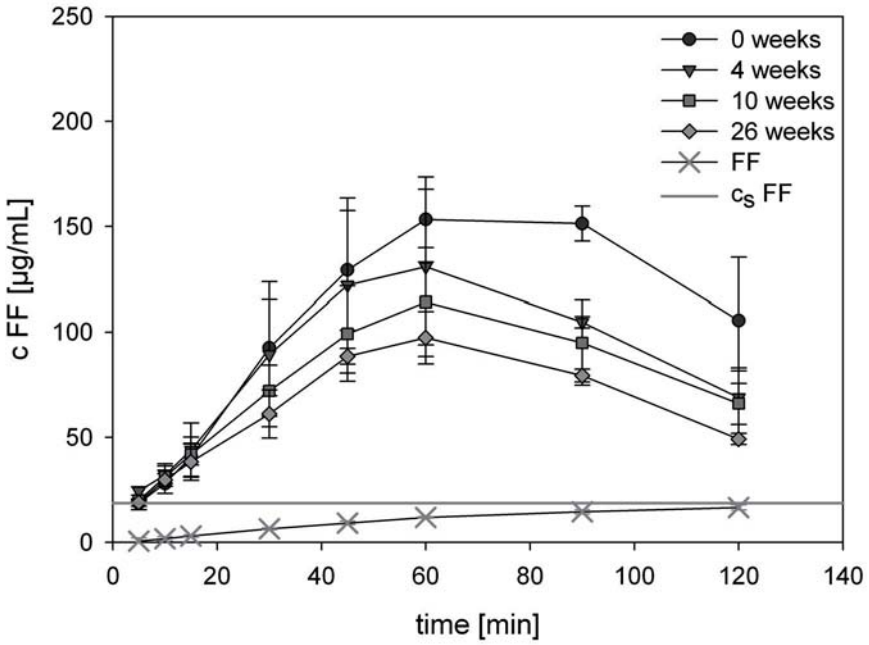


Figure A.8: Dissolution profiles of formulation FF-H pellets stored at 25 °C /60 % rH for 0, 4, 10 and 26 weeks

## A.2 Dissolution profiles of oxeglitazar extrudates

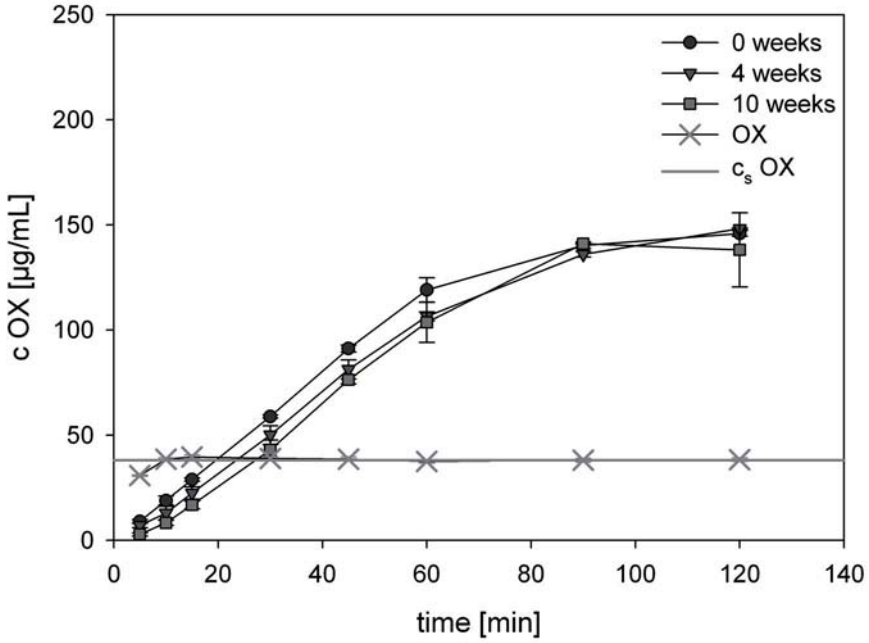


Figure A.9: Dissolution profiles of OX-B pellets stored at 25 °C /60 % rH for 0, 4 and 10 weeks

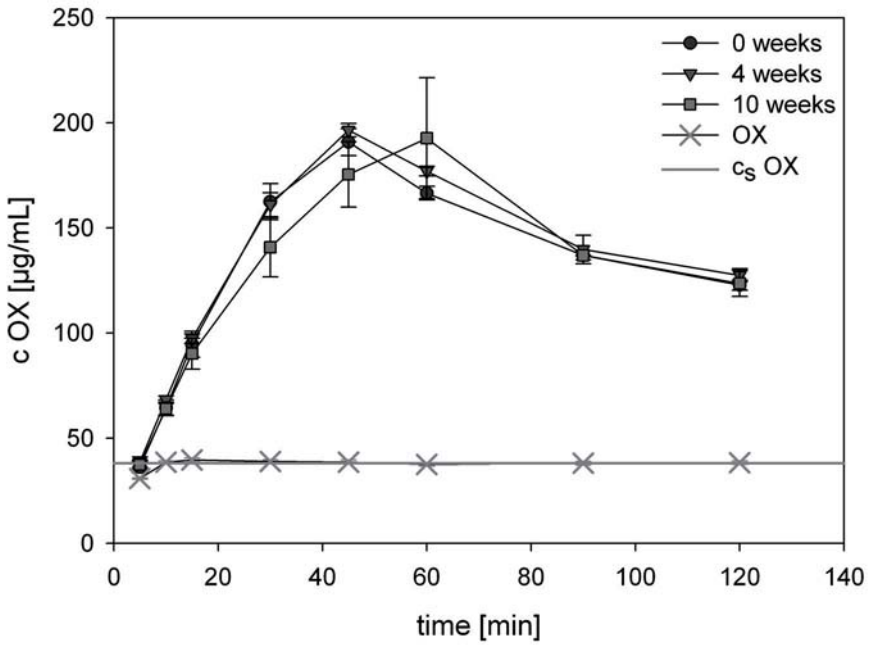


Figure A.10: Dissolution profiles of OX-D pellets stored at 25 °C /60 % rH for 0, 4 and 10 weeks

## A.3 Pellet sizes of extrudates

Table A.1: Pellet sizes of single polymeric FF formulations FF-A, FF-B and FF-C

| Pellet | FF-A | | | FF-B | | | FF-C | | |
|---|---|---|---|---|---|---|---|---|---|
| | Diameter [mm] | Length [mm] | Weight [mg] | Diameter [mm] | Length [mm] | Weight [mg] | Diameter [mm] | Length [mm] | Weight [mg] |
| 1 | 1.50 | 1.49 | 3.37 | 2.73 | 1.00 | 6.66 | 1.47 | 1.25 | 2.55 |
| 2 | 1.60 | 1.25 | 3.10 | 2.57 | 1.19 | 6.87 | 1.56 | 1.43 | 3.43 |
| 3 | 1.65 | 1.31 | 3.29 | 2.63 | 1.12 | 7.29 | 1.45 | 1.64 | 3.23 |
| 4 | 1.59 | 1.27 | 3.11 | 2.85 | 1.07 | 7.40 | 1.59 | 1.37 | 3.33 |
| 5 | 1.76 | 1.26 | 3.20 | 2.45 | 1.28 | 7.47 | 1.27 | 1.07 | 1.36 |
| 6 | 1.72 | 1.72 | 4.60 | 2.87 | 1.09 | 7.60 | 1.47 | 1.46 | 3.15 |
| 7 | 1.60 | 1.16 | 2.93 | 2.84 | 1.13 | 7.67 | 1.54 | 1.56 | 3.47 |
| 8 | 1.56 | 1.28 | 2.99 | 2.59 | 1.26 | 7.67 | 1.52 | 1.48 | 3.36 |
| 9 | 1.49 | 1.24 | 2.68 | 2.79 | 1.11 | 7.71 | 1.57 | 1.36 | 3.09 |
| 10 | 1.55 | 1.18 | 2.50 | 2.91 | 1.01 | 7.80 | 1.50 | 1.61 | 3.54 |
| 11 | 1.64 | 1.70 | 4.01 | 2.75 | 1.13 | 7.85 | 1.56 | 1.49 | 3.63 |
| 12 | 1.59 | 1.59 | 3.79 | 2.80 | 1.01 | 8.03 | 1.52 | 1.36 | 2.88 |
| 13 | 1.56 | 1.56 | 3.02 | 2.86 | 1.11 | 8.22 | 1.53 | 1.43 | 3.25 |
| 14 | 1.58 | 1.61 | 3.63 | 2.82 | 1.10 | 8.26 | 1.55 | 1.13 | 2.51 |
| 15 | 1.55 | 1.36 | 2.76 | 2.81 | 1.18 | 8.30 | 1.49 | 1.55 | 3.26 |
| 16 | 1.61 | 1.41 | 3.33 | 2.62 | 1.30 | 8.34 | 1.48 | 1.53 | 3.25 |
| 17 | 1.55 | 1.35 | 3.14 | 2.91 | 1.45 | 11.85 | 1.46 | 1.48 | 2.84 |
| 18 | 1.54 | 1.42 | 3.21 | 2.82 | 1.15 | 8.40 | 1.56 | 1.33 | 3.06 |
| 19 | 1.59 | 1.37 | 3.39 | 2.97 | 1.08 | 8.43 | 1.53 | 1.34 | 3.07 |
| 20 | 1.45 | 1.46 | 2.97 | 2.98 | 1.06 | 8.44 | 1.62 | 1.59 | 3.78 |
| 21 | 1.65 | 1.39 | 3.60 | 2.85 | 1.09 | 8.55 | 1.47 | 1.58 | 3.09 |
| 22 | 1.67 | 1.16 | 2.77 | 2.58 | 1.38 | 8.55 | 1.56 | 1.39 | 3.32 |
| 23 | 1.58 | 1.36 | 2.98 | 2.84 | 1.26 | 8.68 | 1.49 | 1.77 | 3.56 |
| 24 | 1.47 | 1.27 | 2.64 | 2.95 | 1.15 | 8.71 | 1.47 | 1.32 | 2.67 |
| 25 | 1.49 | 1.21 | 2.58 | 2.89 | 1.19 | 8.71 | 1.52 | 1.71 | 3.64 |
| 26 | 1.58 | 1.41 | 3.30 | 2.89 | 1.13 | 8.74 | 1.59 | 1.50 | 3.63 |
| 27 | 1.56 | 1.52 | 3.49 | 2.77 | 1.31 | 8.76 | 1.57 | 1.56 | 3.60 |
| 28 | 1.62 | 1.64 | 4.00 | 2.79 | 1.29 | 8.78 | 1.50 | 1.43 | 3.10 |
| 29 | 1.60 | 1.33 | 3.34 | 2.78 | 1.18 | 8.92 | 1.51 | 1.48 | 3.24 |
| 30 | 1.47 | 1.53 | 3.14 | 2.92 | 1.20 | 8.93 | 1.47 | 1.41 | 2.88 |
| 31 | 1.60 | 1.50 | 3.50 | 3.00 | 1.11 | 8.94 | 1.61 | 1.46 | 3.78 |
| 32 | 1.60 | 1.39 | 3.43 | 2.84 | 1.35 | 9.65 | 1.46 | 1.44 | 2.84 |
| 33 | 1.71 | 1.40 | 3.85 | 2.82 | 1.32 | 9.74 | 1.46 | 1.26 | 2.61 |
| 34 | 1.71 | 1.14 | 3.11 | 2.73 | 1.35 | 9.76 | 1.48 | 1.55 | 3.32 |
| 35 | 1.76 | 1.27 | 3.60 | 2.89 | 1.34 | 9.84 | 1.53 | 1.51 | 3.27 |
| 36 | 1.63 | 1.34 | 3.08 | 2.97 | 1.17 | 9.91 | 1.55 | 1.41 | 3.30 |
| 37 | 1.67 | 1.68 | 4.42 | 2.82 | 1.43 | 10.00 | 1.53 | 1.57 | 3.59 |
| 38 | 1.58 | 1.37 | 3.31 | 2.77 | 1.43 | 10.10 | 1.47 | 1.47 | 3.05 |
| 39 | 1.59 | 1.59 | 3.79 | 2.87 | 1.41 | 10.20 | 1.62 | 1.55 | 3.96 |
| 40 | 1.70 | 1.33 | 3.70 | 2.90 | 1.39 | 10.79 | 1.55 | 1.45 | 3.26 |
| 41 | 2.16 | 1.48 | 6.11 | 2.90 | 1.43 | 10.94 | 1.51 | 1.51 | 3.41 |
| 42 | 1.55 | 1.46 | 3.23 | 2.83 | 1.60 | 11.01 | 1.56 | 1.12 | 2.67 |
| 43 | 1.63 | 1.47 | 3.59 | 2.81 | 1.60 | 11.07 | 1.54 | 1.37 | 2.82 |
| 44 | 1.59 | 1.40 | 3.17 | 3.08 | 1.26 | 11.20 | 1.56 | 1.73 | 3.81 |
| 45 | 1.59 | 1.34 | 2.62 | 2.94 | 1.48 | 11.20 | 1.61 | 1.61 | 3.92 |
| 46 | 1.52 | 1.46 | 3.08 | 2.86 | 1.54 | 11.21 | 1.50 | 1.32 | 2.87 |
| 47 | 1.58 | 1.98 | 4.19 | 2.80 | 1.52 | 11.61 | 1.48 | 1.42 | 2.97 |
| 48 | 1.54 | 1.81 | 3.73 | 3.02 | 1.42 | 11.64 | 1.46 | 1.42 | 2.96 |
| 49 | 1.65 | 1.55 | 3.91 | 2.93 | 1.63 | 11.73 | 1.57 | 1.36 | 3.16 |
| 50 | 1.60 | 1.34 | 3.00 | 2.94 | 1.57 | 11.84 | 1.55 | 1.40 | 3.28 |
| Mean value | 1.61 | 1.42 | 3.39 | 2.83 | 1.27 | 9.20 | 1.52 | 1.45 | 3.19 |
| Std deviation | 0.11 | 0.17 | 0.61 | 0.12 | 0.17 | 1.46 | 0.06 | 0.14 | 0.44 |

## A.4 AUC values for manufactured formulations

Table A.2: AUC values for drug dissolution from manufactured formulations and untreated APIs calculated from the first to the last sampling point (5 min - 120 min)

| Formulation | AUC values [µg/mLmin] | | | | |
|---|---|---|---|---|---|
| | 0 weeks | 4 weeks | 10 weeks | 26 weeeks | PM |
| US-A | 2007 | - | - | - | 1158 |
| US-B | 2241 | - | - | - | 1157 |
| US-C | 2698 | - | - | - | 1600 |
| US-D | 2269 | - | - | - | 1597 |
| US-E | 2481 | - | - | - | 1304 |
| FD-A | 5978 | 5017 | 6199 | - | 3096 |
| FD-B | 2832 | - | - | - | 3716 |
| FD-C | 351 | - | - | - | 3088 |
| FD-D | 2845 | - | - | - | 3447 |
| FD-E | 971 | - | - | - | 2708 |
| FD-F | 1453 | - | - | - | 3723 |
| FF-A | 10426 | 11185 | 7570 | 5674 | 1158 |
| FF-B | 4905 | 5164 | 4905 | 4351 | 1157 |
| FF-C | 6486 | 7458 | 6563 | 9008 | 1600 |
| FF-D | 11486 | 8881 | 7648 | 6881 | 1025 |
| FF-E | 11687 | 10612 | 9381 | 7306 | 978 |
| FF-F | 15282 | 11935 | 10225 | 9923 | 1024 |
| FF-G | 15431 | 9694 | 9209 | 8003 | 1150 |
| FF-H | 13497 | 10952 | 9605 | 8138 | 1000 |
| FF-J | 3355 | - | - | - | 1597 |
| FF-K | 281 | - | - | - | 1304 |
| OX-A | 11029 | 10571 | 10704 | - | 5552 |
| OX-B | 11735 | 10978 | 10645 | - | 4145 |
| OX-C | 1484 | - | - | - | 5186 |
| OX-D | 16358 | 16863 | 16356 | - | 4371 |
| OX-E | 5192 | - | - | - | 5063 |
| OX-F | 5036 | - | - | - | 4670 |
| OX-G | 11986 | - | - | - | - |
| OX-H | 17333 | - | - | - | - |
| OX-J | 16974 | - | - | - | - |
| OX-K | 12337 | - | - | - | - |
| OX-CL 1 | 1243 | - | - | - | - |
| OX-CL 2 | 1646 | - | - | - | - |
| FD | | | 2853 | | |
| FF | | | 1227 | | |
| OX | | | 4391 | | |

## A.5 XRD patterns of felodipine extrudates

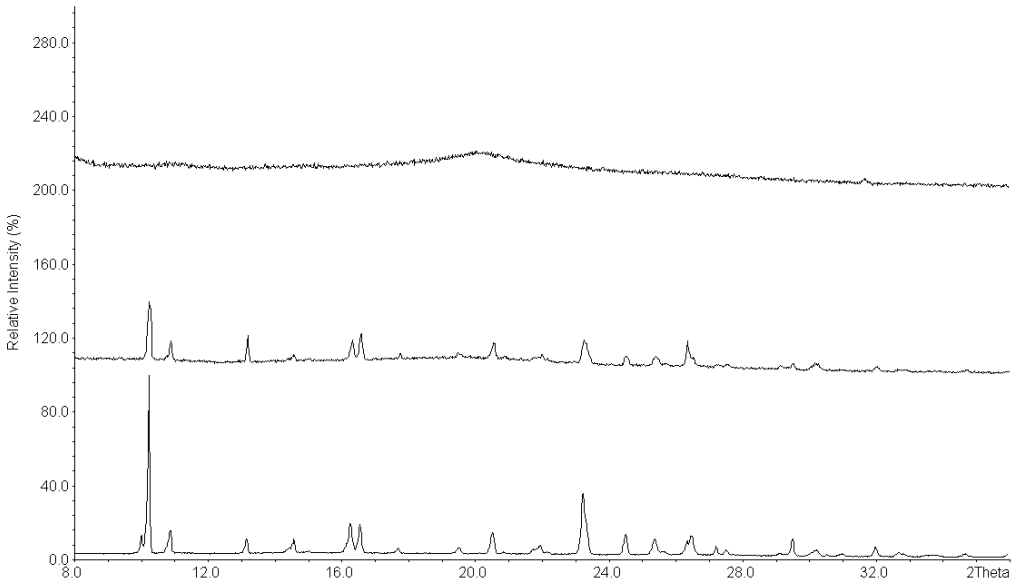


Figure A.11: XRD pattern of FD-B extrudate with the following data displayed from top to bottom: pelletized extrudate, physical mixture of the components, pure FD

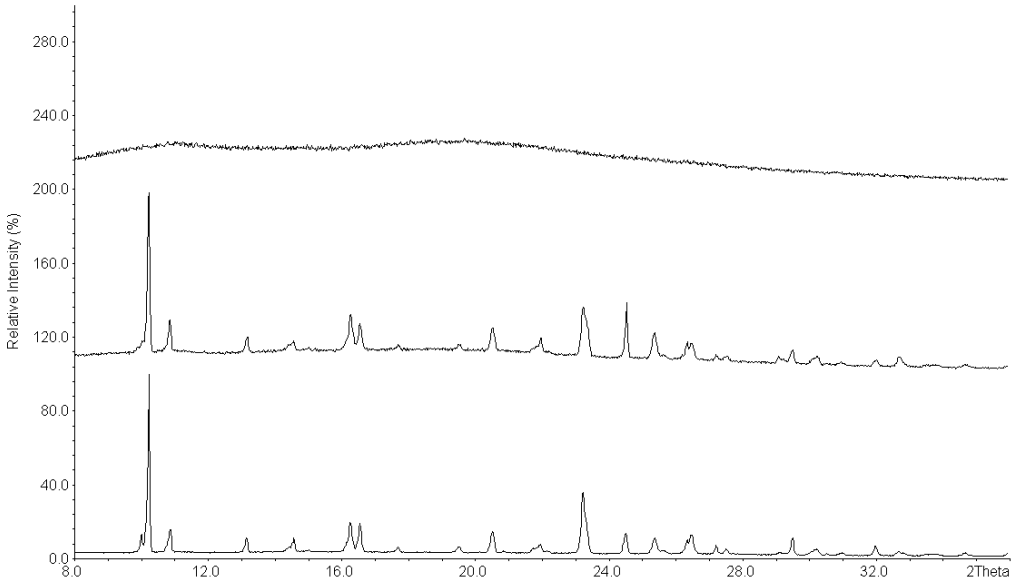


Figure A.12: XRD pattern of FD-C extrudate with the following data displayed from top to bottom: pelletized extrudate, physical mixture of the components, pure FD

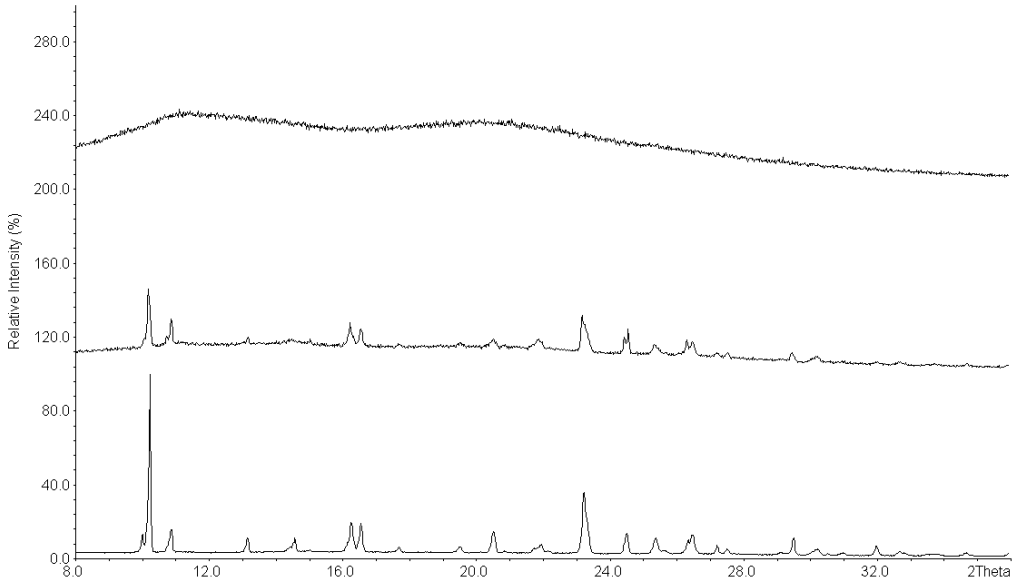


Figure A.13: XRD pattern of FD-E extrudate with the following data displayed from top to bottom: pelletized extrudate, physical mixture of the components, pure FD

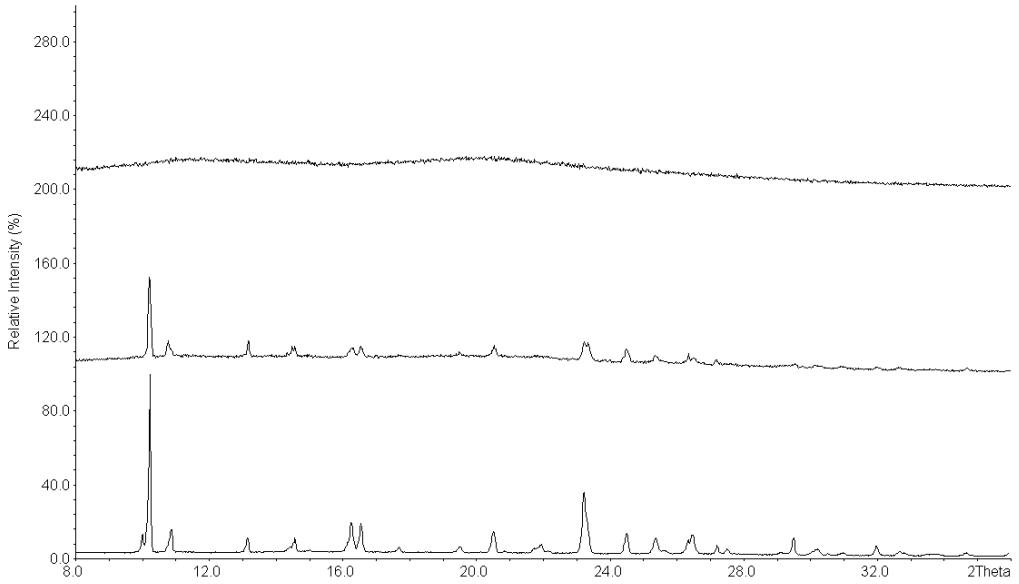


Figure A.14: XRD pattern of FD-F extrudate with the following data displayed from top to bottom: pelletized extrudate, physical mixture of the components, pure FD

## A.6 XRD patterns of fenofibrate extrudates

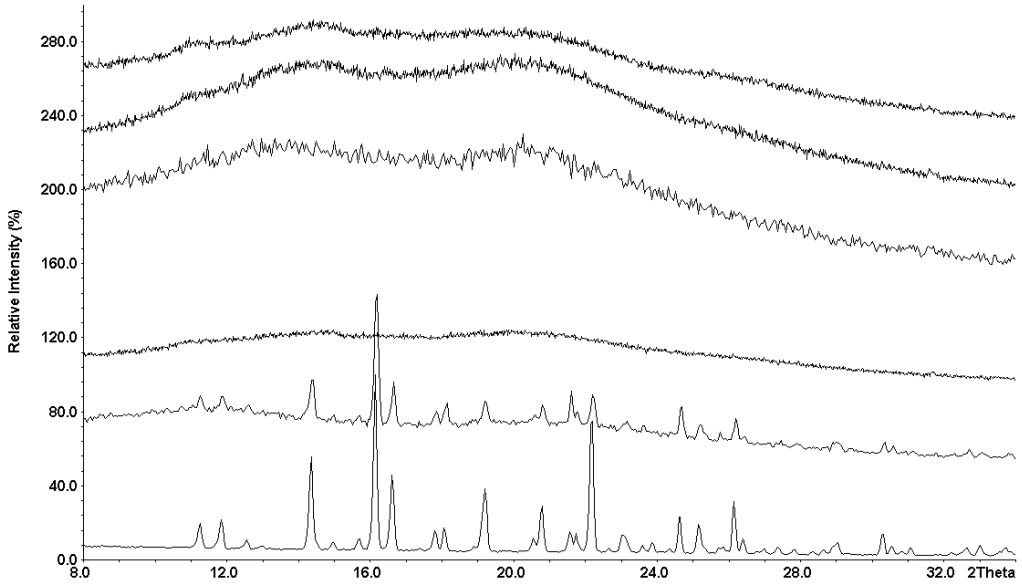


Figure A.15: XRD pattern of FF-D extrudate with the following data displayed from top to bottom: pellets after 0, 4, 10 and 26 weeks of storage at 25 °C /60 % rH, physical mixture of the components, pure FF

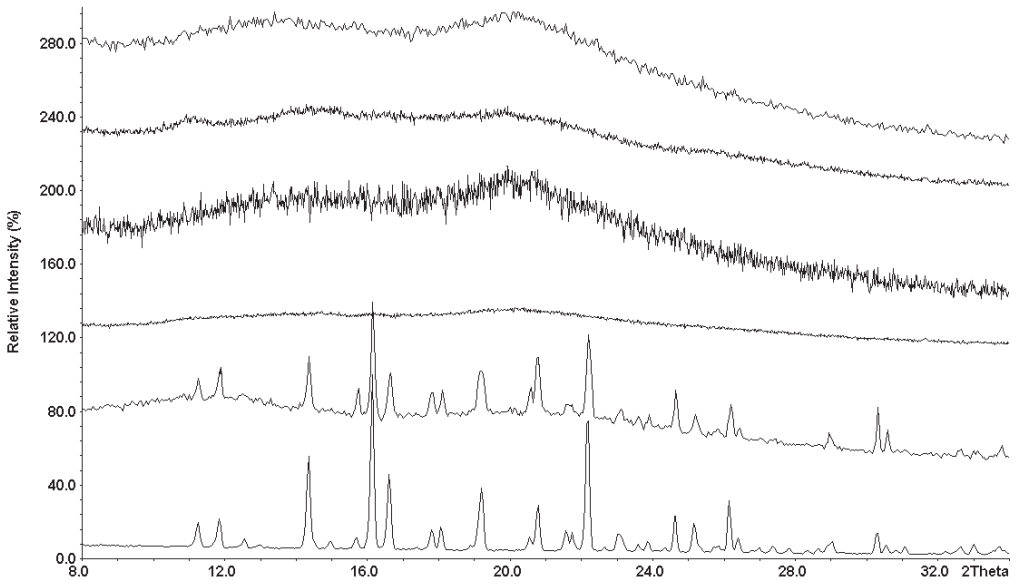


Figure A.16: XRD pattern of FF-E extrudate with the following data displayed from top to bottom: pellets after 0, 4, 10 and 26 weeks of storage at 25 °C /60 % rH, physical mixture of the components, pure FF

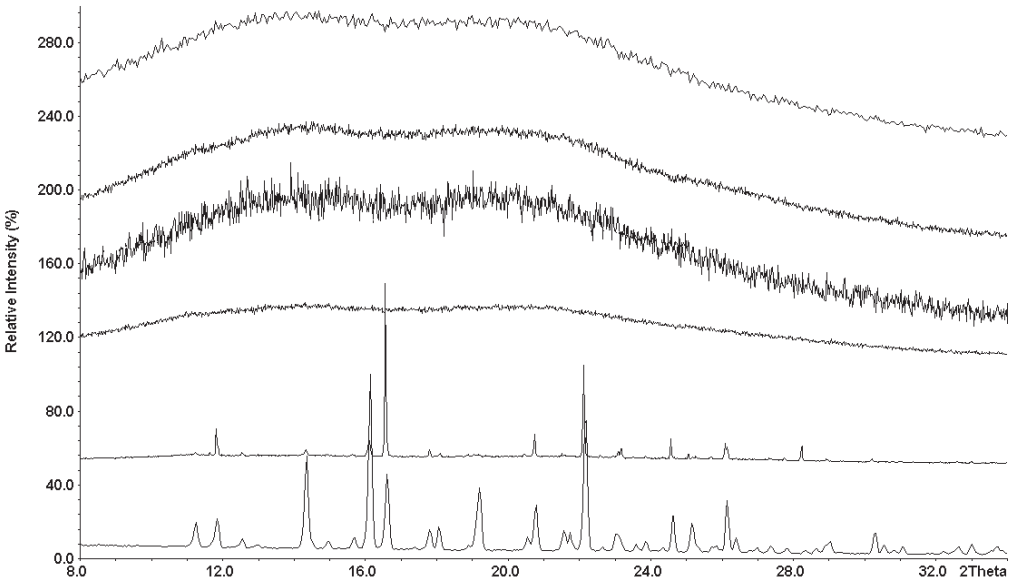


Figure A.17: XRD pattern of FF-F extrudate with the following data displayed from top to bottom: pellets after 0, 4, 10 and 26 weeks of storage uat 25 °C /60 % rH, physical mixture of the components, pure FF

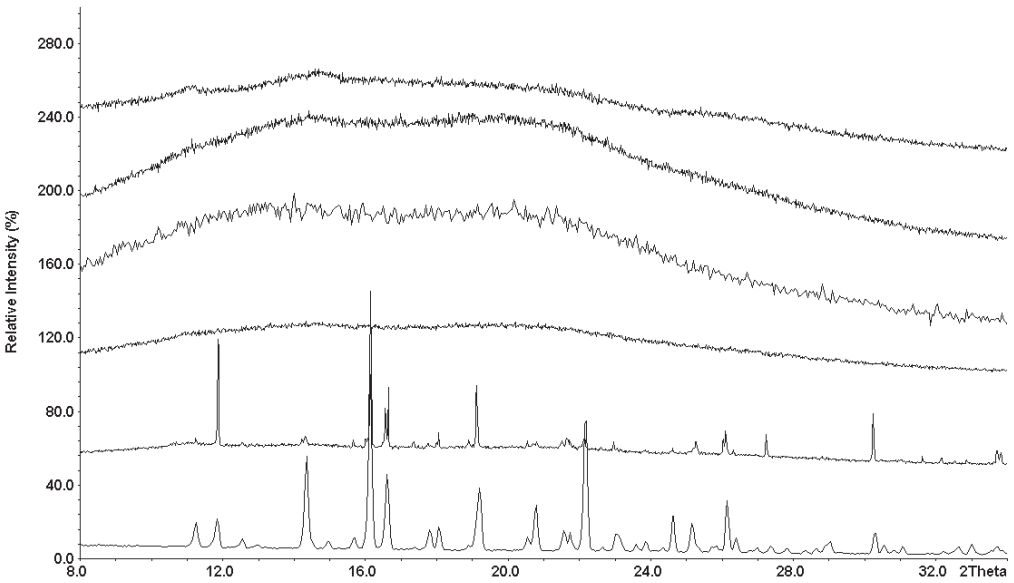


Figure A.18: XRD pattern of FF-G extrudate with the following data displayed from top to bottom: pellets after 0, 4, 10 and 26 weeks of storage uat 25 °C /60 % rH, physical mixture of the components, pure FF

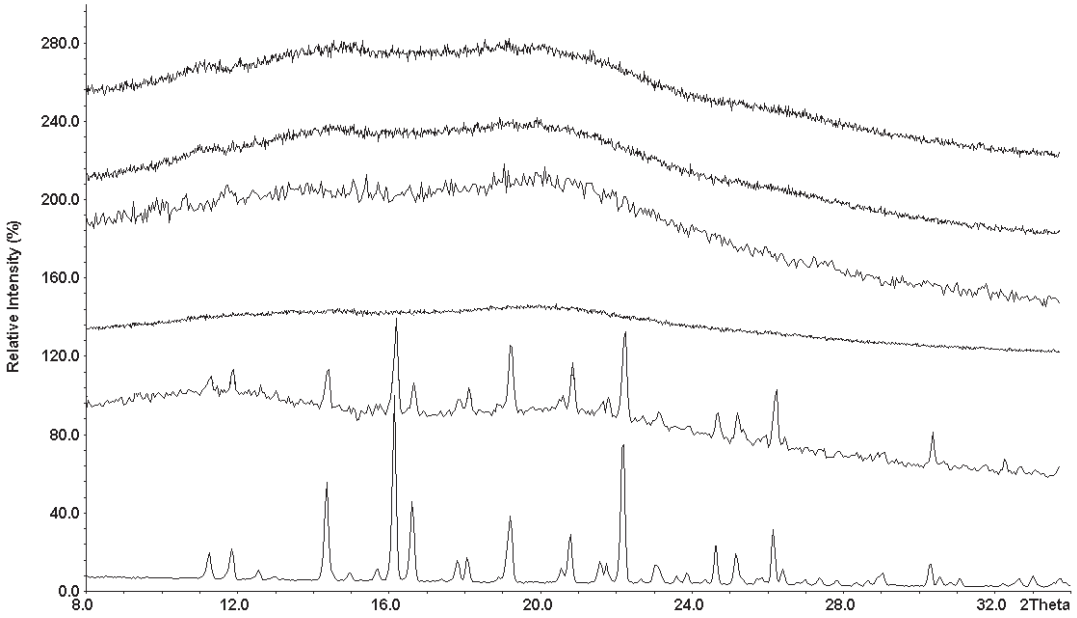


Figure A.19: XRD pattern of FF-H extrudate with the following data displayed from top to bottom: pellets after 0, 4, 10 and 26 weeks of storage uat 25 °C /60 % rH, physical mixture of the components, pure FF

## A.7 XRD patterns of oxeglitazar extrudates

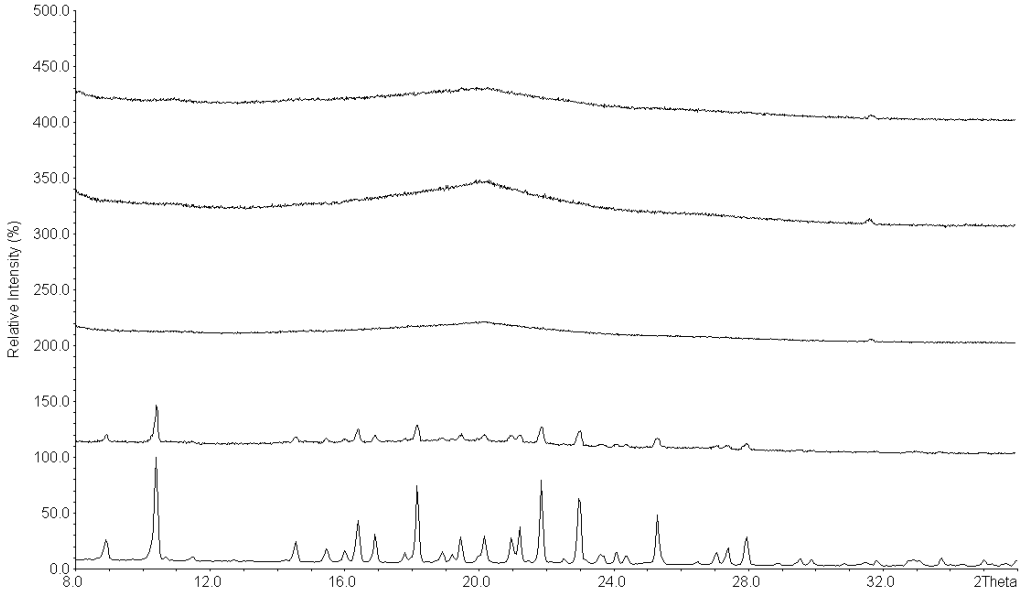


Figure A.20: XRD pattern of OX-B extrudates with the following data displayed from top to bottom: pellets after 0 weeks, 4 weeks, 10 weeks of storage under long-term storage conditions (25 °C /60 % rH), physical mixture of the components, pure OX

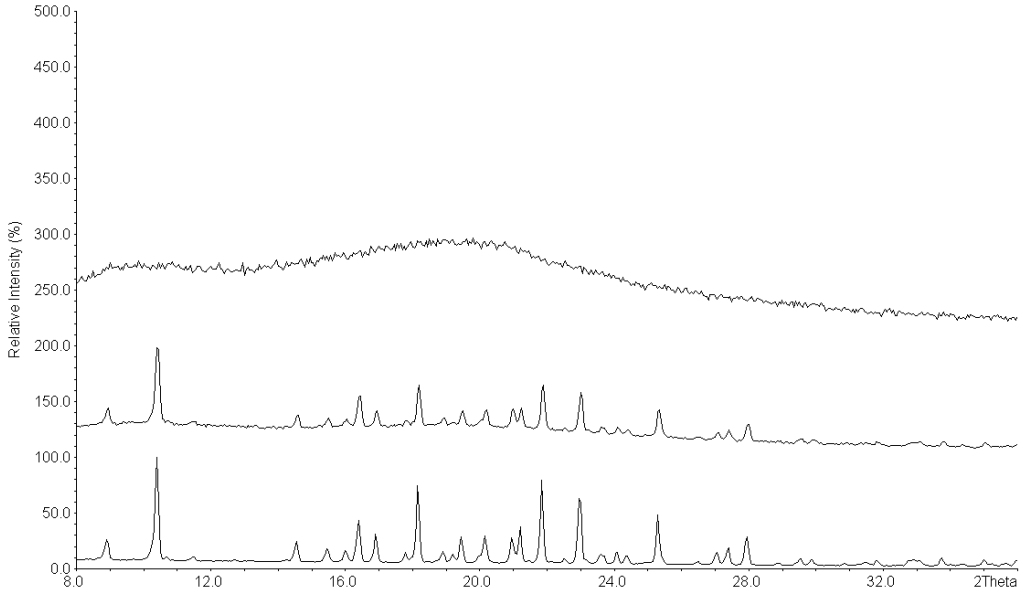


Figure A.21: XRD pattern of OX-C extrudates with the following data displayed from top to bottom: pellets directly after manufacture, physical mixture of the components, pure OX

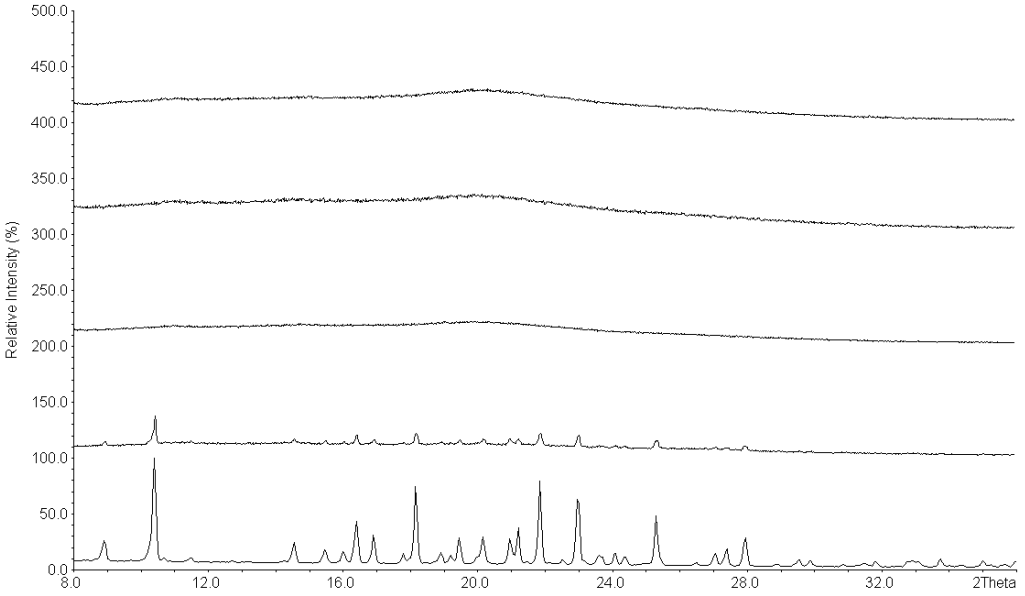


Figure A.22: XRD pattern of OX-D extrudates with the following data displayed from top to bottom: pellets after 0 weeks, 4 weeks, 10 weeks of storage under long-term storage conditions (25 °C /60 % rH), physical mixture of the components, pure OX

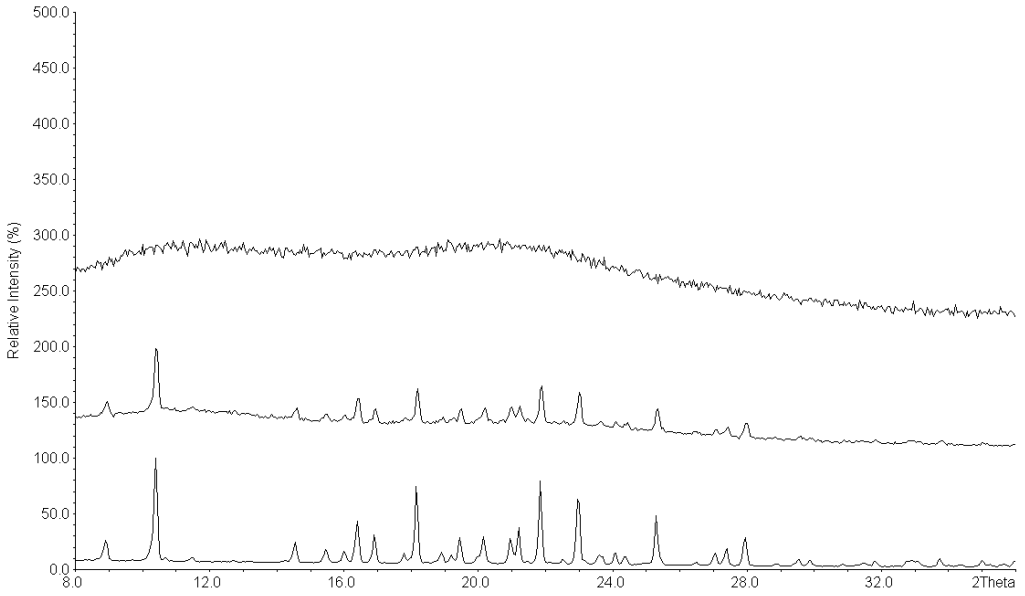


Figure A.23: XRD pattern of OX-E extrudates with the following data displayed from top to bottom: pellets directly after manufacture, physical mixture of the components, pure OX

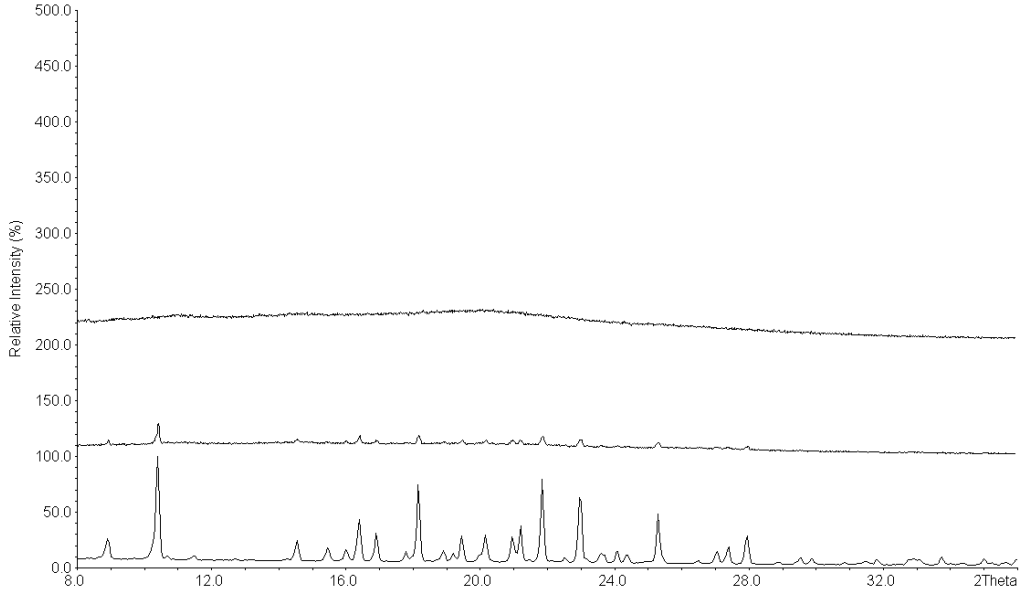


Figure A.24: XRD pattern of OX-F extrudates with the following data displayed from top to bottom: pellets directly after manufacture, physical mixture of the components, pure OX

## A.8 DSC thermograms of single components

Table A.3: DSC analysis of APIs and carriers

| Sample | $1^{st}$ heating cycle | | | $2^{nd}$ heating cycle | | |
|---|---|---|---|---|---|---|
| | | $T_{onset}$ [°C] | $T_{midpt,peak}$ [°C] | | $T_{onset}$ [°C] | $T_{midpt,peak}$ [°C] |
| FD | $T_m$ | 145.1 | 148.3 | - | - | - |
| FF | $T_m$ | 81.4 | 83.2 | $T_g$ | -19.2 | -18.5 |
| OX | $T_m$ | 158.2 | 160.8 | $T_g$ | 38.4 | 39.7 |
| | | | | $T_m$ | 153.8 | n/a |
| | | | | $T_m$ | n/a | 158.3 |
| COP | - | - | - | $T_g$ | 100.8 | 104.9 |
| HPMC | $T_g$ | 174.3 | 175.4 | - | - | - |
| PVCL-PVAc-PEG | - | - | - | - | - | - |
| aPMMA | $T_g$ | 48.1 | 50.5 | $T_g$ | 32.3 | 38.2 |
| PVA-AA-MMA | - | - | - | $T_g$ | 64.9 | 69.6 |

While in the first heating cycle, only one endothermic event was observed for OX, multiple events were detected in the second heating cycle (see Figure A.25). The thermogram shows a distinct melting peak in the first heating cycle at 158.2 °C. In the second heating cycle, a glass transition was detected at approximately 50 °C. At approximately 103 °C, an exothermic event takes place which can be associated with a recrystallization of the amorphous API.

At 154 °C, a double peak was observed. This endothermic event indicates the presence of two polymorphic forms with similar melting temperatures leading to an overlaying of the two melting peaks. Two polymorphic forms of OX have been described in literature thus supporting the approach to the interpretation of the DSC curve (Majerik et al., 2007).

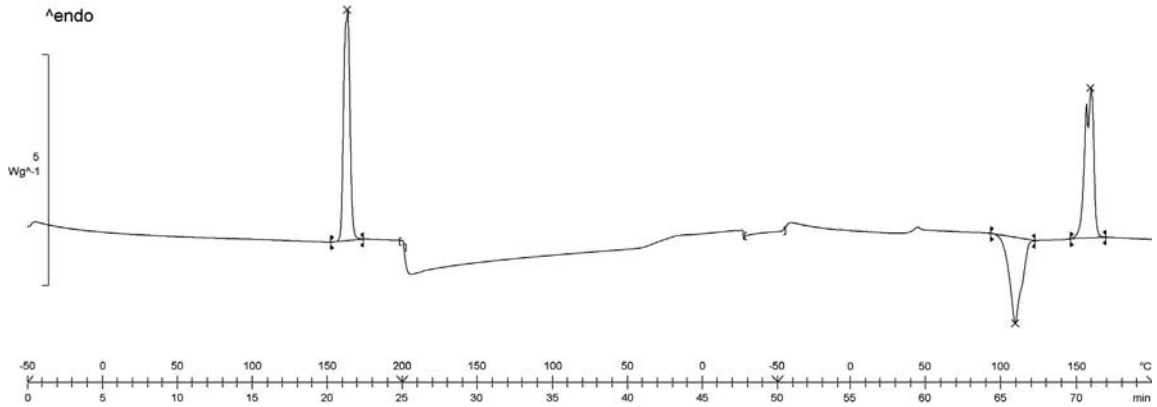


Figure A.25: DSC thermogram of pure OX powder

## A.9 DSC thermograms of felodipine extrudates

Table A.4: DSC analysis of FD extrudates in comparison to the physical mixtures (PM)

| Sample | | | $1^{st}$ heating cycle | | | $2^{nd}$ heating cycle | |
|---|---|---|---|---|---|---|---|
| | | | $T_{onset}$ [°C] | $T_{midpt,peak}$ [°C] | | $T_{onset}$ [°C] | $T_{midpt,peak}$ [°C] |
| FD-A | 0 weeks | $T_g$ | 70.1 | 73.8 | $T_g$ | 88.2 | 91.6 |
| | 4 weeks | $T_g$ | 82.6 | 86.9 | $T_g$ | 83.5 | 88.4 |
| | 10 weeks | $T_g$ | 76.8 | 78.1 | $T_g$ | 85.8 | 90.3 |
| | PM | $T_m$ | 140.0 | 147.0 | $T_g$ | 82.8 | 87.0 |
| FD-B | 0 weeks | $T_g$ | 52.0 | 56.6 | - | - | - |
| | PM | $T_m$ | 143.9 | 147.6 | - | - | - |
| FD-C | 0 weeks | $T_g$ | 46.4 | 50.4 | $T_g$ | 48.3 | 48.0 |
| | PM | $T_m$ | 141.2 | 146.4 | $T_g$ | 40.6 | 54.5 |
| FD-D | 0 weeks | $T_g$ | 76.2 | 80.4 | $T_g$ | 88.2 | 91.1 |
| | PM | $T_m$ | 140.5 | 147.4 | $T_g$ | 85.8 | 91.8 |
| FD-E | 0 weeks | $T_g$ | | | $T_g$ | 81.5 | 84.9 |
| | PM | $T_m$ | 139.0 | 146.5 | $T_g$ | 84.9 | 91.8 |
| FD-F | 0 weeks | $T_g$ | - | - | $T_g$ | 86.0 | 89.5 |
| | PM | $T_m$ | 141.5 | 148.2 | $T_g$ | 84.9 | 90.7 |

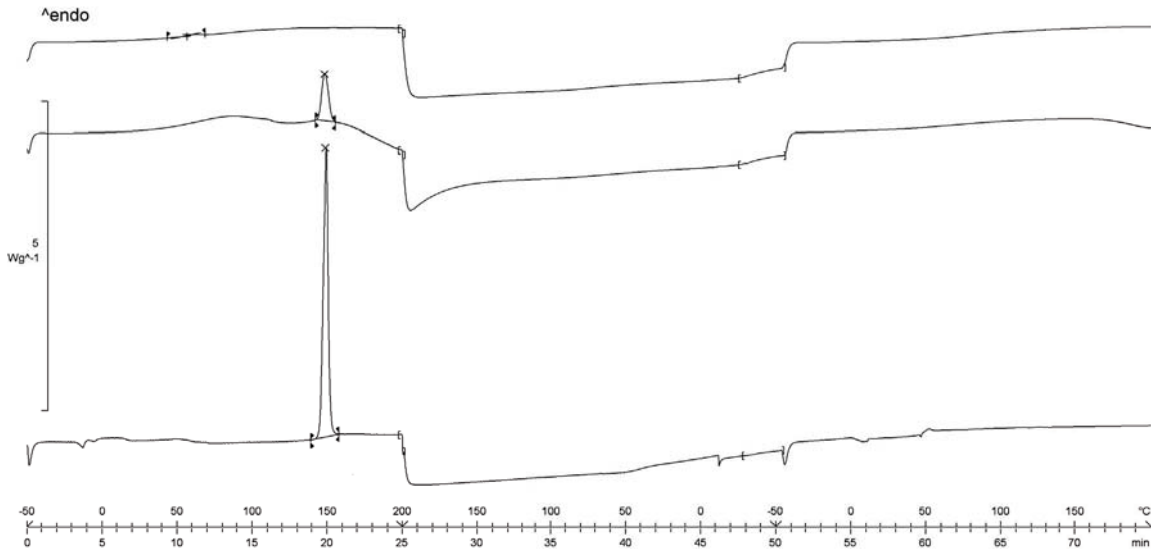


Figure A.26: DSC thermogram of FD-B extrudate with the following data displayed from top to bottom: extrudate, the corresponding physical mixture, pure FD

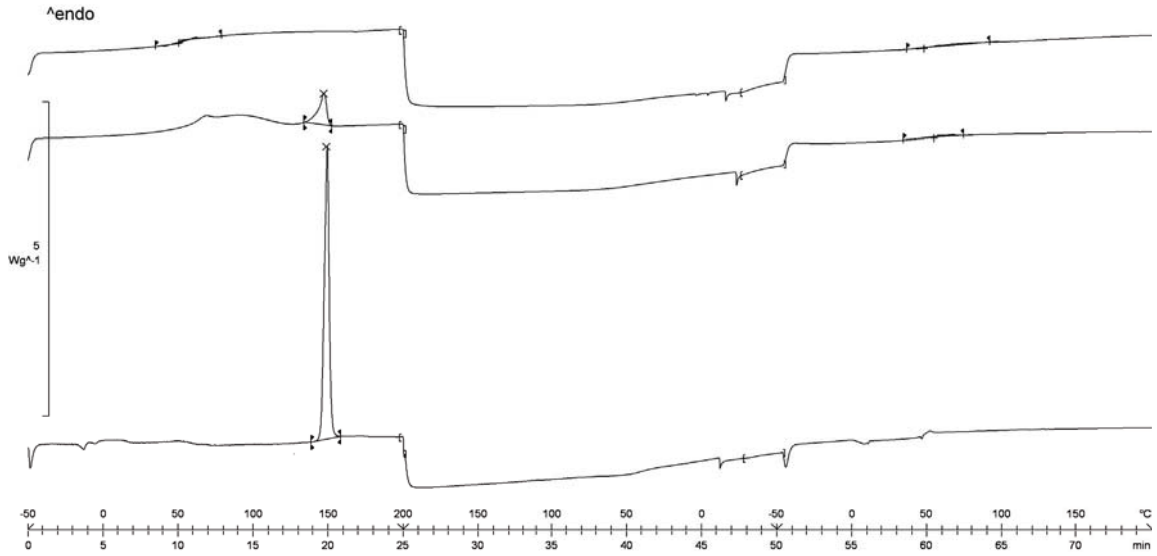


Figure A.27: DSC thermogram of FD-C extrudate with the following data displayed from top to bottom: extrudate, the corresponding physical mixture, pure FD

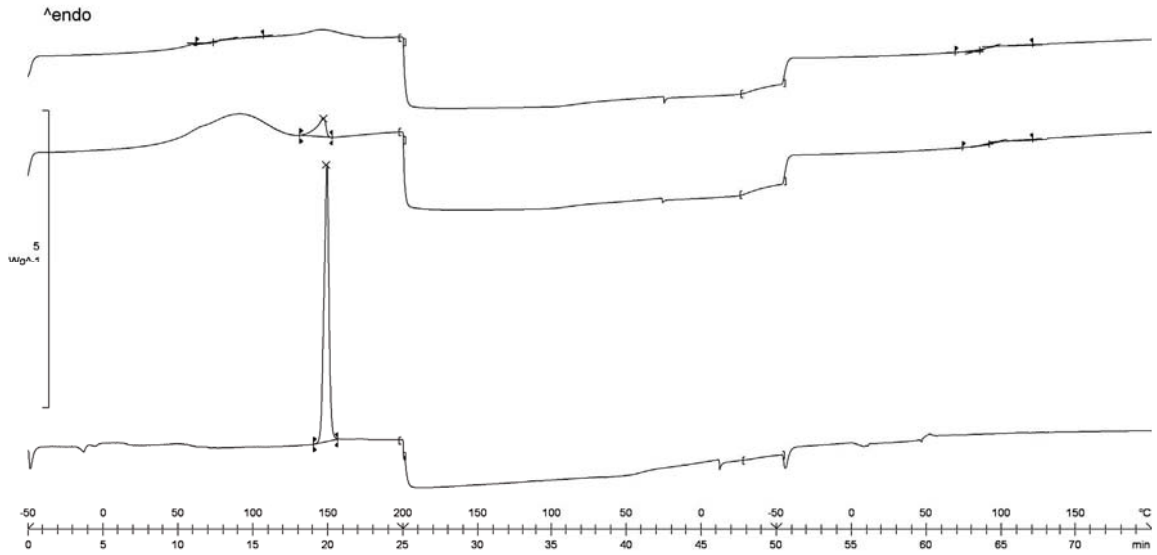


Figure A.28: DSC thermogram of FD-E extrudate with the following data displayed from top to bottom: extrudate, the corresponding physical mixture, pure FD

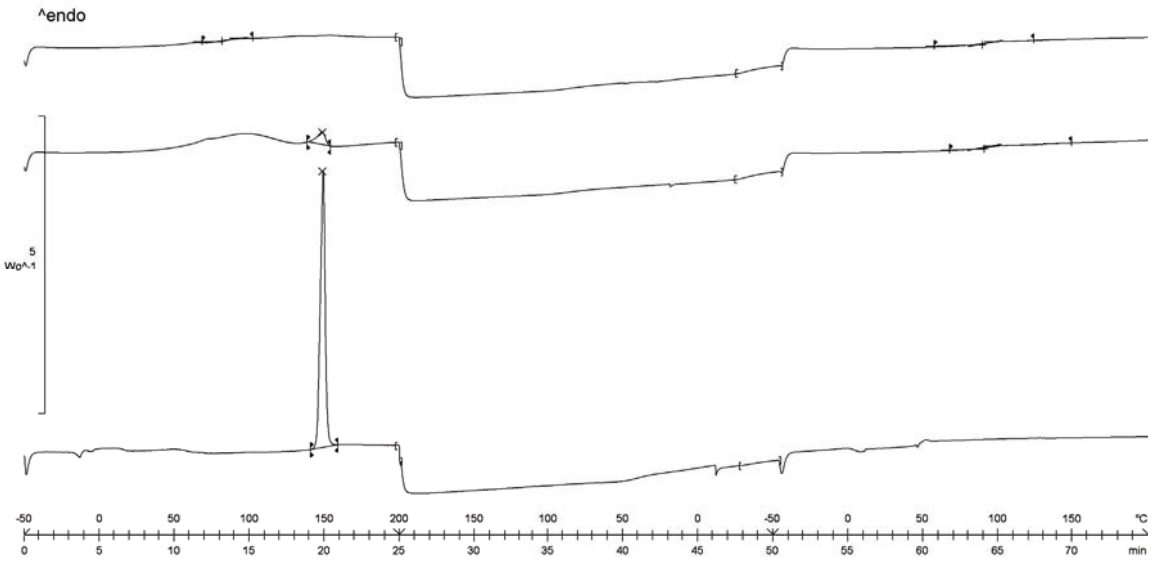


Figure A.29: DSC thermogram of FD-F extrudate with the following data displayed from top to bottom: extrudate, the corresponding physical mixture, pure FD

## A.10 DSC thermograms of fenofibrate extrudates

Table A.5: DSC analysis of FF extrudates directly after manufacture (0 weeks) and after removal from storage in comparison to the physical mixtures (PM)

| Sample | | | $1^{st}$ heating cycle | | | $2^{nd}$ heating cycle | |
|---|---|---|---|---|---|---|---|
| | | | $T_{onset}$ [°C] | $T_{midpt,peak}$ [°C] | | $T_{onset}$ [°C] | $T_{midpt,peak}$ [°C] |
| FF-A | 0 weeks | $T_g$ | 35.0 | 39.1 | $T_g$ | 49.8 | 55.0 |
| | 4 weeks | $T_g$ | 45.6 | 47.4 | $T_g$ | 45.0 | 55.9 |
| | 10 weeks | $T_g$ | 38.1 | 41.1 | $T_g$ | 49.6 | 56.4 |
| | 26 weeks | $T_g$ | 43.9 | 45.1 | $T_g$ | 52.1 | 56.6 |
| | PM | $T_m$ | 79.8 | 82.8 | $T_g$ | 43.6 | 55.0 |
| FF-B | 0 weeks | $T_g$ | 47.4 | 52.6 | - | - | - |
| | 4 weeks | $T_g$ | 46.0 | 51.2 | - | - | - |
| | 10 weeks | $T_g$ | 47.8 | 52.8 | - | - | - |
| | | $T_m$ | 82.3 | 85.7 | | | |
| | 26 weeks | $T_g$ | 55.7 | 57.9 | - | - | - |
| | | $T_m$ | 81.7 | 83.1 | | | |
| | PM | $T_m$ | 80.4 | 83.2 | - | - | - |
| FF-C | 0 weeks | $T_g$ | 29.2 | 37.3 | $T_g$ | 13.3 | 29.5 |
| | 4 weeks | $T_g$ | 29.0 | 34.2 | $T_g$ | 15.5 | 30.0 |
| | 10 weeks | $T_g$ | 22.0 | 42.6 | $T_g$ | 25.8 | 30.3 |
| | | $T_m$ | 75.8 | 80.6 | | | |
| | 26 weeks | $T_g$ | 20.1 | 37.8 | $T_g$ | 17.5 | 38.7 |
| | | $T_m$ | 77.4 | 81.5 | | | |
| | PM | $T_m$ | 80.3 | 84.4 | $T_g$ | 22.6 | 33.5 |
| FF-D | 0 weeks | $T_g$ | 44.5 | 45.8 | $T_g$ | 41.3 | 43.5 |
| | 4 weeks | $T_g$ | 48.4 | 49.3 | $T_g$ | 41.2 | 41.8 |
| | 10 weeks | - | - | - | - | - | - |
| | 26 weeks | $T_g$ | 30.9 | 36.1 | $T_g$ | 48.8 | 53.7 |
| | PM | $T_m$ | 79.9 | 83.6 | $T_g$ | 41.3 | 48.6 |
| FF-E | 0 weeks | $T_g$ | 43.6 | 47.8 | $T_g$ | 54.4 | 59.8 |
| | 4 weeks | $T_g$ | 53.6 | 54.4 | $T_g$ | 55.3 | 60.1 |
| | 10 weeks | - | - | - | - | - | - |
| | 26 weeks | $T_g$ | 38.7 | 42.1 | $T_g$ | 46.5 | 55.9 |
| | PM | $T_m$ | 79.8 | 83.3 | $T_g$ | 45.0 | 54.3 |
| FF-F | 0 weeks | $T_g$ | 39.7 | 39.3 | $T_g$ | 55.6 | 61.0 |
| | 4 weeks | $T_g$ | 49.7 | 50.4 | $T_g$ | 54.9 | 61.5 |
| | 10 weeks | - | - | - | - | - | - |
| | 26 weeks | $T_g$ | 47.8 | 48.0 | $T_g$ | 54.0 | 60.4 |
| | PM | $T_m$ | 80.3 | 84.2 | $T_g$ | 59.0 | 61.4 |
| FF-G | 0 weeks | $T_g$ | 36.5 | 43.8 | $T_g$ | 42.2 | 50.3 |
| | 4 weeks | $T_g$ | 49.2 | 50.3 | $T_g$ | 46.3 | 49.6 |
| | 10 weeks | - | - | - | - | - | - |
| | 26 weeks | $T_g$ | 50.4 | 52.3 | $T_g$ | 45.5 | 49.3 |
| | PM | $T_m$ | 80.2 | 83.7 | $T_g$ | 49.6 | 60.4 |
| FF-H | 0 weeks | $T_g$ | 44.6 | 47.7 | $T_g$ | 63.7 | 65.5 |
| | 4 weeks | $T_g$ | 44.8 | 45.5 | $T_g$ | 63.3 | 66.8 |
| | 10 weeks | - | - | - | - | - | - |
| | 26 weeks | $T_g$ | 43.7 | 45.3 | $T_g$ | 62.6 | 67.1 |
| | PM | $T_g$ | 174.3 | 175.9 | - | - | - |
| FF-J | 0 weeks | $T_g$ | -13.4 | -5.7 | $T_g$ | -14.3 | -6.1 |
| | PM | $T_m$ | 80.2 | 83.8 | $T_g$ | -13.3 | -6.0 |
| FF-K | 0 weeks | $T_g$ | 65.4 | 66.6 | $T_g$ | 62.1 | 74.7 |
| | | $T_m$ | 78.9 | 84.8 | | | |
| | PM | $T_m$ | 81.5 | 85.6 | $T_g$ | -18.9 | -17.1 |
| | | | | | $T_g$ | 61.8 | 70.4 |

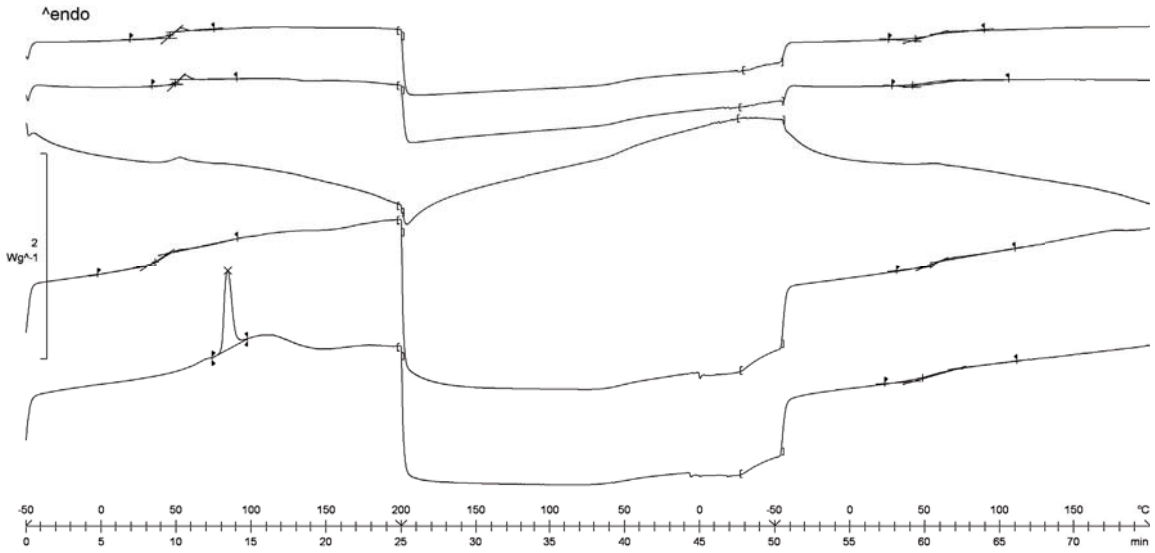


Figure A.30: DSC thermogram of FF-D extrudate with the following data displayed from top to bottom: Pellets after 0 weeks, 4 weeks, 10 weeks, 26 weeks of storage at 25 °C /60 % rH, physical mixture

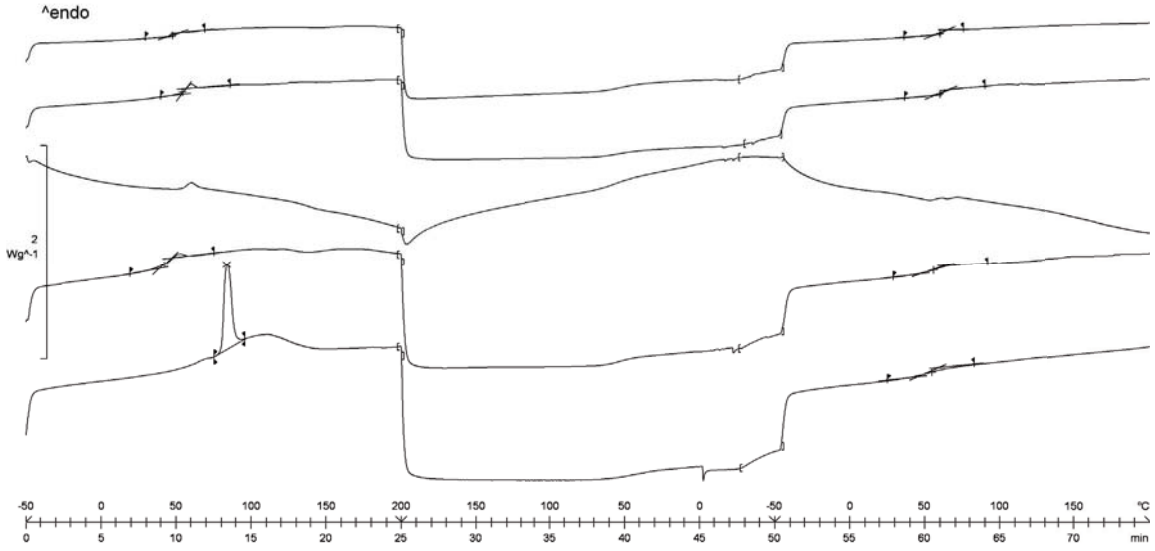


Figure A.31: DSC thermogram of FF-E extrudate with the following data displayed from top to bottom: Pellets after 0 weeks, 4 weeks, 10 weeks, 26 weeks of storage at 25 °C /60 % rH, physical mixture

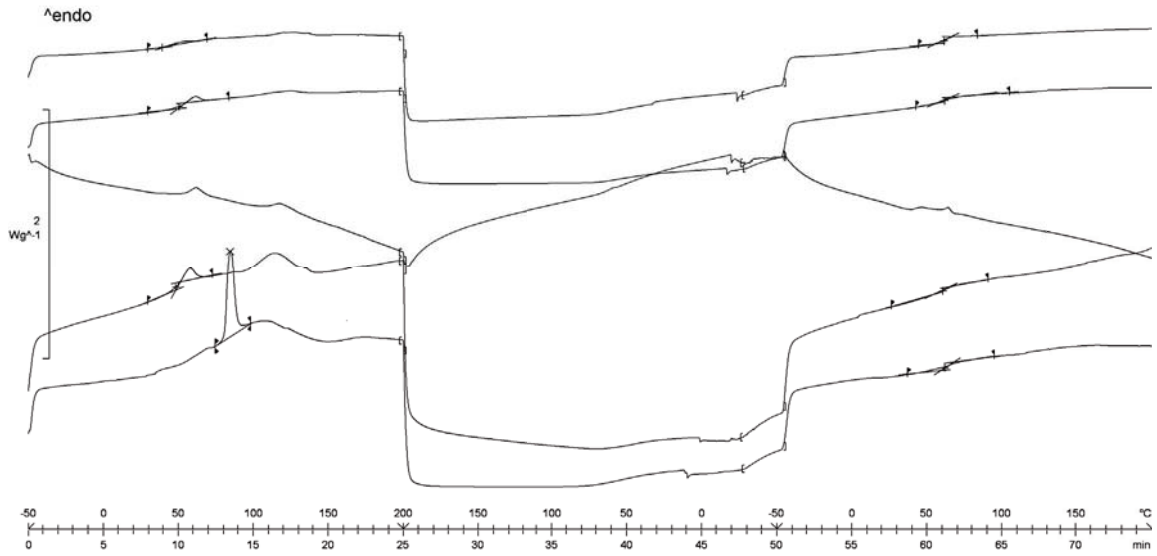


Figure A.32: DSC thermogram of FF-F extrudate with the following data displayed from top to bottom: Pellets after 0 weeks, 4 weeks, 10 weeks, 26 weeks of storage at 25 °C /60 % rH, physical mixture

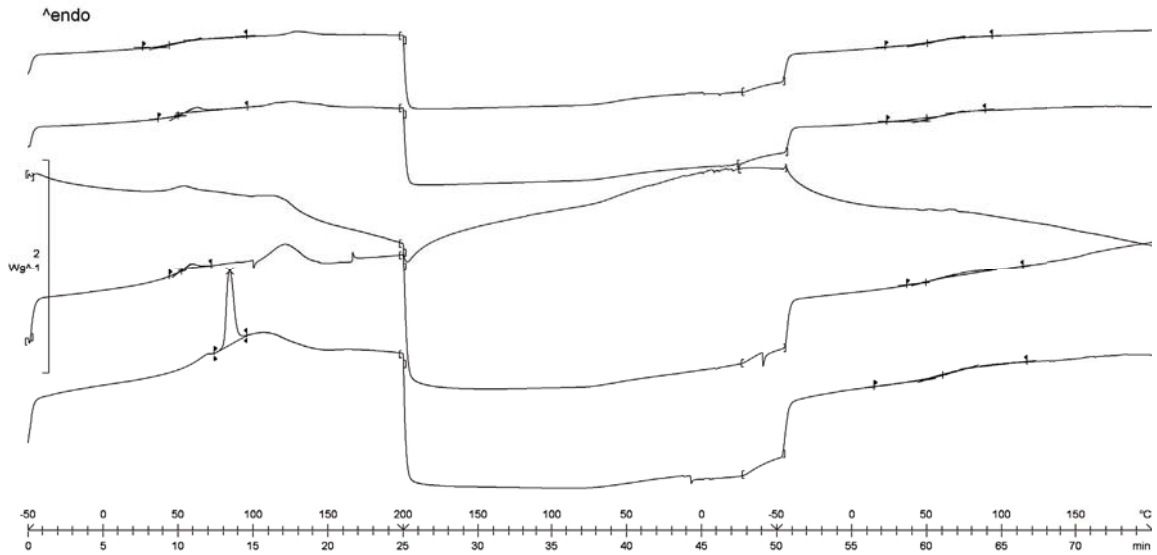


Figure A.33: DSC thermogram of FF-G extrudate with the following data displayed from top to bottom: Pellets after 0 weeks, 4 weeks, 10 weeks, 26 weeks of storage at 25 °C /60 % rH, physical mixture

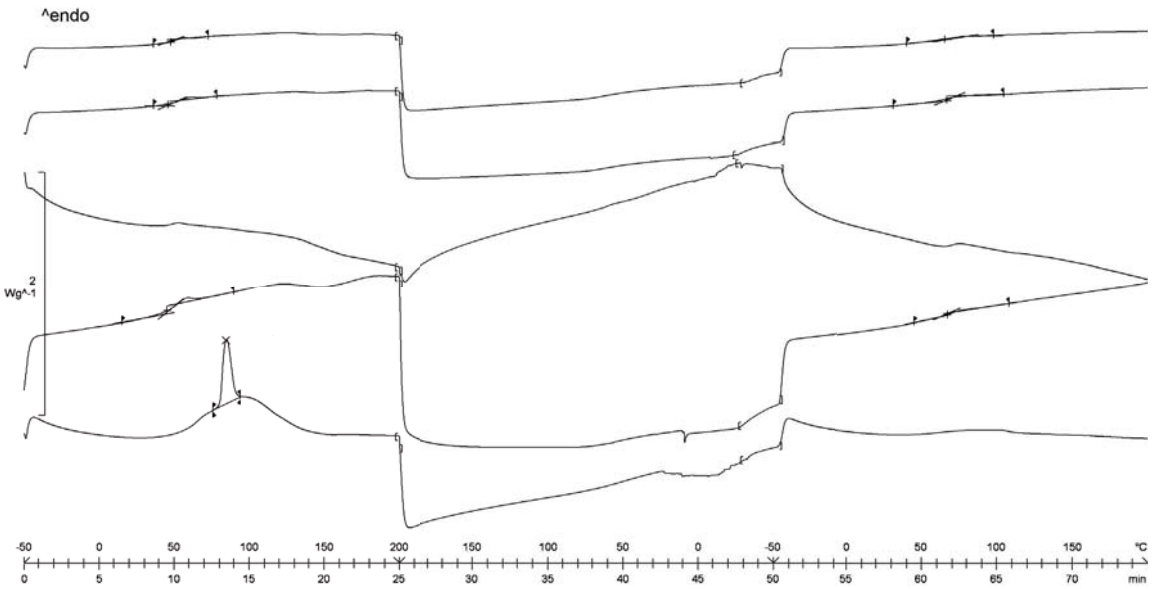


Figure A.34: DSC thermogram of FF-H extrudate with the following data displayed from top to bottom: Pellets after 0 weeks, 4 weeks, 10 weeks, 26 weeks of storage at 25 °C /60 % rH, physical mixture

## A.11 DSC thermograms of oxeglitazar extrudates

Table A.6: DSC analysis of OX extrudates directly after manufacture (0 weeks) and after removal from storage in comparison to the physical mixtures (PM)

| Sample | | | $1^{st}$ heating cycle | | | $2^{nd}$ heating cycle | |
|---|---|---|---|---|---|---|---|
| | | | $T_{onset}$ [°C] | $T_{midpt,peak}$ [°C] | | $T_{onset}$ [°C] | $T_{midpt,peak}$ [°C] |
| OX-A | 0 weeks | $T_g$ | 80.5 | 86.6 | $T_g$ | 78.3 | 82.7 |
| | 4 weeks | $T_g$ | 80.3 | 89.2 | $T_g$ | 76.6 | 81.4 |
| | 10 weeks | $T_g$ | 63.8 | 67.9 | $T_g$ | 76.7 | 84.9 |
| | PM | $T_m$ | 153.0 | 158.9 | $T_g$ | 78.9 | 80.8 |
| OX-B | 0 weeks | $T_g$ | 51.5 | 55.6 | $T_g$ | 56.1 | 71.5 |
| | 4 weeks | $T_g$ | 55.3 | 54.7 | $T_g$ | 53.0 | 71.3 |
| | PM | $T_m$ | 148.6 | 156.2 | - | - | - |
| OX-C | 0 weeks | $T_g$ | 37.7 | 39.6 | $T_g$ | 57.2 | 63.1 |
| | PM | - | - | - | $T_g$ | 53.0 | 63.8 |
| OX-D | 0 weeks | $T_g$ | 77.4 | 84.4 | $T_g$ | 79.5 | 81.8 |
| | 4 weeks | $T_g$ | 57.1 | 74.2 | $T_g$ | 77.7 | 83.8 |
| | PM | - | - | - | $T_g$ | 82.2 | 87.3 |
| OX-E | 0 weeks | $T_g$ | 46.2 | 52.5 | $T_g$ | 76.3 | 82.3 |
| | | $T_g$ | 67.8 | 74.9 | | | |
| | PM | $T_m$ | 151.8 | 157.1 | $T_g$ | 82.4 | 83.8 |
| OX-F | 0 weeks | - | - | - | $T_g$ | 79.7 | 84.2 |
| | PM | - | - | - | $T_g$ | 82.3 | 88.8 |
| OX-G | 0 weeks | $T_g$ | 78.8 | 85.0 | $T_g$ | 83.6 | 87.9 |
| OX-H | 0 weeks | - | - | - | $T_g$ | 74.7 | 80.0 |
| OX-J | 0 weeks | $T_g$ | 72.0 | 76.0 | $T_g$ | 72.1 | 78.3 |
| OX-K | 0 weeks | - | - | - | $T_g$ | 64.4 | 78.7 |

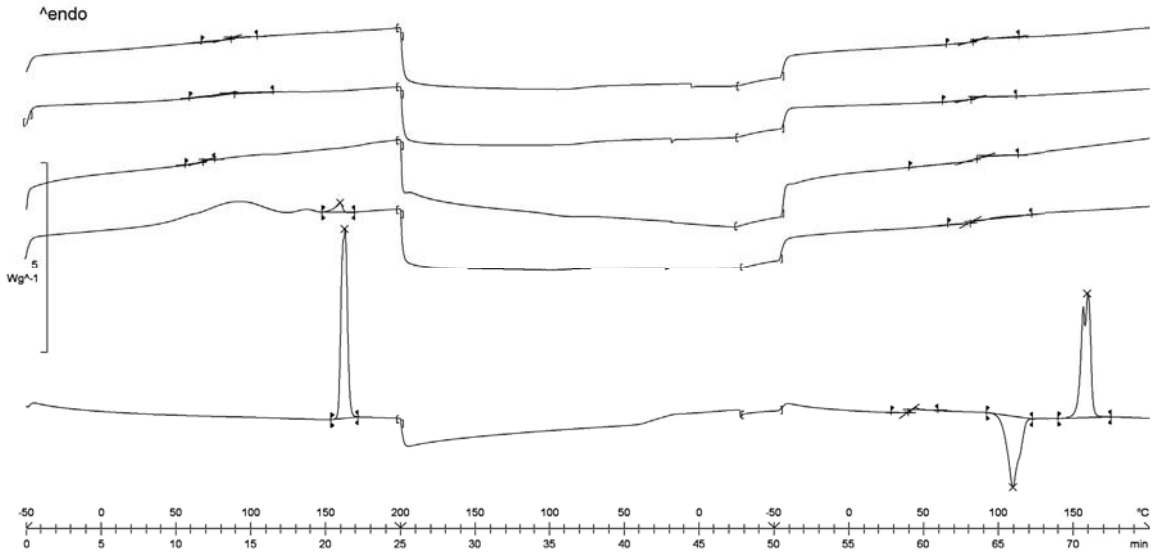


Figure A.35: DSC thermogram of OX-A extrudate with the following data displayed from top to bottom: Pellets after 0 weeks, 4 weeks, 10 weeks of storage at 25 °C / 60 % rH, physical mixture, pure OX

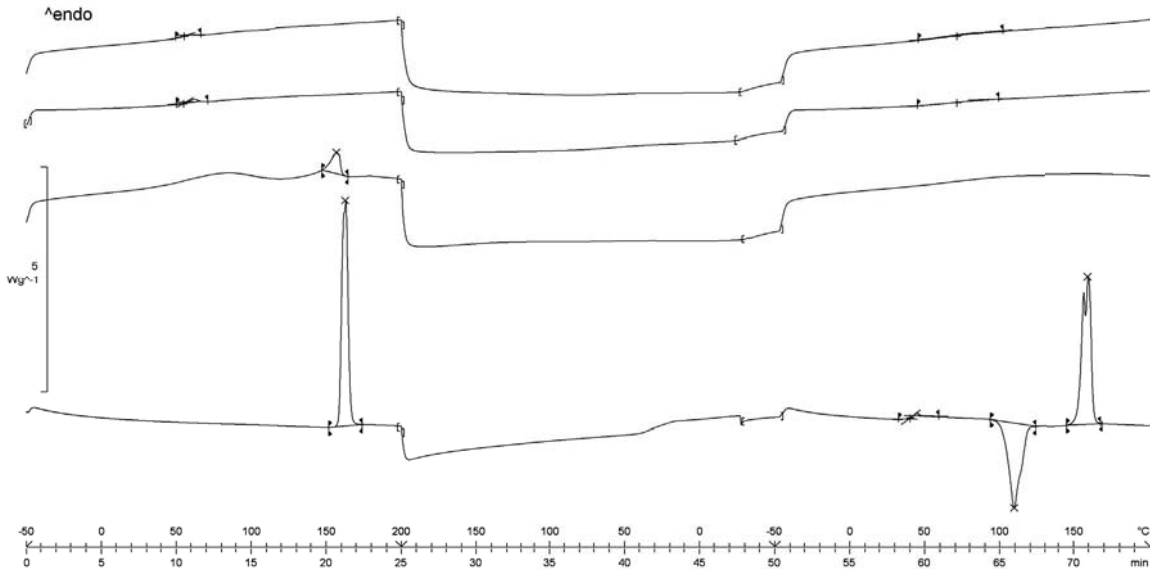


Figure A.36: DSC thermogram of OX-B extrudate with the following data displayed from top to bottom: Pellets after 0 weeks, 4 weeks of storage at 25 °C /60 % rH, physical mixture, pure OX

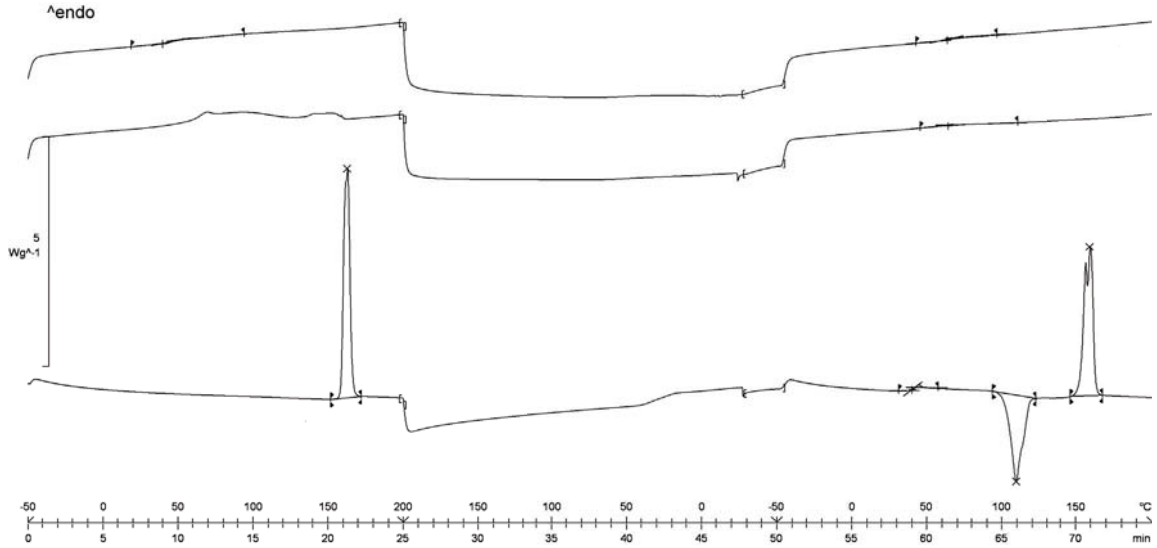


Figure A.37: DSC thermogram of OX-C extrudate with the following data displayed from top to bottom: Pellets directly after manufacture, physical mixture, pure OX

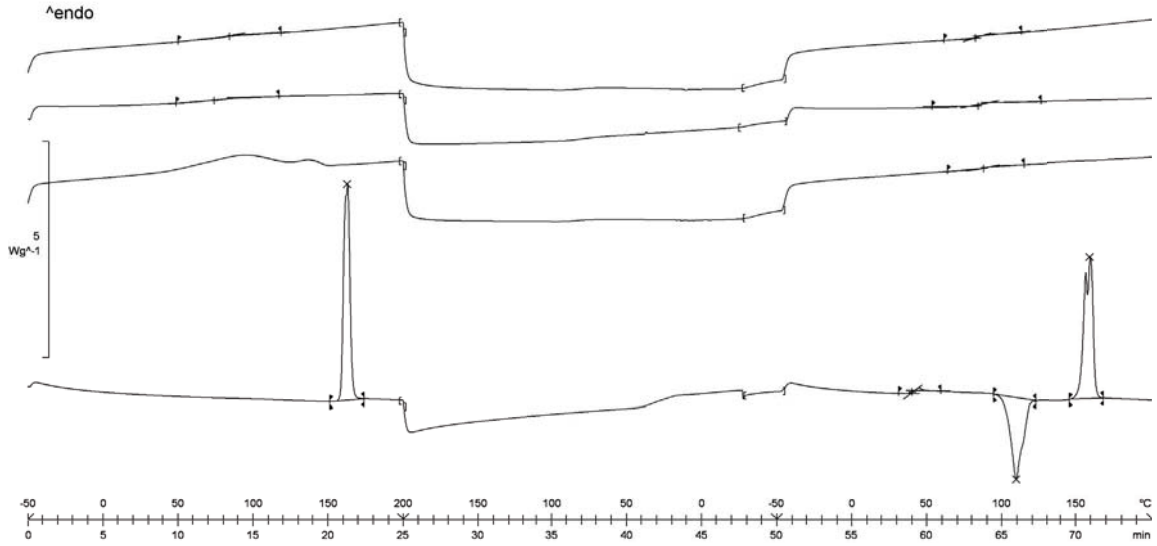


Figure A.38: DSC thermogram of OX-D extrudate with the following data displayed from top to bottom: Pellets after 0 weeks, 4 weeks of storage at 25 °C/60 % rH, physical mixture, pure OX

## A.12 Surface morphology of oxeglitazar extrudates

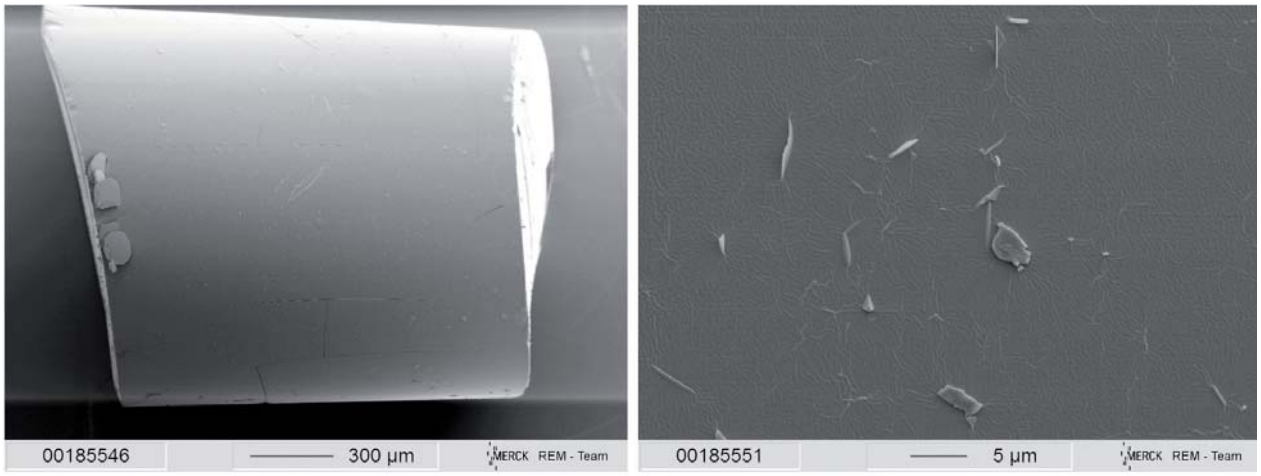


(a) (b)

Figure A.39: SEM images of OX-A pellets before exposure to the dissolution medium

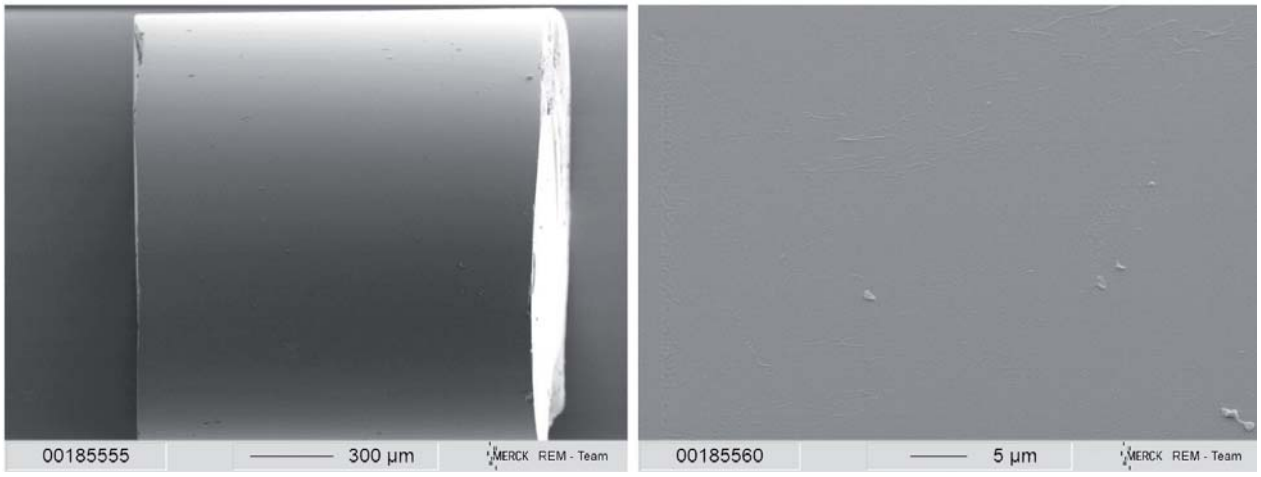


(a) (b)

Figure A.40: SEM images of OX-C pellets before exposure to the dissolution medium

# B Dissolution profiles of physical mixtures

## B.1 Felodipine

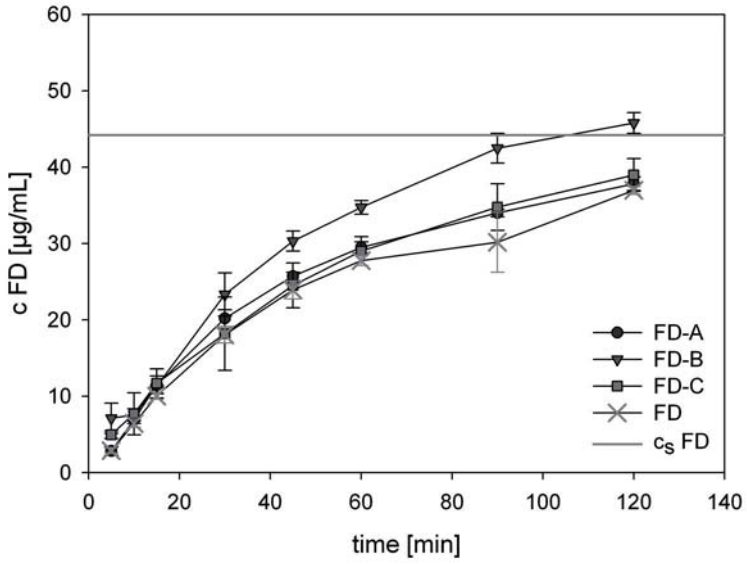


(a)

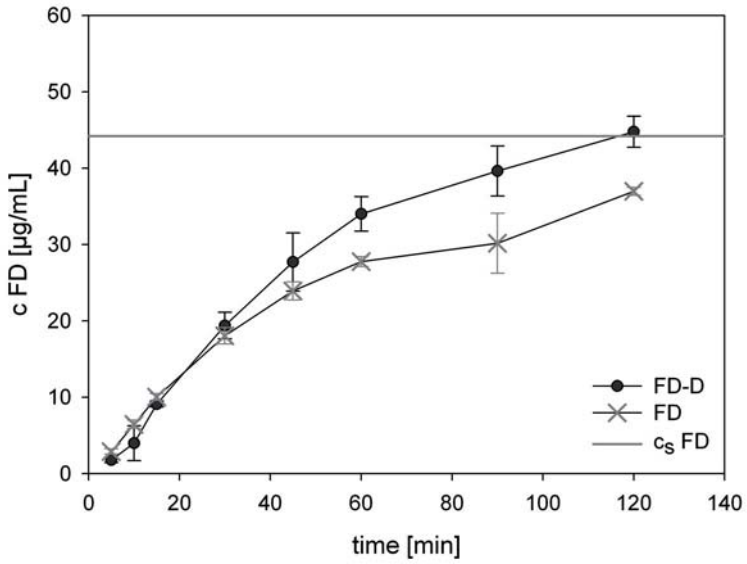


(b)

Figure B.41: Dissolution profiles of physical mixtures of felodipine and carrier(s)

## B.2 Fenofibrate

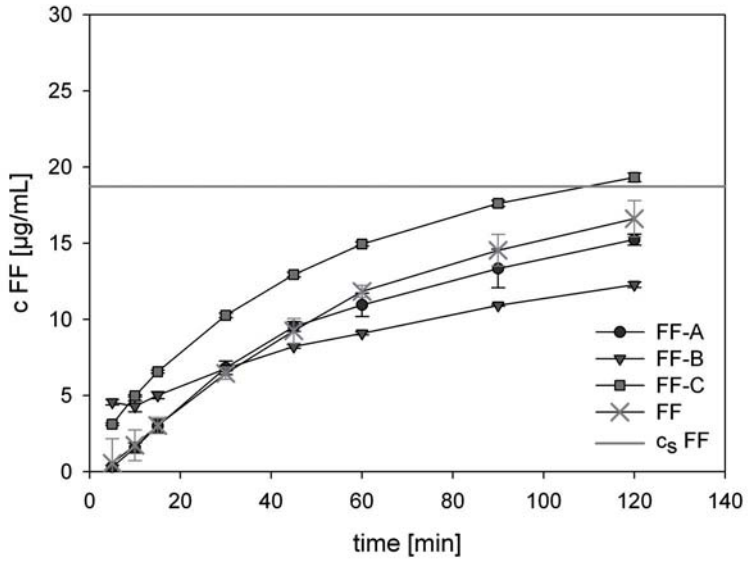


(a)

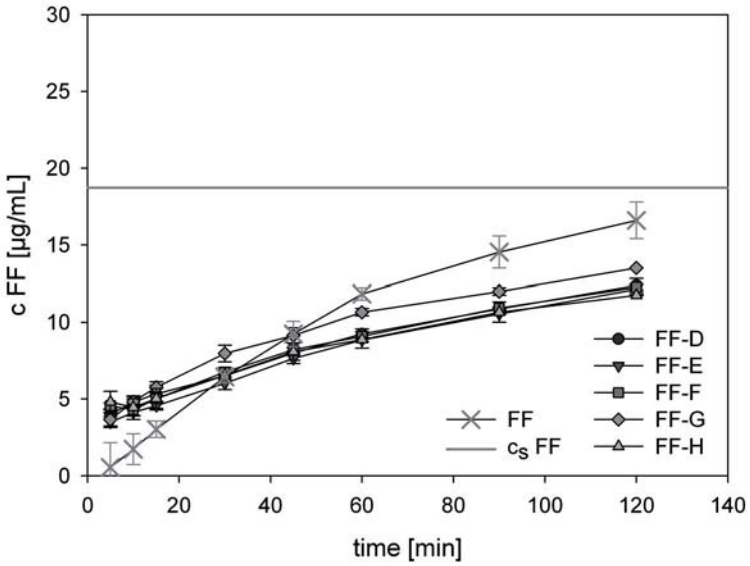


(b)

Figure B.42: Dissolution profiles of physical mixtures of fenofibrate and carrier(s)

## B.3 Oxeglitazar

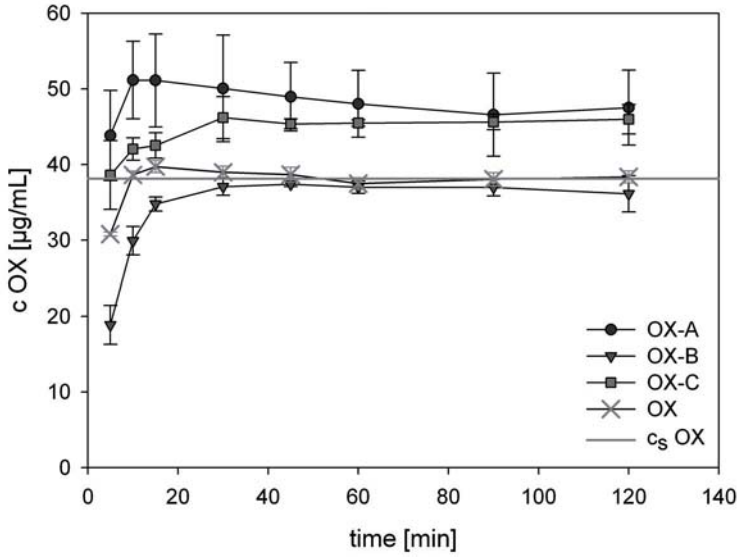


(a)

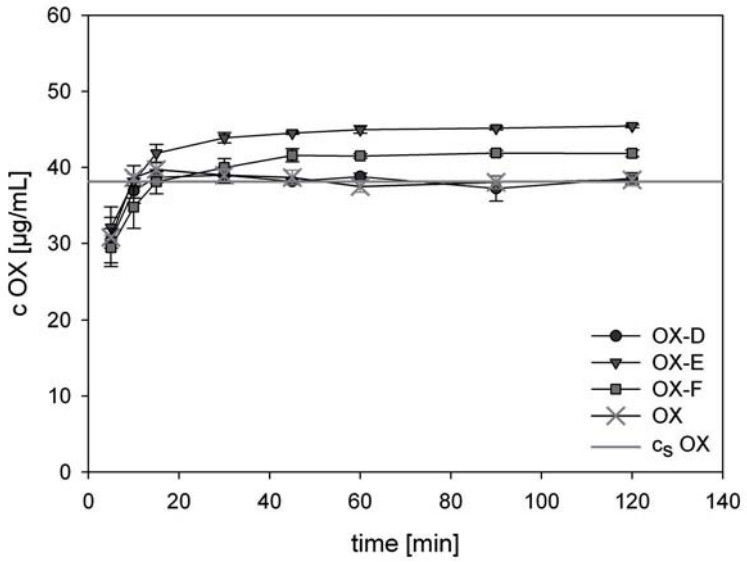


(b)

Figure B.43: Dissolution profiles of physical mixtures of oxeglitazar and carrier(s)

# C Limits of detection

In this work, the samples were referred to as "amorphous" if no crystallinity was found with both XRD and DSC analysis. It goes without saying that the presence of minimal amounts of crystalline substances may remain undetected if below the LOD of the analytical method.

## C.1 X-ray diffraction

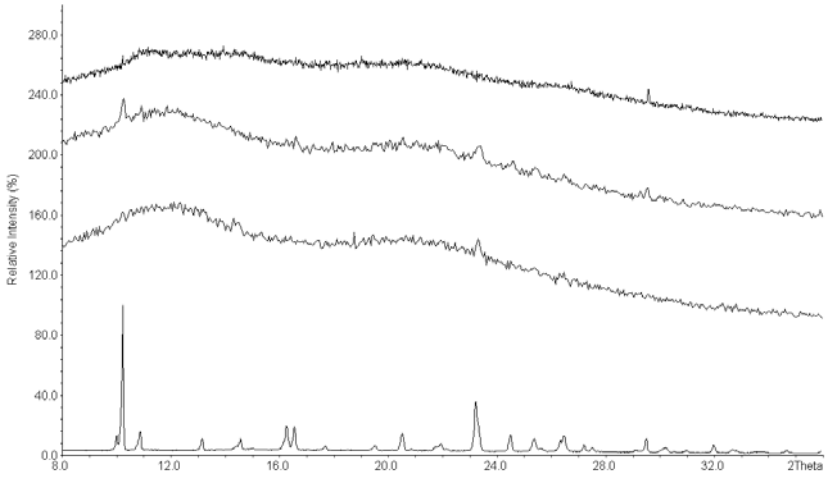


Figure C.44: XRD LOD determination for physical mixtures of FD and COP with the following data displayed from top to bottom: drug content 1 %, 2 %, 5 % (w/w), pure API

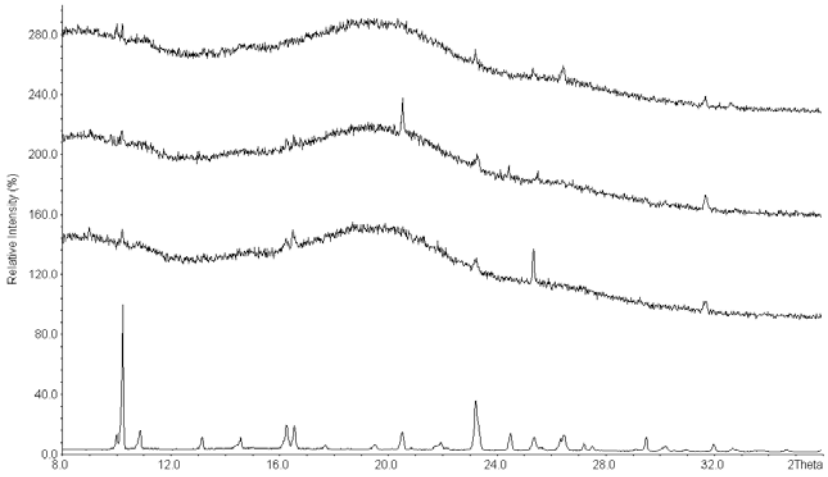


Figure C.45: XRD LOD determination for physical mixtures of FD and HPMC with the following data displayed from top to bottom: drug content 1 %, 2 %, 5 % (w/w), pure API

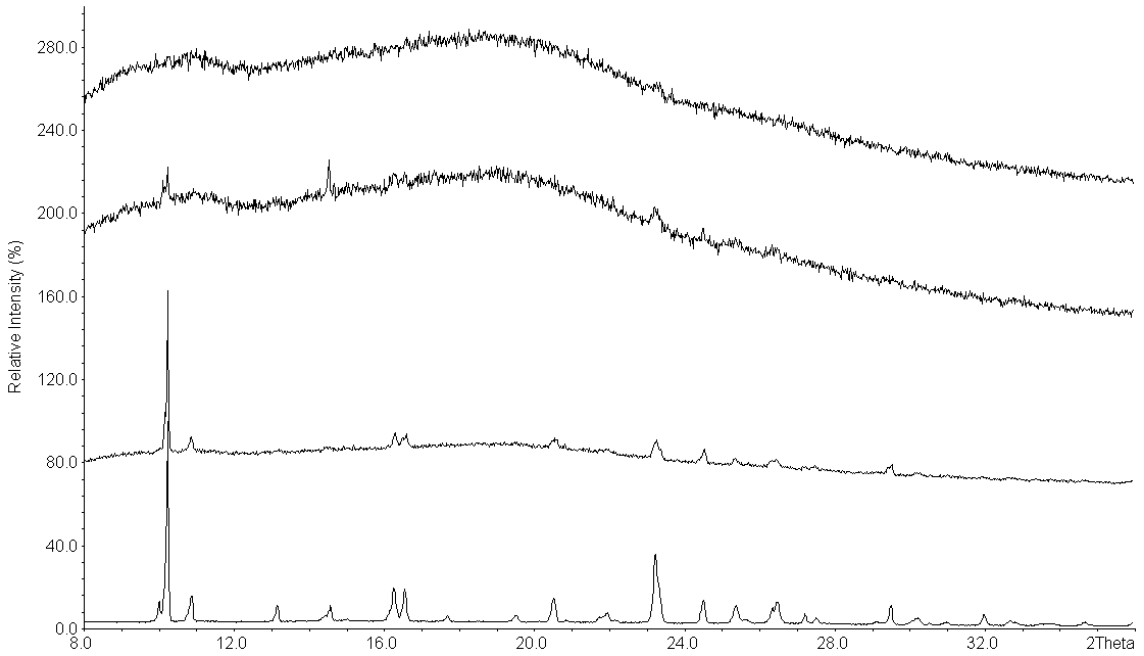


Figure C.46: XRD LOD determination for physical mixtures of FD and PVCL-PVAc-PEG with the following data displayed from top to bottom: drug content 1 %, 2 %, 5 % (w/w), pure API

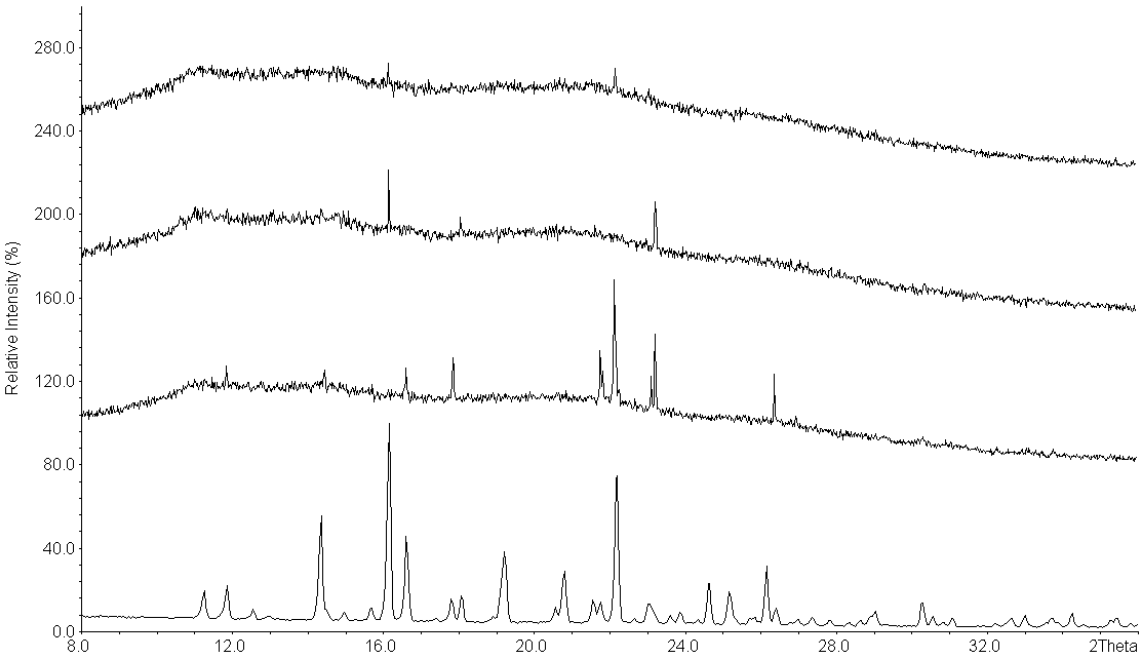


Figure C.47: XRD LOD determination for physical mixtures of FF and COP with the following data displayed from top to bottom: drug content 1 %, 2 %, 5 % (w/w), pure API

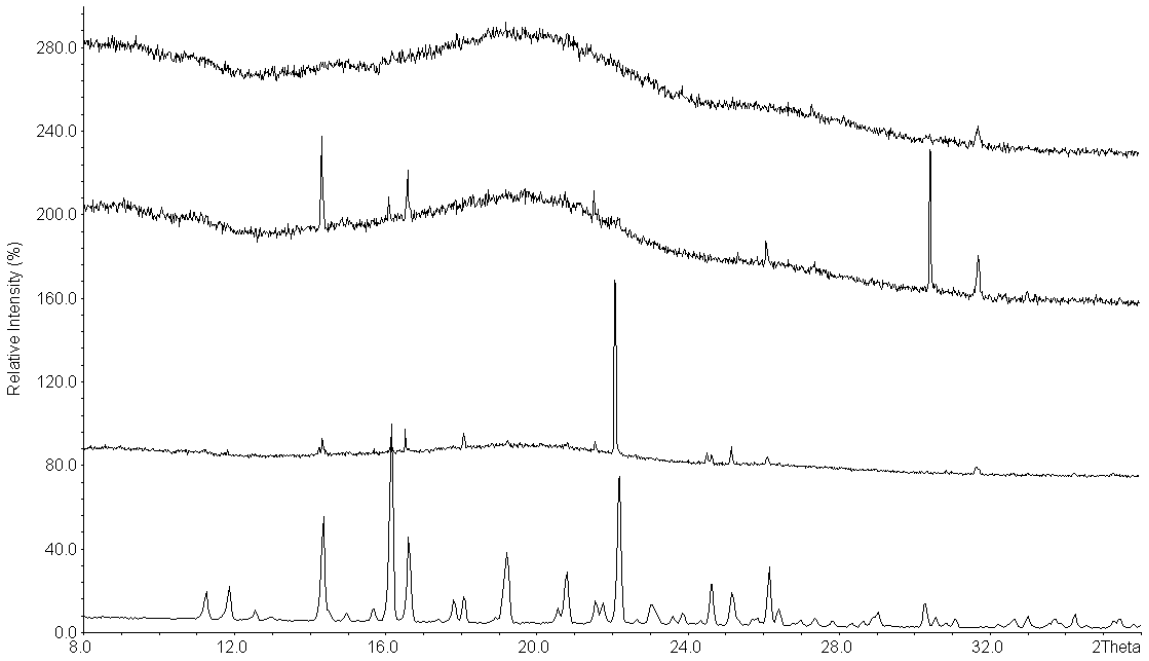


Figure C.48: XRD LOD determination for physical mixtures of FF and HPMC with the following data displayed from top to bottom: drug content 1 %, 2 %, 5 % (w/w), pure API

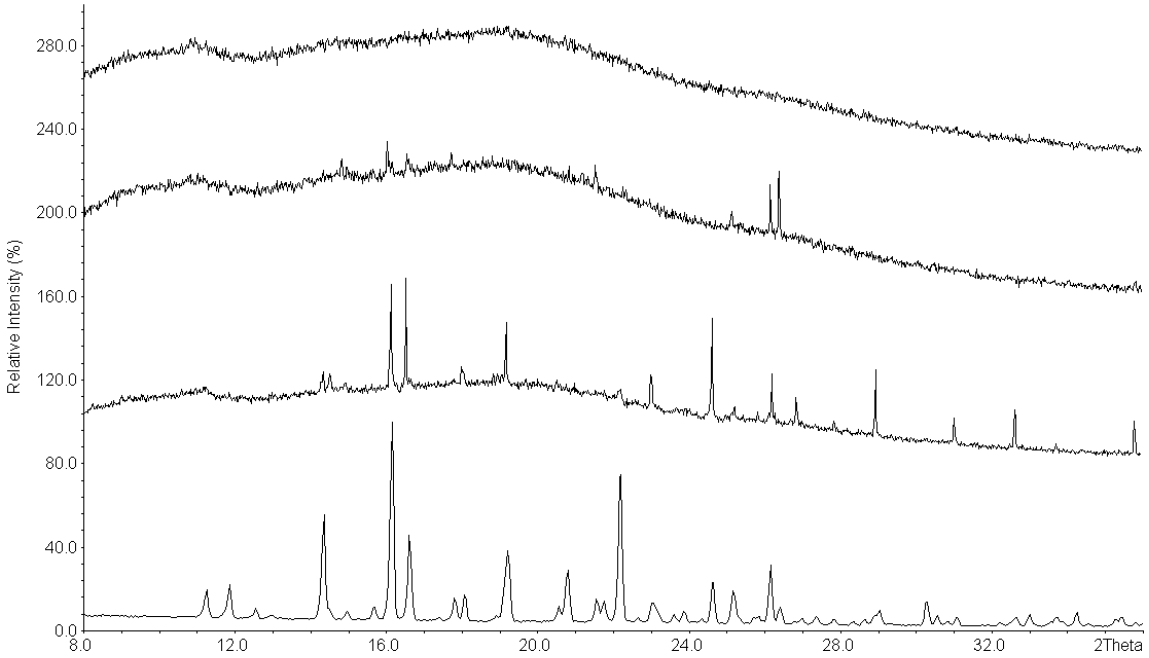


Figure C.49: XRD LOD determination for physical mixtures of FF and PVCL-PVAc-PEG with the following data displayed from top to bottom: drug content 1 %, 2 %, 5 % (w/w), pure API

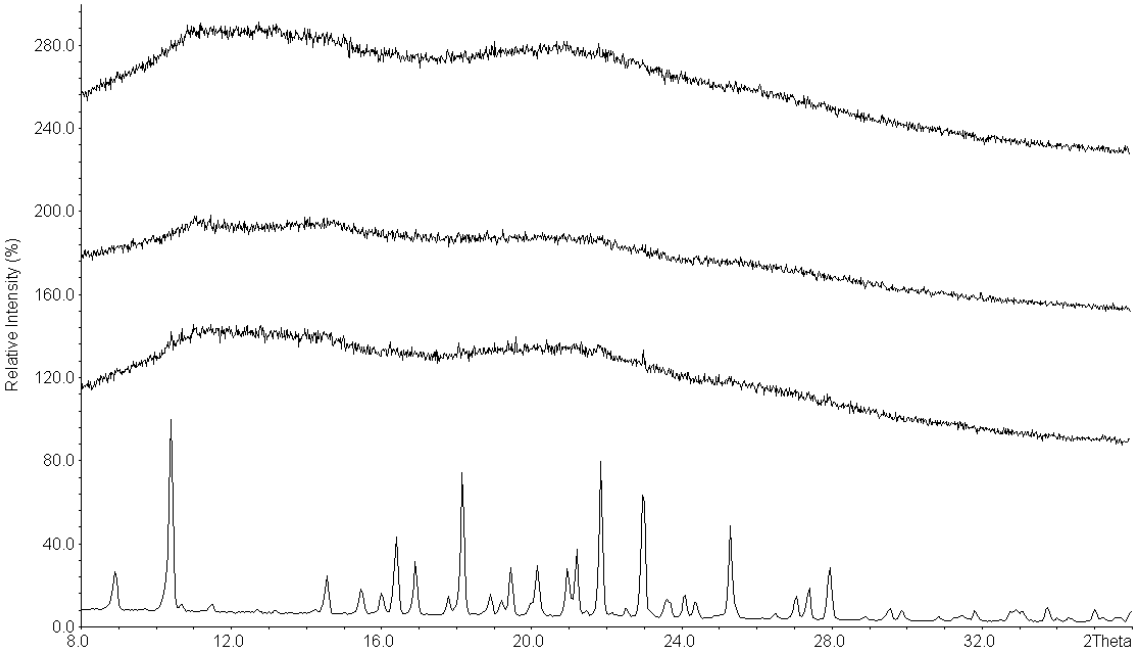


Figure C.50: XRD LOD determination for physical mixtures of OX and COP with the following data displayed from top to bottom: drug content 1 %, 2 %, 5 % (w/w), pure API

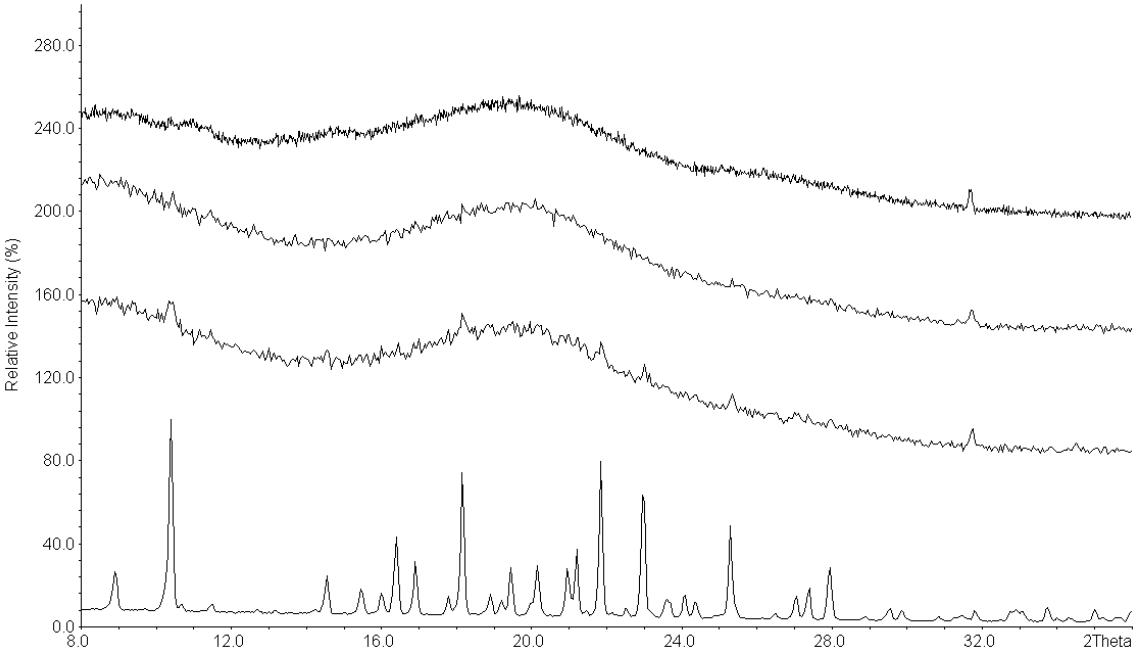


Figure C.51: XRD LOD determination for physical mixtures of OX and HPMC with the following data displayed from top to bottom: drug content 1 %, 2 %, 5 % (w/w), pure API

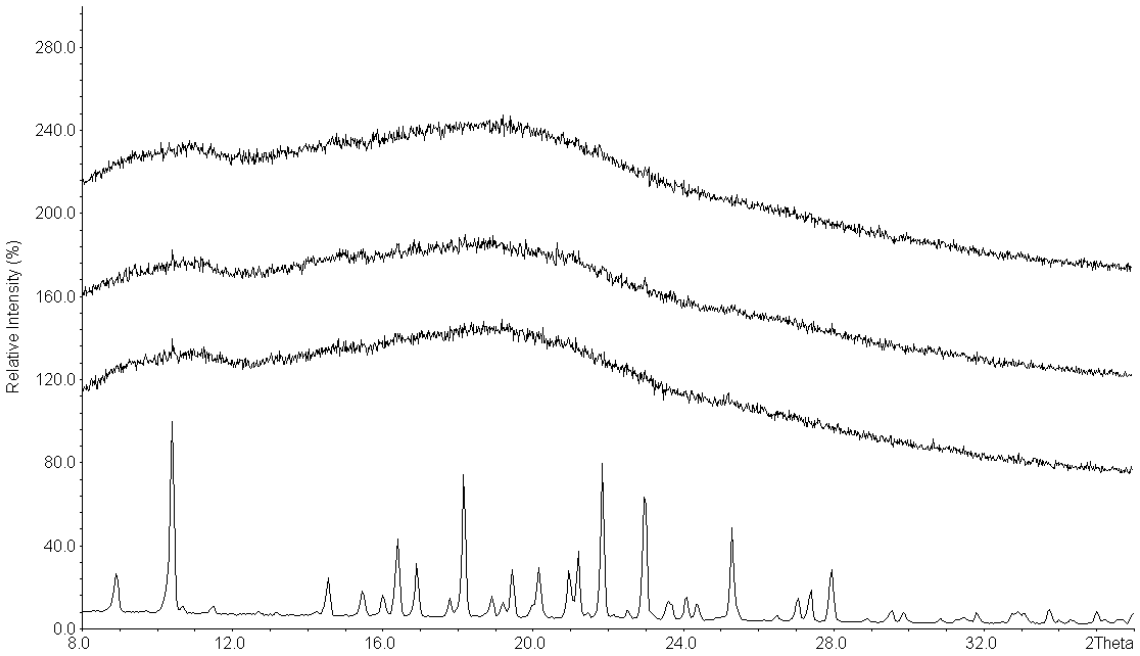


Figure C.52: XRD LOD determination for physical mixtures of OX and PVCL-PVAc-PEG with the following data displayed from top to bottom: drug content 1 %, 2 %, 5 % (w/w), pure API

## C.2 Differential scanning calorimetry

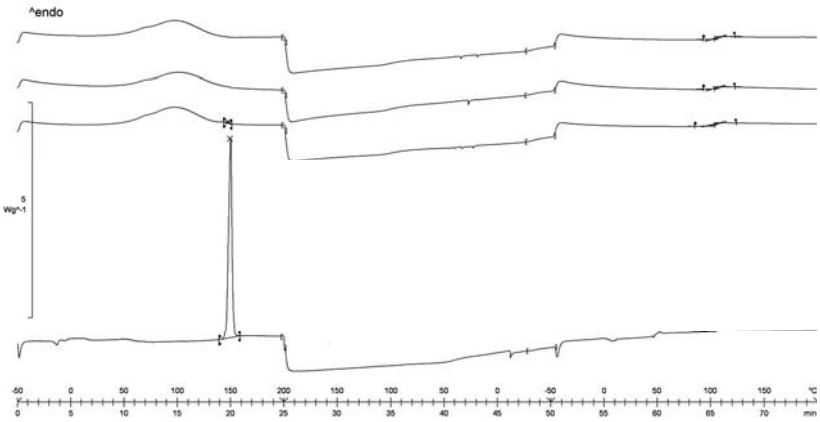


(a) Physical mixtures of FD and COP

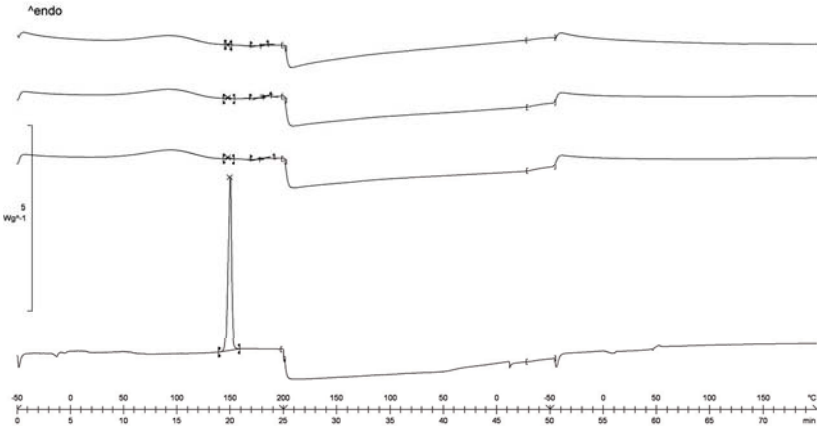


(b) Physical mixtures of FD and HPMC

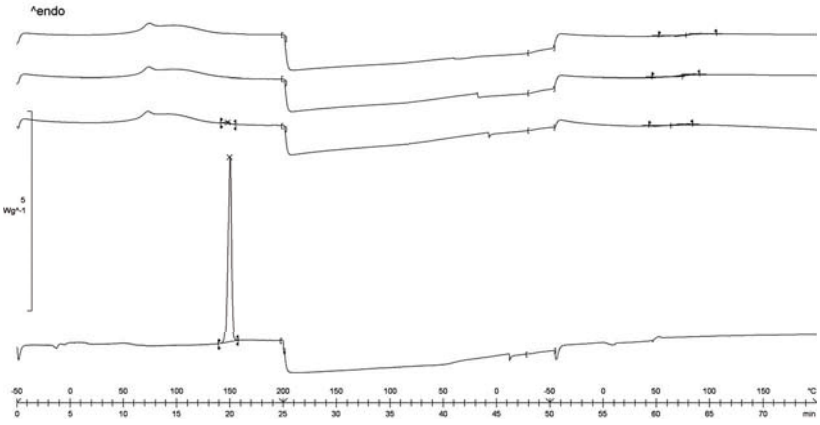


(c) Physical mixtures of FD and PVCL-PVAc-PEG

Figure C.53: DSC LOD determination for FD with the following data displayed from top to bottom: drug content 1 %, 2 %, 5 % (w/w), pure API

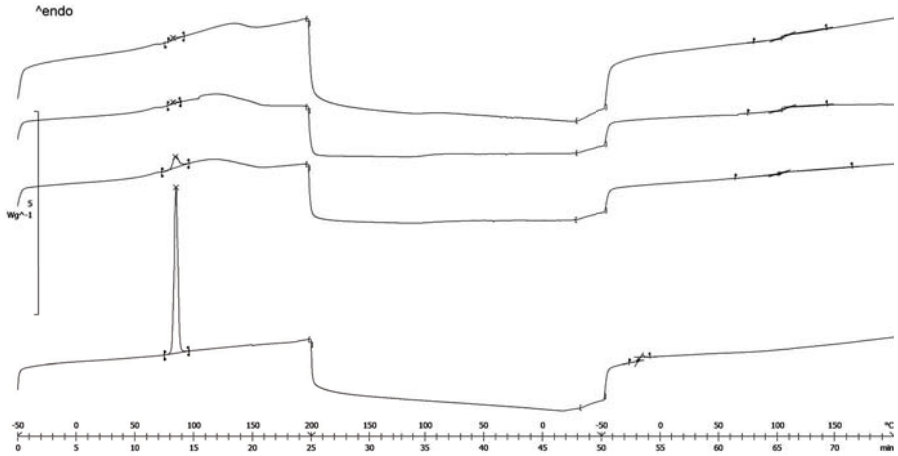


(a) Physical mixtures of FF and COP

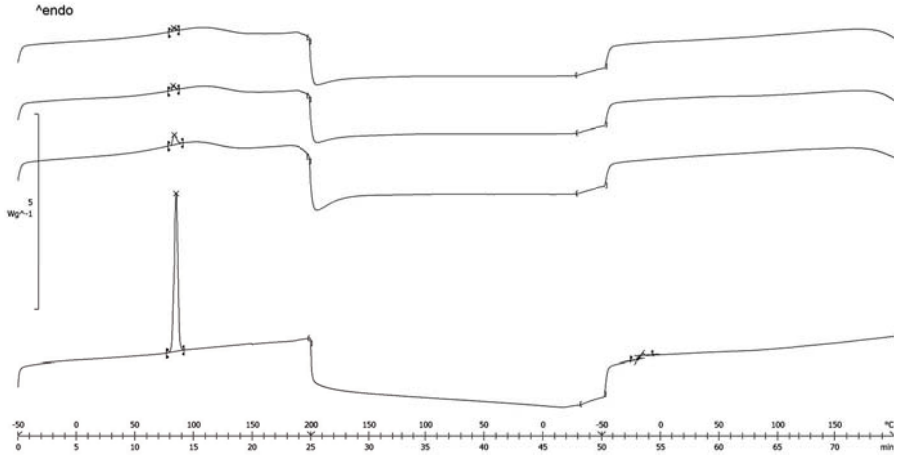


(b) Physical mixtures of FF and HPMC

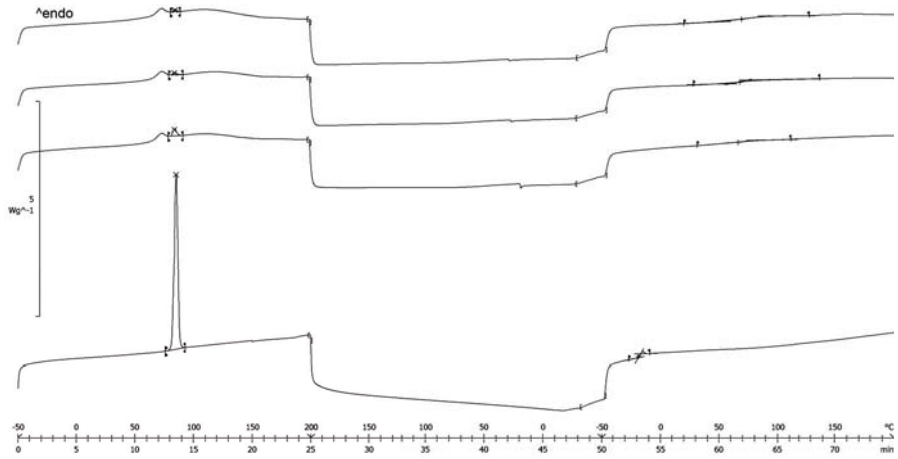


(c) Physical mixtures of FF and PVCL-PVAc-PEG

Figure C.54: DSC LOD determination for FF with the following data displayed from top to bottom: drug content 1 %, 2 %, 5 % (w/w), pure API

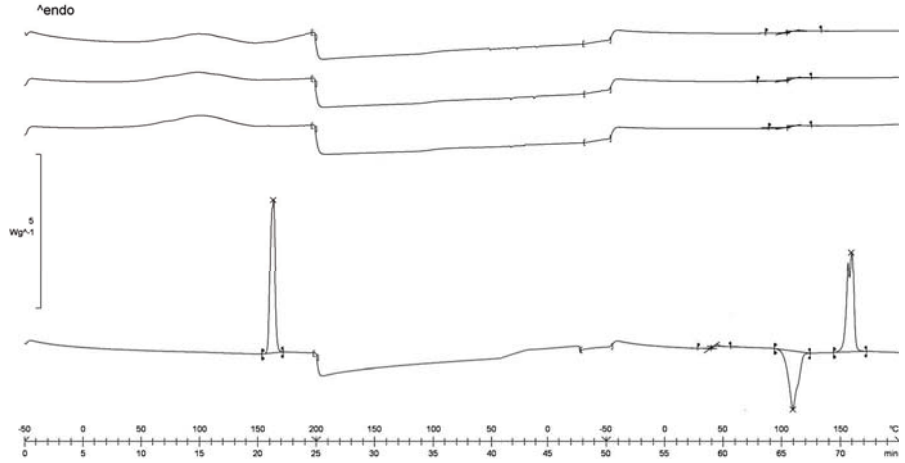


(a) Physical mixtures of OX and COP

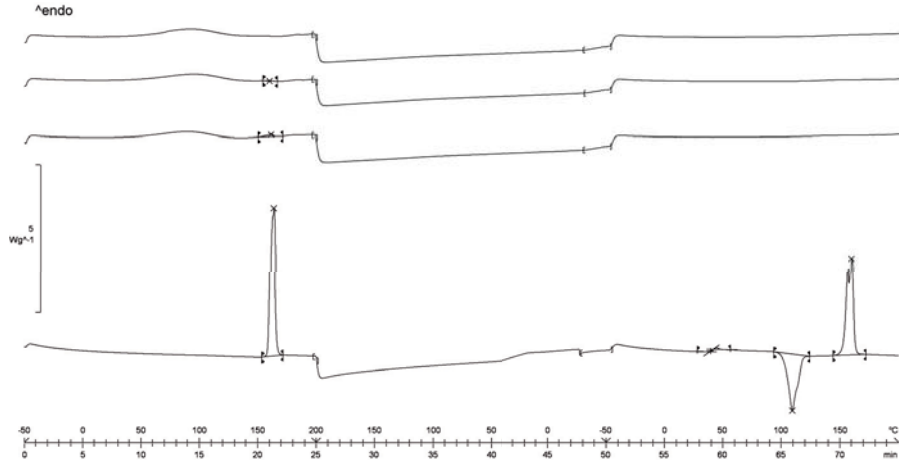


(b) Physical mixtures of OX and HPMC

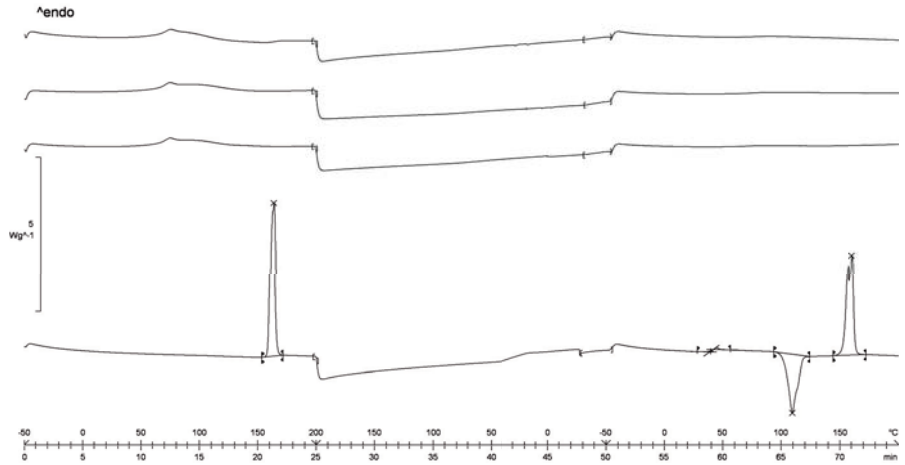


(c) Physical mixtures of OX and PVCL-PVAc-PEG

Figure C.55: DSC LOD determination for OX with the following data displayed from top to bottom: drug content 1 %, 2 %, 5 % (w/w), pure API

# D Characterization of applied drugs

## D.1 Solubility

Table D.7: Solubility of the applied drugs in the dissolution media at 37 °C

| API | Solvent | Solubility [µg/mL] |
|---|---|---|
| FD | Hydrochloric acid medium pH 1.2 + 0.1 % polysorbate 80 | 44.2 |
| FF | Hydrochloric acid medium pH 1.2 + 0.1 % polysorbate 80 | 18.7 |
| OX | Phosphate buffer solution pH 6.4 + 0.1 % polysorbate 80 | 38.1 |

## D.2 Surface morphology of oxeglitazar

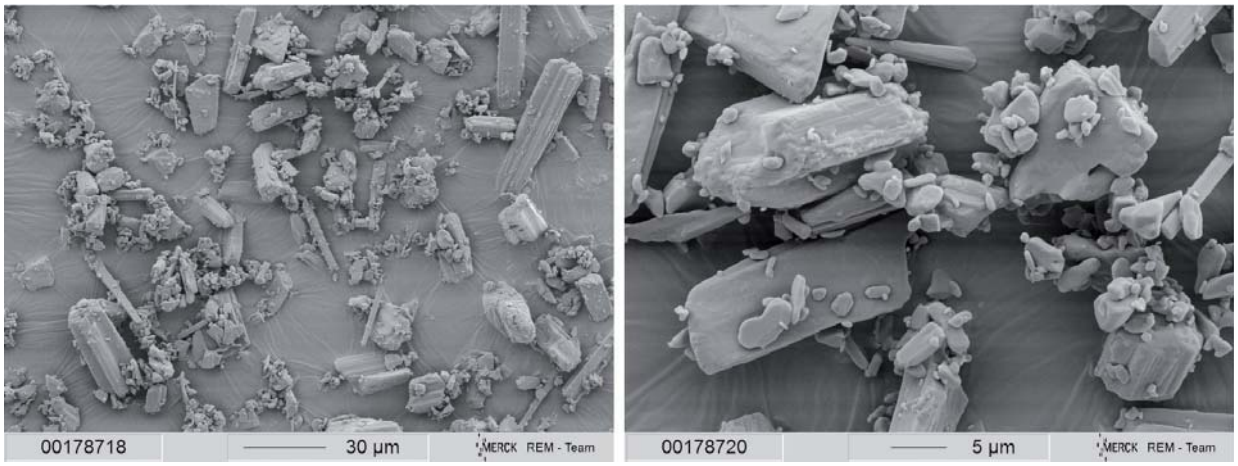


(a) (b)

Figure D.56: SEM image of untreated OX powder

# Bibliography


Albers J. Hot-melt extrusion with poorly soluble drugs. Ph.D. thesis, Goettingen: Cuvillier, 1 edn. (2008).

Albers J, Alles R, Matthée K, Knop K, Schulze-Nahrup J, Kleinebudde P. Mechanism of drug release from polymethacrylate-based extrudates and milled strands prepared by hot-melt extrusion. *European Journal of Pharmaceutics and Biopharmaceutics* 71 (2009) 387–394.

Alonzo DE, Gao Y, Zhou D, Mo H, Zhang GGZ, Taylor LS. Dissolution and precipitation behavior of amorphous solid dispersions. *Journal of Pharmaceutical Sciences* 100 (2011) 3316–3331.

Aly AM, Semreen M, Qato MK. Superdisintegrants for solid dispersion to produce rapidly disintegrating tenoxicam tablets via camphor sublimation. *Pharmaceutical Technology* 29 (2005) 68–78.

Amidon GL, Lennernäs H, Shah VP, Crison JR. A theoretical basis for a biopharmaceutic drug classification: The correlation of in vitro drug product dissolution and in vivo bioavailability. *Pharmaceutical Research* 12 (1995) 413–420.

Badens E, Majerik V, Horváth G, Szokonya L, Bosc N, Teillaud E, Charbit G. Comparison of solid dispersions produced by supercritical antisolvent and spray-freezing technologies. *International Journal of Pharmaceutics* 377 (2009) 25–34.

Blaschek W, Ebel S, Hackenthal E, Holzgrabe U, Keller K, Reichling J (Eds.). HagerROM Hagers Handbuch der Drogen und Arzneistoffe. London: Springer (2002).

Breitenbach J. Melt extrusion: From process to drug delivery technology. *European Journal of Pharmaceutics and Biopharmaceutics* 54 (2002) 107–117.

Brunner E. Reaktionsgeschwindigkeit in heterogenen Systemen. *Zeitschrift für Physikalische Chemie* 43 (1904) 56–102.

Cadogan DF, Howick CJ. Plasticizers. In: G Bellussi, M Bohnet, J Bus, K Drauz, H Faulhammer, H Greim, KP Jäckel, U Karst, W Klaffke, A Kleemann, T Laird, W Meier, J Mukherjee, E Ottow, M Röper, K Sundmacher, R Ulber, B van Dyk, J von Heimburg, K Wagemann, U Wietelmann (Eds.), Ullmann's Encyclopedia of Industrial Chemistry, Wiley-VCH Verlag (2000) 599–618.

Caraballo I, Millán M, Fini A, Rodriguez L, Cavallari C. Percolation thresholds in ultrasound compacted tablets. *Journal of Controlled Release* 69 (2000) 345–355.

Characteristization of Povacoat (2010). http://www.daido-chem.co.jp/english/techinfo/pdf/pova-e.pdf (available online: 2012-02-22).

Chiou WL, Riegelman S. Preparation and dissolution characteristics of several fast-release solid dispersions of griseofulvin. *Journal of Pharmaceutical Sciences* 58 (1969) 1505–1510.

Chiou WL, Riegelman S. Pharmaceutical applications of solid dispersion systems. *Journal of Pharmaceutical Sciences* 60 (1971) 1281–1302.

Chowdary K, Rao S. Investigation of dissolution enhancement of itraconazole by solid dispersion in superdisintegrants. *Drug Development and Industrial Pharmacy* 26 (2000) 1207–11.

Coppens K, Hall M, He V, Larsen P, Koblinski B, Read M, Shrestha U. Excipient blends in hot melt extrusion. Conference poster, Annual Meeting and Exposition of the American Association of Pharmaceutical Scientists, San Antonio, TX, USA. (2006).

Corrigan OI. Mechanisms of dissolution of fast release solid dispersions. *Drug Development and Industrial Pharmacy* 11 (1985) 697–724.

Craig DQM. The mechanisms of drug release from solid dispersions in water-soluble polymers. *International Journal of Pharmaceutics* 231 (2002) 131–144.

Craig DQM, Royall PG, Kett VL, Hopton ML. The relevance of the amorphous state to pharmaceutical dosage forms: Glassy drugs and freeze dried systems. *International Journal of Pharmaceutics* 179 (1999) 179–207.

Crowley MM, Zhang F, Koleng JJ, McGinity JW. Stability of polyethylene oxide in matrix tablets prepared by hot-melt extrusion. *Biomaterials* 23 (2002) 4241–4248.

Crowley MM, Zhang F, Repka MA, Thumma S, Upadhye SB, Battu SK, McGinity JW, Martin C. Pharmaceutical applications of hot-melt extrusion: Part I. *Drug Development and Industrial Pharmacy* 33 (2007) 909 – 926.

Diez I, Colom H, Moreno J, Obach R, Peraire C, Domenech J. A comparative in vitro study of transdermal absorption of a series of calcium channel antagonists. *Journal of Pharmaceutical Sciences* 80 (1991) 931–934.

Dittgen M, Fricke S, Gerecke H, Osterwald H. Hot spin mixing: A new technology to manufacture solid dispersions. I: Testosterone. *Pharmazie* 50 (1995) 225–226.

Djuric D, Kolter K. Bioavailability enhancement of fenofibrate and itraconazole by forming solid solutions with an innovative amphiphilic copolymer. Conference poster, 7th World Meeting on Pharmaceutics, Biopharmaceutics and Pharmaceutical Technology, Valetta, Malta. (2010).

Doktycz S, Suslick K. Interparticle collisions driven by ultrasound. *Science* 247 (1990) 1067–1069.

Dubois JL, Ford JL. Similarities in the release rates of different drugs from polyethylene glycol 6000 solid dispersions. *Journal of Pharmacy and Pharmacology* 37 (1985) 494–495.

El-Egakey M, Soliva M, Speiser P. Hot extruded dosage forms. *Pharmaceutica Acta Helvetiae* 46 (1971) 31–52.

European Pharmacopoeia. 7. ed. Council of Europe, Strasbourg, France (2007).

Fini A, Cavallari C, Ospitali F. Effect of ultrasound on the compaction of ibuprofen/isomalt systems. *Pharmaceutics* 1 (2009) 3–19.

Fini A, Fernández-Hervás MJ, Holgado MA, Rodriguez L, Cavallari C, Passerini N, Caputo O. Fractal analysis of ß-cyclodextrin–indomethacin particles compacted by ultrasound. *Journal of Pharmaceutical Sciences* 86 (1997) 1303–1309.

Fini A, Holgado MA, Rodriguez L, Cavallari C. Ultrasound-compacted indomethacin/polyvinylpyrrolidone systems: Effect of compaction process on particle morphology and dissolution behavior. *Journal of Pharmaceutical Sciences* 91 (2002a) 1880–1890.

Fini A, Rodriguez L, Cavallari C, Albertini B, Passerini N. Ultrasound-compacted and spray-congealed indomethacin/polyethyleneglycol systems. *International Journal of Pharmaceutics* 247 (2002b) 11–22.

Ford JL. The current status of solid dispersions. *Pharmaceutica Acta Helvetiae* 61 (1986) 69–88.

Ghaderi R, Artursson P, Carlfors J. Preparation of biodegradable microparticles using solution-enhanced dispersion by supercritical fluids (SEDS). *Pharmaceutical Research* 16 (1999) 676–681.

Goldberg AH, Gibaldi M, Kanig JL. Increasing dissolution rates and gastrointestinal absorption of drugs via solid solutions and eutectic mixtures I. Theoretical considerations and discussion of the literature. *Journal of Pharmaceutical Sciences* 54 (1965) 1145–1148.

Goldberg AH, Gibaldi M, Kanig JL. Increasing dissolution rates and gastrointestinal absorption of drugs via solid solutions and eutectic mixtures II: Experimental evaluation of a eutectic mixture: Urea-acetaminophen system. *Journal of Pharmaceutical Sciences* 55 (1966a) 482–487.

Goldberg AH, Gibaldi M, Kanig JL. Increasing dissolution rates and gastrointestinal absorption of drugs via solid solutions and eutectic mixtures III: Experimental evaluation of griseofulvin-succinic acid solid solution. *Journal of Pharmaceutical Sciences* 55 (1966b) 487–492.

Goldberg AH, Gibaldi M, Kanig JL, Mayersohn M. Increasing dissolution rates and gastrointestinal absorption of drugs via solid solutions and eutectic mixtures IV: Chloramphenicol-urea system. *Journal of Pharmaceutical Sciences* 55 (1966c) 581–583.

Graeser K. On the stability prediction of amorphous drugs. Ph.D. thesis, University of Otago, Dunedin, New Zealand (2009).

Gueret JLH. Process for the compaction of a powder mixture providing an absorbent or partially friable compact product and the product obtained by this process. US patent 5,211,892 (1993).

Guichard JP, Blouquin P, Qing Y. A new formulation of fenofibrate: Suprabioavailable tablets. *Current Medical Research and Opinion* 16 (2000) 134–138.

Guo JH, Robertson RE, Amidon GL. Influence of physical aging on mechanical properties of polymer free films: The prediction of long-term aging effects on the water permeability and dissolution rate of polymer film-coated tablets. *Pharmaceutical Research* 8 (1991) 1500–1504.

Haleblian J, McCrone W. Pharmaceutical applications of polymorphism. *Journal of Pharmaceutical Sciences* 58 (1969) 911–929.

Hardung H, Djuric D, Ali S. Combining HME and solubilization: Soluplus® the solid solution. *Drug Delivery Technology* 10 (2010).

Harwood RJ. Hypromellose. In: RC Rowe, PJ Sheskey, PJ Weller (Eds.), Handbook of Pharmaceutical Excipients, London: Pharmaceutical Press, 4 (2003) 297–300.

He H, Yang R, Tang X. In vitro and in vivo evaluation of fenofibrate solid dispersion prepared by hot-melt extrusion. *Drug Development and Industrial Pharmacy* 36 (2010) 681–687.

He X. Integration of physical, chemical, mechanical, and biopharmaceutical properties in solid oral dosage form development. In: Y Qiu, Y Chen, G Zhang, L Liu, W Porter (Eds.), Developing Solid Oral Dosage Forms: Pharmaceutical Theory and Practice, Burlington: Elsevier (2009) 429–430.

Higuchi WI, Mir NA, Desai SJ. Dissolution rates of polyphase mixtures. *Journal of Pharmaceutical Sciences* 54 (1965) 1405–1410.

Janssens S, des Armas HN, Roberts CJ, van den Mooter G. Characterization of ternary solid dispersions of itraconazole, PEG 6000, and HPMC 2910 E5. *Journal of Pharmaceutical Sciences* 97 (2008) 2110–2120.

Kanaujia P, Lau G, Ng WK, Widjaja E, Schreyer M, Hanefeld A, Fischbach M, Saal C, Maio M, Tan RB. Investigating the effect of moisture protection on solid-state stability and dissolution of fenofibrate and ketoconazole solid dispersions using PXRD, HSDSC and Raman microscopy. *Drug Development and Industrial Pharmacy* 37 (2011) 1026–1035.

Kanig JL. Properties of fused mannitol in compressed tablets. *Journal of Pharmaceutical Sciences* 53 (1964) 188–192.

Kolter K, Karl M, Nalawade S, Rottmann N. Hot-melt extrusion with BASF pharma polymers. Extrusion compendium. Ludwigshafen: BASF (2010).

Konno H, Handa T, Alonzo DE, Taylor LS. Effect of polymer type on the dissolution profile of amorphous solid dispersions containing felodipine. *European Journal of Pharmaceutics and Biopharmaceutics* 70 (2008) 493–499.

Lakshman JP, Cao Y, Kowalski J, Serajuddin ATM. Application of melt extrusion in the development of a physically and chemically stable high-energy amorphous solid dispersion of a poorly water-soluble drug. *Molecular Pharmaceutics* 5 (2008) 994–1002.

Law D, Wang W, Schmitt EA, Qiu Y, Krill SL, Fort JJ. Properties of rapidly dissolving eutectic mixtures of poly(ethylene glycol) and fenofibrate: The eutectic microstructure. *Journal of Pharmaceutical Sciences* 92 (2003) 505–515.

Leuner C, Dressman J. Improving drug solubility for oral delivery using solid dispersions. *European Journal of Pharmaceutics and Biopharmaceutics* 50 (2000) 47–60.

Levina M, Rubinstein MH. The effect of ultrasonic vibration on the compaction characteristics of paracetamol. *Journal of Pharmaceutical Sciences* 89 (2000) 705–723.

Levina M, Rubinstein MH. The effect of ultrasonic vibration on the compaction characteristics of ibuprofen. *Drug Development and Industrial Pharmacy* 28 (2002) 495 – 514.

Levina M, Rubinstein MH, Rajabi-Siahboomi AR. Principles and application of ultrasound in pharmaceutical powder compression. *Pharmaceutical Research* 17 (2000) 257–265.

Linn M, Collnot EM, Djuric D, Hempel K, Fabian E, Kolter K, Lehr CM. Soluplus® as an effective absorption enhancer of poorly soluble drugs in vitro and in vivo. *European Journal of Pharmaceutical Sciences* 45 (2011) 336–343.

Liu H, Wang P, Zhang X, Shen F, Gogos CG. Effects of extrusion process parameters on the dissolution behavior of indomethacin in Eudragit® E PO solid dispersions. *International Journal of Pharmaceutics* 383 (2010) 161–169.

Lloyd G, Craig D, Smith A. A calorimetric investigation into the interaction between paracetamol and polyethylene glycol 4000 in physical mixes and solid dispersions. *European Journal of Pharmaceutics and Biopharmaceutics* 48 (1999) 59–65.

Majerik V. Improvement of bioavailability of LM4156 using supercritical and cryogenic technologies. Ph.D. thesis, Doctoral School of Chemical Engineering, University of Veszprém; Doctoral School of Environmental Sciences, University of Aix-Marseille III (2006).

Majerik V, Charbit G, Badens E, Horváth G, Szokonya L, Bosc N, Teillaud E. Bioavailability enhancement of an active substance by supercritical antisolvent precipitation. *The Journal of Supercritical Fluids* 40 (2007) 101–110.

Majerik V, Horváth G, Charbit G, Badens E, Szokonya L, Bosc N, Teillaud E. Solid dispersions of oxeglitazar in PVP K17 and poloxamer 407 by supercritical antisolvent and co-evaporation methods. *Hungarian Journal of Industrial Chemistry* 34 (2006) 41–49.

Marciniec B, Ogrodowczyk M. Thermal stability of 1,4-dihydropyrinine derivatives in solid state. *Acta Poloniae Pharmaceutica - Drug Research* 63 (2006) 477–484.

Marsac P, Konno H, Rumondor A, Taylor L. Recrystallization of nifedipine and felodipine from amorphous molecular level solid dispersions containing poly(vinylpyrrolidone) and sorbed water. *Pharmaceutical Research* 25 (2008) 647–656.

Matsumoto T, Zografi G. Physical properties of solid molecular dispersions of indomethacin with poly(vinylpyrrolidone) and poly(vinylpyrrolidone-co-vinyl-acetate) in relation to indomethacin crystallization. *Pharmaceutical Research* 16 (1999) 1722–1728.

McGinity JW, Maincent P, Steinfink H. Crystallinity and dissolution rate of tolbutamide solid dispersions prepared by the melt method. *Journal of Pharmaceutical Sciences* 73 (1984) 1441–1444.

Meng X, Chen Y, Chowdhury SR, Yang D, Mitra S. Stabilizing dispersions of hydrophobic drug molecules using cellulose ethers during anti-solvent synthesis of micro-particulates. *Colloids and Surfaces B: Biointerfaces* 70 (2009) 7–14.

Millán M, Caraballo I. Effect of drug particle size in ultrasound compacted tablets: Continuum percolation model approach. *International Journal of Pharmaceutics* 310 (2006) 168–174.

Munoz A, Guichard JP, Reginault P. Micronised fenofibrate. *Atherosclerosis* 110 (1994) S45–S48.

Nakamichi K, Nakano T, Yasuura H, Izumi S, Kawashima Y. The role of the kneading paddle and the effects of screw revolution speed and water content on the preparation of solid dispersions using a twin-screw extruder. *International Journal of Pharmaceutics* 241 (2002) 203–211.

Nernst W. Theorie der Reaktionsgeschwindigkeit in heterogenen Systemen. *Zeitschrift für Physikalische Chemie* 47 (1904) 52–55.

Nollenberger K, Gryczke A, Meier C, Dressman J, Schmidt M, Brühne S. Pair distribution function X-ray analysis explains dissolution characteristics of felodipine melt extrusion products, 98. Wiley Subscription Services, A Wiley Company (2009a).

Nollenberger K, Gryczke A, Takayuki M, Tatsuya I. Using polymers to enhance solubility of poorly soluble drugs. *Pharmaceutical Technology* (2009b) s20–s25.

Noyes AA, Whitney WR. The rate of solution of solid substances in their own solutions. *Journal of the American Chemical Society* 19 (1897) 930–934.

O'Donnell K, Williams III RO. Optimizing the formulation of poorly water-soluble drugs. In: RO Williams III, AB Watts, DA Miller (Eds.), Formulating poorly water soluble drugs, New York: Springer (2009) 40–41.

Papageorgiou GZ, Bikiaris D, Kanaze FI, Karavas E, Stergiou A, Georgarakis E. Tailoring the release rates of fluconazole using solid dispersions in polymer blends. *Drug Development and Industrial Pharmacy* 34 (2008) 336–346.

Patel AR, Vavia PR. Preparation and in vivo evaluation of SMEDDS (self-microemulsifying drug delivery system) containing fenofibrate. *AAPS Journal/Journal of Pharmacy and Pharmacology* 9 (2007) E344–E352.

Paul DW, Crawford RJ. Ultrasonic moulding of plastic powders. *Ultrasonics* 19 (1981) 23–27.

Prodduturi S, Urman K, Otaigbe J, Repka M. Stabilization of hot-melt extrusion formulations containing solid solutions using polymer blends. *AAPS PharmSciTech* 8 (2007) E152–E161.

Qi S, Belton P, Nollenberger K, Clayden N, Reading M, Craig D. Characterisation and prediction of phase separation in hot-melt extruded solid dispersions: A thermal, microscopic and NMR relaxometry study. *Pharmaceutical Research* 27 (2010) 1869–1883.

Repka MA, Gerding TG, Repka SL, McGinity JW. Influence of plasticizers and drugs on the physical-mechanical properties of hydroxypropylcellulose films prepared by hot melt extrusion. *Drug Development and Industrial Pharmacy* 25 (1999) 625–633.

Repka MA, Majumdar S, Kumar Battu S, Srirangam R, Upadhye SB. Applications of hot-melt extrusion for drug delivery. *Expert Opinion on Drug Delivery* 5 (2008) 1357–1376.

Repka MA, McGinity JW. Influence of Vitamin E TPGS on the properties of hydrophilic films produced by hot-melt extrusion. *International Journal of Pharmaceutics* 202 (2000) 63–70.

Rodriguez L, Cini M, Cavallari C, Passerini N, Saettone MF, Fini A, Caputo O. Evaluation of theophylline tablets compacted by means of a novel ultrasound-assisted apparatus. *International Journal of Pharmaceutics* 170 (1998) 201–208.

Rodriguez L, Cini M, Cavallari C, Passerini N, Saettone MF, Monti D, Caputo O. Ultrasound-assisted compaction of pharmaceutical materials. *Farmacevtski Vestnik* 46 (1995) 241–242.

Rumondor A, Ivanisevic I, Bates S, Alonzo D, Taylor L. Evaluation of drug-polymer miscibility in amorphous solid dispersion systems. *Pharmaceutical Research* 26 (2009a) 2523–2534.

Rumondor A, Stanford L, Taylor L. Effects of polymer type and storage relative humidity on the kinetics of felodipine crystallization from amorphous solid dispersions. *Pharmaceutical Research* 26 (2009b) 2599–2606.

Saettone MF, Giannaccini B, Monti D, Cabani I, Rodriguez L, Cini M, Cavallari C, Caputo O. Ultrasound-assisted compaction of pharmaceutical materials. 2. Preparation of matrices for sustained release of theophylline. *Bollettino chimico farmaceutico* 135 (1996) 142–144.

Sancin P, Caputo O, Cavallari C, Passerini N, Rodriguez L, Cini M, Fini A. Effects of ultrasound-assisted compaction on Ketoprofen/Eudragit® S100 Mixtures. *European Journal of Pharmaceutical Sciences* 7 (1999) 207–213.

Sato T, Okada A, Sekiguchi K, Thusa Y. Difference in Physico-Pharmaceutical Properties between Crystalline and Noncrystalline 9,3''-Diacetylmidecamycin. *Chemical & Pharmaceutical Bulletin* 29 (1981) 2675–2682.

Sears JK, Darby JR. The Technology of Plasticizers. New York: John Wiley & Sons (1982).

Sekiguchi K, Obi N. Studies on absorption of eutectic mixture. I. A comparison of the behavior of eutectic mixture of sulfathiazole and that of ordinary sulfathiazole in man. *Chemical & Pharmaceutical Bulletin* 9 (1961) 866–872.

Serajuddin ATM. Solid dispersion of poorly water-soluble drugs: Early promises, subsequent problems, and recent breakthroughs. *Journal of Pharmaceutical Sciences* 88 (1999) 1058–1066.

Sheu MT, Yeh CM, Sokoloski TD. Characterization and dissolution of fenofibrate solid dispersion systems. *International Journal of Pharmaceutics* 103 (1994) 137–146.

Six K, Berghmans H, Leuner C, Dressman J, Van Werde K, Mullens J, Benoist L, Thimon M, Meublat L, Verreck G, Peeters J, Brewster M, Van den Mooter G. Characterization of solid dispersions of itraconazole and hydroxypropylmethylcellulose prepared by melt extrusion, Part II. *Pharmaceutical Research* 20 (2003) 1047–1054.

Sjökvist E, Nyström C. Physicochemical aspects of drug release. VI. Drug dissolution rate from solid particulate dispersions and the importance of carrier and drug particle properties. *International Journal of Pharmaceutics* 47 (1988) 51–66.

Sjökvist Saers E, Craig DQM. An investigation into the mechanisms of dissolution of alkyl p-aminobenzoates from polyethylene glycol solid dispersions. *International Journal of Pharmaceutics* 83 (1992) 211–219.

Srinarong P, Faber JH, Visser MR, Hinrichs WLJ, Frijlink HW. Strongly enhanced dissolution rate of fenofibrate solid dispersion tablets by incorporation of superdisintegrants. *European Journal of Pharmaceutics and Biopharmaceutics* 73 (2009) 154–161.

Suslick KS, Casadonte DJ, Green MLH, Thompson ME. Effects of high intensity ultrasound on inorganic solids. *Ultrasonics* 25 (1987) 56–59.

Suslick KS, Doktycz SJ. Effects of ultrasound on surfaces and solids. In: TJ Mason (Ed.), Advances in sonochemistry, London: JAI Press, 1 (1990) 187–230.

Technical Information Soluplus (2010). http://www.pharma-ingredients.basf.com/Statements/TechnicalInformations/EN/PharmaSolutions/03_090801e_Soluplus.pdf (available online: 2012-01-24).

Tu J, Shen Y, Mahalingam R, Jasti B, Li X. Polymers in oral modified release systems, Hoboken: John Wiley & Sons (2010) 77–79.

Uemura T, Uramatsu S, Akiyama S, Ichikawa H, Fukumori Y. Application of poly(vinylalcohol/acrylic acid/methyl methacrylate) (PVA copolymer) as a solid dispersion matrix. *The AAPS Journal* 11 ().

Uramatsu S, Shinike H, Kida A, Uemura T, Ichikawa H, Fukumori Y. Application of poly(vinylalcohol/acrylic acid/methyl methacrylate) (PVA copolymer) as a solid dispersion matrix. Conference poster, First Asian Symposium on Pharmaceutical Sciences and Technology, July 28-30, 2007, Shenyang, China. (2007).

Van Nijlen T, Brennan K, Van den Mooter G, Blaton N, Kinget R, Augustijns P. Improvement of the dissolution rate of artemisinin by means of supercritical fluid technology and solid dispersions. *International Journal of Pharmaceutics* 254 (2003) 173–181.

Vasanthavada M, Tong WQ, Joshi Y, Kislalioglu MS. Phase behavior of amorphous molecular dispersions I: Determination of the degree and mechanism of solid solubility. *Pharmaceutical Research* 21 (2004) 1598–1606.

Verreck G, Six K, Van den Mooter G, Baert L, Peeters J, Brewster ME. Characterization of solid dispersions of itraconazole and hydroxypropylmethylcellulose prepared by melt extrusion–part I. *International Journal of Pharmaceutics* 251 (2003) 165–174.

Vogt M, Kunath K, Dressman JB. Dissolution enhancement of fenofibrate by micronization, cogrinding and spray-drying: Comparison with commercial preparations. *European Journal of Pharmaceutics and Biopharmaceutics* 68 (2008) 283–288.

Wypych G. Introduction. In: G Wypych (Ed.), Handbook of plasticizers, Ontario: ChemTec Publishing (2004a) 2–5.

Wypych G. Introduction. In: G Wypych (Ed.), Handbook of plasticizers, Ontario: ChemTec Publishing (2004b) 280–282.

Zhang GGZ, Zhou D. Crystalline and amorphous solids. In: Y Qiu, Y Chen, G Zhang, L Liu, W Porter (Eds.), Developing Solid Oral Dosage Forms: Pharmaceutical Theory and Practice, Burlington: Elsevier (2009) 53–54.

Zhu Y, Shah NH, Malick AW, Infeld MH, McGinity JW. Solid-state plasticization of an acrylic polymer with chlorpheniramine maleate and triethyl citrate. *International Journal of Pharmaceutics* 241 (2002) 301–310.

# List of Publications

## Peer-reviewed articles

1. Kalivoda A, Fischbach M, Kleinebudde P. Application of mixtures of polymeric carriers for dissolution enhancement of fenofibrate using hot-melt extrusion. *International Journal of Pharmaceutics* 429 (2012) 58-68.
2. Kalivoda A, Fischbach M, Maio M, Kleinebudde P. Preliminary studies to assess ultrasound-assisted compaction as a potential novel technique in solid dispersion preparation. *Die Pharmazeutische Industrie* 4 (2012) 652-662.

## In preparation

1. Kalivoda A, Fischbach M, Kleinebudde P. Application of mixtures of polymeric carriers for dissolution enhancement of oxeglitazar using hot-melt extrusion.

## Poster presentations

1. Kalivoda A, Fischbach M, Maio M, Kleinebudde P. Application of polymeric blends as carrier for dissolution enhancement using hot-melt extrusion. 8th World Meeting on Pharmaceutics, Biopharmaceutics and Pharmaceutical Technology, March 19-22, 2012, Istanbul, Turkey
2. Kalivoda A, Fischbach M, Maio M, Kleinebudde P. Application of hot melt extrusion for dissolution enhancement of fenofibrate - a comparison of various polymeric carriers and their influence on the dissolution profile. AAPS Annual Meeting and Exposition, October 23–27, 2011, Washington, D.C., USA
3. Kalivoda A, Fischbach M, Maio M, Kleinebudde P. Preliminary studies to assess ultrasound-assisted compaction technique as a new technology. 7th World Meeting on Pharmaceutics, Biopharmaceutics and Pharmaceutical Technology, March 8-11, 2010, Valetta, Malta

# Danksagung

Die vorliegende Arbeit entstand am Institut für Pharmazeutische Technologie und Biopharmazie der Heinrich-Heine-Universität Düsseldorf unter der Leitung von Herrn Prof. Dr. Peter Kleinebudde in Zusammenarbeit mit der Merck Serono GmbH, Darmstadt.

Meinem Doktorvater Prof. Dr. Peter Kleinebudde danke ich ganz herzlich für die Überlassung des interessanten Themas, für die außergewöhnlich gute wissenschaftliche Betreuung und für seine stete Diskussionsbereitschaft. Insbesondere seine Anregungen und kritischen Einwände haben mir immer wieder neue Anstöße bei der Bearbeitung des Themas gegeben.

Dr. Matthias Fischbach von der Merck Serono GmbH gilt mein besonderer Dank für seine hervorragende Betreuung während meiner Promotionszeit. Sein stets offenes Ohr für meine Fragen und die Zeit für gemeinsame Diskussionen, die er trotz immervollem Terminkalender doch immer für mich gefunden hat, haben mich häufig wieder auf die richtige Spur gebracht.

Bei beiden Betreuern möchte ich mich für die Möglichkeit, an internationalen Kongressen und Seminaren teilzunehmen, bedanken - überaus spannende und lehrreiche Erfahrungen, die ich nicht missen möchte.

Ebenfalls möchte ich mich bei den Mitarbeitern der Merck Serono GmbH bedanken, die mich bei meinen Versuchen tatkräftig unterstützt haben: dem Labor AD2, insbesondere Eckard Garrandt, für das Erhören meiner Hilferufe, wenn die HPLC mal nicht so wollte wie sie sollte...Andreas Swoboda und Bianca Jordan für die Durchführung unzähliger XRD-Messungen...Steffen Merk und Norbert Halder für die schnelle Unterstützung bei kleinen und großen Extruder-Problemen...Ioannis Chartomatsidis und dem gesamten Labor AD8 für ihre Hilfsbereitschaft in allen Dissolution-Dingen (und dafür, dass ich ungehindert in ihrem Labor herumwuseln durfte)...dem Spitzencluster-Mittagessensteam...und all den anderen, die ich hier nicht genannt habe.

Ganz herzlich bedanke ich mich auch bei meinen Mit-Doktoranden Tobias Miller und Alexandra Hill für die gute Zusammenarbeit, fachliche Diskussionen und die schöne Zeit. Ein großes HURRA und Dankeschön geht an Dr. Alena Wieber und Gudrun Birk - für die großartige Zeit im Büro und Unterstützung in jeder Lebenslage, auch nach Feierabend.

Von ganzem Herzen danke ich meiner Familie für ihre uneingeschränkte Unterstützung, den Rückhalt und ihr Verständnis, ohne die ich dieses Ziel nicht erreicht hätte.

Schließlich möchte ich mich bei Peter bedanken - für die Bearbeitung der Bilder, das Korrekturlesen, die viele Geduld bei meinen soziallegasthenischen Anwandlungen in Zeiten, in denen einfach nichts geklappt hat, das klaglose Ertragen der wochenlangen Schreibphase und vor allem für den Halt und die Ermutigung während dieser Zeit.